Establishment of novel options for quantification of bioactive compounds via planar chromatography–effect-directed analysis combined with nuclear magnetic resonance spectroscopy

Cumulative inaugural dissertation

For the degree of

***Doctor rerum naturalium* (*Dr. rer. nat.*)**

By

Ebrahim Azadniya, M. Sc.

Sari, Iran

Submitted to the

Faculty of Agricultural Science, Nutritional Science,

and Environmental Management

Prepared at

Department of Food Science

Institute of Nutritional Science

Justus Liebig University Giessen, Germany

Giessen, 2019

TABLE OF CONTENT

LIST OF FIGURES

Dissertation reviewers and examiners

1st Reviewer

Prof. Dr. Gertrud Morlock

Chair of Food Science, Institute of Nutritional Science, Justus Liebig University Giessen

2nd Reviewer

Prof. Dr. Richard Göttlich

Institute of Organic Chemistry, Justus Liebig University Giessen

1st Examiner

Prof. Dr. Wolfgang Schwack

Chair of Food Science, Institute of Nutritional Science, Justus Liebig University Giessen

2nd Examiner

Prof. Dr. Jan Siemens

Department of Soil Science and Soil Conservation, Justus Liebig University Giessen

Declaration

I declare: this dissertation submitted is a work of my own, written without any illegitimate help by any third party and only with materials indicated in the dissertation. I have indicated in the text where I have used texts from already published sources, either word for word or in substance, and where I have made statements based on oral information given to me. At any time during the investigations carried out by me and described in the dissertation, I followed the principles of good scientific practice as defined in the "Statutes of the Justus Liebig University Giessen for the Safeguarding of Good Scientific Practice".

Giessen, September 2019

_____

Ebrahim Azadniya

Acknowledgements

Special thanks to

My supervisor Professor Dr. Gertrud Morlock,

My co-supervisor Professor Dr. Richard Göttlich,

My colleagues, Dr. Maryam Jamshidi-Aidji, Dr. Salim Hage, Dr. Tim Häbe.

Dedicated to

Whom I owe my life, my wonderful parents,

My unique brother Mohammad-Hossein,

My resourceful sisters, Hamideh, Akram and Azam,

My cute nieces and nephews, Shokraneh, Yeganeh, Amirali, Abolfazl and Ashkan,

My kind accompanier, Sahar,

Finally dedicated to my beloved grandfather

Gholamali Barzegar

Scientific contributions

Peer-reviewed original research papers

1) Azadniya, E., Morlock, G.E., ***J. Chromatogr. A* 1533 (2018) 180-192**

   Bioprofiling of *Salvia miltiorrhiza* via planar chromatography linked to (bio)assays, high-resolution mass spectrometry and nuclear magnetic resonance spectroscopy

2) Azadniya, E., Morlock, G.E., ***J. Chromatogr. A* 1602 (2019) 458-466**

   Automated piezoelectric spraying of biological and enzymatic assays for effect-directed analysis of planar chromatograms

3) Azadniya, E., Morlock, G.E., ***Anal. Methods,* accepted**
   https://doi.org/10.1039/C9AY01465A

   Equivalency calculation of enzyme inhibiting unknowns *in situ* the adsorbent of the effect-directed autogram

4) Mollergues, J., Azadniya, E., Stroheker, T., Billerbeck, K., Morlock, G.E., ***in submission***

   Incorporating the S9 system into methods for acetylcholinesterase inhibition and application to food contact materials

5) Azadniya, E., Goldoni, L., Bandiera, T., Morlock, G.E., ***in submission***

   From bioprofiling to quantification of bioactive compounds via a direct workflow of planar chromatography–effect-directed analysis-nuclear magnetic resonance spectroscopy

SCIENTIFIC CONTRIBUTIONS

Poster presentations

Presenter is underlined

1) Azadniya, E., Morlock, G.E**., 8th Annual GGL Conference, Giessen**, 31.09-01.10.2015:
"Crucial aspects of structural elucidation of bioactive compounds in medicinal herbal extracts by hyphenation of HPTLC with NMR"

2) Azadniya, E., Morlock, G.E., **9th Annual GGL Conference, Giessen**, 20.09.-21.09.2016:
"Comprehensive HPTLC–bioassay–MS method for bioactivity screening of *Salvia miltiorrhiza*"

3) Azadniya, E., Morlock, G.E., **International Symposium for HPTLC 2017, Berlin**, 04.-08.07.2017:
"HPTLC–EDA–HRMS and PLC-NMR spectroscopy for structural elucidation of active compounds in *Salvia miltiorrhiza*"

4) Azadniya, E., Goldoni, L., Bandiera, T., Morlock, G.E., **11th Annual GGL Conference, Giessen**, 19.-20.09.2018:
"HPTLC-qNMR to quantify co-eluted isomers in (bio)active zones"

Oral presentations

5) Azadniya, E., Morlock, G.E., **International Symposium for HPTLC 2017, Berlin**, 04.-08.07.2017:
"HPTLC–EDA–HRMS and PLC-NMR to reveal co-eluting isomers of bioactive zones"

6) Azadniya, E., Morlock, G.E., **10th Annual GGL Conference 2017, Giessen**, 28.-29.09.2017:
"HPTLC–(bio)assays–HRMS and PLC-NMR spectroscopy for structural elucidation of active compounds in *Salvia miltiorrhiza*"

7) Azadniya, E., Morlock, G.E., **Nestlé Research Center, Chemical Food Safety, Lausanne**, 5.11.2018:
"Screening of acetylcholinesterase inhibitors in migration extracts via HPTLC–S9–AChE"

Abstract

Hyphenation between high-performance thin-layer chromatography and effect-directed analysis (HPTLC–EDA) via immersion/spraying is a simple and fast procedure for bioprofiling to find the responses of known and unknown compounds *in situ* a complex sample matrix. In order to benefit the bioanalytical potential of HPTLC–EDA, several obstacles of the automated immersion needed to be avoided such as the (1) required high volumes of solutions, (2) tailing, distortion or shifting zones due to long/slow immersion times/speeds, (3) gradual inactivation of the re-used enzyme solution, and (4) lack of covering the whole plate surface. Using automated piezoelectric spraying for performing an assay was an alternative but challenging. In this research we reached this milestone via optimization of important aspects *i.e.*, plate pre-wetting, spraying nozzle type and applied volumes for microorganism suspension or enzyme and substrate-chromogenic solutions. To overcome above challenges, piezoelectric spraying provided (1) using by a factor of 4 to 27 less solutions consumption than by immersion (cheaper and environment-friendly workflow), (2) better resolved autogram zones and no zone distortion or shift (good for quantification), (3) covering the whole plate surface (both sides of plate can be used) and (4) using always a fresh solution (just defrost the needed aliquot of enzyme solution, 3 mL instead of 70 mL) would be the best practice with regard to the standardization of HPTLC–EDA procedure. Finally, the newly developed automated piezoelectric spraying procedures for the application of biological (*Aliivibrio fischeri*) and enzymatic acetyl- and butyrylcholinesterase (AChE/BChE) assays were used for bioprofiling of *Peganum harmala* seed extract. By their *in situ* high-resolution mass spectrometry (HRMS) spectra, the active zones in the *P. harmala* seed extract were assigned to be harmine and harmaline as AChE inhibitors and harmol, vasicine and deoxyvasicine as BChE-inhibitors.

Then the enzyme inhibitory potency of the active compounds was estimated via two different modes of equivalency calculation, referring to a potent inhibitor as a reference. These two modes were designed as applied ChE inhibitors on a HPTLC plate (no chromatography) and developed ChE inhibitors with the same chromatographic condition used for the sample extract, and then performed, validated and compared exemplarily on the AChE/BChE inhibition of *P. harmala* seed extract. Among Physostigmine (PHY), rivastigmine and piperine, PHY reveled the most similar properties (brightness against

the plate background, hR_F value and band shape) to the unidentified inhibitors of sample, and thus selected as reference. The results showed that the enzyme inhibition equivalency calculated via developed reference bands was more reliable and sensitive, if compared to applied mode results. In case of using as a compromise the faster procedure of an applied band pattern for routine equivalency calculation, a potential bias should be considered (here ca. 30%). Finally, it was the first time; the found inhibitors were calculated equivalently to their well-matched reference inhibitor and thus, the automated piezoelectric spraying was proven to be quantitative.

In another part of our study, the HPTLC–(bio)assays–HRMS workflow followed by an scale-up to preparative layer chromatography combined with nuclear magnetic resonance (PLC-NMR) spectroscopy was used. It included using four different (bio)assays for activity screening of both polar and nonpolar extracts of *Salvia miltiorrhiza* Bunge root (Danshen) on the same HPTLC plate after a two-step development. It followed by MS recording of active compounds and finally a high concentration nonpolar extract was applied as an area for isolation of unidentified active zone for NMR spectroscopy. The ^{1}H-NMR and ^{1}H-^{13}C Heteronuclear Single Quantum Coherence spectra (1) confirmed the existence of two potential candidates among others which (2) revealed a coelution of two tanshinones (1,2-dihydrotanshinone I and methylenetanshinquinone) and (3) relatively quantify them in the ratio of 2:1. Compare to former reports about an unknown band among tanshinones, it was the first report, a multipotent unidentified active zone in the *Bacillus subtilis, A. fischeri* and AChE fingerprints was identified as a coeluted band.

In order to reach absolute quantitative NMR (qNMR) spectroscopy, the efficiency of planar chromatography isolation as a sample preparation method for NMR spectroscopy needed to be investigated. The HPTLC/PLC isolation needs to provide the enough amounts of the active compounds from a planar chromatogram in detectable rang of NMR spectroscopy (sensitivity gap). In this research, a straight-forward HPTLC-NMR spectroscopy workflow using a fix chromatographic condition from bioprofiling to isolation of the active zones was established. The dried extracts containing different structural isomers e.g. ursolic (UA), oleanolic (OA), betulinic acids (all $C_{30}H_{48}O_3$) with potential of coelution, were selected as the extreme case studies. The HPTLC–EDA revealed the UA-OA as a coeluted bioactive zone, and then collected via HPTLC isolation (using

one plate) for qNMR spectroscopy. In contrast to NP-HPTLC and HRMS, ^{1}H NMR spectra indicated UA and OA via a distinct allylic 1H-18 signals (UA 2.20 ppm and OA 2.85 ppm). The PUlse Length-based CONcentration determination (PULCON) procedure calibrated by maleic acid standard solution was used for UA and OA quantification. The results of two orthogonal methods (PULCON and pre- and post-chromatographic derivatization HPTLC) revealed a high correlation (R^2 = 0.972). The efficiency of HPTLC isolation procedure was assessed by comparing the amount of UA and OA in the isolated samples and the crude extracts solutions via derivatization HPTLC. The HPTLC isolation using the same chromatographic condition from bioprofiling to isolation showed 82 % (mean) efficiency and provided detectable amount for qNMR spectroscopy. The direct HPTLC-NMR workflow with low solvent consumption (16 mL) as an environment-friendly procedure can be a proper alternative for bioactivity-guided fractionation strategy to reach the NMR spectra of the active compounds and quantify them considering the isolation efficiency.

In one of our last projects, the metabolizing S9 enzyme mixture, mimicking the biotransformation reactions in the liver, was incorporated into two orthogonal methods (HPTLC–AChE and fluorometric microtiter plate AChE assay). The incorporated S9 mixture in fluorometric microtiter plate assay interfered with the final detection product and reduced that to a non-fluorescent product (hydroresorufin). In contrast, S9 mixture was successfully incorporated into HPTLC–AChE and used as the alternative method to assess the toxicity of food contact materials (FCMs) migrants and extract. After on-plate metabolization and one or two-step HPTLC development, the recently developed automated piezoelectric spraying procedure for AChE was used to detect the inhibitors. The determined limits of detection (LODs) of six AChE inhibiting chemicals, including PHY, chlorpyrifos, quinalphos, parathion, tris(nonylphenyl) phosphite and nonylphenol were compared between both methods and with/without S9 metabolic activation. According to LODs obtained by the HPTLC–S9–AChE method, the thresholds of toxicological concern (TTCs) of migrates and extract of a white polyurethane coated can was achieved by a 200-fold enrichment, simply by solvent evaporation during spray-on area application. Hence, two migrates and one extract were directly analyzed without pre-dilution/concentration with this straightforward HPTLC–S9–AChE method, which was standardized, automated in its important steps, and highly efficient.

1. Introduction

1.1.High-performance thin-layer chromatography (HPTLC)

Planar chromatography was termed HPTLC because of the latest improvements by moving towards lower size and narrower distribution of stationary phase particles as well as more automated TLC instruments making this technique faster, more sensitive and reliable than before for qualitative/quantitative analysis.[1]

Some exclusive features of HPTLC are[1-3]:

- Reduced sample preparation which protects the main structure of a sample and the matrix components remain at the start/solvent front of the plate. Whereas in gas chromatography (GC) these remain in the liner or in high-performance liquid chromatography (HPLC) held on the column
- Most parts of the sample are on the plate for further study (in HPLC, it goes to the waste)
- Each sample benefits from a new adsorbent and complex matrix do not change the stationary phase unlike to the sequential analysis of column-based methods
- Parallel analysis allowing comparison of several samples on one plate, on one run with the same mobile phase and other parameters (not possible in HPLC and GC)
- Derivatization by selective/specific chemical reagents provides thorough view about sample, especially for investigation of unknown compounds
- HPTLC is compatible with other complementary methods e.g. ultraviolet-visible (UV-Vis) light, florescence (FL), mass spectrometry (MS), nuclear magnetic resonance (NMR) spectroscopy, and effect-directed analysis (EDA).

1.2.Hyphenations of HPTLC with EDA

In cuvette, petri dish, microtiter plate or dot-blot assays only a sum parameter is achievable for either a complex sample or isolated fractions. In contrast, HPTLC–EDA separates complex samples and points to active zones *in situ* the autogram (Fig. 1). HPTLC–EDA allows detecting unknown (bio)active metabolites, side products, process contaminants,

degradation products, adulterants, packaging migrants, or residues in the complex samples.

The offline/open format HPTLC has some uniqueness for hyphenation with EDA such as[1]:

- The matrix-robust HPTLC allows avoiding a long sample preparation, leading to a comprehensive overview on the sample
- Cost-effective in comparison with other types of online methods
- Solvents-free chromatograms fit better to living organisms and enzymes
- A multi-fold HPTLC run provides comprehensive information of different bioassays and helps choosing the zone of interest for further analysis.

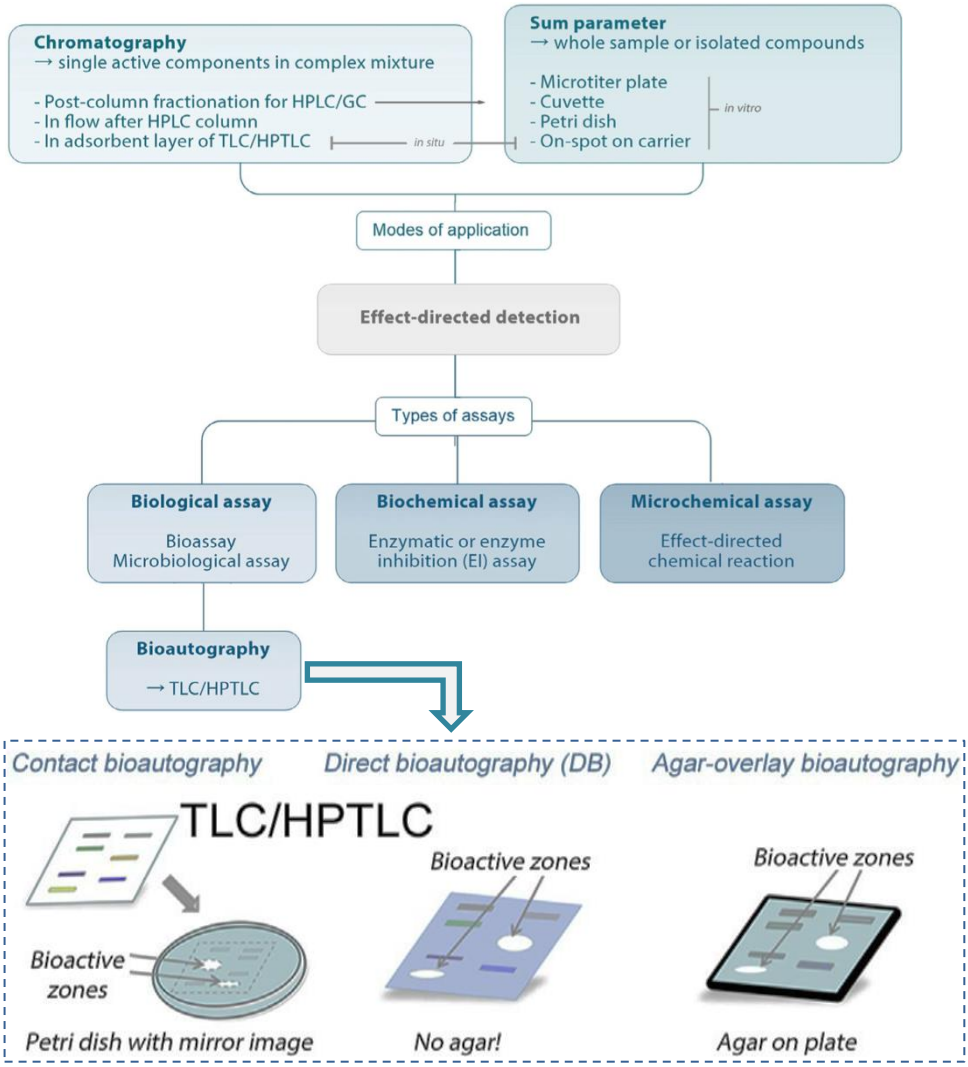

Figure 1. Overview on HPTLC–EDA compare to other methods and bioautography classification.[4]

EDA comprises all detection procedures indicating an effect that can affect biological systems/inhibit enzymes/scavenge free radicals. (HP)TLC–EDA was already established for three different groups including biological, biochemical and microchemical assays (Fig. 1). Hyphenation of (HP)TLC with bioassays termed as bioautography. Direct bioautography (DB) is a straightforward and efficient workflow for bioprofiling considering handling, detectability, resolution and analysis time compare to contact and agar-overlay bioautography.[4-6] The DB procedure can be used for biochemical assays as well via immersion[7-9], manual spraying[10] or a combination of both[11].

Application: HPTLC–EDA allows a fast biochemical and biological profiling *i.e.* finding enzyme inhibitors[8,12-15], antibacterial[6,16], antifungal[17,18] and antioxidant compounds[19] in complex samples. HPTLC–EDA–(HR)MS combined with NMR spectroscopy was demonstrated as a straightforward strategy to reach bioactive compounds structure (Fig. 2).[9,20]

In current research: Recently an automated piezoelectric spraying of biological and biochemical reagents were set up for *Aliivibrio fischeri* and acetyl- and butyrylcholinesterase (bio)assays.[21]

Figure 2. HPTLC-EDA-HRMS followed by preparative layer chromatography (PLC) isolation and NMR spectroscopy.[9]

1.2.1. HPTLC–*A. fischeri* bioassay

A. fischeri is a non-pathogenic Gram-negative marine bacterium with a bioluminescence emitting a blue-green (480 nm) lights in a critical density. Bioluminescence is directly linked to the bacteria's metabolism; a decrease in light intensity shows a disturbance of the metabolism. Luciferase, the bioluminescence catalyst, is expressed and catalyzes an oxidation reaction that releases excess energy in the form of light.[22]

After immersion, the plate surface is coated with a film of the bioluminescent bacteria (after removing the excess liquid) which produce dark zones on a luminescent background. Dark zones indicated the luminescence inhibition of the bacteria with tox-

ic/bioactive compounds.[23] The change in the luminescent bioautogram was immediately monitored and documented with the BioLuminizer (CAMAG) using an exposure time and trigger intervals.

Application: This method is suitable for the detection of bioactive compounds in plant extracts[7], beverages[24], *Bacillus* lipopeptides extracts[25], parabens in cosmetics[26] or water quality control[27].

In current research: HPTLC–*A. fischeri* either via immersion or automated piezoelectric spraying (for the first time) procedure was used for bioprofiling of *Salvia miltiorrhiza* Bunge root (Danshen)[9] and *P. harmala* seed[21] extracts.

1.2.2. HPTLC–*Bacillus subtilis* bioassay

B. subtilis is a non-pathogenic Gram-positive aerobic bacterium found in soil[28] and the gastrointestinal tract[29] of ruminants and humans. HPTLC–*B. subtilis* bioassay offers a fast bioprofiling to find the anti-bacterial compounds in a complex matrix of natural samples. HPTLC–*B. subtilis* bioassay was modified as a streamlined and reliable method to discover antimicrobials in herbal extracts. Among others, incubation time of the seeded plate and the neutralization procedure to remove residual acid traces from the planar chromatogram can influence the results of HPTLC–*B. subtilis*.[6]

For HPTLC–*B. subtilis*, the chromatogram was immersed into a suspension of bacteria, followed by incubation. For visualization, a live/dead cell staining assay, 3-(4,5-dimethylthiazol-2-yl)-2,5-diphenyltetrazolium bromide (MTT), was used. The dehydrogenases of viable cells reduced MTT into a colored formazan (Fig. 3). Pale yellow zones on a purple background visualized the position of antimicrobial compounds.[30]

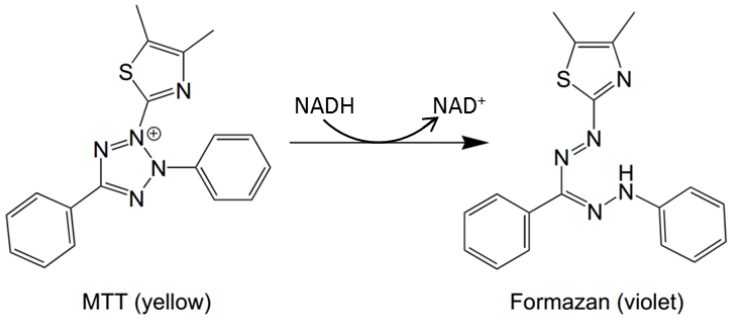

Figure 3. Reduction on MTT during the live/dead cell staining assay.

Application: (HP)TLC–*B. subtilis* was already used for finding antibacterial in Cow's milk[31,32], beverages[24], lipopeptides[25] and plant extracts[6,33,34].

In current research: HPTLC–*B. subtilis* was applied for bioprofiling of Danshen[9], *Lamiaceae* and apple peel extracts[35].

1.2.3. HPTLC–tyrosinase assay

Tyrosinase (EC 1.14.18.1) is an oxidase enzyme containing two copper ions connected to six histidine residues in catalytic site[36] (Fig. 4), distributed in plants, fungi and animals. It is responsible for enzymatic browning of fruits[37] or controls the melanin production and human skin color[38]. Browning changes the fruit/vegetables appearance and nutritional quality which encouraged researchers to find new potent tyrosinase inhibitors for food industry. Melanin is the most important chromophore of human skin. Melanogenesis is induced by the upregulation of tyrosinase after UV exposure in order to self-protect of the skin; however, abnormal accumulation of melanin causes undesirable aesthetic problems.[39] Hyperpigmentation enhanced by UV exposure such as freckles, melasma and lentigines which can be treated by using whitening agents, such as hydroquinone.[40] Nevertheless, hyperpigmentation can cause invasive forms of skin cancer.[41]

Some of the tyrosinase inhibitors are hydroquinone, arbutin, aloesin, kojic acid and Licorice extract. Kojic acid inhibits tyrosinase by binding to copper while hydroquinone does it by binding histidines at the active site. Hydroquinone is banned in Europe due to toxicity and carcinogenicity issues which brought the seeking for safe and effective tyrosinase inhibitor into focus.

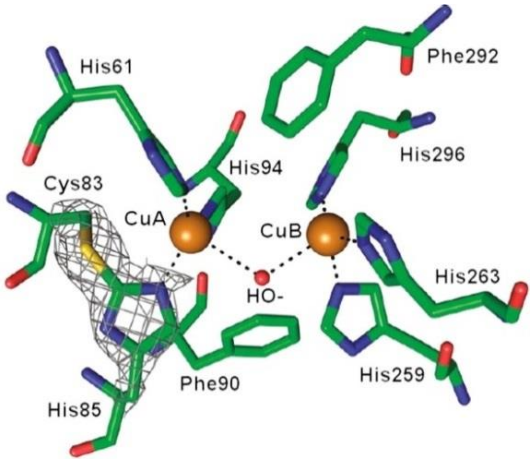

Figure 4. Crystal structure of mushroom tyrosinase.[42,43]

Tyrosinase catalyzes the hydroxylation of L-tyrosine to L-3,4-dihydroxyphenylalanine (L-DOPA). Then secondly involves oxidation of L-DOPA to L-DOPAquinine which is precursor for other steps to result melanin (Fig. 5).[44]

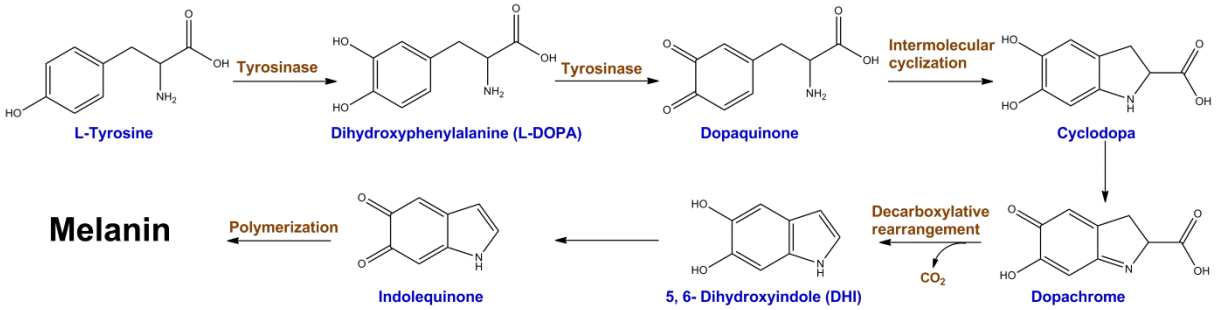

Figure 5. Mechanism of melanin production from tyrosine amino acid.

HPTLC–tyrosinase assay is a fast method to discover tyrosinase inhibitors using the CAMAG suggested procedure which was recently improved in our laboratory.[14,40] The planar chromatogram was placed in the Derivatizer (CAMAG), sprayed with substrate solution (L-DOPA), and subsequently dried using a cold stream of hair dryer. Then, it was sprayed with enzyme solution and incubated at room temperature in a humid box followed by drying. The tyrosinase inhibitors appeared as white/light yellow zones in a gray background.

Application: HPTLC–tyrosinase was already used for finding tyrosinase inhibitors or anti-melanogenic drug screening in natural samples[38,45-47] and *Bacillus* lipopeptide extracts[14].

In current research: HPTLC–tyrosinase was applied for tyrosinase inhibitory screening of *Lamiaceae* and apple peel extracts.[35]

1.2.4. HPTLC–cholinesterase assay

Acetylcholinesterase (AChE, EC. 3.1.1.7) and butyrylcholinesterase (BChE, EC. 3.1.1.8) are hydrolase enzymes. AChE known as true ChE is found in synaptic clefts of the central and peripheral nervous system. Its active sides consists the esteratic site (serine) binging to acetyl part of acetylcholine (ACh) and the anionic site binding to quaternary ammonium of ACh (Fig. 6A).[48-50] BChE known as pseudo-ChE or nonspecific ChE is mainly found in plasma, liver and muscle tissue, yet its function is not completely clear but it

hydrolyses ACh at a slower rate. AChE as the main catalytic enzyme is essential for returning the neuron to its resting phase by cleaving ACh. The acyl group of ACh is initially transferred to an active-site serine, then a water nucleophile attacks this ester, resulting acetate and completing the hydrolysis (Fig. 6B).[48,51,52]

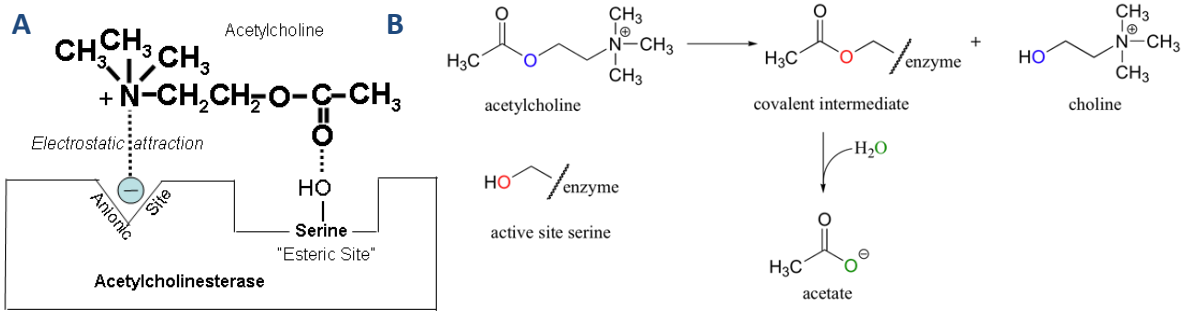

Figure 6. Interaction between ACh with two site of AChE (A)[50] ACh hydrolysis via AChE (B)[52].

The neurotransmitter ACh is an ester of acetic acid and choline, contradictory to the most amino acids based neurotransmitters. The choline acetyltransferase synthesizes ACh from acetyl-CoA and choline in the presynaptic axon. Encapsulated ACh is released into the synaptic cleft, and then bonded to cholinergic receptors enable the signal transmission. (Fig. 7).[48,53]

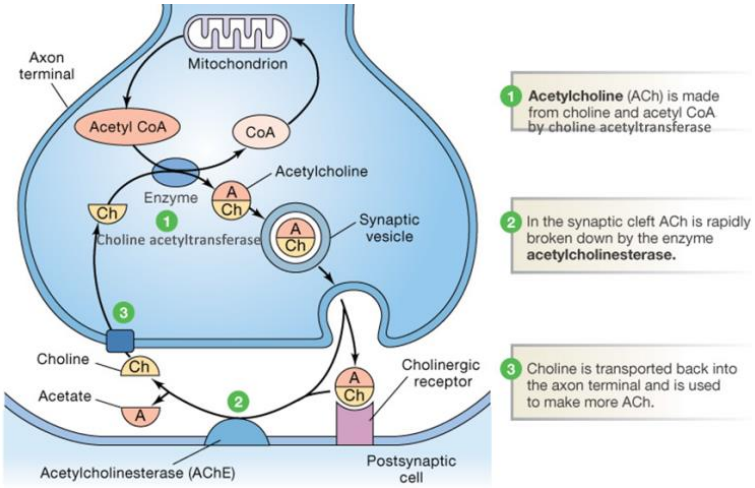

Figure 7. The cycle of ACh synthesis and hydrolysis via choline acetyltransferase and AChE, respectively during a neural transmission.[53]

ChE inhibition deactivates the enzymatic hydrolysis of ACh and consequently increases the ACh levels in the synaptic cleft and prolongs nerve stimulation. The ChE inhibitors can be divided into irreversible and reversible groups according to their pharmacological or toxicological functions. The reversible inhibitors (competitive or noncompetitive)

are used for treatment of Alzheimer's and Parkinson's diseases, myasthenia gravis, Lewy bodies by slowing down the ACh hydrolysis rate.[48]

While some of reversible (carbamate) and irreversible (organophosphates, OPs) inhibitors exhibit toxic function and used as insecticides by disrupting neurotransmission. Some OPs pesticides like chlorpyrifos and parathion require cytochrome P450-mediated metabolism to produce their respective oxon forms and increase their ChE inhibitory potency. However some of OPs showed therapeutic effects in the treatment of chronic glaucoma.[49] Some of ChE inhibitors used in disease treatments are donepezil, rivastigmine, galantamine and physostigmine (PHY, Fig. 8).[48,52]

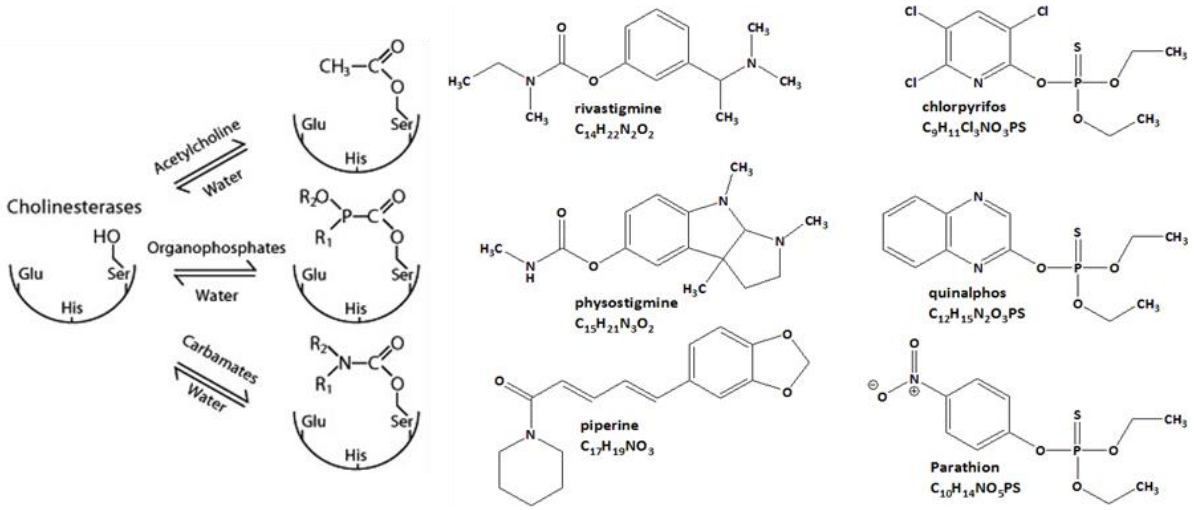

Figure 8. Inhibition mechanism of ChE enzymes modified from ref[54] and ChE inhibitors.

The HPTLC–ChE assays were carried out either according to our latest piezoelectric spaying procedure[21] (Derivatizer, CAMAG) or immersion procedure using the modified Marston's method[8,55,56]. Briefly, piezoelectric spaying procedure[21]: the planar chromatogram was wetted via spraying Tris-HCl buffer. Then, the enzyme solution was sprayed and the plate was incubated in a humid plastic box, followed by spraying of substrate-chromogenic solution and drying. While in immersion procedure planar chromatogram was directly immersed into enzyme and after incubation step followed by immersed into the substrate-chromogenic solution and drying. The ChE inhibitors were documented as white bands on a purple plate background at white light illumination. AChE hydrolyses the 1-naphthyl (substrate) to 1-naphthol reacting with Fast Blue B salt (chromogenic agent) to produce a purple plate background.[56]

Application: The HPTLC–AChE was not only used for finding AChE inhibitors as anti-Alzheimer's disease agents in medicinal plants[21,57,58], but also for detection of organophosphate and carbamate insecticides[59-62] and chemical warfare agents[63].

In current research: HPTLC–ChE was used for ChE inhibitory screening of Danshen[9] and *P. harmala* seed[21], *Lamiaceae* and apple peel[35] extracts, and food contact materials (FCMs) migrants and extract[64] as well as equivalency inhibitory calculation of active compounds of *P. harmala* seed extract refereed to applied and developed PHY[65].

1.3.HPTLC–(HR)MS

The first step of structural elucidation is recording the mass spectra of the unidentified bioactive compounds *in situ* the planar chromatogram. Thus, using the TLC-MS interface allowed the usage of HRMS besides the full potential of HPTLC separation and accelerated the workflow to gain structural information directly from favorite zone.[9,14,21,25] Generally, transferring methods are divided into two branches: elution-based and desorption-based techniques. The elution-based techniques uses a tight elution head and a solvent follow to transfer the zone of interest *in situ* planar chromatogram to MS spectra.[1]

Application in current research: TLC-MS interface coupled with the heated electrospray ionization (HESI) source connected to a hybrid quadrupole-orbitrap mass spectrometer was used for MS measurements of all favorite active compounds such as tanshinones and phenolics in Danshen[9], alkaloids in *P. harmala* seed[21] and hydroxy pentacyclic triterpen acids in *Lamiaceae* and apple peel[35] extracts.

1.4.Direct workflow from HPTLC to quantitative NMR spectroscopy

Structural confirmation and quantification of bioactive compounds are the ultimate targets after (HP)TLC–EDA. NMR spectra of bioactive compounds provide the structural information to confirm the chemical structure and quantify the analyte by quantitative NMR (qNMR) spectroscopy.[9,20,66] The sensitivity gap was the main obstacle to achieve a direct workflow to provide the active compounds *in situ* planar chromatogram in detectable range of NMR spectroscopy.[9,35] Using column based separation[17,57,67] or TLC elution head-based interface[20,66,68] for NMR spectroscopy sample preparation were inef-

ficient procedures because of time-consuming steps including fractionation/stamping, evaporation and high consumption of solvent and HPTLC plates.[17,20,57,66-68]

NMR spectroscopy is an orthogonal technique for simultaneous identification and quantification of several compounds. In comparison to chromatographic methods, qNMR spectroscopy analysis is based on the identification of resolved signals of the analyets in the mixture rather than achieving resolution of individual components.[69] In addition, qNMR spectroscopy quantifies all the analytes of several spectra, just with a single reference compound.[70] In NMR spectroscopy the peak intensity is directly proportional to the number of nuclei, in the NMR active volume, generating such a signal which is linearly related to the analyte amount in solution (absolute concentration).[70-73] qNMR spectroscopy can be fulfilled by relative and absolute quantitation methods. Relative mode provides molar ratio between two compounds[9] while the absolute quantitation measures the actual amount of an analyte[70,72]. Absolute mode requires an internal or external reference compound to calibrate the NMR signal. In the internal standard method, a weighed amount of a reference standard (or a measured volume of a known concentration solution) is added into a fix volume of sample and the intensity of its signal is used for quantification of all the other species in the same spectrum. The main drawback of internal standard is the sample contamination with the added standard, on the contrary, the external methods utilize a reference compound in a separate solution and its NMR signal intensity is used to quantify several compounds in different spectra.[72] Among external methods one of the most innovative is the PUlse Length-based CONcentration determination (PULCON) method, that correlates the NMR signal intensity of a reference standard to those ones of analytes in different spectra, after the 90° pulse correction on each sample tube, according to the principle of reciprocity.[74,75]

The former studies in the field of planar chromatography and qNMR spectroscopy mostly focused on comparison of two methods, and qNMR spectroscopy measurements were performed on crude dried extract.[69,76-79] In some cases, TLC was used after/between several column chromatography steps to select or purify the best fraction containing favorite compounds for qNMR spectroscopy via internal standard[80] or calibration curve[81]. In order to record 1D and 2D NMR spectra of two pure bioactive isomers, a flash chromatographic fraction was purified five times by semipreparative HPLC-DAD.[82] Isolation of bioactive compounds *in situ* planar chromatogram (high number of plates) via

TLC-MS interface coupled with a HPLC pump was used for NMR spectroscopy sample preparation to confirm the structure[20,66] or qNMR (PULCON)[68,83].

Application: Using the high field magnets and cryoprobes improved the sensitivity of NMR spectrometers, lowering down the limit of detection (LOD) to the µM range to measure low amount analytes even in complex biological matrices.[84] The ^{1}H-qNMR was used in quantification of several metabolites of drugs and plants.[2,70,85-88]

In current research: The direct PLC/HPTLC-qNMR workflows were established in this research and used for quantification of challenging bioactive structural isomers.[9,35] Two structural isomers of tanshinones,1,2-dihydrotanshinone I (1,2-DHTI) and methylenetanshinquinone (MTQ)[9] and another two hydroxy pentacyclic triterpen acids (ursolic and oleanolic acids)[35] were isolated via a one-step PLC/HPTLC development and resulting fraction, dissolved in deuterated methanol, was measured via relative qNMR[9] or PULCON[35] (Fig. 9).

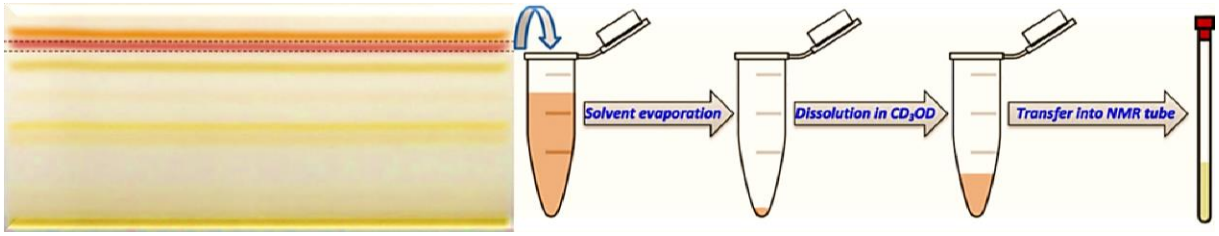

Figure 9. PLC isolation of an unidentified active zone *in situ* the planar chromatogram of Danshen extract for NMR spectroscopy.

1.5.Quantitative planar chromatographic–effect-directed analysis

First step to perform a quantitative analysis after a biological/biochemical assays is measuring and quantifying a resulting autogram via scanning densitometer (scanner). It is equipped with the continuous light sources a deuterium lamp (190 to 450 nm) and a tungsten lamp (370 to 800 nm) as well as a discrete light source a mercury vapor lamp (several individual wavelengths). Densitometry can be performed in absorbance or fluorescence modes. In absorbance measurement, the reflected light from the plate represents the baseline signal, which is lowered when the light beam hits an absorbing zone of the track, and then electronically inverted signal is presented as a positive peak in the densitogram. The resulting densitogram can be integrated and quantitatively evaluated.

Fluorescence measurement is performed when a substance can be excited to fluoresce by UV light. It needs a bandpass or cutoff filter between the plate and the detector to efficiently eliminate the UV light used for excitation. The reflected light from plate background is blocked by filter (zero signal, baseline) and emission light from fluorescing zone with a longer wavelength can pass the filter and reaches the photomultiplier detector (no need of inversion).

The relation between the measured signal and the amount of substance in a zone is either linear like fluorescence mode or nonlinear for absorption mode (Kubelka-Munk equation). In absorption measurement, signal increases with increasing substance amount and in most cases, data are best fitted to polynomial functions.

Two major categories were evident to indicate the active zones in resulting chromatogram after performing a bioassay (bioautogram). First, the bioactive substances are detected as fluorescent zones and densitometric measurement was performed at UV range, e.g. pYES.[89,90] Second, bioactive substances were indicated as white zones in a stained background such as *B. subtilis*[6], AChE/BChE[21], α-, β-glucosidase[13], tyrosinase[14] and α-amylase[15] (bio)assays.

Application in current research: Densitometric measurement of the autogram was performed at the selected wavelength using an inverse scan. At the mercy of no inversion of fluorescence measurement and adjustment of no cutoff filter, the reflected light from white zone was recorded as positive densitogram for equivalency calculation of ChE inhibitors in *P. harmala* seed extract.[21,65] In order to estimate the efficiency of HPTLC isolation, amount of ursolic and oleanolic acids was densitometicaly measured in the isolated samples and the crude extracts at absorption mode after a pre- and post-chromatographic derivatization HPTLC.[35]

1.6.Equivalency calculation

Quantitative measurement is relative, meaning that a response generated by unknown amount of a substance needs to be compared with those of known amount of that (calibration curve). In case of unknown or unidentified enzyme inhibitors discovered in a complex sample, an external standard calibration cannot be performed and their inhibition potency needs to be estimated by alternative means as equivalency calculation refer

to a well-known active compound known as positive control. According to the classical procedure, the reference compound and sample containing unknown or unidentified enzyme inhibitors have to be chromatographed on the same plate. However, the integration of a reference compound relevant to an enzymatic assay causes a challenging method development for new samples due to the different chromatographic interactions with mobile/stationary phases. Then, application of different amount of positive control (as a pattern after development) is a fast alternative to perform equivalency calculation.

Application: The equivalency calculation has been reported in reference to a well-known active compounds such as ciprofloxacin or marbofloxacin[34] as reference antibiotics in *B. subtilis* bioassays, alkaloids like (±)-huperzine-A[91] and galantamine[57], or carbamates like PHY[58] in AChE/BChE assays, kojic acid[14,47] in tyrosinase assays and ascorbic[92,93]/gallic acid[92] in 2,2-diphenyl-1-picrylhydrazyl radical scavenging assays.

In current research: Two different modes of equivalency calculation, referring to a potent inhibitor that was either applied or also developed were investigated, validated and compared, exemplarily on the AChE/BChE inhibition of *P. harmala* seed extract. Three potent inhibitors, PHY, rivastigmine and piperine, were evaluated with regard to their hR_F value, band shape and inhibition brightness against the plate background and the well-matched one (PHY) considered for equivalency calculation. Finally the potency of AChE and BChE inhibitory of each active band of *P. harmala* seed extract was reported as ng of PHY.[65]

1.7.Medicinal plant extracts

1.7.1. *Salvia miltiorrhiza* Bunge root

Salvia miltiorrhiza Bunge root (Danshen) as one of the most commonly used traditional medicines. It possesses several curative properties that have been applied to treat different diseases such as Alzheimer's, cerebrovascular, coronary heart disease and skin lesions.[94] A variety of Danshen preparations and formulations are on the market, *i.e.* dripping pills, tablets, injections, capsules, syrups and sprays.[95]

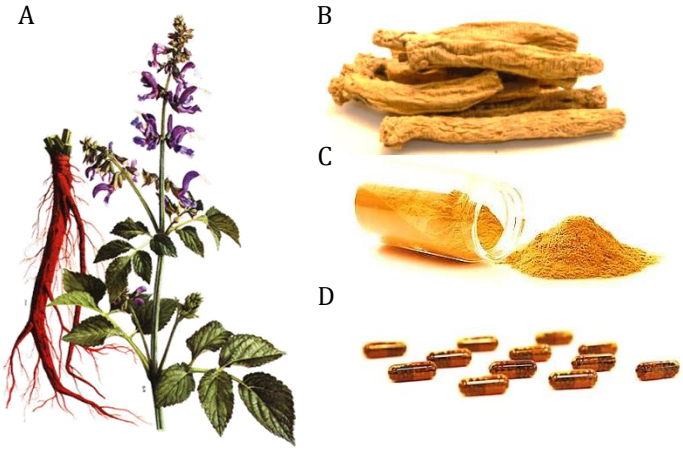

Figure 10. *Salvia miltiorrhiza* (A), dried root (B), root powder (C) and Danshen capsules (D).

Danshen's well-known bioactive components include two major groups, hydrosoluble phenolics (phenolic acids) and lipophilic diterpenoid quinones (tanshinones). So far, 37 phenolics and 55 tanshinones have been reported for Danshen.[96] In order to obtain the chemical profiles of the main phenolics and tanshinones, several separation methods like HPLC-MS[97-99], HPLC-UV[99-101], countercurrent chromatography[102], non-aqueous capillary electrophoresis[103] and (HP)TLC[5,34,100,104,105] were employed.

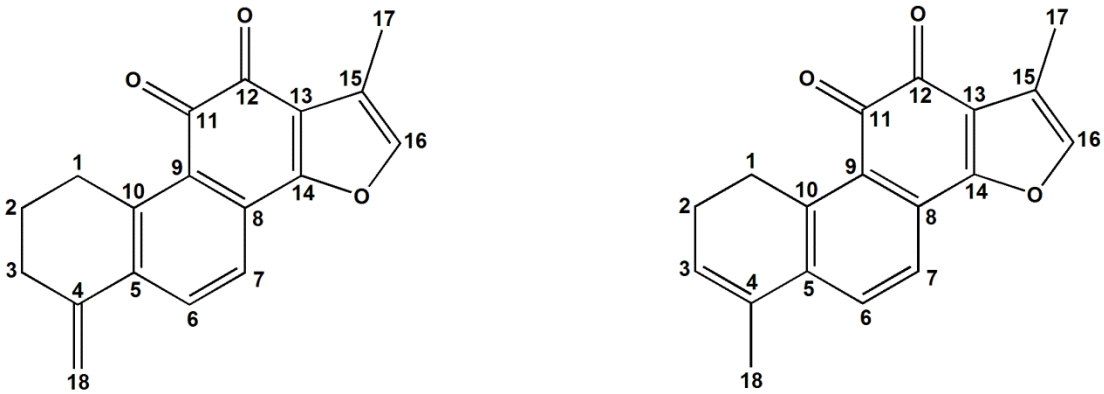

Figure 11. Structures of two tanshinones identified and relatively quantified via qNMR.

In current research: This study aimed at developing a streamlined, yet comprehensive bioanalytical method from screening to structures. Therefore, HPTLC-(bio)assay-HRMS of the polar and the nonpolar Danshen extracts was followed by a fast scale-up to PLC

isolation for ^{1}H-NMR spectroscopy to identify and relatively quantify the two coeluted tanshinones (MTQ and 1,2-DHTI) in a multipotent unidentified zone.[9]

1.7.2. *Peganum harmala* seed

P. harmala (Zygophyllaceae) is known as Espand or Syrian Rue, with pharmacological effects including anticancer, gastrointestinal and antimicrobial activities.[106] The *P. harmala* seed extract contains vasicine and vasicinone (quinazoline alkaloids) as well as harmine, harmaline, harman and harmalol (β-carbolines)[106], showed inhibition via TLC-AChE[57,58]. (Fig. 12 and 13)

In current research: The main ChE inhibition zones of *P. harmala* seed extract, detected without any tailing and diffusion, were equivalently calculated to PHY as a well-known ChE-inhibitor, to demonstrate the quantitative capability and performance of the newly developed automated piezoelectric spraying AChE/BChE workflow.

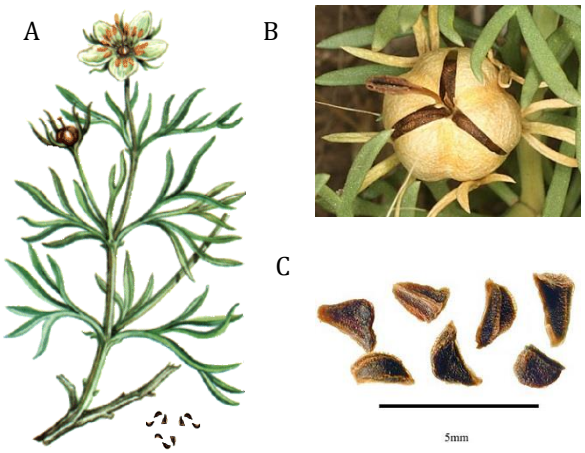

Figure 12. *P. harmala* (A) as well as its fruit (B) and seeds (C).

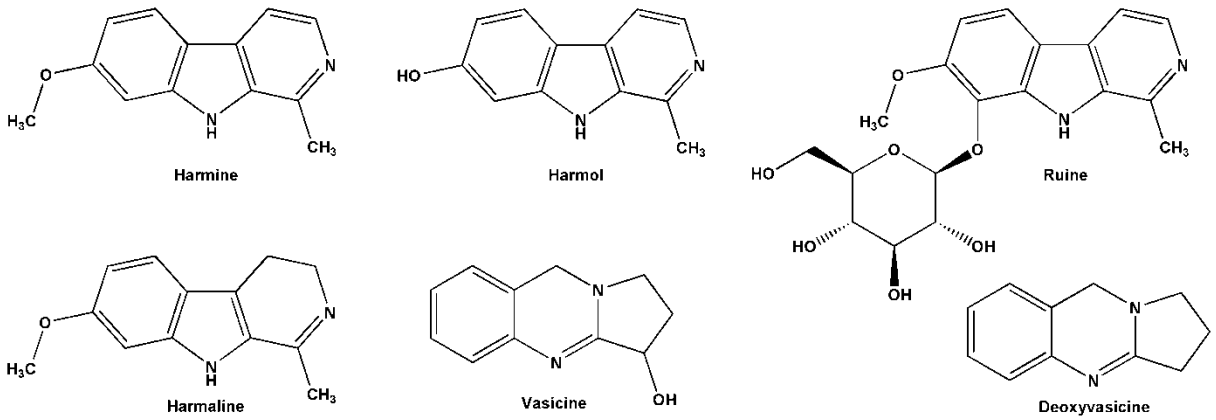

Figure 13. Main ChE inhibitors of *P. harmala* seed extract, found via HPTLC–AChE/BChE

1.7.3. *Lamiaceae* leaves, *Malus domestica* fruit peels

Salvia officinalis, *Thymus vulgaris* and *Origanum vulgare* leaves (*Lamiaceae*), red and green apple peel (*Malus domestica*) extracts contain several structural isomers like ursolic, oleanolic, betulinic acids (all $C_{30}H_{48}O_3$), corosolic, maslinic acids (both $C_{30}H_{48}O_4$), as well as thymol and carvacrol (both $C_{10}H_{14}O$).

In current research: the mentioned extracts were selected as case studies to find a coeluted bioactive zone contains two or more compounds. After bioprofiling, the ursolic and oleanolic acids, as a coeluted active zone, were chosen to be isolated via HPTLC followed by an already set up qNMR spectroscopy (PULCON). Finally, the results of PULCON were compared with those obtained from pre- and post-chromatographic derivatization HPTLC.

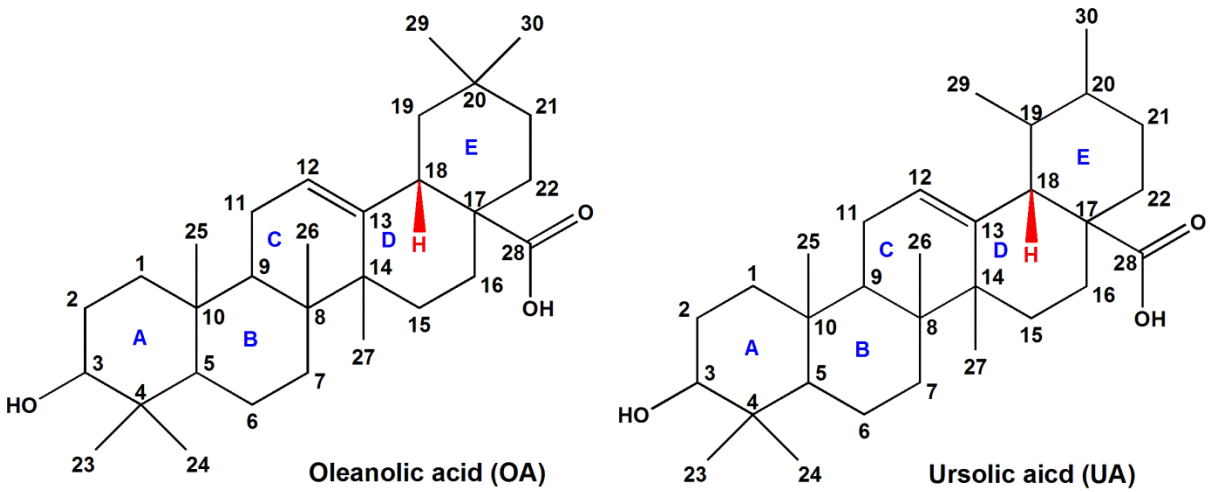

Figure 14. Structures of ursolic and oleanolic acid that were quantified according to their significant 1H-18 signals in ^{1}H-NMR spectra.

1.8.Food contact materials, articles and chemicals

Food contact materials (FCMs) are all materials and articles come into contact with food and beverages during its production, processing, storage, transporting, preparation and serving such as packaging materials, containers, kitchenware, cutlery and dishes as well as water bottles.[107,108] FCMs can be made from different materials including metal, plastics, rubber, and paper.[109] Chemicals in form of nanoparticles so-called food contact chemicals (FCCs) can migrate from food contact articles into foodstuffs, and thus be ingested. FCCs categorized as intentionally added substances (IAS) such as monomers,

additives, and catalysts[110] or non-intentionally added substances (NIAS) such as impurities in the starting materials, and newly formed substances such as degradation products, reaction by-products, or various contaminants from the recycling process[111,112]. These substances should not change the composition of the food in an unacceptable way or interfere with the organoleptic and sensory aspects of the food, and more important should not hazard the safety of the packed food.[107,108,113] The risk assessment strategy for IAS is clear and their safety is currently ensured as rarely problematic. However, risk assessment of NIAS as a significant part of the overall migrate is much more difficult to ascertain because many NIAS remain completely unknown and their chemical identification and toxicological testing is highly time and resource-consuming and thus the toxicological evaluation of these single substances cannot be performed.[114] The Threshold of Toxicological Concern (TTC) concept has been developed as a pragmatic and convenient tool for risk assessment of NIAS and other chemicals with limited toxicological data.[115-119] The TTC concept assesses if intake is below an accepted threshold of no concern, defined by assigning a Cramer class based on the chemical structure.[120]

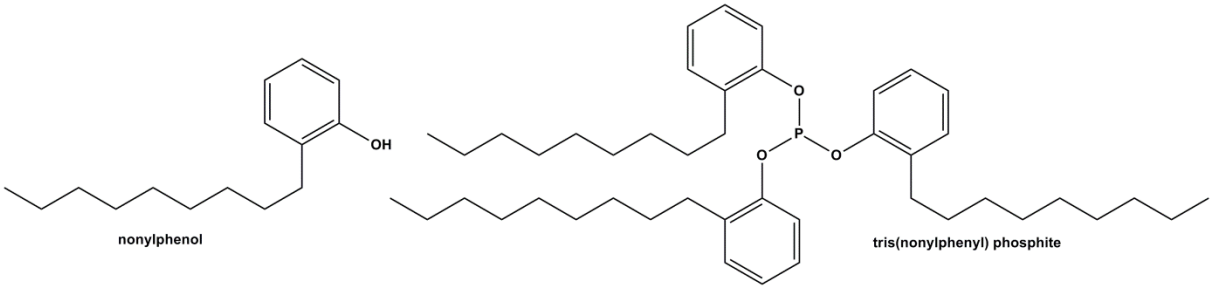

Figure 15. Two chemical packaging which were tested via HPTLC–S9–AChE.

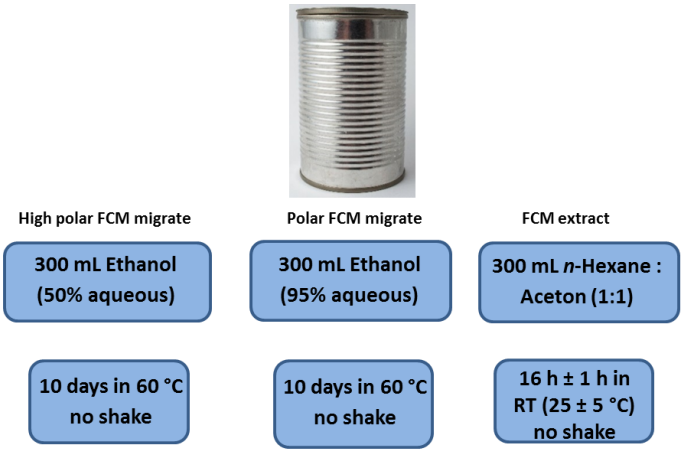

Figure 16. Procedures of FCM migrates and extract preparation.

In current research: The new HPTLC–S9–AChE workflow, after on-plate metabolization and separation, the AChE/substrate-chromogenic reagent solutions were sprayed piezoelectrically, resulting a homogeneous plate background. The LODs of six chemicals, including physostigmine, chlorpyrifos, quinalphos and parathion as well as tris(nonylphenyl) phosphite and nonylphenol were compared between a fluorometric microtiter plate assay and our new HPTLC–S9–AChE workflow. The direct toxicity assessment of FCMs via their respective TTCs was achieved by a 200-fold enrichment of the two migrates and one extract of a white polyurethane coated can, by solvent evaporation during spray-on area application.

1.9.Aim of research

The current research mainly focused on quantification of bioactive compounds *in situ* autogram via equivalency calculation refer to an applied/developed well-known active compound or *ex situ* planar chromatogram via relative/absolute qNMR spectroscopy.

Quantification of unidentified or unknown bioactive compounds is challenging. All information about polarity, functional groups and sum formula of bioactive compounds can be obtained via hR_F value, derivatization, HRMS, respectively, but for quantification as a relative procedure the expensive external standards, sometimes not provided, are needed. In this research, two alternative procedures, independent of bioactive compounds reference standards, were designed, developed, validated and applied on quantification of bioactive compounds found in plant extracts.

In addition, an automated piezoelectric spraying was set up to be more close to the standardization of HPTLC–EDA procedure to provide more reproducible results.

Another alternative for quantification of bioactive compounds is relative or absolute qNMR spectroscopy using an external standard maleic acid. The relative qNMR spectroscopy can be done as a molar ratio after confirmation of the structure among two co-eluted compounds which appear at the same hR_F value as one band in planar chromatogram. For performing of an absolute qNMR spectroscopy of bioactive compounds found via HPTLC–EDA, a traceable sample preparation was needed, thus a direct workflow from bioprofiling to NMR spectroscopy was developed and the efficiency of planar isolation via HPTLC was needed to be determined.

1.10. References

1. G. Morlock and W. Schwack, *J. Chromatogr. A*, 2010, **1217**, 6600-6609.

2. T. K. T. Do, F. Hadji-Minaglou, S. Antoniotti and X. Fernandez, *J. Chromatogr. A*, 2014, **1325**, 256-260.

3. R. Vijayalakshmi and R. Ravindhran, *Asian J. Pharm. Clin. Res.*, 2012, **5**, 170-174.

4. G. E. Morlock, in *Reference Module in Chemistry, Molecular Sciences and Chemical Engineering*, Elsevier, Third edn., 2018, DOI: https://doi.org/10.1016/B978-0-12-409547-2.13959-9.

5. G. E. Morlock, in *Instrumental Methods for the Analysis and Identification of Bioactive Molecules*, American Chemical Society, 2014, vol. 1185, ch. 5, pp. 101-121.

6. M. Jamshidi-Aidji and G. E. Morlock, *J. Chromatogr. A*, 2015, **1420**, 110-118.

7. S. Krüger, L. Hüsken, R. Fornasari, I. Scainelli and G. Morlock, *J. Chromatogr. A*, 2017, **1529**, 93-106.

8. S. Hage and G. E. Morlock, *J. Chromatogr. A*, 2017, **1490**, 201-211.

9. E. Azadniya and G. E. Morlock, *J. Chromatogr. A*, 2018, **1533**, 180-192.

10. A. Schoenborn, P. Schmid, S. Braem, G. Reifferscheid, M. Ohlig and S. Buchinger, *J. Chromatogr. A*, 2017, **1530**, 185-191.

11. L. Stütz, S. C. Weiss, W. Schulz, W. Schwack and R. Winzenbacher, *J. Chromatogr. A*, 2017, **1524**, 273-282.

12. I. A. Ramallo, S. A. Zacchino and R. L. Furlan, *Phytochem. Anal.*, 2006, **17**, 15-19.

13. C. A. Simões-Pires, B. Hmicha, A. Marston and K. Hostettmann, *Phytochem. Anal.*, 2009, **20**, 511-515.

14. M. Jamshidi-Aidji and G. E. Morlock, *Anal. Chem.*, 2018, **90**, 14260-14268.

15. S. Agatonovic-Kustrin and D. W. Morton, *J. Chromatogr. A*, 2017, **1530**, 197-203.

16. G. W. Jóźwiak, B. Majer-Dziedzic, W. Jesionek, W. Zieliński and M. Waksmundzka-Hajnos, *J. Liq. Chromatogr. Relat. Technol.*, 2016, **39**, 281-285.

17. E. F. Queiroz, J.-L. Wolfender, K. Atindehou, D. Traore and K. Hostettmann, *J. Chromatogr. A*, 2002, **974**, 123-134.

18. Q. Favre-Godal, E. F. Queiroz and J.-L. Wolfender, *J. AOAC Int.*, 2013, **96**, 1175-1188.

19. V. Danciu, A. Hosu and C. Cimpoiu, *J. Planar Chromatogr.-Mod. TLC*, 2016, **29**, 306-309.

20. E. M. Grzelak, C. Hwang, G. Cai, J.-W. Nam, M. P. Choules, W. Gao, D. C. Lankin, J. B. McAlpine, S. G. Mulugeta and J. G. Napolitano, *ACS Infect. Dis.*, 2016, **2**, 294-301.

21. E. Azadniya and G. E. Morlock, *J. Chromatogr. A*, 2019, **1602**, 458–466.

22. V. Baumgartner, Dissertation (Dr. rer. nat.), University Hohenheim, 2013.

23. A. A. Bulich, presented in part at the Aquatic Toxicology: Proceedings of the Second Annual Symposium on Aquatic Toxicology, 1979.

24. P. Ristivojević and G. E. Morlock, *Food Chem.*, 2018, **260**, 344-353.

25. M. Jamshidi-Aidji, I. Dimkić, P. Ristivojević, S. Stanković and G. E. Morlock, *J. Chromatogr. A*, 2019, 460-466.

26. A. Seigel, B. Milz and B. Spangenberg, *J. Planar Chromatogr.-Mod. TLC*, 2013, **26**, 119-124.

27. W. Schulz, W. Seitz, S. Weiss, W. Weber, M. Böhm and D. Flottmann, *J. Planar Chromatogr.-Mod. TLC*, 2008, **21**, 427-430.

28. J. van Dijl and M. Hecker, *Microb. Cell Fact.*, 2013, **12**, 3.

29. N. K. Tam, N. Q. Uyen, H. A. Hong, L. H. Duc, T. T. Hoa, C. R. Serra, A. O. Henriques and S. M. Cutting, *J. Bacteriol.*, 2006, **188**, 2692-2700.

30. A. Marston, *J. Chromatogr. A*, 2011, **1218**, 2676-2683.

31. I. Choma, *J. Liq. Chromatogr. Relat. Technol.*, 2006, **29**, 2083-2093.

32. A. Ramírez, R. Gutiérrez, G. Díaz, C. González, N. Pérez, S. Vega and M. Noa, *J. Chromatogr. B*, 2003, **784**, 315-322.

33. W. Jesionek, Á. M. Móricz, Á. Alberti, P. G. Ott, B. Kocsis, G. Horváth and I. M. Choma, *J. AOAC Int.*, 2015, **98**, 1013-1020.

34. M. Jamshidi-Aidji and G. E. Morlock, *Anal. Chem.*, 2016, **88**, 10979-10986.

35. E. Azadniya, L. Goldoni, T. Bandiera and E. G. Morlock, *in submission*

36. A. Slominski, D. J. Tobin, S. Shibahara and J. Wortsman, *Physiol. Rev.*, 2004, **84**, 1155-1228.

37. M. Loizzo, R. Tundis and F. Menichini, *Compr. Rev. Food Sci. F.*, 2012, **11**, 378-398.

38. J. Taibon, A. Ankli, S. Schwaiger, C. Magnenat, V.-I. Boka, C. Simões-Pires, N. Aligiannis, M. Cuendet, A.-L. Skaltsounis and E. Reich, *Planta Med.*, 2015, **81**, 1198-1204.

39. F. Solano, S. Briganti, M. Picardo and G. Ghanem, *Pigment Cell Res.*, 2006, **19**, 550-571.

40. D. Krickeberg, S. Hage and G. E. Morlock, Bachelor thesis, Justus Liebig University Giessen, 2017.

41. J. M. Pankovich and K. Jimbow, *Biochem. J.*, 1991, **280**, 721-725.

42. W. T. Ismaya, H. J. Rozeboom, A. Weijn, J. J. Mes, F. Fusetti, H. J. Wichers and B. W. Dijkstra, *Biochemistry*, 2011, **50**, 5477-5486.

43. C. A. Ramsden and P. A. Riley, *Bioorg. Med. Chem.*, 2014, **22**, 2388-2395.

44. C. J. Vavricka, B. M. Christensen and J. Li, *Protein Cell*, 2010, **1**, 830-841.

45. S. Wangthong, I. Tonsiripakdee, T. Monhaphol, R. Nonthabenjawan and S. P. Wanichwecharungruang, *Biomed. Chromatogr.*, 2007, **21**, 94-100.

46. K.-D. Hsu, Y.-H. Chan, H.-J. Chen, S.-P. Lin and K.-C. Cheng, *Sci. Rep.*, 2018, **8**, 401.

47. J. Zhou, Q. Tang, T. Wu and Z. Cheng, *Phytochem. Anal.*, 2017, **28**, 115-124.

48. M. B. Colovic, D. Z. Krstic, T. D. Lazarevic-Pasti, A. M. Bondzic and V. M. Vasic, *Curr. Neuropharmacol.*, 2013, **11**, 315-335.

49. M. G. Lionetto, R. Caricato, A. Calisi, M. E. Giordano and T. Schettino, *BioMed Res. Int.*, 2013, **Article ID 321213**.

50. E. Auf der Heide, Cholinesterase inhibitors; including pesticides and chemical warfare nerve agents, www.atsdr.cdc.gov/csem/cholinesterase/docs/cholinesterase.pdf.

51. J. Massoulié, L. Pezzementi, S. Bon, E. Krejci and F.-M. Vallette, *Prog. Neurobiol.*, 1993, **41**, 31-91.

52. T. Soderberg, *Organic Chemistry with a Biological Emphasis Volume II*, University of Minnesota Morris Digital Well, 2019.

53. M. R. Deschenes, *Curr. Opin. Physiology*, 2019, **10**, 10-16.

54. N. Waiskopf and H. Soreq, in *Handbook of Toxicology of Chemical Warfare Agents*, Elsevier, 2015, pp. 761-778.

55. R. Akkad and W. Schwack, *J. Chromatogr. B*, 2010, **878**, 1337-1345.

56. A. Marston, J. Kissling and K. Hostettmann, *Phytochem. Anal.*, 2002, **13**, 51-54.

57. X.-y. Zheng, Z.-j. Zhang, G.-x. Chou, T. Wu, X.-m. Cheng, C.-h. Wang and Z.-t. Wang, *Arch. Pharmacal. Res.*, 2009, **32**, 1245-1251.

58. H. R. Adhami, H. Farsam and L. Krenn, *Phytother. Res.*, 2011, **25**, 1148-1152.

59. C. Mendoza, P. Wales, H. McLeod and W. McKinley, *Analyst*, 1968, **93**, 34-38.

60. C. Weins and H. Jork, *J. Chromatogr. A*, 1996, **750**, 403-407.

61. R. Akkad and W. Schwack, *J. Chromatogr. A*, 2011, **1218**, 2775-2784.

62. R. Akkad and W. Schwack, *J. AOAC Int.*, 2012, **95**, 1371-1377.

63. Z. Witkiewicz, M. Mazurek and J. Szulc, *J. Chromatogr. A*, 1990, **503**, 293-357.

64. J. Mollergues, E. Azadniya, T. Stroheker, K. Billerbeck and G. E. Morlock, *in submission*.

65. E. Azadniya and G. E. Morlock, *Anal. Methods*, 2019, DOI: https://doi.org/10.1039/C9AY01465A.

66. H. R. Adhami, U. Scherer, H. Kaehlig, T. Hettich, G. Schlotterbeck, E. Reich and L. Krenn, *Phytochem. Anal.*, 2013, **24**, 395-400.

67. L. Gu, T. Wu and Z. Wang, *LWT-Food Sci. Technol.*, 2009, **42**, 131-136.

68. A. Gössi, U. Scherer and G. Schlotterbeck, *CHIMIA Int. J. Chem.*, 2012, **66**, 347-349.

69. A. Choudhary, R. J. Sharma and I. P. Singh, *J. Essent. Oil-Bear. Plants*, 2016, **19**, 20-31.

70. S. K. Bharti and R. Roy, *Trends Anal. Chem.*, 2012, **35**, 5-26.

71. Y. B. Monakhova, M. Kohl-Himmelseher, T. Kuballa and D. W. Lachenmeier, *J. Pharm. Biomed. Anal.*, 2014, **100**, 381-386.

72. C. H. Cullen, G. J. Ray and C. M. Szabo, *Magn. Reson. Chem.*, 2013, **51**, 705-713.

73. R. Watanabe, C. Sugai, T. Yamazaki, R. Matsushima, H. Uchida, M. Matsumiya, A. Takatsu and T. Suzuki, *Toxins*, 2016, **8**, 294.

74. L. Dreier and G. Wider, *Magn. Reson. Chem.*, 2006, **44**, 206-212.

75. G. Wider and L. Dreier, *JACS*, 2006, **128**, 2571-2576.

76. N. Q. Liu, Y. H. Choi, R. Verpoorte and F. van der Kooy, *Phytochem. Anal.*, 2010, **21**, 451-456.

77. I. Saraf, A. Choudhary, R. J. Sharma, K. Dandi, K. J. Marsh, W. J. Foley and I. P. Singh, *Nat. Prod. Commun.*, 2015, **10**, 379-382.

78. K. Kuchta, J. Ortwein, L. Hennig and H. W. Rauwald, *Fitoterapia*, 2014, **96**, 8-17.

79. K. Kuchta, R. Volk and H. Rauwald, *Pharmazie*, 2013, **68**, 534-540.

80. T.-Y. Wu, Y.-C. Du, Y.-M. Hsu, C.-Y. Lu, A. N. B. Singab, M. El-Shazly, T.-L. Hwang, W.-Y. Lin, K.-H. Lai and M.-C. Lu, *Food Res. Int.*, 2013, **51**, 23-31.

81. K. Ioannidis, E. Melliou, P. Alizoti and P. Magiatis, *J. Sci. Food Agric.*, 2017, **97**, 1708-1716.

82. A. g. M. Móricz, P. t. G. Ott, T. T. Häbe, A. Darcsi, A. Böszörményi, Á. Alberti, D. n. Krüzselyi, P. t. Csontos, S. Béni and G. E. Morlock, *Anal. Chem.*, 2016, **88**, 8202-8209.

83. G. Schlotterbeck, *Camag bibliography service (CBS)*, 2013, **111**, 2-4.

84. L. Goldoni, T. Beringhelli, W. Rocchia, N. Realini and D. Piomelli, *Anal. biochem.*, 2016, **501**, 26-34.

85. J. K. H. Gor and H. K. Jain, *Asian J. Biomed. Pharm.*, 2013, **3**, 56-69.

86. V. Exarchou, A. Troganis, I. P. Gerothanassis, M. Tsimidou and D. Boskou, *J. Agric. Food Chem.*, 2001, **49**, 2-8.

87. H. Dai, C. Xiao, H. Liu and H. Tang, *J. Proteome Res.*, 2010, **9**, 1460-1475.

88. A. Gössi, U. Scherer and G. Schtotterbeck, *CHIMIA-Int. J. Chem.*, 2012, **66**, 347.

89. I. Klingelhöfer and G. E. Morlock, *Anal. Chem.*, 2015, **87**, 11098-11104.

90. I. Klingelhöfer and G. E. Morlock, *J. Chromatogr. A*, 2014, **1360**, 288-295.

91. S. Di Giovanni, A. Borloz, A. Urbain, A. Marston, K. Hostettmann, P.-A. Carrupt and M. Reist, *Eur. J. Pharm. Sci.*, 2008, **33**, 109-119.

92. O. N. Pozharitskaya, S. A. Ivanova, A. N. Shikov and V. G. Makarov, *J. Sep. Sci.*, 2007, **30**, 1250-1254.

93. O. N. Pozharitskaya, S. A. Ivanova, A. N. Shikov and V. G. Makarov, *Phytochem. Anal.*, 2008, **19**, 236-243.

94. S. Chun-Yan, M. Qian-Liang, K. Rahman, H. Ting and Q. Lu-Ping, *Chin. J. Nat. Med.*, 2015, **13**, 163-182.

95. L. Zhou, Z. Zuo and M. S. S. Chow, *J. Clin. Pharmacol.*, 2005, **45**, 1345-1359.

96. H. Pang, L. Wu, Y. Tang, G. Zhou, C. Qu and J.-a. Duan, *Molecules*, 2016, **21**, 51-79.

97. M. Yang, A. Liu, S. Guan, J. Sun, M. Xu and D. Guo, *Rapid Commun. Mass Spectrom.*, 2006, **20**, 1266-1280.

98. S. Yang, X. Wu, W. Rui, J. Guo and Y. Feng, *Acta Chromatogr.*, 2015, **27**, 711-728.

99. M.-J. Don, H.-C. Ko, C.-W. Yang and Y.-L. Lin, *J. Food Drug Anal.*, 2006, **14**, 254-259.

100. P. Hu, G.-A. Luo, Z. Zhao and Z.-H. Jiang, *Chem. Pharm. Bull.*, 2005, **53**, 481-486.

101. G. Zeng, J. Liu, L. Wang, Q. Xu, H. Xiao and X. Liang, *J. Chromatogr. Sci.*, 2006, **44**, 591-595.

102. H.-B. Li and F. Chen, *J. Chromatogr. A*, 2001, **925**, 109-114.

103. M. Gu, S. Zhang, Z. Su, Y. Chen and F. Ouyang, *J. Chromatogr. A*, 2004, **1057**, 133-140.

104. J. Yang, L.-l. Choi, D.-q. Li, F.-q. Yang, L.-j. Zeng, J. Zhao and S.-p. Li, *J. Planar Chromatogr.-Mod. TLC*, 2011, **24**, 257-263.

105. Z. Yang, X. Zhang, D. Duan, Z. Song, M. Yang and S. Li, *J. Sep. Sci.*, 2009, **32**, 3257-3259.

106. M. C. Niroumand, M. H. Farzaei and G. Amin, *J.Tradit. Chin. Med.*, 2015, **35**, 104-109.

107. EFSA, Food contact materials, http://www.efsa.europa.eu/en/topics/topic/food-contact-materials.

108. European Commission, Food Contact Materials https://ec.europa.eu/food/safety/chemical_safety/food_contact_materials_en.

109. European Commission, Public Consultation for the Study supporting the Evaluation of Food Contact Materials (FCM) legislation - (Regulation (EC) No 1935/2004), https://ec.europa.eu/info/law/better-regulation/initiatives/ares-2017-5809429/public-consultation_en.

110. J. Muncke, T. Backhaus, B. Geueke, M. V. Maffini, O. V. Martin, J. P. Myers, A. M. Soto, L. Trasande, X. Trier and M. Scheringer, *Environ. Health Perspect.*, 2017, **125**, 095001.

111. S. Koster, W. Leeman, E. Verheij, E. Dutman, L. van Stee, L. M. Nielsen, S. Ronsmans, H. Noteborn and L. Krul, *Food Chem. Toxicol.*, 2015, **80**, 163-181.

112. K. Grob, P. Camus, N. Gontard, H. Hoellinger, C. Joly, A. Macherey, D. Masset, F. Nesslany, J. Régnier and A. Riquet, *Food Control*, 2010, **21**, 763-769.

113. EU, Official Journal of the European Union, 2004, vol. L 338/4.

114. K. J. Groh and J. Muncke, *Compr. Rev. Food Sci. Food Saf.*, 2017, **16**, 1123-1150.

115. I. Munro, E. Kennepohl and R. Kroes, *Food Chem. Toxicol.*, 1999, **37**, 207-232.

116. R. Kroes, C. Galli, I. Munro, B. Schilter, L.-A. Tran, R. Walker and G. Würtzen, *Food Chem. Toxicol.*, 2000, **38**, 255-312.

117. R. Kroes, A. Renwick, M. Cheeseman, J. Kleiner, I. Mangelsdorf, A. Piersma, B. Schilter, J. Schlatter, F. Van Schothorst and J. Vos, *Food Chem. Toxicol.*, 2004, **42**, 65-83.

118. EFSA and WHO, *EFSA Supporting Publications*, 2016, **13**, 1006E.

119. U. S. FDA, https://www.ecfr.gov/cgi-bin/text-idx?SID=fff8b1d85cc676bb4a448a1f84d7b443&mc=true&node=se21.3.170_139&rgn=div8, 1995.

120. E. N. Pieke, K. Granby, B. Teste, J. Smedsgaard and G. Rivière, *Regul. Toxicol. Pharmacol.*, 2018, **97**, 134-143.

2. PUBLICATION 1

Bioprofiling of *Salvia miltiorrhiza* via planar chromatography linked to (bio)assays, high resolution mass spectrometry and nuclear magnetic resonance spectroscopy

Ebrahim Azadniya[a], Gertrud E. Morlock[a,*]

[a]*Chair of Food Science, Institute of Nutritional Science, Interdisciplinary Research Center (IFZ), Justus Liebig University Giessen, Heinrich-Buff-Ring 26-32, 35392, Giessen, Germany*

Published in

Journal of Chromatography A, 1533 (2018) 180–192

Received 28 August 2017, Received in revised form 4 December 2017, Accepted 5 December 2017, Available online 6 December 2017

Journal of Chromatography A, 1533 (2018) 180–192

Contents lists available at ScienceDirect

Journal of Chromatography A

journal homepage: www.elsevier.com/locate/chroma

Bioprofiling of *Salvia miltiorrhiza* via planar chromatography linked to (bio)assays, high resolution mass spectrometry and nuclear magnetic resonance spectroscopy

Ebrahim Azadniya, Gertrud E. Morlock*

Chair of Food Science, Institute of Nutritional Science, Interdisciplinary Research Center (IFZ), Justus Liebig University Giessen, Heinrich-Buff-Ring 26-32, 35392, Giessen, Germany

ARTICLE INFO

Article history:
Received 28 August 2017
Received in revised form 4 December 2017
Accepted 5 December 2017
Available online 6 December 2017

Keywords:
HPTLC
Direct bioautography (DB)
High resolution mass spectrometry (HRMS)
Preparative layer chromatography (PLC)
NMR
Salvia miltiorrhiza root (Danshen)

ABSTRACT

An affordable bioanalytical workflow supports the collection of data on active ingredients, required for the understanding of health-related food, superfood and traditional medicines. Targeted effect-directed responses of single compounds in a complex sample highlight this powerful bioanalytical hyphenation of planar chromatography with (bio)assays. Among many reports about biological properties of *Salvia miltiorrhiza* Bunge root (Danshen) and their analytical methods, the highly efficient direct bioautography (DB) workflow has not been considered so far. There was just one TLC-acetylcholinesterase (AChE) method with a poor zone resolution apart from our two HPTLC-DB studies, however, all methods were focused on the nonpolar extracts of Danshen (tanshinones) only. The current study on HPTLC-UV/Vis/FLD-(bio)assay-HRMS, followed by streamlined scale-up to preparative layer chromatography (PLC)-^{1}H-NMR, aimed at an even more streamlined, yet comprehensive bioanalytical workflow. It comprised effect-directed screening of both, its polar (containing phenolics) and nonpolar extracts (containing tanshinones) on the same HPTLC plate, the biochemical and biological profiling with four different (bio)assays and elucidation of structures of known and unidentified active compounds. The five AChE inhibitors, salvianolic acid B (SAB), lithiospermic acid (LSA) and rosmarinic acid (RA) as well as cryptotanshinone (CT) and 15,16-dihydrotanshinone I (DHTI) were confirmed, but also unidentified inhibitors were observed. In the polar extracts, SAB, LSA and RA exhibited free radical scavenging properties in the 2,2-diphenyl-1-picrylhydrazyl assay. CT, DHTI and some unidentified nonpolar compounds were found active against Gram-positive *Bacillus subtilis* and Gram-negative *Aliivibrio fischeri* (LOD 12 ng/band for CT, and 5 ng/band for DHTI). For the first time, the most multipotent unidentified active compound zone in the *B. subtilis*, *A. fischeri* and AChE fingerprints of the nonpolar Danshen extract was identified as co-eluted band of 1,2-dihydrotanshinone and methylenetanshinquinone in the ratio of 2:1.

1. Introduction

The unique hyphenation portfolio of high-performance thin-layer chromatography (HPTLC) with other complementary techniques makes HPTLC a versatile tool from bioactivity screening to structural characterization. All the relevant steps can be covered by the planar format, and thus, easily adapted and combined with (bio)assays, derivatization reagents and different detection techniques, *e.g.* UV/Vis/FLD/MS detection [1], nuclear magnetic resonance (NMR) [2–6] and attenuated total reflection Fourier transform infrared spectroscopies [7]. Exclusive features of HPTLC, like simple preparation of complex samples (keeping sample extracts as native as possible) and parallel matrix-robust analyses, allow an ideal direct comparison of the chromatographic fingerprints of complex sample extracts side by side. (HP)TLC is a cost-effective and time-saving method in the field of natural product analysis [8–12], and diverse publications in the field of bioautography [2,6,8–15] reported its benefits for chemical and biological profiling. Compared to contact and agar overlay bioautography, direct bioautography (DB) is a more streamlined workflow for bioprofiling, considering detectability, resolution and analysis time [12]. Different types of effect-directed analysis (EDA) combined with TLC/HPTLC have been employed, *e.g.*, to screen for

* Corresponding author.
E-mail addresses: Ebrahim.Azadniya@chemie.uni-giessen.de (E. Azadniya), Gertrud.Morlock@uni-giessen.de (G.E. Morlock).

https://doi.org/10.1016/j.chroma.2017.12.014
0021-9673/

enzyme inhibitors [4,15–17] as well as antibacterial [8,12], antifungal [6,14] and antioxidant compounds [10,11] in a wide range of different sample types.

With regard to structure elucidation of unidentified active compounds, the hyphenation between TLC/HPTLC and NMR has not been considered enough due to the notable difference between the sensitivity of TLC/HPTLC (mainly ng/band) and NMR spectroscopy (hundreds of μg to some mg per vial) [18]. The use of an elution head-based interface for the zone collection from the plate for NMR [2,4] led to consume a high number of HPTLC plates to reach the required analyte amount. Thus subsequent to EDA, other separation techniques were mostly used for NMR compound collection, such as column chromatography (CC) [19], high-performance liquid chromatography (HPLC) [11] and low-flow LC-NMR with microfractionation [6].

In this study, *Salvia miltiorrhiza* Bunge root (Danshen) was selected, as one of the most commonly used traditional medicines in China, Japan, USA and other western countries [20]. It possesses several curative properties that have been applied to treat different diseases such as Alzheimer's, Parkinson's, cerebrovascular and coronary heart diseases, besides cancer, renal deficiency, bone loss, hepatocirrhosis, gynecologic disorders and skin lesions like chilblains, psoriasis, and carbuncle [20]. A variety of Danshen preparations and formulations are on the market, *i.e.* dripping pills, tablets, injections, capsules, syrups and sprays [21]. Danshen's well-known bioactive components include two major groups, hydrosoluble phenolics (phenolic acids) and lipophilic diterpenoid quinones (tanshinones). So far, 37 phenolics and 55 tanshinones have been reported for Danshen [22]. In order to obtain the chemical profiles of the main phenolics and/or tanshinones, several separation methods like HPLC-MS [23–25], HPLC-UV [25–27], countercurrent chromatography (CCC) [28], non-aqueous capillary electrophoresis [29] and HPTLC [26,30] were employed. Among the many reports about biological properties of Danshen and their analytical methods [20], DB has not been considered so far. To the best of our knowledge, only one biochemical assay (falsely named bioautographic method) was combined with TLC in 2009 [16]. Thus, for the first time in our previous studies [31,32], DB of the nonpolar extract of Danshen was shown using Gram-negative *Aliivibrio fischeri* and Gram-positive *Bacillus subtilis* bacteria for bioquantification. The directly obtained bioactive responses of single compounds in the complex Danshen samples encouraged us to proceed with this streamlined hyphenation of chromatography and bioassays to demonstrate an even more powerful bioanalytical option in contrast to the *status quo*, *e.g.*, analytical and fractional workflows followed by microtiter plate assays. This study aimed at developing a streamlined, yet comprehensive bioanalytical method, *i.e.* the fastest approach from screening to structures. Therefore, biological and biochemical profiling by HPTLC-(bio)assay-HRMS of both, the polar and the nonpolar Danshen extracts on the same plate, was followed by characterization and identification of known and unidentified bioactive compounds by a fast scale-up to preparative layer chromatography (PLC)-^{1}H-NMR spectroscopy.

2. Material and methods

2.1. Chemicals and materials

Solvents were of analytical grade. toluene, ethyl acetate, chloroform, methanol, formic acid (96%), ammonia (25%), sulfuric acid (98%), petroleum ether (60–80 °C), cyclohexane, Müller–Hinton broth, anisaldehyde, protocatechuic aldehyde (PCAD) and 3-(4,5-dimethylthiazol-2-yl)-2,5-diphenyltetrazolium bromide (MTT, ≥98%) were purchased from Carl Roth (Karlsruhe, Germany). Fast Blue B salt, α-naphthyl acetate, acetylcholinesterase (AChE) lyophylisate (*Electrophorus electricus*, electric eel), hydrochloric acid (32%), sodium chloride, sodium monohydrogen phosphate, pentyl acetate, bovine serum albumin, tris(hydroxymethyl)aminomethane (TRIS) and 2,2-diphenyl-1-picrylhydrazyl (DPPH•) were provided from Sigma–Aldrich (Steinheim, Germany). *B. subtilis* spores (BGA, ATCC 6633), citric acid as well as HPTLC (0.2 mm layer thickness) and PLC (0.5 mm layer thickness) plates silica gel 60, also with F_{254}, were delivered by Merck (Darmstadt, Germany). Luminescent marine bacteria *A. fischeri* (DSM no. 5171) were obtained from the Leibniz Institute DSMZ, German Collection of Microorganisms and Cell Cultures (Braunschweig, Germany). Bidistilled water was prepared with a Destamat Bi 18 E (Heraeus, Hanau, Germany). The standard compounds of rosmarinic acid (RA), caffeic acid (CA), tanshinone I (TI), tanshinone IIA (TIIA), cryptotanshinone (CT), 15,16-dihydrotanshinone I (DHTI) were purchased from Sigma-Aldrich, whereas salvianolic acids A (SAA) and B (SAB) as well as lithospermic acid (LSA) were provided by Phytolab (Vestenbergsgreuth, Germany). NMR tubes (5 mm) were purchased from VWR (Darmstadt, Germany), and deuterated methanol (D ≥99.80%, H_2O <0.03%) from Eurisotop (Saarbrücken, Germany). Two Danshen samples were purchased from pharmacies (sample A, HerbaSinica Hilsdorf, Rednitzhembach, Germany, and sample B, meine-teemischung, Hofapotheke St. Afra, Augsburg, Germany).

2.2. Standard solutions and sample preparation

Methanolic solutions of DHTI (20 ng/μL), CT (100 ng/μL), TI (100 ng/μL), TIIA (100 ng/μL), SAB (1000 ng/μL), LSA (500 ng/μL), SAA (500 ng/μL), PCAD (500 ng/μL), CA (250 ng/μL) and RA (150 ng/μL) were prepared. For subsequent sample preparation, the following steps were in common for all the different extracts (Table S-1 with concentrations of Danshen in mg/mL solvent): 15 min in the ultrasonic bath at room temperature, centrifugation at 756 × *g* for 5 min and vortexing for 1 min.

2.2.1. Polar extracts 1–3

Milled Danshen (1 g each of samples A and B) were decocted on the hotplate stirrer with 50 mL distilled water at 70 °C for 30 min, followed by ultrasonication and centrifugation (20 mg/mL). For the first extract (1), the resulting supernatant was acidified with hydrochloric acid (32%, 12 M) to pH 3.0. After centrifugation, the supernatant was transferred into a 50-mL volumetric flask, filled up to the mark with bidistilled water and extracted 5 times with 5 mL ethyl acetate (40 mg/mL). After centrifugation, 15 mL of this upper ethyl acetate phase was concentrated to dryness under a nitrogen stream. The residue was dissolved in 2 mL ethyl acetate (300 mg/mL).

For the second extract (2), 10 mL aqueous supernatant of sample B (20 mg/mL) was acidified by adding 200 μL hydrochloric acid (32%). After centrifugation, 0.5 g sodium chloride was added (salting-out effect). After vortexing, this suspension was extracted with 4 mL of a 1:1 (*V*/*V*) mixture of ethyl acetate (extractant) and acetone (disperser solvent) as dispersive liquid-liquid extraction (DLLE), vortexed and centrifuged. The upper ethyl acetate phase was used (2 mL, 100 mg/mL). For the third extract (3) as a reference, milled Danshen (1 g) was extracted two times with 5 mL methanol (100 mg/mL), vortexed, ultrasonicated and centrifuged. The supernatant was used.

2.2.2. Non-polar extracts 4 and 5

The fourth extract (4) was extracted as for (3), but two times with 5 mL ethanol - pentyl acetate (4:1, *V*/*V*). A 5-mL aliquot of the supernatant (100 mg/mL) was evaporated to dryness. The residue

was dissolved in 2 mL methanol (250 mg/mL). The fifth extract (5) was extracted as for (3), but using ethanol (100 mg/mL).

2.3. HPTLC separation

Standard solutions and the five different extracts of Danshen were applied as 6-mm bands on a HPTLC plate silica gel 60 F_{254} using the Automatic TLC Sampler 4 (ATS 4, CAMAG). Depending on the (bio)assay, 0.5–5 μL/band were applied for standard solutions and 0.25–10 μL/band for sample extracts (Table S-1). The Automatic Development Chamber 2 (ADC 2, CAMAG) was saturated for 5 min with 10 mL mobile phase (MP). The separations were performed at a relative humidity of the air between 45 and 55% at 23–26 °C. The optimal separation was as follows (all ratios given as *V*/*V*): As first development, phenolics were separated with 10 mL toluene - chloroform - ethyl acetate - methanol - formic acid 4:6:8:1:1 (Table S-2, MP 6) up to 45 mm, followed by automatic drying for 3 min. After documentation of the chromatogram at UV 254 nm, UV 366 nm and white light illumination, a second development was performed with 10 mL petroleum ether - cyclohexane - ethyl acetate 5:2.8:2.2 (Table S-2, MP 12) up to 85 mm, followed by drying and documentation of the chromatogram as described. For the separate polar and nonpolar chromatograms, the standard solutions and the five different extracts of Danshen were applied as 8-mm bands on a HPTLC plate silica gel 60 F_{254} and developed with MP 6 or MP 12 up to 7 cm using the same development parameters as for the two-step method.

2.4. Derivatization

The nonpolar chromatograms were immersed in anisaldehyde sulfuric acid reagent for 2 s with 2.5 cm/s immersion speed using the TLC Immersion Device (CAMAG) and heated at 110 °C for 3 min on the TLC Plate Heater (CAMAG).

2.5. Neutralization of chromatograms

Chromatograms intended for *B. subtilis* and *A. fischeri* bioassays were dried for 30 min in the ADC 2, neutralized by 3-s immersion (2.5 cm/s immersion speed) into a phosphate - citrate buffer (4% or 8%, *W*/*V*, pH 7.8) using the TLC Immersion Device (CAMAG) and dried for 5 min under a cold stream of air of a hair dryer (Table S-3, methods 1 and 2). For the AChE assay, chromatograms were neutralized by exposure to ammonia vapor in a twin-trough chamber (20 cm × 10 cm, CAMAG) for 8 min, then dried in the ADC 2 for 8 min using an activated molecular sieve (0.3 nm pearls, grade 564, filled up to 3-cm high in the gas wash bottle of the humidity control device) to reduce the relative humidity to around 0.1% at 22 °C (Table S-3, method 3).

2.6. Effect-directed detection

Two-step developed HPTLC chromatograms as well as separately polar or nonpolar chromatograms were subjected to the respective (bio)assays, if required after neutralization. Immersion was performed via the TLC Immersion Device (CAMAG) at an immersion speed of 2.5 cm/s and documentation via the TLC Visualizer (CAMAG), if not stated otherwise.

2.6.1. A. fischeri *bioassay and limit of detection (LOD) of tanshinones*

The Gram-negative antimicrobial profiling was performed according to [33]. In brief, the neutralized chromatogram was immersed for 2 s into the luminescent *A. fischeri* suspension (the proper luminescence was visually checked by shaking the flask in a dark room, the medium was prepared according to DIN EN ISO 11348-1 [34]). The change over time of the instantly luminescent bioautogram was monitored for 30 min and documented with the BioLuminizer (CAMAG) using an exposure time of 50 s and 1 min trigger intervals. Dark zones indicated the luminescence inhibition of the bacteria [35] and thus bioactive compounds. For LOD study, DHTI (1-5 ng/band), CT (5-100 ng/band), TI (50-300 ng/band) and TIIA (50-400 ng/band) as well as extract 4 of each sample (2 μL) were applied in duplicate. After development with MP 12 up to 70 mm, the chromatogram was immersed into the *A. fischeri* suspension and documented. The bioautogram at 30 min was processed by the open source rTLC V.1.0 [36] to produce inhibition values.

2.6.2. B. subtilis *bioassay*

The Gram-positive antibacterial screening was performed according to [12]. Briefly, the neutralized chromatogram was dipped for 6 s with 3.5 cm/s immersion speed into the *B. subtilis* suspension ($OD_{600\,nm}$ = 0.8), incubated at 37 °C for 2 h and then visualized by immersion into a 0.2% PBS-buffered MTT solution for 1 s with 3.5 cm/s immersion speed and incubation at 37 °C for 30 min followed by heating at 50 °C for 5 min on the TLC Plate Heater (CAMAG). Active microorganisms reduced MTT into purple formazan, whereas antimicrobials were observed as white zones on a purple background [12,37] and documented under white light illumination (reflectance mode).

2.6.3. AChE assay

The AChE assay was performed based on the latest modified procedures [16,38] of the Marston's method [39]. Concisely, the neutralized chromatogram was immersed for 2 s into the enzyme solution (100 mL TRIS buffer, 0.05 M, pH 7.8, plus 666 units AChE and 100 mg bovine serum albumin). The plate was incubated at 37 °C for 25 min and immersed for 1 s into the substrate (90 mg α-naphthyl acetate and 160 mg Fast Blue B salt in 90 mL water – ethanol, 2:1), followed by drying at ambient temperature. Enzyme inhibitors were documented as white zones on a purple background under white light illumination (transmission and reflection modes).

2.6.4. DPPH• *assay*

For the DPPH• assay, the chromatogram was immersed into a 0.2 mg/mL methanolic DPPH• solution for 2 s. After drying for 2 min at ambient temperature in the dark, the plate was documented under white light illumination (transmission and reflection modes). After 30 min, the chromatogram was measured at 520 nm using the tungsten-halogen lamp in the fluorescence mode without optical filter (inverse scan).

2.7. HPTLC-HRMS

The extracts were applied in triplicate (the first section for (bio)assay, the second section for derivatization with anisaldehyde sulfuric acid reagent and the third section for HRMS) and separated by MP 6 or MP 12. The chromatogram was cut (smartCut Plate Cutter, CAMAG) and each section subjected to the intended detection. For HRMS recordings, the positions of the active zones on the (bio)autograms were transferred and marked on the chromatogram for HRMS at UV 254 nm and 366 nm using a soft pencil. An elution head-based interface (Plate Express, Advion, Ithaca, NY, USA) was used to introduce the sample to the heated electrospray ionization (HESI) source, which was connected to a Q Exactive Plus Hybrid Quadrupole-Orbitrap Mass Spectrometer (Thermo Fisher Scientific, Dreieich, Germany). The zone of interest, tightly fixed by the oval elution head (4 mm × 2 mm, 320 N) was eluted for 60 s at a flow rate of 0.1 mL/min using methanol for the positive ionization mode and acidified methanol (plus 0.1% formic acid) for the negative ionization mode. All mass spectra were recorded in the full scan mode

between m/z 50 and m/z 800 in both ionization modes. Two lock masses were used, *i.e.* monosodium diformate (m/z 112.98563) for negative and sodium dibutyl phthalate (m/z 301.14103) for positive ionization mode. The settings (positive/negative mode, if different) included spray voltage +3.7/−3.5 kV, capillary temperature 270 °C, resolution 70.000/140.000, automatic gain control target $3 \times 10^6/2 \times 10^5$ and maximum injection time 10/200 ms. The MS data was processed with Xcalibur 3.0.63 software (Thermo Fisher Scientific). A representative plate/system background (located at a similar hR_F position as the zone of interest) was always subtracted from the analyte mass spectrum.

2.8. PLC-NMR spectroscopy

The sample A (10 g) was extracted with 50 mL solvent as for extract 4. After evaporation, the residue was dissolved in 4 mL methanol. Thereof, 2 mL were applied as band (185 mm × 3 mm) on the PLC plate (cut to 20 cm × 10 cm using the smartCut and prewashed with methanol and water, 3:2), which was developed with MP 12 up to 10 cm in the Twin Trough Chamber (CAMAG). The active zone was scraped off and extracted three times with 2 mL methanol and the supernatant was centrifuged and evaporated to dryness under a nitrogen stream. The residue was dissolved in 600 μL deuterated methanol and transferred into a 5-mm NMR tube (VWR) and measured with the NMR spectrometer AV 600 (Avance III HD 600 MHz, Bruker, Rheinstetten, Germany) equipped with a 5-mm BBO Z-gradient probe. All spectra were collected and processed with TopSpin 3.5 (Bruker), and the acquisition parameters were 64 K data points with 1024 transients and a delay time of 6 s. The CHD_2OD signal at 3.31 ppm originating from the residual methanol solvent was used as reference for the chemical shift.

3. Results and discussion

3.1. Two-step development for a comprehensive profiling

The chemical profiling of the different Danshen extracts was aimed at covering effective compounds as comprehensively as possible. Due to the different polarities of tanshinones and phenolics, two types of MPs were optimized to separate both groups on the same plate through a two-step development. Especially for separation of polar Danshen extracts [30], the MPs contained a high percentage of acids. In contrast, the acid content was required to be as low as possible for a subsequent bioprofiling. Hence, various MPs were investigated for separation of polar and nonpolar extracts (Table S-2). With regard to an acceptable resolution of all the components and a good response of the acid-sensitive bioassays, MP 6 and MP 12 were preferred for polar and nonpolar developments, respectively. If required, halogenated solvents like chloroform can be avoided for separation of the main phenolics (SAB, LSA and RA) in the Danshen extracts (Fig. S-1; substitution of chloroform by pentyl acetate).

3.2. Neutralization of the chromatograms prior to bioassays

Earlier investigations proved that a high percentage of acid in the MP along with an insufficient neutralization hampered the response of specific bioassays. Hence, the acidity of the MP was reduced to 5% (Table S-2, MP 6) to be within the buffer capacity [12]. Among three different investigated neutralization procedures (Table S-3), method 2 was suited for *A. fischeri* and *B. subtilis* bioassays, and method 3 for the AChE assay.

3.3. Impact of different extraction methods on effect-directed profiles

The polar part of Danshen containing phenolic acids was extracted with methanol *versus* water, followed by an acidified ethyl acetate partitioning, whereas the nonpolar part containing diterpenoid quinones was extracted with ethanol *versus* its mixture with pentyl acetate. The effectivity of these extractions was evaluated regarding their biological, biochemical and chemical profiles. Differing application volumes of the extracts eased the qualitative comparison of the fingerprints, however, needed to be factorized for quantitative conclusions. In comparison to agar diffusion and agar overlay bioautography, DB was preferred to screen antimicrobial activities of Danshen extracts due to its good capability of detection, time-saving direct application and minor impact on the resolution of compounds [12].

The different extracts of Danshen provided strong (bio)profiles, whereas the reference extract 3, covering both nonpolar and polar components, had almost the same (bio)activity as the extracts 2 and 5 with the same concentration of 100 mg/mL. For example for nonpolar compounds in the *A. fischeri* bioassay, extract 3 (Fig. 1e, tracks 10–13) was similar in the intensity to extract 5 (tracks 19–22). For polar compounds, extract 3 (Fig. 5) was almost similar in the intensity to extract 2 in the AChE (Fig. 5c) and DPPH• (Fig. 5d) assays. The differing (bio)activity behavior of extracts 1–5 was evident by comparing polar with nonpolar extractions (Fig. 1, left *versus* right plate side). Unique responses were observed even among the extractions of a similar polarity (polar extracts 1 and 2 as well as nonpolar extracts 4 and 5). For instance, if compared to extract 1 of Danshen sample B (Fig. S-2a–c), extract 2 showed more pronounced bands in the phenolics chromatogram (Fig. S-2a–c) and also more and stronger active zones in the *A. fischeri* and *B. subtilis* bioautogram due to the salting-out effect and DLLE (ethyl acetate as extractant and acetone as disperser solvent). Regarding nonpolar extracts, extract 4 seemed at first glance to show a much stronger bioactivity profile than extract 5 (Fig. 2d *versus* e), but it was also by a factor of 2.5 higher in the amount on the plate.

Consequently, the reference extract 3 was an appropriate compromise for both, polar and nonpolar (bio)profilings on the same plate, though intensity of the zones was weaker, if compared to the separate, more polar and more nonpolar extracts. The polar extract 2 led to more intense zones than extract 1, whereas nonpolar extracts 4 and 5 were considered to be comparable.

3.4. Gram-negative antimicrobials discovered via HPTLC-A. fischeri *bioassay*

Literature on antimicrobial activity of Danshen against Gram-negative bacteria showed that sensitive methods and isolated compounds led to lower minimum inhibitory concentration (MIC) values and revealed more accurate values for activities. Ethanolic Danshen extracts exhibited 15.6 mg/mL as MIC against *Aggregatibacter actinomycetemcomitans* and *Porphyromonas gingivalis* [40], which was a relatively high MIC. In contrast, the antibacterial activity of single active compounds of Danshen such as CT and DHTI showed MIC of 100 μg/mL against 8 Gram-negative bacteria (agar dilution method), except *Alcaligenes faecalis* [41]. The antimicrobial activities of 4 tanshinones and 3 phenolics (bioassay-guided fractions of the ethanolic Danshen extract) against 5 Gram-negative bacteria through spore germination and micro-dilution-colorimetric assays showed lower MICs of all phenolics and tanshinones for Gram-negative bacteria *versus* Gram-positive ones. Additionally, DHTI and CT with MICs of 6 to 25 μg/mL had a stronger antimicrobial activity than TI and TIIA with MICs of 25 to 50 μg/mL. Phenolic compounds like RA and

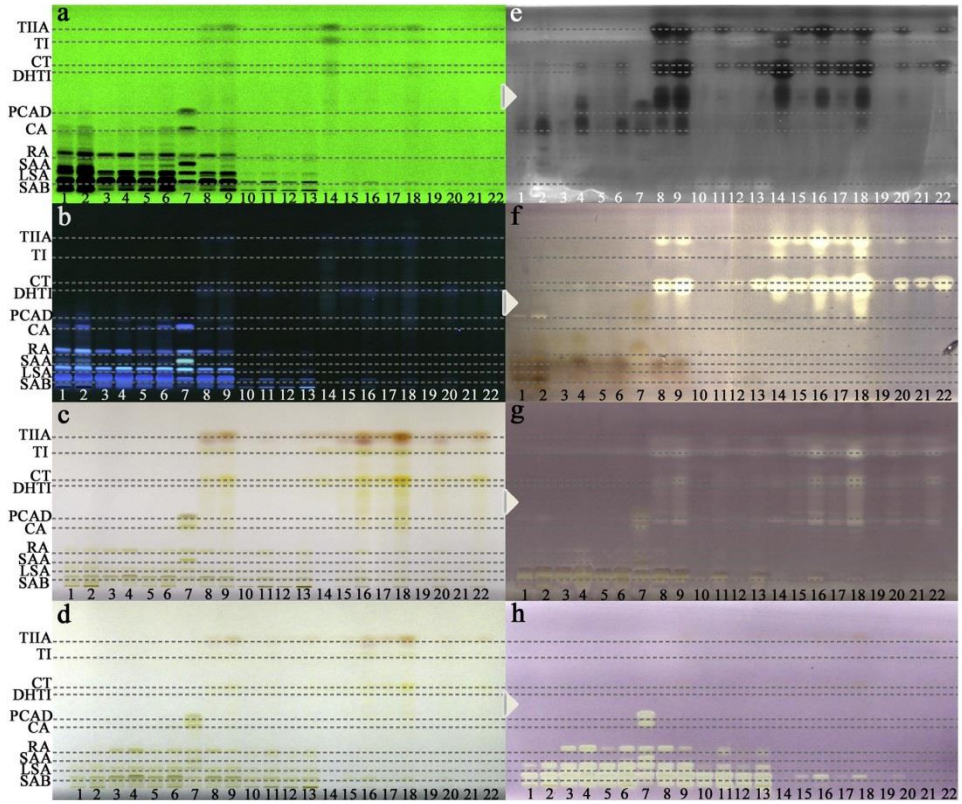

Fig. 1. Chromatograms of the two-step development on HPTLC plates silica gel 60 F_{254} (first toluene - chloroform - ethyl acetate - methanol - formic acid 4:6:8:1:1 up to 45 mm, and second, petroleum ether (60–80 °C) - cyclohexane - ethyl acetate 5:2.8:2.2 up to 85 mm) of 5 Danshen extracts (tracks 1–6, 8–13, 15–22; assignments and individual application volumes in Table S-1) as well as 2 standard mixture solutions with 10 substances (tracks 7 and 14); each plate documented either at UV 254 nm (a) or UV 366 nm (b) or white light (c and d, transmission mode) and to the right the respective bioautograms using *A. fischeri* (e) and *B. subtilis* (f) bioassays as well as AChE inhibition (g) and DPPH• scavenging assays (h).

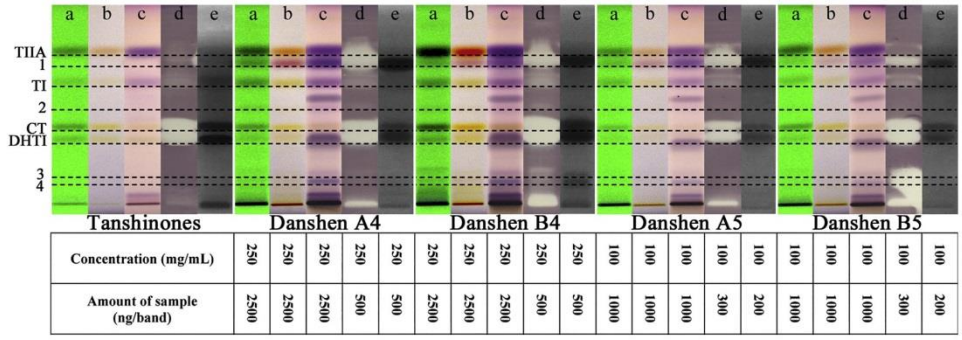

Concentration (mg/mL)	250	250	250	250	250	250	250	250	250	250	100	100	100	100	100	100	100	100	100	100
Amount of sample (ng/band)	2500	2500	2500	500	500	2500	2500	2500	500	500	1000	1000	1000	300	200	1000	1000	1000	300	200

Fig. 2. Chromatograms of tanshinones (in *B. subtilis* and *A. fischeri* DHTI 20 and 10 ng/band, CT 150 and 50 ng/band, TI in both 300 ng/band, and TIIA in both 200 ng/band, respectively) and the nonpolar Danshen extracts 4 and 5 on HPTLC plates silica gel 60 F_{254} with petroleum ether (60–80 °C) - cyclohexane - ethyl acetate 5:2.8:2.2, documented at UV 254 nm (a), white light illumination (b) and after derivatization via anisaldehyde sulfuric acid reagent (c) as well as respective bioautograms after *B. subtilis* (d) and *A. fischeri* (e) bioassays.

CA had a weaker antimicrobial activity (MICs 50–100 μg/mL), if compared to tanshinones [42]. Such bioassays described do only deliver a sum parameter of the bioactivity of complex samples or require tedious pre-fractionation to obtain individual compounds to test.

In our study, HPTLC combined with a bioassay directly indicated bioactive component in the extract without need for fractionation and without discrimination of compounds. The non-pathogenic marine *A. fischeri* bacteria were chosen, which produce an instant luminescent signal and are convenient to use as indicator. Bacteria of a higher clinical relevance often need a special laboratory safety level. Our bioautograms revealed that polar and nonpolar Danshen extracts had a substantial effect on the Gram-negative *A. fischeri* bacteria, whereby the nonpolar portion located at a higher hR_F range was more bioactive than the polar components at a lower hR_F (Fig. 1e). This confirmed initial results for the nonpolar compounds [31].

For detailed investigation, polar and nonpolar extracts were individually developed with the respective optimized MPs up to a migration distance of 70 mm (Figs. 2 and S-2, a–c). The higher migration distances resulted in a better zone resolution, if compared to the two-step development (Fig. 1a–d). Our results showed that among the 4 tanshinone standards, DHTI and CT had a higher Gram-negative antimicrobial activity against *A. fischeri* than TI and TIIA (Fig. 2e). Moreover, three unidentified nonpolar active compounds 1, 3 and 4 were discovered in the Danshen extracts. Among the 6 phenolic standards, SAA, PCAD, CA, SAB and RA showed an antimicrobial activity at the studied amounts on the plate. Apart from these, three unidentified compounds 5–7 (Fig. S-2e) were discovered in the polar Danshen extracts. Our results about antimicrobial activity of polar and nonpolar compounds in Danshen against Gram-negative *A. fischeri* bacteria were in accordance with former results on Gram-negative antimicrobial phenolics and tanshinones in Danshen [42]. In addition, both results confirmed that tanshinones such as DHTI and CT as well as a similar unidentified compound had much stronger antimicrobial activity than phenolics. This proves and outlines the suitability of the streamlined DB workflow to be an efficient alternative with several advantages as discussed.

The HPTLC-*A. fischeri* bioassay can be used not only for bioactivity screening but also for LOD determination of active compounds on the plate [43]. LODs of tanshinones were determined using the bioautogram after 30 min. For DHTI and CT, LODs were exemplarily calculated to be 5 and 12 ng/zone, respectively, based on the extracted digital values of the antimicrobial activity in the bioautogram against *A. fischeri* (Fig. 3b) using an open source software called rTLC [36]. Such LOD values represent the lowest detectable active amount of a substance on the HPTLC plate and can be compared with MIC values. In contrast to tanshinones, phenolic compounds had an inferior *A. fischeri* antimicrobial activity (Fig S-2e), clearly underlined by their antimicrobial activity at higher amounts, *i.e.* 10 μg/zone for SAB, 2.5 μg/zone for LSA, 2.5 μg/zone for SAA, 1.5 μg/zone for RA, 0.75 μg/zone for CA and 1.5 μg/zone for PCAD. To conclude, the HPTLC-*A. fischeri* bioassay workflow was not only fast and cost-efficient, but also more sensitive than the agar dilution method to detect activities, *i.e.*, by a factor of 20 for DHTI with 100 μg/mL [41] *versus* 5 ng/zone or by a factor of 8 for CT with 100 μg/mL [41] *versus* 12 ng/zone, when referred to a 1-μL/zone application volume. In that sense, the HPTLC-*A. fischeri* bioassay workflow was comparable to the MIC range of spore germination and micro-dilution-colorimetric assays (for DHTI 6–25 μg/mL [42] *versus* 5 ng/zone or for CT 6–12 μg/mL [42] *versus* 12 ng/zone), though it is expected to be more sensitive for higher application volumes, *e.g.*, by a factor of 100 for an application of 100 μL.

3.5. Gram-positive antimicrobials discovered via HPTLC-B. subtilis *bioassay*

In antimicrobial studies of Danshen against Gram-positive bacteria [44,45], the ethanolic (MICs 15.6 to 62.5 mg/mL via cup-plate method) and methanolic extracts (MICs 8 to 64 μg/mL via broth dilution method) exhibited antimicrobial activities on pathogenic bacteria in the mouth such as *Streptococcus* (*S.*) *mutans*, *Lactobacillus, S. sanguinis, S. sobrinus, S. ratti, S. criceti, S. anginosus and S. gordonii*. These MIC values were wondering due to their difference by a factor of 1000. In contrast to no antimicrobial activity (disc diffusion assay) of water, butanol and ethyl acetate fractions of methanol extract of Danshen, its *n*-hexane and chloroform fractions as well as whole methanol extract demonstrated strong effects against *Staphylococcus aureus,* even against a methicillin-resistant one, with MICs of 1 to 128 μg/mL through broth microdilution method [46]. CT and DHTI showed antibacterial activity (agar dilution method) against a wide range of Gram-positive bacteria with MICs of 3 to ca. 100 μg/mL [41]. Moreover, CT had strong antimicrobial activity against 21 *S. aureus* as well as methicillin- and vancomycin-resistant *S. aureus* strains by broth macro/microdilution method [47,48]. A coculture of *Salvia miltiorrhiza* root with *Bacillus cereus* bacteria showed an increase in the accumulation of tanshinones, produced as a defensive reaction for inhibition of the bacterial growth due to the antimicrobial effects of CT, TI and TIIA [49]. The activity of tanshinones and phenolics against three Gram-positive bacteria (*B. subtilis*, *S. aureus* and *S. haemolyticus*) via bioassay-guided fractionation of an ethanolic Danshen extract showed that CT and DHTI had a stronger antimicrobial activity than TI and TIIA. If compared to tanshinones, phenolic compounds like RA and CA had a lower Gram-positive antimicrobial activity with regard to the MIC level [42].

In our study, the ubiquitous, non-pathogenic *B. subtilis* bacteria were chosen, as bacteria of a higher clinical relevance often need a special laboratory safety level. To compare our results with the mentioned studies, first, the antimicrobial responses of the whole polar extracts (Fig. 1f, 1–6, 500–2250 ng/μL, Table S-1, *B. subtilis*) were compared with the nonpolar extract responses (Fig. 1f, 15–22, 100–500 ng/μL). Even though the polar extract was at least at a factor of 4.5 higher amount on the plate, it was less active in the response, if compared to the nonpolar extracts. Therefore, it was evident that the most antimicrobial compounds were found in the nonpolar extract, which was retained at higher hR_F values. This result was in accordance with the results of the mentioned studies for antimicrobial investigation of both isolated polar and nonpolar compounds of Danshen [41,42,47–49] and its extract solutions [44–46]. Nevertheless, some weak zones were observed in the lower, polar hR_F range. For further study, the polar and nonpolar extracts were also developed separately up to 70 mm. In the nonpolar extracts, not only DHTI, CT, TI, TIIA, but also the unidentified compound zones 1 to 4 showed a strong bioactivity (Fig. 2d). Moreover, derivatization with anisaldehyde sulfuric acid reagent revealed a violet zone (Fig. 2c) co-eluting with the yellow (Fig. 2b), bioactive (Fig. 2d) DHTI zone in the Danshen extracts. In the polar Danshen extracts, bioactive zones at the same hR_F value as SAB (Fig. S-2d), LSA (only in Danshen extract B2) and RA (only in Danshen extract A1) as well as the unidentified compound 6 were observed. The bioactive zone 5 at a higher hR_F (Fig. S-2d) was assumed to belong to the group of tanshinones extracted at a lower amount during the polar extraction.

To conclude, the visual antibacterial activities of the tanshinones and phenolics were observed in the following descending order: DHTI > CT > TI ≈ TIIA ⋙ phenolics. Despite of the structural similarity of all tanshinones, they showed a differing bioactivity. The dihydrofurane ring might explain this. Having a dihydrofurane ring, a higher, but similar antimicrobial activity of CT and DHTI was

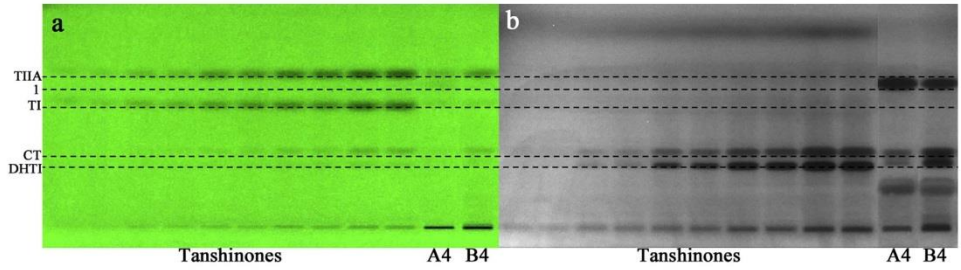

Fig. 3. Chromatogram of tanshinones (DHTI 1-5 ng/band, CT 5-100 ng/band, TI 50-300 ng/band and TIIA 50-400 ng/band) and the nonpolar extract of Danshen (2 µL/band each) on HPTLC plates silica gel 60 F_{254} with petroleum ether (60–80 °C) - cyclohexane - ethyl acetate 5:2.8:2.2, documented at UV 254 nm (a) as well as respective *A. fischeri* bioquantogram (b, 2 sections of one plate).

observed in comparison to the bioactivity of T1 and TIIA with a furane ring (C-15 and C-16). Also, DHTI with an aromatic ring A had a higher activity in contrast to CT with a perhydrated six-membered ring A [42]. The HPTLC-*B. subtilis* bioassay was a fast and sensitive method for investigation of the Gram-positive antimicrobial activity of these complex extracts, and again, directly indicated their bioactive components without need for fractionation or discrimination of compounds.

3.6. AChE inhibitors discovered by HPTLC-AChE assay

Isolated DHTI and CT were inhibitors of AChE with IC_{50} values of 0.89 and 4.67 µM, respectively, using the Ellman colorimetric method [50]. After modification of this method, DHTI and CT (isolated by vacuum liquid chromatography followed by CC) had anti-cholinesterase activity with IC_{50} values 1.0 and 7.0 µM; whereas, isolated TI and TIIA showed a weak AChE inhibition [51]. The AChE inhibitory activity of DHTI and CT was confirmed *ex-vivo* for 3 h and 6 h, respectively, while their *in vitro* IC_{50} values were 25 and 82 µM, respectively [52]. Substantial AChE inhibition (enzyme from homogenated rat brain) of TI, DHTI, total tanshinones and an ethanolic Danshen extract was also proven via the Ellman colorimetric method; whereas CT and TIIA did not exhibit any activity in contrast to previous studies [53]. Among IC_{50} values of tanshinones, DHTI with a dihydrofurane ring had the highest inhibitory activity in comparison to TI and TIIA. In a recent structural study using recombinant human AChE, DHTI revealed a selective peripheral site binding in a special orientation of the dihydrofurane ring [54].

Our AChE profiling of Danshen extracts showed AChE inhibitors in all extracts (Fig. 1g). Via separation of the nonpolar extracts, DHTI, CT and the two unidentified compounds 1 and 3 (also detected via *A. fischeri* and *B. subtilis* bioassays) were found to be AChE inhibitors (Fig. 4). The partition-coefficient factor clogP of 2.4 for DHTI and 3.4 for CT showed that they are able to penetrate the blood-brain barrier [51]. In other words, any AChE inhibitors need to penetrate the blood-brain barrier to inhibit AChE, and consequently, increasing the acetylcholine levels to restore its physiological effects. Therefore, the clogP value is an important parameter for AChE inhibitors. Apart from tanshinones, polyphenols are also a main source of AChE inhibitors [53]. In the polar extract, the six phenolics SAB, SAA, LSA, RA, CA and PCAD showed a strong inhibition of AChE (Fig. 5c). SAB, LSA and RA were detected as given, whereas CA and PCAD were first detected at a higher sample amount (data not shown). Additionally, the unidentified compound 8 was revealed in the Danshen extracts A3 and B3 (Fig. 5). The inhibition mechanism of phenolic compounds with a similar structure to caffeic acid is assumed to be done by fitting the inhibitors into

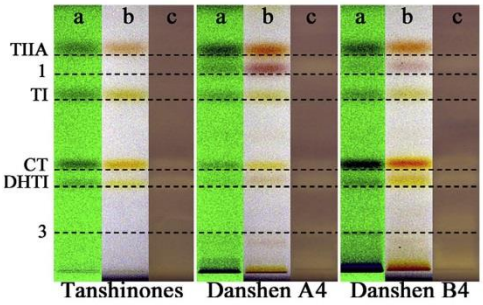

Fig. 4. Chromatograms of tanshinones (DHTI 40 ng/band, CT 300 ng/band, TI 200 ng/band and TIIA 300 ng/band) and the nonpolar extracts of Danshen (2 µL/band each) on HPTLC plates silica gel 60 F_{254} with petroleum ether (60–80 °C) - cyclohexane - ethyl acetate 5:2.8:2.2, documented at UV 254 nm (a) and white light illumination (b) as well as after AChE inhibition (c).

the gorge of the active AChE site via aromatic ring positioning into the peripheral anionic site (except for phenolics with the orientation of the aromatic ring towards the anionic site) [55]. The results of HPTLC-AChE assay showed that this method has a considerable potential for high-throughput screening of a wide range of active compounds with differing polarities.

3.7. Free radical scavengers discovered by HPTLC-DPPH• assay

The antioxidant activitiy of phenolic compounds is related to the compound structure such as the number of hydroxyl groups present in the aromatic ring(s) and their positions (ortho, meta and para). Phenolic antioxidants can inactivate the free radical generation by transfering a hydrogen atom to radicals [56] and generation of own stable radicals which are stabilized through resonance [57]. Antioxidants can interrupt the oxidizing chain reactions in different ways, including disactivation of reactive oxygen species, inhibition of enzymes, and chelating of metal ions. For these protective functions, two mechanisms have been proposed. The first mechanism is the hydrogen atom transfer from the antioxidant to the free radical, depending on the dissociation energy of the OH bond. The second mechanism is the electron transfer reaction by giving an electron from the antioxidant to the free radical, depending on the ionization potential [56]. Among the stable radical assays, the DPPH• scavenging activity depends on the hydrogen atom transfer (first mechanism). Obtained results may differ to the unstable superoxide anion assay [58].

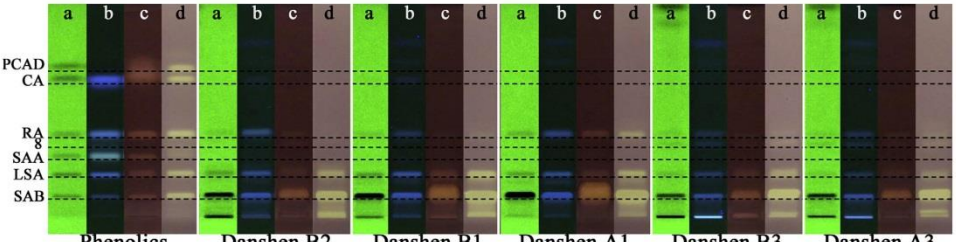

Phenolics	Danshen B2				Danshen B1				Danshen A1				Danshen B3				Danshen A3			
Concentration (mg/mL)	100	100	100	1.7	300	300	300	5.0	300	300	300	5.0	100	100	100	3.4	100	100	100	3.4
Amount of sample (ng/band)	300	300	300	17	600	600	600	50	600	600	600	50	200	200	200	34	200	200	200	34

Fig. 5. Chromatograms of phenolics (50 ng/band for DPPH• and 400 ng/band for AChE) and the polar extracts of Danshen on HPTLC plates silica gel 60 F_{254} with toluene - chloroform - ethyl acetate - methanol - formic acid 4:6:8:1:1, documented at UV 254 nm (a), UV 366 nm (b), after AChE inhibition assay (c) and after DPPH• assay (d).

Most DPPH• studies used conventional spectroscopic methods [57,59–61]. The correlation between high amounts of tanshinones in Danshen extracts and any antioxidant activity, which was attributed to phenolic acids and flavonoids, was found unlikely [59]. Despite of this consideration, the antioxidant activity of tanshinones was reported based on experiments performed by the Rancimat and the Schaal oven-peroxide value method (tanshinones isolated by CC and preparative TLC, and mixed with pork fat at 0.02%, *W*/*W*, compared with a control sample). Except for TIIA, all the diterpenoid quinones such as DHTI, TI, methylenetanshinquinone (MTQ), CT, and tanshinone IIB provided notable antioxidant activity according to a prolonged induction time and lower peroxide values of the fat [62]. Kang et al. found that ethyl acetate and *n*-butanol fractions of methanolic Danshen extracts had considerable scavenging activity against DPPH. Also, 2 phenolics and 3 diterpenoid quinones were isolated from the pentyl acetate, ethyl acetate, *n*-butanol and water fractions by CC. Among these, the 2 phenolics in the ethyl acetate and *n*-butanol fractions showed strong DPPH• scavenging activity, even higher than butylated hydroxytoluene and *L*-ascorbic acid as two well-known antioxidants [57]. In contrast, the 3 diterpenoid quinones (TIIA, TI and CT) had no antioxidative properties and were inactive in all three experiments even at high concentrations [57]. Also salvianic acid A (danshensu), SAB and SAA were found to be effective radical scavengers with antioxidative activities [60,61]. A recent HPTLC-DPPH• investigation of 19 *Salvia* species (but no Danshen) showed that most samples had antioxidative polar compounds covered by flavonoids and phenolic acids. Only four *Salvia* species exhibited free radical scavenging properties also in the less polar fractions [63].

In our study, the effect-directed HPTLC-DPPH analysis seems to be the first for Danshen. It rapidly detects individual free radical scavengers. Only phenolic compounds at a lower hR_F were detected as the major free radical scavengers in Danshen (Fig. 1h). As the response was too intense, the DPPH• assay was repeated after a 1:60 methanolic dilution of the Danshen extract 2 (to be 1.7 mg/mL), extract 1 (5.0 mg/mL) and after 1:30 methanolic dilution of extract 3 (3.4 mg/mL). The phenolic standard solutions were diluted to be 50 ng/μL and 1 μL was applied on the plate via overspraying (50 ng/band). The polar development up to 70 mm showed that all six polar phenolics, *i.e.* SAB, LSA, SAA, RA, CA and PCAD, were free radical scavengers (Fig. 5d). In all Danshen extracts, DPPH•-effective bands were detected at the same hR_F as SAB, LSA, RA, and only in extract 3, an additional weak unidentified compound 8 was detected (Fig. 5d). To conclude, SAB, LSA and RA showed the most intense free radical scavenging activity and substantially contributed to the antioxidative potential of the Danshen extracts. Our densitometric results also showed that free radical scavenging activities of the phenolics were obtained in the following descending order for a 50 ng/zone each (peak area percentage): RA > CA ≈ LSA > SAB ≈ PCAD > SAA (Fig. S-3).

3.8. HPTLC-HRMS for the identification of known active compounds

The preliminary assignment of discovered active compounds to standard substances based on the hR_F value and spectral properties, was proved by recording of mass spectra of both the standard and sample zones. This way, CT, TI and TIIA were confirmed in the nonpolar extracts 4 and 5, and SAB, LSA, SAA, RA, CA and PCAD in the polar extracts 1 and 2 (Fig. 6). The HRMS results confirmed a co-elution at the same hR_F values of DHTI in the samples, as the prior derivatization results had revealed. According to the measured exact mass of *m*/*z* 303.09917 $[M2+Na]^+$, the co-eluting compound was assumed to be either methylenedihydrotanshinquinone (MDHTQ) or danshenxinkun B (DXB) or 1,2,15,16-tetrahydrotanshinone I (THT) or their combinations (Fig. 6 DHTI and Table 1). As most important active zone among all the unidentified zones in the bioautogram and fingerprint of the nonpolar extract of Danshen, the compound zone 1 was selected and revealed *m*/*z* 301.08354 $[M+Na]^+$. According to [20,23,64–68], four tanshinones were potential candidates, *i.e.* 1,2-dihydrotanshinone I (1,2-DHTI), MTQ, *iso*-dihydrotanshinone I (*iso*DHTI), and *iso*-dihydrotanshinone II (*iso*DHTII) (Fig. 7). To accept or reject the mentioned potential candidates, ^{1}H-NMR spectroscopy was performed next.

3.9. Structural elucidation of unidentified active compounds via PLC-NMR spectroscopy

Most reported isolation strategies were uneconomical even those approaches with a direct elution of the zone from the plate. A high number of TLC/HPTLC plates was required for zone elution using an elution head-based interface to collect a sufficient analyte amount for NMR spectroscopy [2,4]. Although good results were reported for quantification of standards [5], the small elution area of the elution head is not considered as an appropriate option for extended compound isolation from complex samples. A single PLC

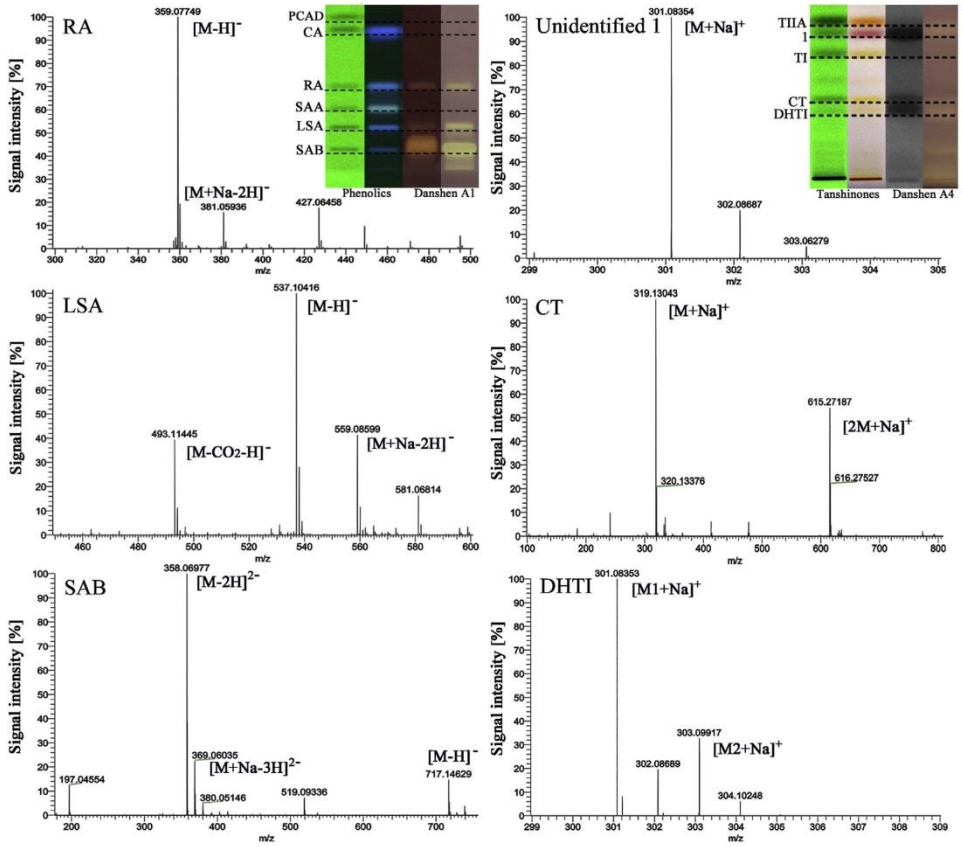

Fig. 6. HPTLC-HRMS spectra of the polar bioactive compounds (RA, LSA, SAB) in polar extract A1 and the nonpolar unidentified bioactive compound 1 as well as CT and DHTI, which were tentatively assigned (via standard comparison) in the nonpolar Danshen extract A4.

plate was preferred instead of using several HPTLC plates and developments, a hundred elutions and pilling up of binder and solvent impurities. A large volume of a highly concentrated sample was applied to yield the relevant amount in the low mg-range. The PLC-NMR workflow was fast (separation took ca. 0.5 h), user-friendly (direct method transfer) and environmentally friendly (less solvent comsumption *versus* CC).

Among the unidentified active zones, the multipotent compound zone 1 was selected. Among the four potential candidates according to HPTLC-HRMS, 1,2-DHTI and MTQ contain vinylic protons that are not present in *iso*DHTI and *iso*DHTII. Moreover, the vinylic protons at C-3 and C-18 of 1,2-DHTI and MTQ, respectively, were expected to appear at different chemical shifts. Hence, discrimination via the protons at C-3 in the structure of 1,2-DHTI and at C-18 in MTQ (4.6–6.0 ppm) was possible. The recorded ^{1}H-NMR spectrum (Fig. 8) revealed two singlet signals which were related to MTQ (5.10 ppm, 5.58 ppm) and one multiplet signal for 1,2-DHTI (6.08 ppm). The COSY spectra demonstrated that two singlet signals at 5.10 ppm and 5.58 ppm correlated with each other. The multiplet signal also revealed a coupling with the signal at 2.08 ppm that was related to the methyl protons at C-18 of 1,2-DHTI. The 600 MHz ^{1}H-NMR signals (Fig. 8) were assigned to the MTQ protons at (ppm): 1.81 (2H, m, H-3), 2.24 (3H, d, J = 1.35 Hz, H-17), 2.52 (2H, t, J = 6.4 Hz, H-2), 3.16 (2H, t, J = 6.5 Hz, H-1), 5.10 (1H, s, H-18), 5.58 (1H, s, H-18), 7.48 (1H, q, J = 1.35 Hz, H-16), 7.77 (1H, d, J = 8.2 Hz, H-6), 8.0 (1H, d, J = 8.2 Hz, H-7), and to the 1,2-DHTI protons at (ppm): 2.08 (3H, q, J = 1.6 Hz, H-18), 2.23 (2H, d, J = 1.37 Hz, H-2), 2.24 (3H, d, J = 1.35 Hz, H-17), 3.27 (2H, t, J = 6.4 Hz, H-1), 6.08 (1H, m, H-3), 7.45 (1H, q, J = 1.35 Hz, H-16), 7.54 (1H, d, J = 8.0 Hz, H-6), 7.63 (1H, d, J = 8.0 Hz, H-7). According to the NMR integrations, the active zone contained 1,2-DHTI and MTQ in the ratio 2:1, and only the ^{1}H-NMR results revealed this co-elution. The HSQC spectrum (Fig. S-4) confirmed that the two singlet signals at 5.10 ppm and 5.58 ppm correlated with the same carbon at 110 ppm, and the multiplet signal at 6.08 ppm also had coupling with the carbon at 128 ppm, which were all in the olefinic carbon region (100–150 ppm).

This compound zone 1, a red purple band in the HPTLC fingerprint located between TI and TIIA, was not identified in former (HP)TLC studies of Danshen [26,30–32,69]. Furthermore, it was shown as unidentified peak between TI and TIIA in HPLC research

Table 1
HPTLC-HRMS data of selected bioactive compounds in the two Danshen extracts A1 and A4.

A1	hR_F	Observed m/z	Theoretical m/z	Sum formula	Mass error (ppm)	Assignment	Confirmed substance
R	38	359.07749	359.07724	$C_{18}H_{15}O_8^-$	0.70	$[M-H]^-$	RA
		381.05936	381.05918	$C_{18}H_{14}NaO_8^-$	0.45	$[M+Na-2H]^-$	Sodium adduct of RA
L	20	493.11445	493.11402	$C_{26}H_{21}O_{10}^-$	0.87	$[M-CO_2-H]^-$	Fragment of LSA
		537.10416	537.10385	$C_{27}H_{21}O_{12}^-$	0.57	$[M-H]^-$	LSA
		559.08599	559.08579	$C_{27}H_{20}NaO_{12}^-$	0.35	$[M+Na-2H]^-$	Sodium adduct of LSA
B	10	197.04554	197.04554	$C_9H_9O_5^-$	0.00	$[M-C_{27}H_{21}O_{11}]^-$	Fragment of SAB
		358.06977	358.06942	$C_{36}H_{28}O_{16}^{2-}$	0.99	$[M-2H]^{2-}$	Fragment of SAB
		369.06035	369.06039	$C_{36}H_{27}NaO_{16}^{2-}$	−0.10	$[M+Na-3H]^{2-}$	Sodium adduct of SAB
		519.09336	519.09328	$C_{27}H_{19}O_{11}^-$	0.14	$[M-C_9H_{11}O_5]^-$	Fragment of SAB
		717.14629	717.14611	$C_{36}H_{29}O_{16}^-$	0.25	$[M-H]^-$	SAB
A4							
1	68	301.08354	301.08352	$C_{18}H_{14}NaO_3^+$	0.06	$[M+Na]^+$	1,2-DHTI/MTQ[d]
		579.17813	579.17781	$C_{36}H_{28}NaO_6^+$	0.55	$[2M+Na]^+$	Dimer of 1,2-DHTI/MTQ[b]
C	38	319.13043	319.13047	$C_{19}H_{20}NaO_3^+$	- 0.11	$[M+Na]^+$	CT[c]
		615.27187	615.27171	$C_{38}H_{40}NaO_6^+$	0.26	$[2M+Na]^+$	Dimer of CT[b]
D	33	301.08353	301.08352	$C_{18}H_{14}NaO_3^+$	0.03	$[M1+Na]^+$	DHTI[c]
		579.17801	579.17781	$C_{36}H_{28}NaO_6^+$	0.34	$[2M1+Na]^+$	Dimer of DHTI[b]
		303.09917	303.09916	$C_{18}H_{16}NaO_3^+$	0.02	$[M2+Na]^+$	MDHTQ/DXB/THTI[a,b]

[a] Methylenedihydrotanshinquinone (MDHTQ)/danshenxinkun B (DXB)/1,2,15,16-tetrahydrotanshinone I (THTI); compound was assumed to be either one of these or their combinations.
[b] Tentatively assigned according to exact mass.
[c] Assigned according to exact mass and confirmed with standards.
[d] Confirmed according to exact mass and ^{1}H-NMR spectra.

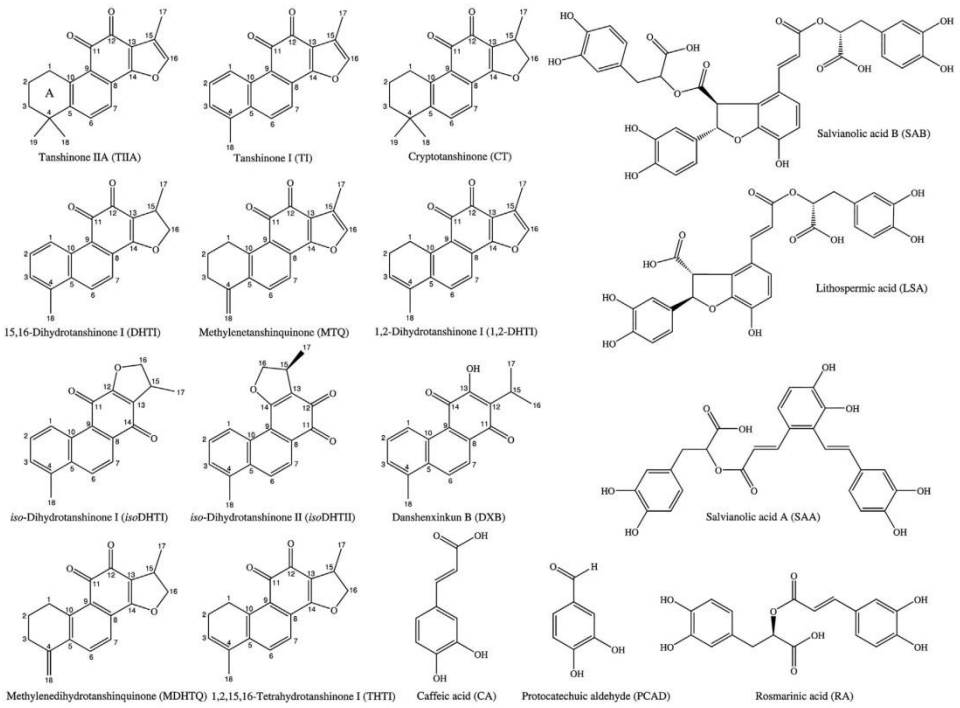

Fig. 7. Structures of tanshinones and phenolic compounds in Danshen, discussed in this study.

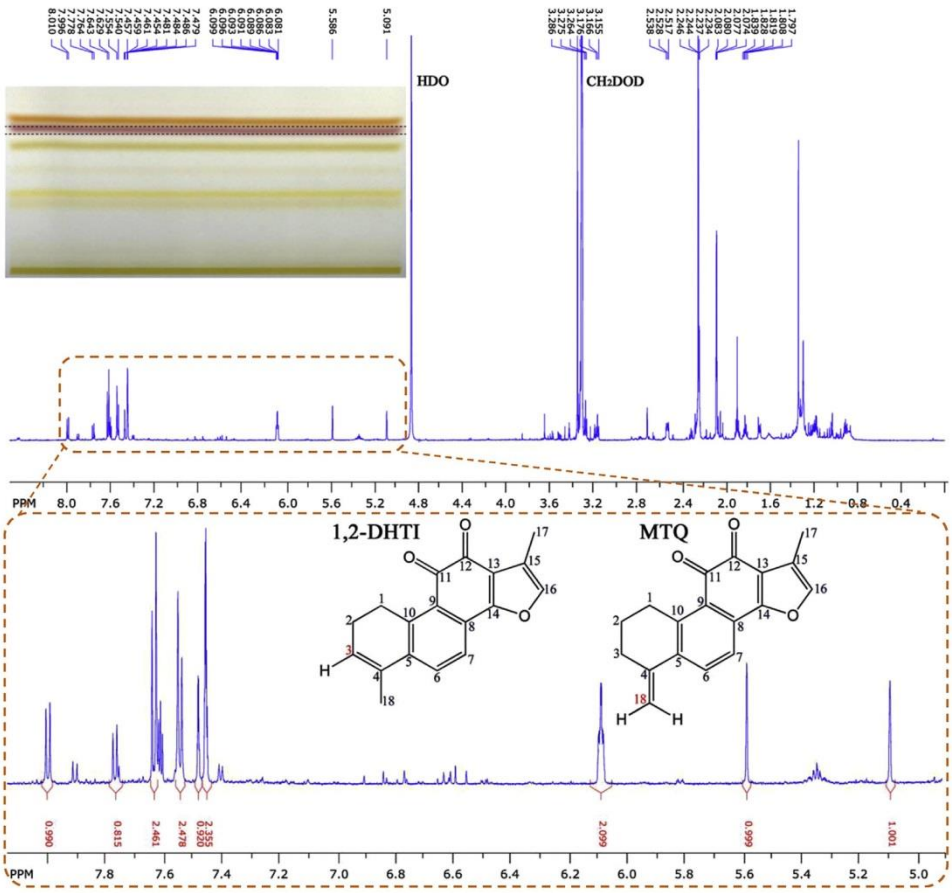

Fig. 8. ^{1}H-NMR spectrum of the unidentified compound zone 1, which was identified to be a critical pair of 1,2-DHTI and MTQ.

[70]. In other LC studies without DHTI and MTQ standards as a reference, the isolated compound was reported as one of them, especially with retention time between TI and TIIA [28,71]. In simultaneous studies of DHTI and MTQ, both were evident as overlapped peak [64,72] and only in a few cases as separated peaks [73]. The results revealed that the physicochemical interaction of both compounds were almost the same with regard to mobile and stationary phases in different separation systems. The (bio)activity of this zone may be related to both compounds, and a further study may reveal their relative activity or any synergy.

3.10. *Streamlined effect-directed profiling in contrast to* status quo

Sum parameter bioassays do only deliver the total bioactivity of complex samples or require tedious pre-fractionation to draw conclusions on single bioactive compounds. In the most previous studies on Danshen, a combination of several chromatographic methods was used such as CC, preparative TLC and preparative HPLC with fraction collection. The bioactivity of each extract was tested and the most active extracts were chosen for further investigation via fractionation. The bioactivity of each fraction was checked after each step, so called bioactivity-guided-fractionation [57]. Purity was checked and further fractionation for the isolation of compounds or fractions of interest followed [62,65–67]. Such workflows and methods required a large amount of sample (hundreds of g to kg), of solvent volumes for extraction and fractionation through the column (tens of L) and time-consuming and tedious evaporation steps [65]. Also, cuvette or microtiter plate assays are not compatible with organic solvents and the full range of sample ingredients is not represented in these assays, meaning that more middle polar to nonpolar compounds are discriminated due to the requirement for aqueous solubility.

Hence, the combination of such assays with planar chromatography, which directly indicates active compounds, does not have these limitations and extraordinary streamlines the workflow. A comparison of the *A. fischeri* cuvette assay (known as Microtox assay) with DB showed by a factor of 3, both faster analyses and higher cost savings [74]. The developed bioprofiling workflow, using the same mobile phase for HPTLC–UV/Vis/EDA–HRMS

and subsequent PLC–NMR, was demonstrated to be a streamlined option, being fast, user-friendly, cost-effective and environmentally friendly. Bioactivity screening (bioprofiling of the whole, natural sample extracts in parallel), effect-directed detection and characterization of active sample constituents were integrated in the workflow on the same plate. Only few plates were required to gain a wealth of information on active compounds in complex sample extracts.

4. Conclusion

The two-step HPTLC-EDA and parallel screening of different extracts allowed a comprehensive bioprofiling of Danshen. In a streamlined workflow, several individually active constituents of the sample were discovered. Instead of the switch to other methods like CC and CCC, the fast and cost-efficient scale-up to PLC enabled a direct transfer using the same mobile phase. Although, Danshen is one of the most popular traditional Chinese medicines, still some of the major active compounds have not been investigated satisfyingly, such as the relative activity of MTQ and 1,2-DHTI. First our ^{1}H-NMR results revealed that both compounds were identified as a co-eluting critical pair in the nonpolar HPTLC fingerprint of Danshen, which was not noticed in available literature. The proven activity of single compounds in Danshen as AChE inhibitors, DPPH• scavengers and antimicrobials against Gram-positive and Gram-negative bacteria explains and confirms its worldwide acceptance as multipotent natural product.

Acknowledgments

Thank is owed to Dr. H. Hausmann, Institute of Organic Chemistry, Justus Liebig University Giessen, for NMR measurements, Merck, Darmstadt, Germany for HPTLC and PLC plates and Phytolab, Vestenbergsgreuth, Germany for phenolic standards. Instrumentation used was partially funded by the German Research Foundation, Bonn, Germany (DFG project no. INST 162/471-1 FUGG).

Appendix A. Supplementary data

Supplementary material related to this article can be found, in the online version, at doi:https://doi.org/10.1016/j.chroma.2017.12.014

References

[1] G.E. Morlock, Planar chromatography mass spectrometry, in: Reference Module in Chemistry, Molecular Sciences and Chemical Engineering, Elsevier, 2014.
[2] E.M. Grzelak, C. Hwang, G. Cai, J.-W. Nam, M.P. Choules, W. Gao, D.C. Lankin, J.B. McAlpine, S.G. Mulugeta, J.G. Napolitano, Bioautography with TLC-MS/NMR for rapid discovery of anti-tuberculosis lead compounds from natural sources, ACS Infect. Dis. 2 (2016) 294–301.
[3] I. Yüce, G.E. Morlock, Streamlined structure elucidation of an unknown compound in a pigment formulation, J. Chromatogr. A 1469 (2016) 120–127.
[4] H.R. Adhami, U. Scherer, H. Kaehlig, T. Hettich, G. Schlotterbeck, E. Reich, L. Krenn, Combination of bioautography with HPTLC–MS/NMR: a fast identification of acetylcholinesterase inhibitors from Galbanum, Phytochem. Anal. 24 (2013) 395–400.
[5] A. Gössi, U. Scherer, G. Schlotterbeck, Thin-layer chromatography–nuclear magnetic resonance spectroscopy – a versatile tool for pharmaceutical and natural products analysis, CHIMIA Int. J. Chem. 66 (2012) 347–349.
[6] E.F. Queiroz, J.-L. Wolfender, K. Atindehou, D. Traore, K. Hostettmann, On-line identification of the antifungal constituents of *Erythrina vogelii* by liquid chromatography with tandem mass spectrometry, ultraviolet absorbance detection and nuclear magnetic resonance spectrometry combined with liquid chromatographic micro-fractionation, J. Chromatogr. A 974 (2002) 123–134.
[7] E. Dytkiewitz, G.E. Morlock, Analytical strategy for rapid identification and quantification of lubricant additives in mineral oil by high-performance thin-layer chromatography with UV absorption and fluorescence detection combined with mass spectrometry and infrared spectroscopy, J. AOAC Int. 91 (2008) 1237–1244.
[8] G.W. Jóźwiak, B. Majer-Dziedzic, W. Jesionek, W. Zieliński, M. Waksmundzka-Hajnos, Thin-layer chromatography: Direct bioautography as a method of examination of antimicrobial activity of selected *Potentilla* species, J. Liq. Chromatogr. Relat. Technol. 39 (2016) 281–285.
[9] I. Choma, W. Jesionek, TLC-direct bioautography as a high throughput method for detection of antimicrobials in plants, Chromatography 2 (2015) 225–238.
[10] X.-J. Zhang, L.-J. Liu, T.-T. Song, Y.-Q. Wang, X.-h. Yang, An approach based on antioxidant fingerprint–efficacy relationship and TLC bioautography assay to quality evaluation of *Rubia cordifolia* from various sources, J. Nat. Med. 68 (2014) 448–454.
[11] L. Gu, T. Wu, Z. Wang, TLC bioautography-guided isolation of antioxidants from fruit of *Perilla frutescens* var. *acuta*, LWT-Food Sci. Technol. 42 (2009) 131–136.
[12] M. Jamshidi-Aidji, G.E. Morlock, Bioprofiling of unknown antibiotics in herbal extracts: Development of a streamlined direct bioautography using *Bacillus subtilis* linked to mass spectrometry, J. Chromatogr. A 1420 (2015) 110–118.
[13] G.E. Morlock, I. Klingelhöfer, Liquid chromatography-bioassay-mass spectrometry for profiling of physiologically active food, Anal. Chem. 86 (2014) 8289–8295.
[14] Q. Favre-Godal, E.F. Queiroz, J.-L. Wolfender, Latest developments in assessing antifungal activity using TLC-bioautography: A review, J. AOAC Int. 96 (2013) 1175–1188.
[15] I.A. Ramallo, S.A. Zacchino, R.L. Furlan, A rapid TLC autographic method for the detection of xanthine oxidase inhibitors and superoxide scavengers, Phytochem. Anal. 17 (2006) 15–19.
[16] Z. Yang, X. Zhang, D. Duan, Z. Song, M. Yang, S. Li, Modified TLC bioautographic method for screening acetylcholinesterase inhibitors from plant extracts, J. Sep. Sci. 32 (2009) 3257–3259.
[17] M.O. Salazar, R.L. Furlan, A rapid TLC autographic method for the detection of glucosidase inhibitors, Phytochem. Anal. 18 (2007) 209–212.
[18] E. Azadniya, G.E. Morlock, Hyphenation of HPTLC with NMR for structural elucidation of bioactive compounds in medicinal herbal extracts, in: 8th GGL Annual Conference, Giessen, Germany, 2015.
[19] X.-y. Zheng, Z.-j. Zhang, G.-x. Chou, T. Wu, X.-m. Cheng, C.-h. Wang, Z.-t. Wang, Acetylcholinesterase inhibitive activity-guided isolation of two new alkaloids from seeds of *Peganum nigellastrum* Bunge by an *in vitro* TLC-bioautographic assay, Arch. Pharmacal Res. 32 (2009) 1245–1251.
[20] S. Chun-Yan, M. Qian-Liang, K. Rahman, H. Ting, Q. Lu-Ping, *Salvia miltiorrhiza*: Traditional medicinal uses, chemistry, and pharmacology, Chin. J. Nat. Med. 13 (2015) 163–182.
[21] L. Zhou, Z. Zuo, M.S.S. Chow, Danshen: An overview of its chemistry, pharmacology, pharmacokinetics, and clinical use, J. Clin. Pharmacol. 45 (2005) 1345–1359.
[22] H. Pang, L. Wu, Y. Tang, G. Zhou, C. Qu, J.-a. Duan, Chemical analysis of the herbal medicine *Salviae miltiorrhizae* radix et rhizoma (Danshen), Molecules 21 (2016) 51–79.
[23] M. Yang, A. Liu, S. Guan, J. Sun, M. Xu, D. Guo, Characterization of tanshinones in the roots of *Salvia miltiorrhiza* (Dan-shen) by high-performance liquid chromatography with electrospray ionization tandem mass spectrometry, Rapid Commun. Mass Spectrom. 20 (2006) 1266–1280.
[24] S. Yang, X. Wu, W. Rui, J. Guo, Y. Feng, UPLC/Q-TOF-MS analysis for identification of hydrophilic phenolics and lipophilic diterpenoids from *Radix Salviae miltiorrhizae*, Acta Chromatogr. 27 (2015) 711–728.
[25] M.-J. Don, H.-C. Ko, C.-W. Yang, Y.-L. Lin, Detection of polyphenols and tanshinones in commercial Danshen by liquid chromatography with UV and mass spectrometry, J. Food Drug Anal. 14 (2006) 254–259.
[26] P. Hu, G.-A. Luo, Z. Zhao, Z.-H. Jiang, Quality assessment of *Radix Salviae miltiorrhizae*, Chem. Pharm. Bull. 53 (2005) 481–486.
[27] G. Zeng, J. Liu, L. Wang, Q. Xu, H. Xiao, X. Liang, A uniform HPLC method developed for the analysis of *Salvia miltiorrhiza*, *Panax notoginseng*, and Fufang Danshen, J. Chromatogr. Sci. 44 (2006) 591–595.
[28] H.-B. Li, F. Chen, Preparative isolation and purification of six diterpenoids from the Chinese medicinal plant *Salvia miltiorrhiza* by high-speed counter-current chromatography, J. Chromatogr. A 925 (2001) 109–114.
[29] M. Gu, S. Zhang, Z. Su, Y. Chen, F. Ouyang, Fingerprinting of *Salvia miltiorrhiza* Bunge by non-aqueous capillary electrophoresis compared with high-speed counter-current chromatography, J. Chromatogr. A 1057 (2004) 133–140.
[30] J. Yang, L.-l. Choi, D.-q. Li, F.-q. Yang, L.-j. Zeng, J. Zhao, S.-p. Li, Simultaneous analysis of hydrophilic and lipophilic compounds in *Salvia miltiorrhiza* by double-development HPTLC and scanning densitometry, J. Planar Chromatogr.-Mod. TLC 24 (2011) 257–263.
[31] G.E. Morlock, Chromatography combined with bioassays and other hyphenations – the direct link to the compound indicating the effect, in: Instrumental Methods for the Analysis and Identification of Bioactive Molecules, American Chemical Society, 2014, pp. 101–121.
[32] M. Jamshidi-Aidji, G.E. Morlock, From bioprofiling and characterization to bioquantification of natural antibiotics by direct bioautography linked to high-resolution mass spectrometry: Exemplarily shown for *Salvia miltiorrhiza* root, Anal. Chem. 88 (2016) 10979–10986.
[33] S. Krüger, O. Urmann, G.E. Morlock, Development of a planar chromatographic method for quantitation of anthocyanes in pomace, feed, juice and wine, J. Chromatogr. A 1289 (2013) 105–118.
[34] Water quality - Determination of the inhibitory effect of water samples on the light emission of *Vibrio fischeri* (Luminescent bacteria test) - Part 1: Method using freshly prepared bacteria, in: International Organization for Standardization, Geneva, Switzerland, 2007.

[35] A.A. Bulich, Use of luminescent bacteria for determining toxicity in aquatic environments ASTM International, Aquatic Toxicology: Proceedings of the Second Annual Symposium on Aquatic Toxicology (1979).
[36] D. Fichou, P. Ristivojevicí, G.E. Morlock, Proof-of-principle of rTLC, an open-source software developed for image evaluation and multivariate analysis of planar chromatograms, Anal. Chem. 88 (2016) 12494–12501.
[37] A. Marston, Thin-layer chromatography with biological detection in phytochemistry, J. Chromatogr. A 1218 (2011) 2676–2683.
[38] S. Hage, G.E. Morlock, Bioprofiling of *Salicaceae* bud extracts through high-performance thin-layer chromatography hyphenated to biochemical, microbiological and chemical detections, J. Chromatogr. A 1490 (2017) 201–211.
[39] A. Marston, J. Kissling, K. Hostettmann, A rapid TLC bioautographic method for the detection of acetylcholinesterase and butyrylcholinesterase inhibitors in plants, Phytochem. Anal. 13 (2002) 51–54.
[40] J. Deng, D. Zhang, W. Yang, An *in vitro* experiment on the antimicrobial effects of ethanol extract from *Salvia miltiorrhiza* Bunge on several oral pathogenic microbes, Shanghai, J. Stomatol. 15 (2006) 210–212.
[41] D.-S. Lee, S.-H. Lee, J.-G. Noh, S.-D. Hong, Antibacterial activities of cryptotanshinone and dihydrotanshinone I from a medicinal herb, *Salvia miltiorrhiza* Bunge, Biosci. Biotechnol. Biochem. 63 (1999) 2236–2239.
[42] J. Zhao, J. Lou, Y. Mou, P. Li, J. Wu, L. Zhou, Diterpenoid tanshinones and phenolic acids from cultured hairy roots of *Salvia miltiorrhiza* Bunge and their antimicrobial activities, Molecules 16 (2011) 2259–2267.
[43] A. Klöppel, W. Grasse, F. Brümmer, G. Morlock, HPTLC coupled with bioluminescence and mass spectrometry for bioactivity-based analysis of secondary metabolites in marine sponges, J. Planar Chromatogr.-Mod. TLC 21 (2008) 431–436.
[44] K. Jang, H.-Y. Kim, Synergistic effect of methanol extract of *Salvia miltiorrhiza* and antibiotics against dental caries pathogens, Kor. J. Microbiol. Biotechnol. 38 (2010) 289–294.
[45] B.-Q. Wang, *Salvia miltiorrhiza*: Chemical and pharmacological review of a medicinal plant, J. Med. Plants Res. 4 (2010) 2813–2820.
[46] J. Lee, Y. Ji, S. Lee, I. Lee, Effect of *Saliva miltiorrhiza* Bunge on antimicrobial activity and resistant gene regulation against methicillin-resistant *Staphylococcus aureus* (MRSA), J. Microbiol. 45 (2007) 350–357.
[47] H. Feng, H. Xiang, J. Zhang, G. Liu, N. Guo, X. Wang, X. Wu, X. Deng, L. Yu, Genome-wide transcriptional profiling of the response of *Staphylococcus aureus* to cryptotanshinone, J. Biomed. Biotechnol. 2009 (2009) 1–8, 617509.
[48] J.-D. Cha, M.-R. Jeong, K.-M. Choi, J.-H. Park, S.-M. Cha, K.-Y. Lee, Synergistic effect between cryptotanshinone and antibiotics in oral pathogenic bacteria, Adv. Biosci. Biotechnol. 4 (2013) 283–294.
[49] J.-Y. Wu, J. Ng, M. Shi, S.-J. Wu, Enhanced secondary metabolite (tanshinone) production of *Salvia miltiorrhiza* hairy roots in a novel root–bacteria coculture process, Appl. Microbiol. Biotechnol. 77 (2007) 543–550.
[50] K.K.-K. Wong, J.C.-K. Ngo, S. Liu, H.-q. Lin, C. Hu, P.-C. Shaw, D.C.-C. Wan, Interaction study of two diterpenes, cryptotanshinone and dihydrotanshinone, to human acetylcholinesterase and butyrylcholinesterase by molecular docking and kinetic analysis, Chem.-Biol. Interact. 187 (2010) 335–339.
[51] Y. Ren, P.J. Houghton, R.C. Hider, M.-J.R. Howes, Novel diterpenoid acetylcholinesterase inhibitors from *Salvia miltiorrhiza*, Planta Med. 70 (2004) 201–204.
[52] D.H. Kim, S.J. Jeon, J.W. Jung, S. Lee, B.H. Yoon, B.Y. Shin, K.H. Son, J.H. Cheong, Y.S. Kim, S.S. Kang, Tanshinone congeners improve memory impairments induced by scopolamine on passive avoidance tasks in mice, Eur. J. Pharmacol. 574 (2007) 140–147.
[53] Y. Zhou, W. Li, L. Xu, L. Chen, In *Salvia miltiorrhiza*, phenolic acids possess protective properties against amyloid β-induced cytotoxicity, and tanshinones act as acetylcholinesterase inhibitors, Environ. Toxicol. Pharmacol. 31 (2011) 443–452.
[54] J. Cheung, E.N. Gary, K. Shiomi, T.L. Rosenberry, Structures of human acetylcholinesterase bound to dihydrotanshinone I and territrem B show peripheral site flexibility, ACS Med. Chem. Lett. 4 (2013) 1091–1096.
[55] L.B. Roseiro, A.P. Rauter, M.L.M. Serralheiro, Polyphenols as acetylcholinesterase inhibitors: structural specificity and impact on human disease, Nutr. Aging 1 (2012) 99–111.
[56] E. Bendary, R. Francis, H. Ali, M. Sarwat, S. El Hady, Antioxidant and structure–activity relationships (SARs) of some phenolic and anilines compounds, AOAS 58 (2013) 173–181.
[57] H.S. Kang, H.Y. Chung, J.H. Jung, S.S. Kang, J.S. Choi, Antioxidant effect of *Salvia miltiorrhiza*, Arch. Pharmacal Res. 20 (1997) 496–500.
[58] Y. Tohaya, T. Ochiai, A correlation between the superoxide anion scavenging capacity of antioxidants and their antioxidant capacity as measured by the galvinoxyl or DPPH method, Jpn. J. Food Chem. Safety 20 (2013) 61–65.
[59] A. Matkowski, S. Zielińska, J. Oszmiański, E. Lamer-Zarawska, Antioxidant activity of extracts from leaves and roots of *Salvia miltiorrhiza* Bunge, *S. przewalskii* Maxim., and *S. verticillata* L, Bioresour. Technol. 99 (2008) 7892–7896.
[60] Y. Sun, H. Zhu, J. Wang, Z. Liu, J. Bi, Isolation and purification of salvianolic acid A and salvianolic acid B from *Salvia miltiorrhiza* by high-speed counter-current chromatography and comparison of their antioxidant activity, J. Chromatogr. B 877 (2009) 733–737.
[61] G.-R. Zhao, H.-M. Zhang, T.-X. Ye, Z.-J. Xiang, Y.-J. Yuan, Z.-X. Guo, L.-B. Zhao, Characterization of the radical scavenging and antioxidant activities of danshensu and salvianolic acid B, Food Chem. Toxicol. 46 (2008) 73–81.
[62] K.Q. Zhang, Y. Bao, P. Wu, R.T. Rosen, C.T. Ho, Antioxidative components of tanshen (*Salvia miltiorhiza* Bung, J. Agric. Food Chem. 38 (1990) 1194–1197.
[63] Ł. Cieśla, D. Staszek, M. Hajnos, T. Kowalska, M. Waksmundzka-Hajnos, Development of chromatographic and free radical scavenging activity fingerprints by thin-layer chromatography for selected *Salvia* species, Phytochem. Anal. 22 (2011) 59–65.
[64] P. Li, G. Xu, S.-P. Li, Y.-T. Wang, T.-P. Fan, Q.-S. Zhao, Q.-W. Zhang, Optimizing ultraperformance liquid chromatographic analysis of 10 diterpenoid compounds in *Salvia miltiorrhiza* using central composite design, J. Agric. Food Chem. 56 (2008) 1164–1171.
[65] S.Y. Ryu, Z. No, S.H. Kim, J.W. Ahn, Two novel abietane diterpenes from *Salvia miltiorrhiza*, Planta Med. 63 (1997) 44–46.
[66] Y.-L. Lin, C.-Y. Liu, T.-H. Chen, M.-Y. Kang, M.-J. Don, Acetyl danshenxinkun A from *Salvia miltiorrhiza*, J. Chin. Med. 14 (2003) 123–128.
[67] W.-L. Wu, W.-L. Chang, C.-F. Chen, Cytotoxic activities of tanshinones against human carcinoma cell lines, Am. J. Chin. Med 19 (1991) 207–216.
[68] X. Yan, Dan Shen (*Salvia miltiorrhiza*) in medicine biology and chemistry, vol. 1, Springer, 2014.
[69] P.-S. Xie, S. Sun, S. Xu, L. Guo, Value the unique merit of HPTLC image analysis and extending its performance by digitalization for herbal medicines quality control, J. Chromatogr. Sep. Tech. 5 (2014) 1–9.
[70] G. Tian, T. Zhang, Y. Zhang, Y. Ito, Separation of tanshinones from *Salvia miltiorrhiza* Bunge by multidimensional counter-current chromatography, J. Chromatogr. A 945 (2002) 281–285.
[71] S. Wu, D. Wu, J. Liang, A. Berthod, Modeling gradient elution in countercurrent chromatography: Efficient separation of tanshinones from *Salvia miltiorrhiza* Bunge, J. Sep. Sci. 35 (2012) 964–976.
[72] N. Okamura, K. Kobayashi, A. Yagi, T. Kitazawa, K. Shimomura, High-performance liquid chromatography of abietane-type compounds, J. Chromatogr. A 542 (1991) 317–326.
[73] S. Ślusarczyk, S. Zimmermann, M. Kaiser, A. Matkowski, M. Hamburger, M. Adams, Antiplasmodial and antitrypanosomal activity of tanshinone-type diterpenoids from Salvia miltiorrhiza, Planta Med. 77 (2011) 1594–1596.
[74] J. Ruh, Wissenschaftliche Abschlussarbeit zum 1. Staatsexamen, Universität Hohenheim, Stuttgart, Germany, 2010.

Supplementary data

Bioprofiling of *Salvia miltiorrhiza* via planar chromatography linked to (bio)assays, high resolution mass spectrometry and nuclear magnetic resonance spectroscopy

Ebrahim Azadniya[a] and Gertrud E. Morlock[a,*]

[a]Chair of Food Science, Institute of Nutritional Science, and Interdisciplinary Research Center (IFZ), Justus Liebig University Giessen, Heinrich-Buff-Ring 26-32, 35392 Giessen, Germany

*Corresponding author. Tel.: +49-641-99-39141; fax: +49-641-99-39149.
E-mail addresses: Gertrud.Morlock@uni-giessen.de (G. E. Morlock),
Ebrahim.Azadniya@chemie.uni-giessen.de (E. Azadniya)

Table of Contents

520 nm (a) and documented under white light illumination after DPPH$^{\bullet}$ (b) and *a priori* at UV 366 nm (c).

Page S-10 **Fig. S-4.** HSQC spectrum of unidentified compound 1, showing the correlation of protons in the range of 5 to 6 ppm with different vinyl carbons as a confirmation of including both, 1,2-DHTI and MTQ.

Table S-1. Application volumes used for two-step development, followed by effect-directed detection.

Track no.	Extract** or standard	Concentration	Application volumes (µL/band) for			
			A. fischeri	*B. subtilis*	AChE	DPPH˙
1	B2	100 mg/mL	5	5	0.25	0.25
2	B2	100 mg/mL	7.5	7.5	0.5	0.5
3	A1	300 mg/mL	5	5	1	1
4	A1	300 mg/mL	7.5	7.5	2	2
5	B1	300 mg/mL	5	5	1	1
6	B1	300 mg/mL	7.5	7.5	2	2
7*	SAB	1000 ng/µL	5	5	3	1
7*	LSA	500 ng/µL	5	5	3	1
7*	SAA	500 ng/µL	5	5	3	1
7*	RA	150 ng/µL	5	5	3	1
7*	CA	250 ng/µL	3	3	3	1
7*	PCAD	500 ng/µL	2	2	3	1
8*	A1	300 mg/mL	5	5	1	1
8*	A4	250 mg/mL	1	1	5	1
9*	B1	300 mg/mL	5	5	1	1
9*	B4	250 mg/mL	1	1	5	1
10	A3	100 mg/mL	0.5	0.5	1	1
11	A3	100 mg/mL	1	1	3	2
12	B3	100 mg/mL	0.5	0.5	1	1
13	B3	100 mg/mL	1	1	3	2
14*	CT	100 ng/µL	1	1	2	0.5
14*	DHTI	20 ng/µL	1	1	3	0.5
14*	TI	100 ng/µL	4	4	4	0.5
14*	TIIA	100 ng/µL	4	4	3	0.5
15	A4	250 mg/mL	0.5	1	5	1
16	A4	250 mg/mL	1	2	10	2
17	B4	250 mg/mL	0.5	1	5	1
18	B4	250 mg/mL	1	2	10	2
19	A5	100 mg/mL	0.5	1	5	1
20	A5	100 mg/mL	1	2	10	2
21	B5	100 mg/mL	0.5	1	5	1
22	B5	100 mg/mL	1	2	10	2

*Oversprayed application

**A: sample A; B: sample B; 1: acidified water-ethyl acetate; 2: acidified water-ethyl acetate, DLLE; 3: methanol; 4: ethanol - pentyl acetate (4:1, *V/V*); 5: ethanol

Table S-2. List of mobile phases (MPs) investigated for polar and nonpolar developments (best MP in bold).

Polar MP	Solvent mixture	Solvent ratio (*V*/*V*)	Acid content (%)
1	Toluene - ethyl acetate - formic acid - water	3:4:1:0.4	12
2	Toluene - ethyl acetate - methanol - formic acid	10:8:1:4	17
3	Toluene - acetone - formic acid	5:4:1	10
4	Toluene - chloroform - ethyl acetate - methanol - formic acid	4:6:8:0.4:4	18
5	Toluene - chloroform - ethyl acetate - methanol - formic acid	4:6:8:0.4:2	10
6	**Toluene - chloroform - ethyl acetate - methanol - formic acid**	**4:6:8:1:1**	**5**
7	Toluene - pentyl acetate - ethyl acetate - methanol - formic acid	4:6:8:1:1	5
Non-polar MP			
8	Toluene - ethyl acetate - formic acid	7:3:0.1	1
9	*n*-Hexane - ethyl acetate	4:1	0
10	*n*-Hexane - ethyl acetate	7:1	0
11	*n*-Hexane - toluene - ethyl acetate	7:1:1	0
12	**Petroleum ether (60-80°C) - cyclohexane - ethyl acetate**	**5:2.8:2.2**	**0**
13	Petroleum ether (40-60 °C) – cyclohexane - ethyl acetate	5:2.8:2.2	0
14	Petroleum ether (40-60 °C) - cyclohexane - ethyl acetate	5:2:3	0
15	*n*-Hexane - cyclohexane - ethyl acetate	5:2.8:2.2	0

Table S-3. Neutralization methods investigated for compatibility with subsequent (bio)assay.

Neutralization method	**Step 1 Drying**	**Step 2 Chemical reagent**	**Step 3 Drying**
1	30 min ADC 2	Immersion into 4% (*W/V*) phosphate-citrate buffer	5 min drying with cold stream of air
2	30 min ADC 2	Immersion into 8% (*W/V*) phosphate-citrate buffer	5 min drying with cold stream of air
3	-	8 min NH_3 vapor exposure	8 min ADC 2

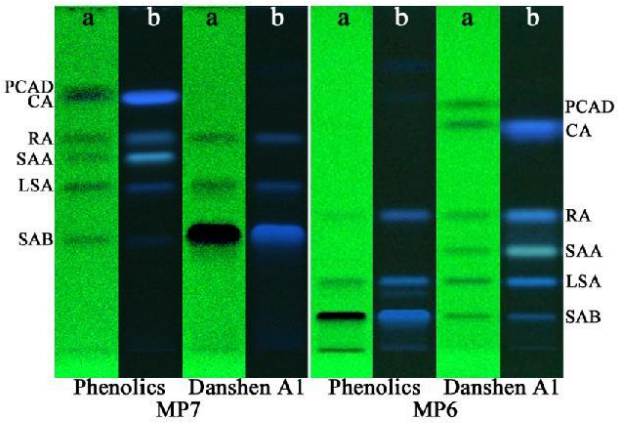

Fig. S-1. Chromatograms of phenolics (0.5 µg/band) and Danshen extract A1 (2 µL/band) at UV 254 nm (a) and UV 366 nm (b) on HPTLC silica gel with toluene - chloroform - ethyl acetate - methanol - formic acid, 4:6:8:1:1 (MP 6) and toluene - pentyl acetate - ethyl acetate - methanol - formic acid, 4:6:8:1:1 (MP 7).

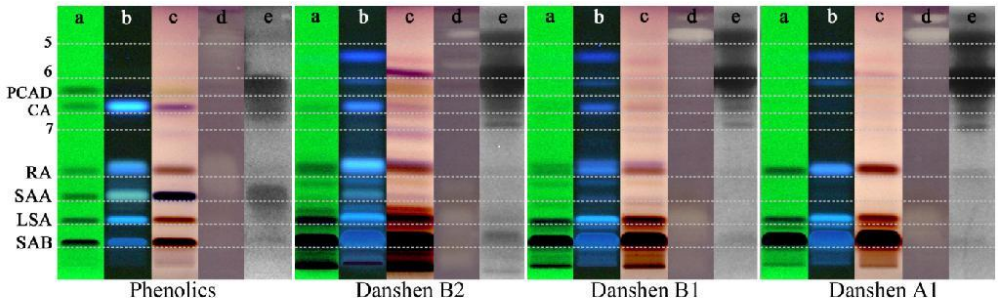

Fig. S-2. Chromatograms of phenolics (SAB 10 µg/band, LSA and SAA 2.5 µg/band as well as RA 0.75/1.5 µg/band, CA 1.25/0.75 µg/band and PCAD 2.5/1.5 µg/band for *B. subtilis/A. fischeri*, respectively) and the polar Danshen extracts (10 µL/band each) on HPTLC silica gel with toluene - chloroform - ethyl acetate - methanol - formic acid, 4:6:8:1:1 (MP 6) documented at UV 254 nm (a), UV 366 nm (b) and after derivatization via anisaldehyde sulfuric acid reagent (c) as well as respective bioautograms after *B. subtilis* (d) and *A. fischeri* bioassays (e).

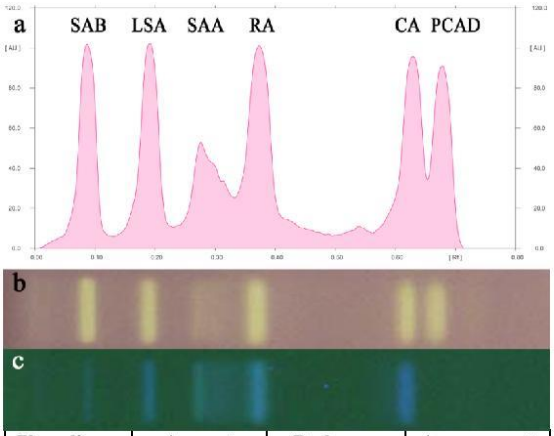

Phenolics	Amount (ng/band)	Peak area (AU)	Area percent (%)
RA	50	2913	22
CA	50	2504	19
LSA	50	2369	18
SAB	50	2180	16
PCAD	50	1962	15
SAA	50	1541	11

Fig. S-3. Comparison of the radical scavenging activity of the different phenolics SAB, LSA, SAA, RA, CA and PCAD (50 ng/band each) on HPTLC silica gel with toluene - chloroform - ethyl acetate - methanol - formic acid, 4:6:8:1:1 (MP 6) after derivatization via DPPH$^{\cdot}$ reagent by inverse scan at 520 nm (a) and documented under white light illumination after DPPH$^{\cdot}$ (b) and *a priori* at UV 366 nm (c).

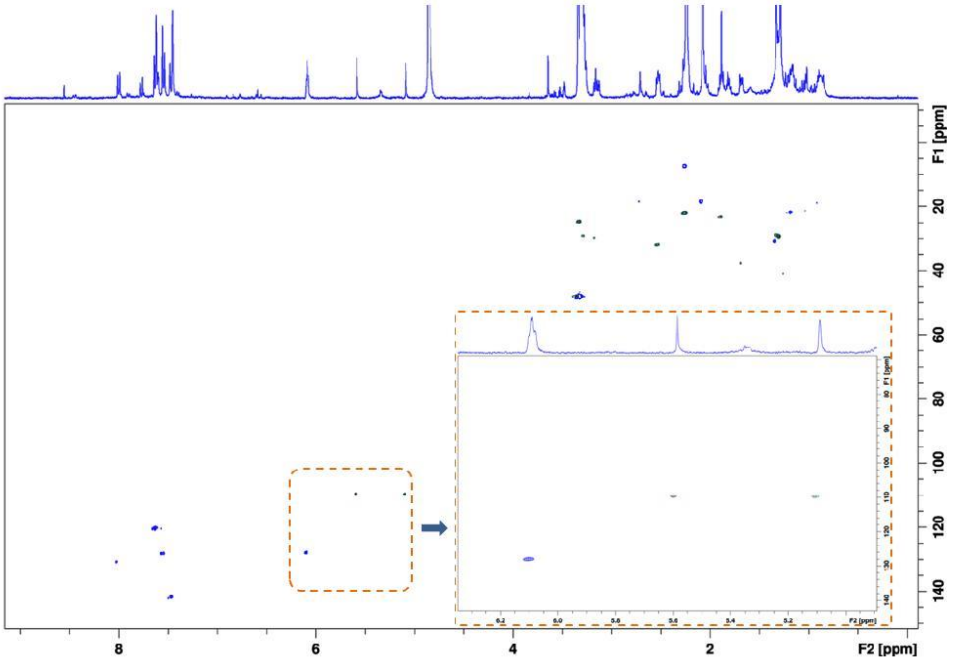

Fig. S-4. HSQC spectrum of unidentified compound 1, showing the correlation of protons in the range of 5 to 6 ppm with different vinyl carbons as a confirmation of including both, 1,2-DHTI and MTQ.

3. PUBLICATION 2

Automated piezoelectric spraying of biological and enzymatic assays for effect-directed analysis of planar chromatograms

Ebrahim Azadniya[a,b], Gertrud E. Morlock[a,b,*]

[a]*Chair of Food Science, Institute of Nutritional Science, Interdisciplinary Research Center (IFZ), Justus Liebig University Giessen, Heinrich-Buff-Ring 26-32, 35392, Giessen, Germany*

[b]*TransMIT Center of Effect-Directed Analysis, Kerkrader Straße 3, 35394 Giessen, Germany*

Published in

Journal of Chromatography A, 1602 (2019) 458–466

Received 14 April 2019, Received in revised form 22 May 2019, Accepted 23 May 2019, Available online 24 May 2019

Journal of Chromatography A, 1602 (2019) 458–466

Contents lists available at ScienceDirect

Journal of Chromatography A

journal homepage: www.elsevier.com/locate/chroma

Automated piezoelectric spraying of biological and enzymatic assays for effect-directed analysis of planar chromatograms

Ebrahim Azadniya[a,b], Gertrud E. Morlock[a,b,*]

[a] Chair of Food Science, Institute of Nutritional Science, and Interdisciplinary Research Center, Justus Liebig University Giessen, Heinrich-Buff-Ring 26-32, 35392 Giessen, Germany
[b] TransMIT Center of Effect-Directed Analysis, Kerkrader Straße 3, 35394 Giessen, Germany

ARTICLE INFO

Article history:
Received 14 April 2019
Received in revised form 22 May 2019
Accepted 23 May 2019
Available online 24 May 2019

Keywords:
Automated quantitative piezoelectric spraying
Acetyl-/butyrylcholinesterase
Aliivibrio fischeri
Peganum harmala
Enzyme inhibitory equivalency
Physostigmine (eserine)

ABSTRACT

Bioanalytical questions are more and more solved by bioassays directly *in situ* the planar separation. If compared to chemical derivatization *in situ*, several reagent applications on the same chromatogram make the workflow for enzymatic and biological assays more complex. Hence, if compared to piezoelectric spraying of chemical derivatization reagents, an assay transfer to the piezoelectric spraying technique was much more challenging. Important aspects were investigated, *i.e.*, plate pre-wetting, spraying nozzle type and applied volumes for microorganism suspension as well as enzyme and substrate-chromogenic solutions. Finally, with the newly developed piezoelectric spraying procedures for the application of biological (*Aliivibrio fischeri*) and enzymatic (acetyl- and butyrylcholinesterase) assays, several obstacles of the state-of-the-art automated immersion were avoided such as the (1) required high volumes of solutions, (2) tailing of highly water-soluble zones upon slow plate withdrawal, (3) zone distortion or shift observed after previous buffer salt applications or long/slow immersion times/speeds, (4) gradual inactivation of the enzyme solution along with its ongoing re-use, and (5) lack of covering the whole plate surface. The benchmarking of both techniques also showed that simplicity remains the key argument for immersion. As proof of concept, piezoelectrically sprayed autograms were compared with those of immersion, by taking the example of *Peganum harmala* (*P. h.*) seed extract. The plate background and thus homogeneity of the applied solutions were found to be almost comparable. Three bands among the pronounced fluorescent bands were responsible for the most antibacterial activity of *P. h.* seed extract in the *A. fischeri* bioassay and were also inhibiting the AChE. These AChE and three further BChE inhibitors were detected, whereby the AChE inhibition was twice as strong as the BChE inhibition. By their *in situ* HRMS spectra, the active zones in the *P. h.* seed extract were assigned to be the AChE-inhibiting β-carboline alkaloids, harmine, harmaline and ruine, as well as the BChE-inhibiting quinazoline alkaloids, vasicine and deoxyvasicine, and the β-carboline alkaloid harmol. For the first time, the found inhibitors were calculated equivalently to the well-known ChE-inhibitor physostigmine, and thus, piezoelectric spraying was proven to be suited for quantifications.

1. Introduction

High-performance thin-layer chromatography (HPTLC) hyphenated with effect-directed analysis (EDA) allows a biochemical and biological profiling of complex samples. For example, HPTLC-EDA was demonstrated to detect enzyme inhibiting [1–4], antibacterial [5,6], antifungal [7,8] and antioxidant compounds [9]. In contrast to dot-blot, microtiter plate and cuvette assays, TLC/HPTLC combined with biological or biochemical assays points to effects of single compound zones in complex sample mixtures without any previous fractionation [10]. If compared to contact and agar-overlay bioautography, direct bioautography (DB) is a more straightforward and efficient workflow for biological profiling, considering handling, detectability, resolution and analysis time [5,11,12]. The ease in the handling of DB is that the microbiological suspensions can be applied on the planar chromatogram in the same mode as microchemical derivatization reagents which is mainly done by immersion [13] or spraying [14]. So far, biochemi-

* Corresponding author at: Chair of Food Science, Institute of Nutritional Science, and Interdisciplinary Research Center, Justus Liebig University Giessen, Heinrich-Buff-Ring 26-32, 35392 Giessen, Germany.
E-mail addresses: Ebrahim.Azadniya@chemie.uni-giessen.de (E. Azadniya), Gertrud.Morlock@uni-giessen.de (G.E. Morlock).
URL: http://mailto:Ebrahim.Azadniya@chemie.uni-giessen.de (E. Azadniya).

https://doi.org/10.1016/j.chroma.2019.05.043
0021-9673/

cal and biological assays, especially the cell suspensions, have been applied *via* immersion [5,10,15,16] or manual spraying [17]. Also a combination of both was used for the HPTLC-acetylcholinesterase (AChE) assay [18]. The ink-jet print on HPTLC plates of a derivatization reagent solution [19] or bacteria suspension that survived the nozzle voltage [20] were shown to open up new opportunities, *e.g.*, selective targeted application and less reagent consumption (μL range).

The latest trends tend to less reagent consumption and higher background homogeneity to make HPTLC-EDA procedures more efficient and environmentally friendly [19,20]. In 2016, an automated piezoelectric spraying device (Derivatizer, CAMAG) was launched on the market for homogeneous application of derivatization reagents on the adsorbent. Generally, a piezoelectric crystal produces the micro-droplets by converting the electric signal to mechanical vibrations [21]. This technology was used in the nozzle which has a palladium-alloy membrane (mesh size 4–12 μm) attached to a piezoelectric ceramic vibrating with an ultrasonic frequency. Among many chemical reagents listed, the Derivatizer was also suggested for application of the tyrosinase assay, which procedure was recently adjusted in our laboratory [22–24]. Further biochemical assays or biological assays applied by piezoelectric spraying have not been reported so far. However, an automated piezoelectric spraying of microorganisms could be an alternative, as experienced for the ink-jet printing of bacteria in 2008 [20].

In this study, piezoelectric spraying was studied for the first time for the application of biological assays, such as the HPTLC-*Aliivibrio fischeri* bioassay, which was used among others in the bioprofiling of herbals [10] or water quality control [25]. To widen the study range, the quality of the piezoelectric spraying was further investigated for enzymatic assays, such as the cholinesterase (ChE) inhibition assays used in the field of drug discovery [26] as well as neurobiology, toxicology, food safety, environmental monitoring and diagnosis after exposure to pesticides [27]. As sample to study, the *Peganum harmala* (*P. h.*, Zygophyllaceae) known as Espand or Syrian Rue, with pharmacological effects including anticancer, gastrointestinal, neurologic, and antimicrobial activities, was selected [28]. The *P. h.* seed extract was reported to contain vasicine and vasicinone (quinazoline alkaloids) as well as harmine, harmaline, harman and harmalol (*β*-carbolines) [28], and showed inhibition zones by visual TLC-AChE evaluation [29,30]. Hence, a reliable quantitative effect-directed evaluation was of interest. Despite of many research about antibacterial effect of the *P. h.* seed extract against Gram-negative [31,32] and Gram-positive [31,32] bacteria, any antimicrobial study against Gram-negative *A. fischeri* bacteria has not been reported so far, and thus, was investigated first in this study. As a proof of principle, the ChE autograms (biochemical profiling) obtained by automated piezoelectric spraying were compared with those of automated immersion (state-of-the-art technique). For the first time, the distinct ChE inhibition zones detected (without any tailing and diffusion) were equivalently calculated to physostigmine as a well-known ChE-inhibitor, to demonstrate the quantitative capability and performance of the newly developed piezoelectric spraying workflow.

2. Material and methods

2.1. Chemicals and reagents

Physostigmine (PHY) and 1-naphthyl acetate were purchased from Santa Cruz Biotechnology, Heidelberg, Germany, and Panreac, Barcelona, Spain, respectively. Lyophilized powder of butyrylcholinesterase (BChE, equine serum) and AChE (*Electrophorus electricus*, electric eel), Fast Blue B salt, caffeine and potassium iodide were provided from Sigma Aldrich, Steinheim, Germany. Luminescent marine *A. fischeri* bacteria (DSM no. 5171) were obtained from the German Collection of Microorganisms and Cell Cultures. Solvents of analytical grade were used. Toluene, ethyl acetate and ammonia (25%) were obtained from Th. Geyer, Berlin, Germany. Bismuth carbonate, hydrogen chloride (HCl), acetic acid, sulfuric acid (98%), formic acid (96%), tris(hydroxymethyl)-aminomethane (Tris), sodium monohydrogen phosphate, bovine serum albumin, and anisaldehyde were purchased from Carl Roth, Karlsruhe, Germany. Ethanol, methanol and its MS-grade were provided from Fisher Scientific, Schwerte, Germany. Citric acid and HPTLC plates silica gel 60 F_{254} were purchased from Merck, Darmstadt, Germany. HPTLC plates were prewashed twice by chromatography with methanol and water 3:1, *V*/*V*, then dried at 120 °C in a clean oven for 1 h, covered with a clean counter glass plate and stored wrapped in aluminum foil.

2.2. Standard solutions and sample preparation

Ground *P. h.* seed (1 g, 0.5-mm sieve) were extracted with 10 mL ethanol and water 3:2, *V*/*V*, on the stirrer at room temperature for 30 min, followed by ultrasonication for 30 min and centrifugation at 756 × *g* for 15 min (100 mg/mL). The resulting supernatant was used directly, or diluted 1:20 and 1:200 with methanol (5 and 0.5 mg/mL). Methanolic standard solutions of PHY (0.1 μg/mL) and caffeine (1 mg/mL) were prepared.

2.3. Pattern application

PHY and caffeine solutions were applied on the HPTLC plate as 6-band-pattern track (8-mm band length and 10–15 mm vertical distance) in the range of 1–15 μL/band (0.1–1.5 ng/band for PHY and 1–15 μg/band for caffeine) using the FreeMode of the winCATS software operated by Automatic TLC Sampler 4 (ATS 4, CAMAG).

2.4. HPTLC method

PHY solution was applied in the range of 1–15 μL/band (0.1–1.5 ng/band) as 8-mm bands on the HPTLC plate using the ATS 4 and winCATS software (CAMAG). *P. h.* seed extract solution (1–10 μL/band, 100 mg/mL) was applied for the *A. fischeri* bioassay (100–1000 μg/band). For the ChE inhibition assay, 0.5–2 μL/band of the 100 mg/mL solution (50–200 μg/band) were applied, whereas 2 and 10 μL/band of the 5 mg/mL solution were used for HRMS and 2 μL/band of the 0.5 mg/mL solution for ChE inhibitory equivalency calculation. After chamber saturation for 5 min, the plates were developed either with an acidic mobile phase (AMP), consisting of ethyl acetate - toluene - formic acid - water 16:4:3:2, *V*/*V*/*V*/*V* [15], or basic mobile phase (BMP) consisting of ethyl acetate - methanol - ammonia (25%) 8.5:1.1:0.4, *V*/*V*/*V*, up to 85 mm (70 mm for *A. fischeri*) in the Twin Trough Chamber (CAMAG). After drying (Table S1), chromatograms were documented at UV 254 nm, UV 366 nm and white light illumination.

2.5. Piezoelectric spraying

The Derivatizer (for 20 × 10 cm plates, CAMAG) was used at the spraying speed of 6 for derivatization, plate neutralization and (bio)assay application. The detailed parameters were listed in Table S2. In case of drying, the plate was dried using the humidity control or drying modes of the Automatic Developing Chamber 2 (ADC 2, CAMAG) as well as a hair dryer (Table S1). For HPTLC-ChE inhibitory assays, the chromatogram developed with AMP was neutralized (not needed for BMP) and pre-wetted (W) with 1 mL Tris-HCl buffer before application of the enzyme (E) solution (3 mL), all piezoelectrically sprayed (Table S2), followed by incubation at

37 °C for 25 min in a humid box. In case of using the same nozzle for two different solutions, it is necessary to clean the nozzle in-between. After spraying the Tris-HCl buffer, a nozzle washing was not necessary for the following spraying of E-solution, but the bottom side of the Green nozzle was dried to avoid dropping on the plate. The ChE-inhibitors were visualized by spraying of 0.5 mL substrate-chromogenic (S) solution, followed by drying (Table S1) and documentation, as white zones on a purple background under white light illumination (transmission and reflection modes, automatic capture of the image).

The *A. fischeri* culture medium was prepared according to DIN EN ISO 11348-1 [33]. Briefly, 150 μL of the bacterial cryostock (−80 °C) were added to 20 mL medium, and this suspension was incubated in a 100 mL Erlenmeyer flask when shaking (75 rpm) at room temperature. After 18–24 h, the bacterial luminescence was visually checked for its brilliance by shaking the flask in a dark room. Bacteria suspensions can be sub-cultivated for approximately 1 week by transferring an aliquot of 1 mL strongly luminescent bacteria suspension into 20 mL fresh medium. The *A. fischeri* suspension (4 mL) was piezoelectrically sprayed on the chromatogram developed with BMP *via* the Derivatizer (Table S2). After settling down of the micro droplets, the plate was immediately transferred to the BioLuminizer (CAMAG) and the hood was closed again to suck out the rest into the trap. The luminescent bioautogram was documented with the BioLuminizer for 30 min, using an exposure time of 60 s and 1.1 min trigger intervals. Dark zones indicated the bioactive compounds inhibiting the luminescence of the *A. fischeri* bacteria [34].

2.6. Automated immersion

The chromatogram was immersed for neutralization and (bio)assay application using the immersion chamber sized 10 × 10 cm or 20 × 10 cm (Biostep, Burkhardtsdorf, Germany) and the TLC Immersion Device (CAMAG). Parameters were listed in Table S3.

2.7. HPTLC-ChE inhibitory equivalency calculation

P. h. seed extract solution was three-fold applied (1 μg/band each). PHY was applied at 6 levels (0.1–1.5 ng/band) for the development with BMP. After drying (Table S1), both ChE assays (AChE and BChE) were performed *via* piezoelectric spraying. The enzyme inhibition densitograms of both assays were obtained by inverse scan measurement (florescence without optical filter) at 546 nm using the mercury lamp (TLC Scanner 4, CAMAG). For information on reproducibility, the experiments for both ChE assays were performed four times ($n = 4$).

2.8. HPTLC-HRMS

The *P. h.* seed extract solution (10 and 50 μg/band) was applied in triplicate on a prewashed HPTLC plate and developed with BMP up to 85 mm. The chromatogram was divided by smartCut Plate Cutter (CAMAG). Two pieces were subjected to the ChE assays and a third piece for HRMS. The positions of the active zones were marked on the HRMS piece under 254 nm and 366 nm using a soft pencil. An elution head-based interface (Plate Express, Advion, Ithaca, NY, USA) transferred the active substances to the heated electrospray ionization (HESI) source connected to a Q Exactive Plus Hybrid Quadrupole-Orbitrap Mass Spectrometer (Thermo Fisher Scientific, Dreieich, Germany). The zone of interest was tightly fixed by the oval elution head (4 mm × 2 mm, 320 N) and eluted for 60 s at a flow rate of 0.1 mL/min using methanol for the positive ionization mode. All mass spectra were recorded in the full scan mode between m/z 50 and m/z 750. Sodium diisooctyl phthalate (m/z 413.26623) was used as lock mass. The settings included spray voltage +3.5 kV and capillary temperature 270 °C. The MS data processing was done with Xcalibur 3.0.63 software (Thermo Fisher Scientific). A representative plate background (located at a similar hR_F position as the zone of interest) was recorded as well as a piece of a clean aluminium plate (system background *via* elution head), which were subtracted from the analyte mass spectrum.

3. Results and discussion

3.1. Challenges

Similar to immersion, piezoelectric spraying should also be able to homogenously cover the chromatogram. The generated fine micro-droplets of respective solutions should be adsorbed on the surface and migrate into the layer depth until saturated with liquid. However, if compared to chemical derivatization reagents, several solutions need to be applied on the same chromatogram for enzymatic and biological assays, which makes the workflow more complex. For example, the chromatogram developed with an acidic mobile phase needs to be neutralized, dried and pre-wetted before enzyme application, and after incubation, the substrate-chromogenic solution needs to be applied. Several drawbacks occurred for such a multi-step usage of the piezoelectric spraying device. For example, the frequent use of the same nozzle for repeated piezoelectric spraying on the same chromatogram tended to cause drops in the chromatogram center or inhomogeneous colored background or a prior reaction within the nozzle (of the previous/residual enzyme with the following substrate-chromogenic reagent). This was solved by nozzle cleaning and/or nozzle change within the workflow.

3.2. Neutralization of the acidic chromatogram prior to the assay

As for the automated immersion, also the results for initial piezoelectric spraying revealed that remaining acid traces after using an acidic mobile phase for separation of compounds in the *P. h.* seed extract (Fig. 1Aa and b) hampered the generation of the purple plate background of the AChE assay (Fig. 1Ac). Thus, a neutralization of the chromatogram was *conditio sine qua non*. The same was evident in case of an insufficient neutralization (Fig. 1A d, with 25% ammonia vapor in the Twin Trough Chamber for 10 min followed by drying, Table S1). Hence, the neutralization was studied using piezoelectric spraying of 2, 3 and 4 mL phosphate-citrate buffer with nozzle G (Table S2). The resulting autograms of 2 and 3 mL buffer showed almost the same image (Fig. 1Ae and f), whereas that of 4 mL buffer (Fig. 1Ag) showed a zone tailing due to the overlaying liquid flowing downwards, while turning the plate in the vertical position after the piezoelectric spraying. For comparison with the state-of-the-art automatic immersion technique, a chromatogram was immersed into the phosphate-citrate buffer (Table S3), which caused a slight zone tailing in the direction of plate withdrawal (Fig. 1Ah). Hence, 2–3 mL buffer were able to neutralize the chromatogram developed with 12% formic acid (AMP) without any tailing or diffusion.

3.3. Optimized piezoelectric spraying for the ChE assays

The comparison with manual spraying was not considered due to the not exactly known consumption of E- and S-solutions. While other methods with a lower concentrated E-solution (1 U/mL) [2] or cheaper S-solution [35] were reported, the ChE assays were carried out based on the latest modified procedure [16,36] of the Marston's method [37], however, using piezoelectric spraying instead of automated immersion. Dry chromatograms were pre-wetted (W) by piezoelectric spraying of two different volumes of Tris-HCl buffer

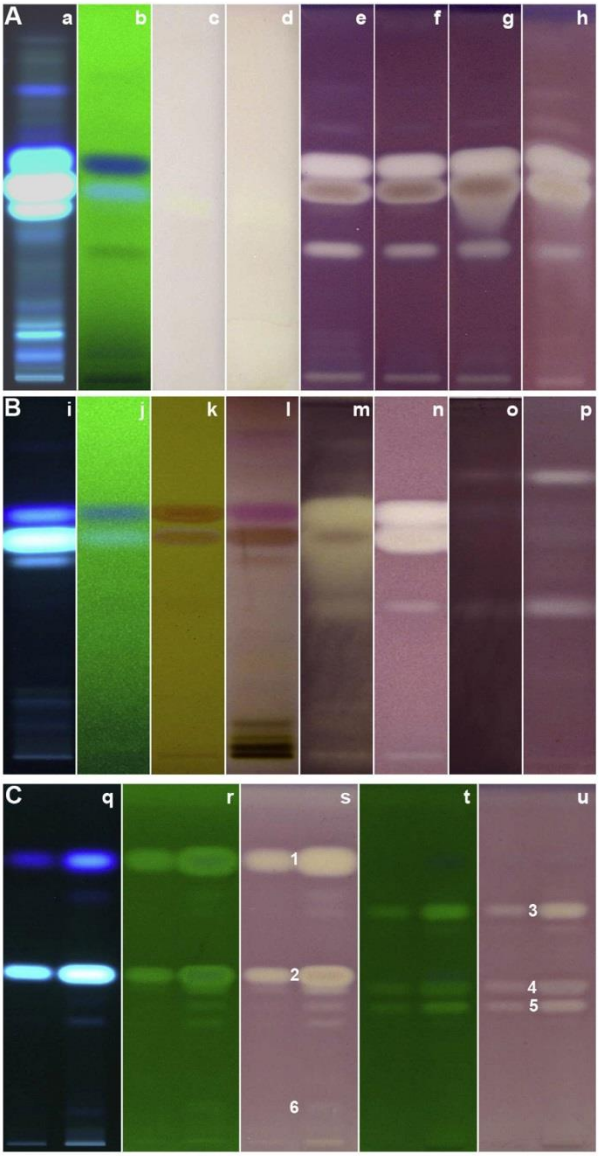

Fig. 1. Study of piezoelectric spraying of chromatograms of *P. h.* seed extract: (A) Separation with AMP of 200-μg applied seed extract detected at 366 nm (a), 254 nm (b) and respective AChE autograms at white light illumination without neutralization (c), with neutralization with ammonia vapor (d), after piezoelectric spraying with 2 (e), 3 (f) and 4 mL (g) of phosphate-citrate buffer (8% *W/V*, pH 7.8) *versus* immersion (h); (B) final workflow for 50-μg applied seed extract at 366 nm (i), 254 nm (j), after derivatization with Dragendorff's (k) and anisaldehyde sulfuric acid (l) reagents, respective AChE (m, n) and BChE autograms (o, p) by immersion (m, o) *versus* piezoelectric spraying (n, p); (C) BMP separation (10 and 50 μg/band) at 366 nm (q) and AChE (r, s) and BChE (t, u) autograms at 254 nm and white light illumination (RT mode); zone no. 1-5 as in Table 2.

(1 and 4 mL), which both were compared with results of the dry chromatogram. Different volumes of E-solution (2, 3 and 4 mL) and S-solution (0.5, 1, 2 and 4 mL) as well as four nozzle types were studied. The nozzle mesh sizes were increasing as follows: green G 4–5 μm < blue B 5–7 μm < yellow Y 7–9 μm < red R 9–12 μm. To study and find the optimal parameters, a PHY pattern was applied, because a chromatographic separation was not necessary for this study. The optimization for the AChE assay comprised five phases,

as described in the supplement along with Figs. S1 and S2. This led to the finally selected W:E:S volume ratio of 1:3:0.5 for the AChE assay. It was transferred to the BChE assay with both nozzles (G and R), used individually or in combination (Fig. S3). The nozzle combination G:G:R for the 1:3:0.5 W:E:S volume ratio was preferred since the nozzle change for the third spraying avoided any residual enzyme reacting with S-solution within the nozzle or a potential dropping of the solutions, which was observed for longer working periods with the same nozzle. Hence, this combination (G:G:R nozzles and 1:3:0.5 mL for W:E:S) was selected for piezoelectric spraying of both ChE inhibition assays.

3.4. *Biochemical profiling of* P. h. *seed extract* via *piezoelectric spraying* versus *immersion*

The ethanol – water (3:2, *V*/*V*) mixture extracted a wide range of compounds from the *P. h.* seed sample, especially polar and mid-polar compounds. Thus, acidic and basic mobile phases (AMP and BMP) were tested. First, the AMP-developed fingerprints (Fig. 1Bi–l) were compared with the resulting autograms obtained by automated immersion (Fig. 1B m and o) *versus* piezoelectric spraying (Fig. 1Bn and p) including plate neutralization. Immersion led to more diffuse and tailing zones than spraying, especially at higher sample amounts (Fig. S4 c and e, more diffuse zones at 200 μg *versus* 50 μg). In contrast, piezoelectric spraying showed clean and sharp bands without any tailing and diffusion (Fig. 1Bn and p, Fig. S4 d and f). The diffusion of BChE active zones in the autogram obtained by immersion (Fig. 1Bo) was less pronounced due to the lower activities of the BChE zones. Although the two main blue fluorescent bands (Fig. 1Aa and b) showed very weak BChE inhibition, their zone shapes were slightly more diffuse by immersion as by piezoelectric spraying. Diffusion/tailing effects are caused by the solubility of the active zones in the different reagent solutions during the immersion process (Figs. 1Bm, S4c). In contrast, even at the same higher sample amount on the plate, piezoelectric spraying showed no diffusion/tailing of the zones (Figs. 1Bn, S4d).

Secondly, the BMP separation was investigated and finally selected for the subsequent experiments due to the faster workflow (no need of neutralization) and better resolution (Fig. 1C), if compared to AMP (Fig. 1A and B) and another mobile phase containing 90% chloroform [29]. Hence, ChE inhibitory screening of *P. h.* seed extract was performed with the final piezoelectric spraying procedure after development with BMP (Fig. 1C). Five major natural ChE inhibitors of *P. h.* seed extract were visualized after both ChE assays (Fig. 1Cr–u). However, the bands 3–5 showed only a light inhibition in the AChE assay at the higher sample amount (50 μg/band), whereas these were more dominant in the BChE assay.

3.5. *Optimized piezoelectric spraying for* A. fischeri *bioassay*

A caffeine pattern (Fig. 2Aa, 1–15 μg/band) was used for 6 different *A. fischeri* experiments. Different volumes of aqueous pre-wetting (0–2 mL), *A. fischeri* suspension (2–4 mL) as well as different nozzle types were tested to find an appropriate condition for piezoelectric spraying. Driven by the experience in the piezoelectric spraying of the ChE assays, the optimization of the Derivatizer parameters for setting up the *A. fischeri* bioassay was started with chromatogram pre-wetting, followed by spraying the *A. fischeri* suspension. The nozzle R with the largest nozzle diameter was selected for spraying the suspension containing the few-micrometer sized *A. fischeri* bacteria. As there was no response detectable in the image (Fig. 2Ab), the volume of the *A. fischeri* suspension was increased and that of pre-wetting decreased (Fig. 2Ac and d). Finally, spraying 4 mL (R nozzle) *A. fischeri* suspension without any pre-wetting showed a better bioactive pattern, and thus, it was tested for the other three nozzles G, B and Y (Fig. 2Ae–g). Nozzles R and B were selected as best, whereas nozzle Y led to dropping (Fig. 2Ag) or/and an uneven background, despite adhering to the nozzle cleaning protocol as recommended by the manufacturer.

3.6. *Bioprofiling of* P. h. *seed extract* via A. fischeri *bioassay*

In contrast to the ChE inhibitory assays, plates were developed with BMP only up to 70 mm (to ease covering the full developing distance by immersion; instead of 85 mm) for the *A. fischeri* bioassay (Figs. 2B, S5). In comparison to immersion (Fig. 2Bj), piezoelectric spraying with the nozzles R (Fig. 2Bk) and B (Fig. 2Bl) led to a pronounced bioactivity response of the *P. h.* seed extract (100 and 500 μg applied as start zone; in Fig. S6 also 1 mg applied) in the bioautogram. The homogeneity of the luminescent background was the main visual difference between piezoelectric spraying and immersion. In conclusion, also piezoelectric spraying of the *A. fischeri* bioassay was successful and showed that the pronounced fluorescent bands were responsible for the most antibacterial activity of the *P. h.* seed extract. Subsequently, these multipotent (antibacterial and AChE inhibiting) bioactive compounds were tentatively assigned by HRMS.

3.7. *Benchmarking of piezoelectric spraying* versus *immersion for (bio)assays*

The piezoelectric spraying for ChE assays led to better resolved autogram zones, if compared to the automated immersion. The optimized piezoelectric spraying protocol produced almost no overlaying liquid on the plate surface, and thus, needed no waiting times for evaporation of E- and S-solutions, whereas evaporation times were needed after immersion. Apart from incubation time, the immersion procedure for ChE assays was faster and took 4 min, whereas the spraying procedure took 3 times longer (12–15 min).

The piezoelectric spraying workflow was more cost-effective, even if compared to a best case scenario for immersion. For this, the E-solution was used as longest as possible for maximum 6 times only (repeated defrosting and use) due to gradual enzyme deactivation and potential cross-contamination from immersed plates. Also, a narrower immersion chamber (glass dip tank, Biostep) was preferred to the wider ones, *i.e.* the durable polypropylene (PP) chamber [38] or glass dip tank (CAMAG), reducing the needed volume around 2–3 times (70 mL Biostep, 170 mL PP chamber and 220 mL CAMAG). Comparing the consumption of E-solutions, piezoelectric spraying needed by a factor of 4 less volume than immersion (18 mL for 6 times spraying of 3 mL on a 20 × 10 cm plate *versus* 82 mL for 6 times immersion in the dipping chamber sized 20 × 10 cm). For the latter, maximal 70 mL can be filled in the 20 × 10-cm narrow dipping chamber to avoid an overflow of the solution by plate immersion, and additionally max. 2 mL per immersion are lost through adsorption on the 20 × 10-cm HPTLC layer, which together sums up to 82 mL, if calculated for six plates immersed. By a factor of 27, less S-solution was consumed (3 mL for 6 times spraying of 0.5 mL *versus* 82 mL for 6 times immersion on the same day).

In case of *A. fischeri* bioassay, even though immersion was much faster, it needed sweeping with a squeegee to remove the overlaying *A. fischeri* microorganism suspension, while piezoelectric spraying with the Derivatizer showed no overlaying liquid. The piezoelectric spraying afforded by a factor of 18 less volume of the *A. fischeri* suspension (4 mL for the Derivatizer *versus* 70 mL for the immersion chamber sized 20 × 10 cm).

Applied piezoelectric spraying solutions covered the whole plate surface, while for immersion the chromatogram was coverable maximal 85 mm. Thus, for immersion, a developing distance < 85 mm is required, which is the usual case and no hindrance. Even a 70-mm migration distance was highly satisfying (Fig. S5), espe-

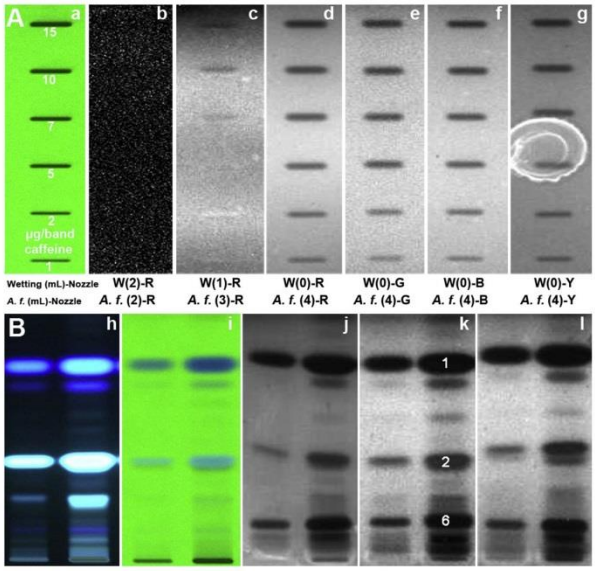

Fig. 2. Piezoelectric spraying of the *A. fischeri* bioassay suspension: (A) Caffeine pattern at 254 nm (a) for optimization of the piezoelectric spraying of and (B) chromatograms of *P. h.* seed extract after BMP separation (100 and 500 µg/band) at 366 nm (h) and 254 nm (i) as well as respective *A. fischeri* bioautograms by immersion (j) versus piezoelectric spraying with nozzles R (k) and B (l); zone no. 1, 2 and 6 as in Table 2.

Table 1
Figures of merit for ChE inhibitory equivalency calculation of *P. h.* seed extract in reference to PHY.

Assays	PHY equivalency calculation	Amount	Intermediate precision		Amount	Intermediate precision	
		ng/band, peak height	SD (n = 3)	*RSD%*	ng/band, peak area	SD (n = 3)	*RSD%*
AChE	PHY equal to **band 1**	0.9	0.05	6	0.9	0.07	8
	PHY equal to **band 2**	0.9	0.05	6	1.0	0.12	12
	PHY equal to **1 µg/band** *P. h.* seed extract	**1.8**	0.09	5	**1.9**	0.19	10
	S/N ratio (0.1 ng/band)	8					
	LOD/LOQ (ng/band)	0.03/0.09			0.04/0.12		
	Determination coefficient R^2	0.999			0.999		
BChE	PHY equal to **band 3**	0.3	0.03	9	0.3	0.03	9
	PHY equal to **band 4**	0.3	0.02	8	0.3	0.01	5
	PHY equal to **band 5**	0.2	0.01	7	0.2	0.01	7
	PHY equal to **1 µg/band** *P. h.* seed extract	**0.8**	0.04	5	**0.8**	0.05	7
	S/N ratio (0.1 ng/band)	5					
	LOD/LOQ (ng/band)	0.05/0.15			0.05/0.15		
	Determination coefficient R^2	0.999			0.999		
AChE/BChE	**Inhibition ratio for *P. h.* seed extract**	**2.3**			**2.4**		

cially for marking of zones for TLC-MS. However, it was a limitation for horizontal antiparallel development, which requires the whole plate format to be usable.

Hence for distinct challenges, the benefit achievable by piezoelectric spraying is evident. Key arguments pro piezoelectric spraying are (1) better resolved autogram zones, (2) covering the whole plate surface, and (3) no zone distortion or shift observed after previous buffer salt applications (required for neutralization or originally acidic/basic plates [39]). (4) The use of always a fresh solution (just defrost the needed aliquot of E-solution, 3 mL instead of 70 mL) would be the best practice with regard to the standardization of autograms. (5) The volume consumption by piezoelectric spraying was by a factor of 4 to 27 less than by immersion.

As a key argument pro immersion remains simplicity, *i. e.* the more simple instrumental workflow, faster handling and rapid cleaning. A tailing of (in the reagent solvent) highly soluble zones upon slow plate withdrawal can be mitigated with a change of the reagent solvent or a fast immersion speed and short immersion time (fast in, fast out). If the above mentioned obstacles do not matter and reagent solutions are cheap and stable, when kept in the refrigerator in the dark over months, immersion remains the technique of choice in our laboratory. All in all, homogeneity of the applied solutions, and thus, the resulting background response/color were almost comparable for both techniques (immersion or piezoelectric spraying), which is the most essential fact to solve analytical tasks.

3.8. Equivalency calculations

After the piezoelectric spraying workflow, distinct inhibition zones on a homogenous background were precondition for quantification. The main active compounds of *P. h.* seed extract were

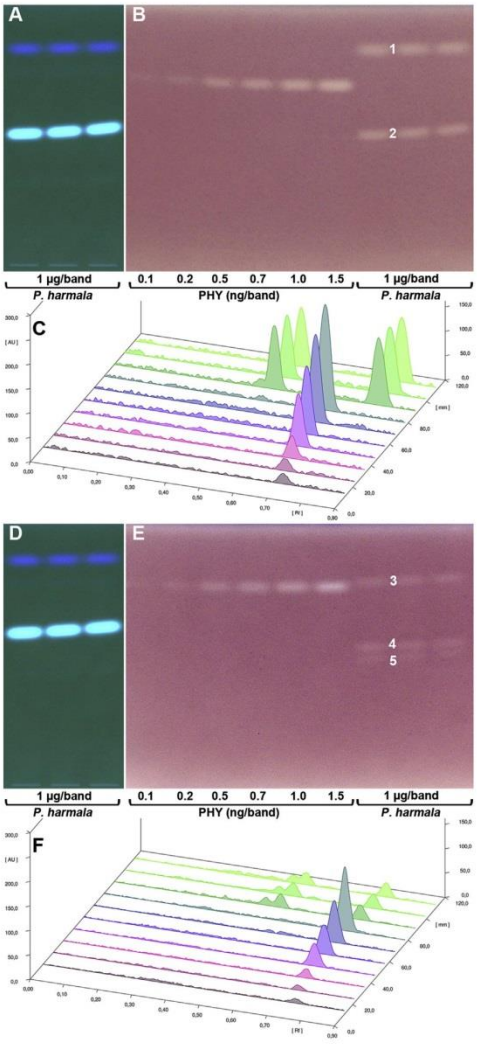

Fig. 3. ChE inhibitory equivalency study of *P. h.* seed extract (1 µg applied) referred to PHY (positive control) and calculated in Table 1. BMP-developed chromatogram of *P. h.* seed extract at 366 nm (A), AChE autogram (B) and enzyme inhibition densitogram (C); analogously for BChE (D–F); zone no. 1-5 as in Table 2.

targeted for ChE inhibitory equivalency calculation with reference to PHY. The threefold application of *P. h.* seed extract (1 µg/band each) and PHY calibration levels (0.1–1.5 ng/band each) were used for calculating the precisions for the application zones (<6 *RSD%*, Table S4) and determination coefficients (0.999, Table 1), respectively (Fig. 3).

The AChE inhibition of 1 µg/band of *P. h.* seed extract was equivalent to 1.8 ng/band PHY (peak height, Table 1) or 1.9 ng/band PHY (peak area, Table 1). The BChE inhibition of 1 µg/band *P. h.* seed extract was equivalent to 0.8 ng/band PHY (peak area and peak height, Table 1). The total AChE inhibition of 1 µg/band of *P. h.* seed extract was more than twice as strong as its BChE inhibition (Table 1, AChE/BChE inhibition ratio of 2.3 or 2.4). The intraday precision on two plates/experiments at the same day showed that the ChE inhibitory equivalency calculation for a developed PHY was *RSD%* of 2–12% (Table S4). The intermediate precision on three days revealed that the ChE inhibitory equivalency calculation with a developed PHY was *RSD%* 5–12% (Table 1).

The ChE inhibition LODs of PHY were calculated based on 3.3 STEYX/Slope (MS-Office) in the linear range of the calibration curves (AChE 0.1-0.7 ng/band and BChE 0.1–1.5 ng/band). The S/N ratio (AChE 8 and BChE 5) for the lowest calibration level (0.1 ng/band) proved that the LODs of PHY for both ChE assays were lower than 0.1 ng/band (Table 1, AChE 0.03 ng/band and BChE 0.05 ng/band). These LODs were much more lower than Marston's method (1 ng/band) [37] and near to the LOD of another study (0.01 ng/band) with round-shape inhibition zones [2]. Our LODs were lower than other TLC-AChE methods with different reagents *i.e.* combination of 4-methoxylphenyl acetate as substrate and mixture of potassium ferricyanide/iron chloride hexahydrate as chromogenic reagent (1 ng/band) [35] and TLC-modified Ellman's method 10–600 ng/band [40–42].

The lowest calibration level of PHY (0.1 ng/band or 3.6×10^{-13} Mol) was considered for calculation of pMIQ (negative logarithm of the minimal inhibitory quantity, in mole, of the least observable band), though LOD was lower. For this level (0.1 ng/band PHY, >LOD), the pMIQ would be 12.4 *via* both HPTLC-AChE and HPTLC-BChE assays performed by piezoelectric spraying. Our results showed a higher value in comparison with reported pMIQ for PHY (11.8), and additionally confirmed the activity of PHY to be above 10.5, which is the cut-off value for considering a compound as an active one [43].

3.9. HPTLC-HRMS for the identification of bioactive compounds

The mass spectra of six natural ChE inhibitors and three antibacterial compounds of *P. h.* seed extract were recorded and compared with literature. The two pronounced fluorescent bands (also orange and pink bands in Dragendorff's and anisaldehyde sulfuric acid reagents in Fig. 1Ak and l) were tentatively assigned to be the β-carboline alkaloids, harmine (zone 1) and harmaline (zone 2). These two and also ruine (zone 6), a glucosidic β-carboline alkaloid, were detected as active zones in the *A. fischeri* bioassay (Fig. 2Bk) as well as AChE assay (Table 2, Fig. 1Cs). The detected BChE inhibitors were tentatively assigned to be the β-carboline alkaloid harmol (zone 3) and the quinazoline alkaloids vasicine (zone 4) and deoxyvasicine (zone 5, Table 2, Fig. 1Cu).

These outcome was in accordance with former TLC-AChE research that reported β-carbolines, especially harmine and harmaline, as main AChE inhibitors of *P. h.* seed extract, while quinazolines as weak AChE inhibitors (such as vasicinone, deoxyvasicinone, deoxyvasicine, nigellastrine I and nigellastrine II). On the contrary, the quinazolines had much more BChE inhibitory activity than β-carbolines [29,30]. Another study showed that the β-carbolines harmane, harmine and harmaline had the lowest IC_{50} values and highest AChE inhibitory activity, while the quinazoline alkaloid vasicine showed the lowest IC_{50} value and highest BChE inhibitory activity among the alkaloids of *Peganum* genus *via* the *in vitro* Ellman method [44]. Deoxyvasicine did not show any IC_{50} value, whereas in our experiment, an inhibition was evident in both ChE assays. Especially for the 1-µg applied *P. h.* seed extract in the BChE assay, the inhibition of zone 5 was equal to 0.2 ng/band of PHY. Another research about the ChE inhibitory activity of a bioassay-guided fractionation of *P. h.* seeds revealed the lowest IC_{50} values for deoxyvasicine, vasicine and harmol in the BChE assay, which proved our results showing the sensitive BChE inhibition for

Table 2
HPTLC-HRMS data of the main (bio)active compound zones 1-6 in the *P. h.* seed extract.

No.	Observed *m/z*	Theoretical *m/z*	Molecular formula	Mass error (ppm)	Tentatively assigned $[M+H]^+$
1	213.10210	213.10224	$C_{13}H_{13}N_2O^+$	−0.65	Harmine
2	215.11780	215.11789	$C_{13}H_{15}N_2O^+$	−0.42	Harmaline
3	199.08654	199.08659	$C_{12}H_{11}N_2O^+$	−0.25	Harmol
4	189.10203	189.10224	$C_{11}H_{13}N_2O^+$	−1.11	Peganine or vasicine
5	173.10725	173.10732	$C_{11}H_{13}N_2^+$	−0.43	Deoxypeganine or deoxyvasicine
	195.08920	195.08926	$C_{11}H_{12}N_2Na^+$	−0.34	Sodium adduct
6	391.14963	391.14998	$C_{19}H_{23}N_2O_7^+$	−0.89	Ruine

these already in the 1-μg applied *P. h.* seed extract [45]. For higher amounts of *P. h.* seed extract applied on the plate, further inhibitors were evident (Fig. S5).

4. Conclusions

New piezoelectric spraying workflows for enzymatic and biological assays were successfully developed. The enzyme inhibitory calculation of potential inhibitors in traditional medicinal plants equal to a known potent and highly selective ChE inhibitor was demonstrated as proof of principle of using the new piezoelectric spraying procedure. If compared with the state-of-the-art automated immersion, the homogeneity of the plate background *via* piezoelectrically spayed solutions was comparable using the newly developed workflow. As benefit, the piezoelectric spraying provided a cost-effective (with regard to expensive reagent solutions) and user-friendly procedure for ChE assays and the *A. fischeri* bioassay without any cross-contamination, zone tailing and zone shift. Advantageous is also the homogenous spraying of the whole plate in case of higher migration distances or antiparallel developments, if compared to automated immersion. The use of always a fresh solution would be the best practice with regard to the standardization of chromatograms/autograms. In contrast, simplicity remains the key argument pro immersion, *i. e.* the simpler instrumental workflow, faster handling and cleaning. Hence, it is advantageous, if the above mentioned drawbacks do not matter and reagent solutions are cheap and stable, when kept in the refrigerator in the dark over months. Several alkaloids of the *Peganum* genus were found as proof of principle of the HPTLC-EDA-HRMS workflow. At the same time, HPTLC-EDA-HRMS is able to reveal further unknown bioactive compound zones that have not been in the focus so far.

Author contributions

Both authors contributed to the study design and instruction of the experimental work of the students. E.A. performed the MS analyses supervised by G.E.M. E.A. has prepared the first draft, which was substantially revised by G.E.M.

Acknowledgements

Thank is owed to Isabelle Thomä, Jonas Baake, and Kathrin Billerbeck to work on this project as part of their bachelor/master theses as well as Merck, Darmstadt, Germany for providing HPTLC plates.

Appendix A. Supplementary data

Supplementary material related to this article can be found, in the online version, at doi:https://doi.org/10.1016/j.chroma.2019.05.043.

References

[1] I.A. Ramallo, S.A. Zacchino, R.L. Furlan, A rapid TLC autographic method for the detection of xanthine oxidase inhibitors and superoxide scavengers, Phytochem. Anal. 17 (2006) 15–19.
[2] Z. Yang, X. Zhang, D. Duan, Z. Song, M. Yang, S. Li, Modified TLC bioautographic method for screening acetylcholinesterase inhibitors from plant extracts, J. Sep. Sci. 32 (2009) 3257–3259.
[3] H.R. Adhami, U. Scherer, H. Kaehlig, T. Hettich, G. Schlotterbeck, E. Reich, L. Krenn, Combination of bioautography with HPTLC–MS/NMR: A fast identification of acetylcholinesterase inhibitors from Galbanum, Phytochem. Anal. 24 (2013) 395–400.
[4] M.O. Salazar, R.L. Furlan, A rapid TLC autographic method for the detection of glucosidase inhibitors, Phytochem. Anal. 18 (2007) 209–212.
[5] M. Jamshidi-Aidji, G.E. Morlock, Bioprofiling of unknown antibiotics in herbal extracts: Development of a streamlined direct bioautography using *Bacillus subtilis* linked to mass spectrometry, J. Chromatogr. A 1420 (2015) 110–118.
[6] G.W. Jóźwiak, B. Majer-Dziedzic, W. Jesionek, W. Zieliński, M. Waksmundzka-Hajnos, Thin-layer chromatography: Direct bioautography as a method of examination of antimicrobial activity of selected *Potentilla* species, J. Liq. Chromatogr. Relat. Technol. 39 (2016) 281–285.
[7] E.F. Queiroz, J.-L. Wolfender, K. Atindehou, D. Traore, K. Hostettmann, On-line identification of the antifungal constituents of *Erythrina vogelii* by liquid chromatography with tandem mass spectrometry, ultraviolet absorbance detection and nuclear magnetic resonance spectrometry combined with liquid chromatographic micro-fractionation, J. Chromatogr. A 974 (2002) 123–134.
[8] Q. Favre-Godal, E.F. Queiroz, J.-L. Wolfender, Latest developments in assessing antifungal activity using TLC-bioautography: A review, J. AOAC Int. 96 (2013) 1175–1188.
[9] V. Danciu, A. Hosu, C. Cimpoiu, Comparative evaluation of antioxidant activity using 1, 1-diphenyl-2-picrylhydrazyl and 2, 2′-azino-bis (3-ethylbenzothiazoline-6-sulphonic acid) methods, J. Planar Chromatogr.-Mod. TLC 29 (2016) 306–309.
[10] E. Azadniya, G.E. Morlock, Bioprofiling of *Salvia miltiorrhiza* via planar chromatography linked to (bio)assays, high resolution mass spectrometry and nuclear magnetic resonance spectroscopy, J. Chromatogr. A 1533 (2018) 180–192.
[11] G.E. Morlock, Chromatography combined with bioassays and other hyphenations – the direct link to the compound indicating the effect, in: in: Instrumental Methods for the Analysis and Identification of Bioactive Molecules, American Chemical Society, 2014, pp. 101–121.
[12] G.E. Morlock, Bioassays and further effect-directed detections in chromatography, in: in: Reference Module in Chemistry, Molecular Sciences and Chemical Engineering, Elsevier Science, Amsterdam, 2019.
[13] S. Kirchert, G.E. Morlock, Simultaneous determination of mono-, di-, oligo- and polysaccharides *via*planar chromatography in 4 different prebiotic foods and 60 naturally degraded inulin samples, J. Chromatogr. A 1569 (2018) 212–221.
[14] A. Sobanska, E. Brzezinska, Rapid HPTLC quantification of p-aminobenzoic acid in complex pharmaceutical preparations, J. Planar Chromatogr.-Mod. TLC 23 (2010) 141–147.
[15] S. Krüger, L. Hüsken, R. Fornasari, I. Scainelli, G. Morlock, Effect-directed fingerprints of 77 botanical extracts *via* a generic high-performance thin-layer chromatography method combined with assays and mass spectrometry, J. Chromatogr. A 1529 (2017) 93–106.
[16] S. Hage, G.E. Morlock, Bioprofiling of *Salicaceae* bud extracts through high-performance thin-layer chromatography hyphenated to biochemical, microbiological and chemical detections, J. Chromatogr. A 1490 (2017) 201–211.
[17] A. Schoenborn, P. Schmid, S. Braem, G. Reifferscheid, M. Ohlig, S. Buchinger, Unprecedented sensitivity of the planar yeast estrogen screen by using a spray-on technology, J. Chromatogr. A 1530 (2017) 185–191.
[18] L. Stütz, S.C. Weiss, W. Schulz, W. Schwack, R. Winzenbacher, Selective two-dimensional effect-directed analysis with thin-layer chromatography, J. Chromatogr. A 1524 (2017) 273–282.
[19] G.E. Morlock, C. Stiefel, W. Schwack, Efficacy of a modified printer for application of reagents in planar chromatography, J. Liq. Chromatogr. Relat. Technol. 30 (2007) 2171–2184.
[20] G.E. Morlock, Miniaturized planar chromatography using office peripherals-office chromatography, J. Chromatogr. A 1382 (2015) 87–96.
[21] Z. Ramshani, Fluid manipulations using a piezo electric transformer for sensing and spray generation applications. Dissertation 3162, Western Michigan University, Kalamazoo, United States, 2017, August.
[22] D. Krickeberg, S. Hage, G.E. Morlock, Discovery and characterization of tyrosinase inhibitors in plants, creams and propolis by optimized

HPTLC-ESI-MS, Master thesis, Justus Liebig University of Giessen, Giessen, Germany, 2017, September.
[23] E. Azadniya, L. Goldoni, T. Bandiera, G.E. Morlock, HPTLC-qNMR to quantify co-eluted isomers in (bio)active zones, Poster, 11th annual GGL conference on life sciences, Giessen, Germany, 2018.
[24] M. Jamshidi-Aidji, G.E. Morlock, Fast equivalency estimation of unknown enzyme inhibitors *in situ* the effect-directed fingerprint, shown for *Bacillus* lipopeptide extracts, Anal. Chem. 90 (2018) 14260–14268.
[25] W. Schulz, W. Seitz, S. Weiss, W. Weber, M. Böhm, D. Flottmann, Use of *Vibrio fischeri* for screening for bioactivity in water analysis, J. Planar Chromatogr.-Mod. TLC 21 (2008) 427–430.
[26] V. Prasasty, M. Radifar, E. Istyastono, Natural peptides in drug discovery targeting acetylcholinesterase, Molecules 23 (2018) 2344–2365.
[27] I.A. Ramallo, P. García, R.L. Furlan, A reversed-phase compatible thin-layer chromatography autography for the detection of acetylcholinesterase inhibitors, J. Sep. Sci. 38 (2015) 3788–3794.
[28] M.C. Niroumand, M.H. Farzaei, G. Amin, Medicinal properties of *Peganum harmala* L. in traditional Iranian medicine and modern phytotherapy: A review, J. Tradit. Chin. Med. 35 (2015) 104–109.
[29] H.R. Adhami, H. Farsam, L. Krenn, Screening of medicinal plants from Iranian traditional medicine for acetylcholinesterase inhibition, Phytother. Res. 25 (2011) 1148–1152.
[30] X.-Y. Zheng, Z.-J. Zhang, G.-X. Chou, T. Wu, X.-M. Cheng, C.-H. Wang, Z.-T. Wang, Acetylcholinesterase inhibitive activity-guided isolation of two new alkaloids from seeds of *Peganum nigellastrum* Bunge by an *in vitro* TLC-bioautographic assay, Arch. Pharmacal. Res. 32 (2009) 1245–1251.
[31] E. Darabpour, A.P. Bavi, H. Motamedi, S.M.S. Nejad, Antibacterial activity of different parts of *Peganum harmala* L. growing in Iran against multi-drug resistant bacteria, EXCLI J. 10 (2011) 252–263.
[32] G. Nenaah, Antibacterial and antifungal activities of (beta)-carboline alkaloids of *Peganum harmala* (L) seeds and their combination effects, Fitoterapia 81 (2010) 779–782.
[33] International Organization for Standardization, Water quality - Determination of the inhibitory effect of water samples on the light emission of *Vibrio fischeri* (Luminescent bacteria test) - Part 1: Method using freshly prepared bacteria, Geneva, Switzerland, 2007.
[34] A.A. Bulich, Use of luminescent bacteria for determining toxicity in aquatic environments, in: Aquatic Toxicology: Proceedings of the Second Annual Symposium on Aquatic Toxicology, ASTM International, 1979.
[35] Z.D. Yang, Z.W. Song, J. Ren, M.J. Yang, S. Li, Improved thin-layer chromatography bioautographic assay for the detection of actylcholinesterase inhibitors in plants, Phytochem. Anal. 22 (2011) 509–515.
[36] R. Akkad, W. Schwack, Multi-enzyme inhibition assay for the detection of insecticidal organophosphates and carbamates by high-performance thin-layer chromatography applied to determine enzyme inhibition factors and residues in juice and water samples, J. Chromatogr. B 878 (2010) 1337–1345.
[37] A. Marston, J. Kissling, K. Hostettmann, A rapid TLC bioautographic method for the detection of acetylcholinesterase and butyrylcholinesterase inhibitors in plants, Phytochem. Anal. 13 (2002) 51–54.
[38] W. Schwack, Glass breakage-free TLC/HPTLC dipping chambers, Poster, International Symposium for High-Performance Thin-Layer Chromatography, Berlin, Germany, 2017.
[39] I. Klingelhöfer, G.E. Morlock, Sharp-bounded zones link to the effect in planar chromatography-bioassay-mass spectrometry, J. Chromatogr. A 1360 (2014) 288–295.
[40] I.K. Rhee, M. van de Meent, K. Ingkaninan, R. Verpoorte, Screening for acetylcholinesterase inhibitors from Amaryllidaceae using silica gel thin-layer chromatography in combination with bioactivity staining, J. Chromatogr. A 915 (2001) 217–223.
[41] I.J. Vieira, W.L. Medeiros, C.S. Monnerat, J.J. Souza, L. Mathias, R. Braz-Filho, A.C. Pinto, P.M. Sousa, C.M. Rezende, R.D.A. Epifanio, Two fast screening methods (GC-MS and TLC-ChEI assay) for rapid evaluation of potential anticholinesterasic indole alkaloids in complex mixtures, An. Acad. Bras. Cienc. 80 (2008) 419–426.
[42] A.H. Abou-Donia, F.A. Darwish, S.M. Toaima, E. Shawky, S.S. Takla, A new approach to develop a standardized method for assessment of acetylcholinesterase inhibitory activity of different extracts using HPTLC and image analysis, J. Chromatogr. B 955 (2014) 50–57.
[43] S. Di Giovanni, A. Borloz, A. Urbain, A. Marston, K. Hostettmann, P.-A. Carrupt, M. Reist, *In vitro* screening assays to identify natural or synthetic acetylcholinesterase inhibitors: Thin layer chromatography *versus* microplate methods, Eur. J. Pharm. Sci. 33 (2008) 109–119.
[44] T. Zhao, K.-M. Ding, L. Zhang, X.-M. Cheng, C.-H. Wang, Z.-T. Wang, Acetylcholinesterase and butyrylcholinesterase inhibitory activities of β-carboline and quinoline alkaloids derivatives from the plants of genus *Peganum*, J. Chem. 2013 (2013), Article ID 717232.
[45] Y. Yang, X. Cheng, W. Liu, G. Chou, Z. Wang, C. Wang, Potent AChE and BChE inhibitors isolated from seeds of *Peganum harmala* Linn by a bioassay-guided fractionation, J. Ethnopharmacol. 168 (2015) 279–286.

Supplementary data

Automated piezoelectric spraying of biological and enzymatic assays for effect-directed analysis of planar chromatograms

Ebrahim Azadniya[a,b] and Gertrud E. Morlock[a,b,*]

[a]Chair of Food Science, Institute of Nutritional Science, and Interdisciplinary Research Center, Justus Liebig University Giessen, Heinrich-Buff-Ring 26-32, 35392 Giessen, Germany

[b]TransMIT Center of Effect-Directed Analysis, Kerkrader Straße 3, 35394 Giessen, Germany

*Corresponding author. Tel.: +49-641-99-39141; fax: +49-641-99-39149

E-mail addresses: Gertrud.Morlock@uni-giessen.de (G. E. Morlock),

Ebrahim.Azadniya@chemie.uni-giessen.de (E. Azadniya)

Table of Contents

Table S-1. Drying conditions used after derivatization, neutralization and (bio)assay application

Drying after	Method	Duration (min)
Development with AMP/BMP	ADC 2, drying mode	10
Dragendorff's reagent	Hairdryer, cold stream	2
Anisaldehyde-sulfuric reagent	CAMAG TLC Plate Heater, 110 °C	3-5
Neutralization	ADC 2, humidity control mode (relative humidity was reduced to 1% with activated molecular sieve, 0.3 nm pearls, grade 564, filled up to 3-cm high in the gas wash bottle)	10
AChE/BChE	Ambient temperature/then in ACD 2, humidity control mode (as mentioned)	5/10

Table S-2. Piezoelectric spraying parameters used for derivatization, neutralization and (bio)assay application

Piezoelectric spraying for	Nozzle type[1]	Spraying volume (mL)	Spraying solution
Derivatization			
- Dragendorff's reagent	R	3	A: 1.1 g bismuth carbonate was dissolved in 40 mL bi-distilled water and 10 mL acetic acid under heating B: 8 g Potassium iodide was dissolved in 30 mL bi-distilled water Reagent: 3 mL of A and B was mixed with 4 mL of acetic acid and 20 mL bi-distilled water.
- Anisaldehyde-sulfuric acid reagent	B	3	10 mL sulfuric acid was carefully added to a cooled mixture of 170 mL methanol and 20 mL acetic acid. Then, 1 mL of anisaldehyde was added.
Neutralization[2]	G	3	Phosphate-citrate buffer (8 % *W/V*, pH 7.8)
AChE/BChE assay			
- Wetting (W)	G	1	Tris-HCl buffer 0.05 M, pH 7.8
- Enzyme application (E)	G	3	100 mL Tris-HCl buffer 0.05 M, pH 7.8 plus 666 units AChE or 334 units BChE and 100 mg bovine serum albumin
- Substrate-chromogenic application (S)	R	0.5	4.5 mg α-naphthyl acetate and 9 mg Fast Blue B salt in 4.5 mL water - ethanol 2:1
A. fischeri bioassay	R/B	4	Medium preparation according to DIN EN ISO 11348-1

[1]Red (R), Blue (B), Green (G)

[2]Needed for AMP-developed plates

Table S-3. Immersion conditions for neutralization and (bio)assay application

Immersion for	Immersion volume (mL) for 10/20 cm × 10 cm plate	Immersion solution	Immersion speed (cm/s)/time (s)
Neutralization*	45/90	Phosphate-citrate buffer (8 % *W/V*, pH 7.8)	2.5/3.0
AChE/BChE assay			
-Enzyme application	45/90	100 mL Tris-HCl buffer 0.05 M, pH 7.8 plus 666 units AChE or 334 units BChE and 100 mg bovine serum albumin	2.5/2.0
-Substrate-chromogenic application	45/90	90 mg α-naphthyl acetate (substrate) and 180 mg Fast Blue B salt (chromogenic agent) in 90 mL water - ethanol 2:1	2.5/1.0
A. fischeri bioassay	45/90	medium preparation was according to DIN EN ISO 11348-1 [31].	2.5/3.0

*Needed for AMP-developed plates

Table S-4. Application precision (n = 4, peak area) and intraday precision of *P. h.* seed extract (n = 2, peak area)

	Application precision		**Intraday precision of ChE inhibitory equivalency calculation**	
	AChE	BChE	AChE	BChE
P. h. band	*RSD* %	*RSD* %	*RSD* %	*RSD* %
1	2	-	2	-
2	3	-	2	-
3	-	6	-	2
4	-	5	-	12
5	-	4	-	5

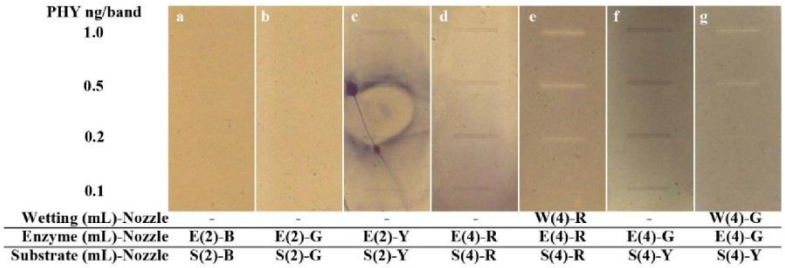

Fig. S-1. Initial experiments of the piezoelectric spraying parameters for the AChE assay with regard to plate pre-wetting, nozzle type and volumes of enzyme and substrate-chromogenic solutions: PHY inhibition patterns (0.1 -1.0 ng/band) obtained for the different settings a-g, showing a first successful response/inhibition (settings e and g) for further optimization (Figure S-2)

Five-phase optimization study

The first phase investigated different combinations and ratios, reported in the mL volumes taken (Figure S-1). If compared to the response on non-wetted plates (Figure S-1 a-d, W:E:S 0:2:2 and Figure S-1 f, W:E:S 0:4:4), the PHY pattern showed a higher visual response using a plate pre-wetting before spraying of the E-solutions (Figure S-1e and g, W:E:S 4:4:4). These initial plates were covered by an extra liquid film and looked oversaturated due to high volume (4 mL) for all W/E/S steps. Therefore, in the second phase, the volume of all W:E:S steps was reduced to the ratio 1:3:3 and 1:3:2 (Figure S-2, no. 1-6) with fixed volume of W/E-solution and the S-volume (2 or 3 mL) was studied. The nozzles combination for second phase, R:R:Y and G:G:R for W:E:S solutions, was selected due to higher visual response in initial study (Figure S-1e and g). The spraying of 2 mL S-solution was stopped when the background color appeared, and still 1 mL S-solution remained in the nozzle R (Figure S-2, no. 6). Then, the S-solution volume was reduced to 1 mL and kept constant in the third phase, in which the E-solution volume was investigated (2 or 3 mL), either with or without pre-wetting with1 mL Tris-HCl buffer (Figure S-2, no. 7-12). The last nozzles combination of second phase (G:G:R, Figure S-2, no. 6) and G:G:Y for W:E:S solutions was selected for third phase. The experiments with 2 mL E-solution (Figure S-2, 7-8 and 11) did not show purple background and a week inhibition for PHY pattern in compare to 3 mL E-solutions (Figure S-2, 9-10 and 12). Then, the 1:3:1 volume ratio was found appropriate, given by the optimum amount of enzyme (3 mL) on a pre-wetted plate. In the fourth phase (Figure S-2, no. 13-16), the ratio 1:3:1 for W:E:S was tested with each single nozzle type for all three steps. The nozzles G and R showed the best results, whereby spraying took longest with the nozzle G (13.4 min) *versus* nozzles R, B and Y (9.5 min). In the fifth phase, the S-solution volume was reduced to 0.5 mL and studied for nozzles G and R (Figure S-2, no. 17 and 18) as the best ones in former step. For the AChE assay, the final W:E:S volume ratio was 1:3:0.5 for both G and R nozzles.

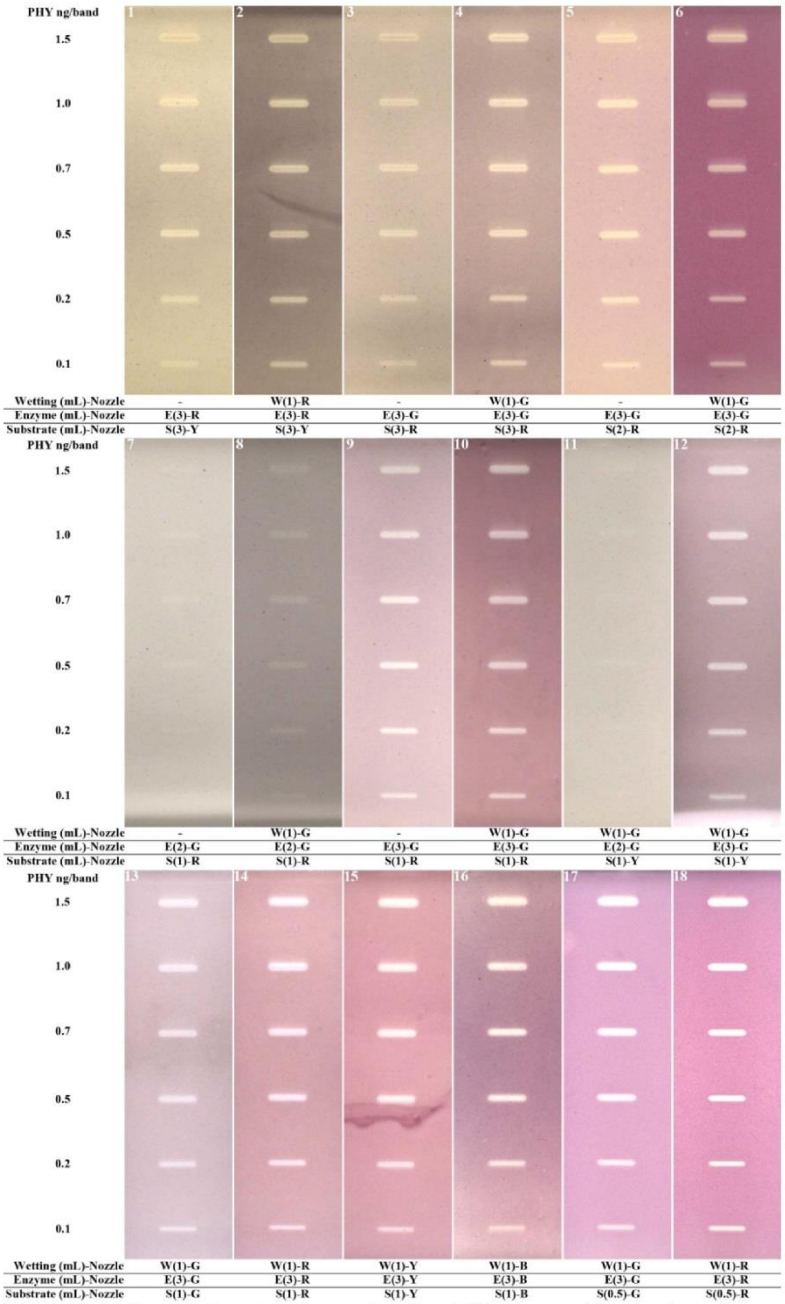

Fig. S-2. Optimization of piezoelectric spraying for AChE assay with regard to plate pre-wetting, nozzle type and volumes of enzyme and substrate-chromogenic solutions: PHY inhibition patterns (0.1 -1.5 ng/band) obtained for 18 different settings

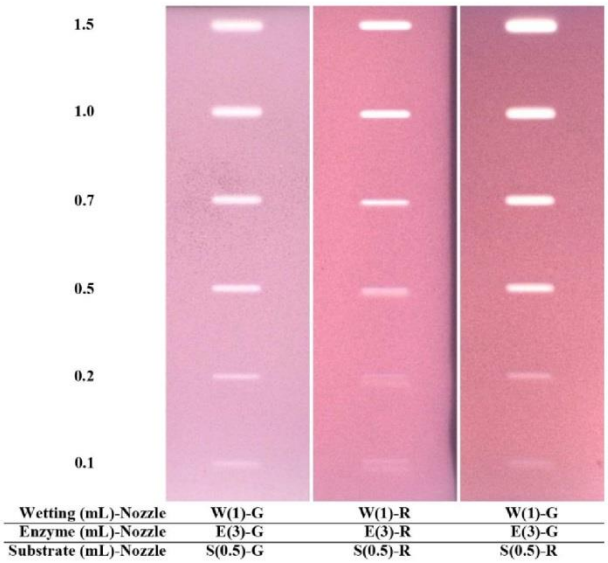

Fig. S-3. Transfer of the optimized settings for piezoelectric spraying (Figure S-2) to the BChE assay and final optimization with regard to the nozzle types: PHY inhibition pattern (0.1 -1.5 ng/band) obtained for 3 different nozzle settings

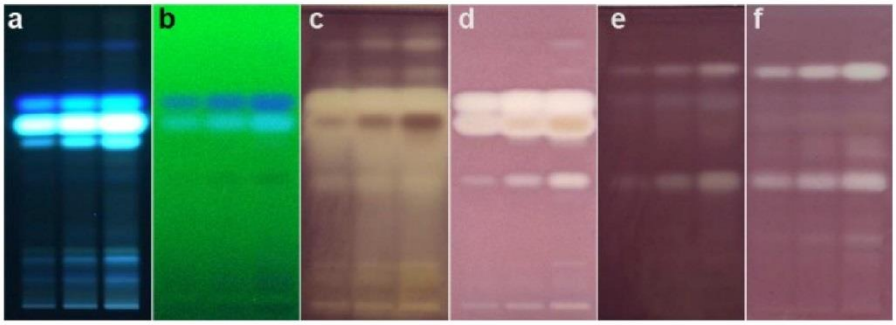

Fig. S-4. Comparison of immersion *versus* piezoelectric spraying: Chromatograms of *P. h.* seed extract (50, 100 and 200 µg/band) on HPTLC plate silica gel 60 developed with acidic mobile phase (AMP) documented at 366 nm (a), 254 nm (b), and white light illumination (RT) of respective AChE and BChE autograms obtained by immersion (c and e) *versus* piezoelectric spraying (d and f)

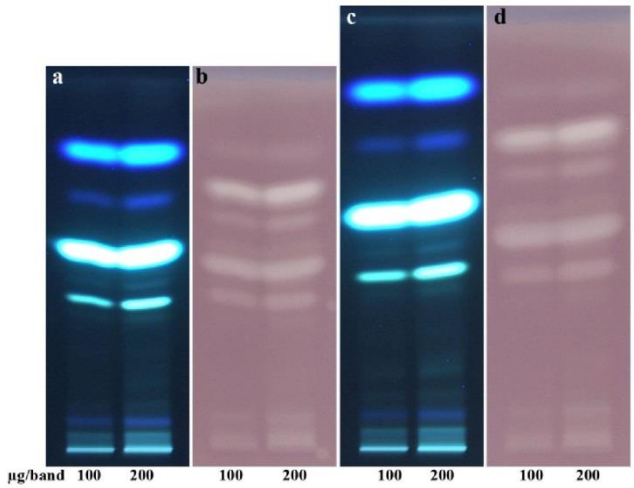

Fig. S-5. Comparison between 70 mm (a and b) and 85 mm (c and d) developing distance of BMP-developed chromatogram of *P. h.* seed extract (100 and 200 µg/band) at 366 nm (a and c) and autograms for BChE inhibitory screening white RT (b and d).

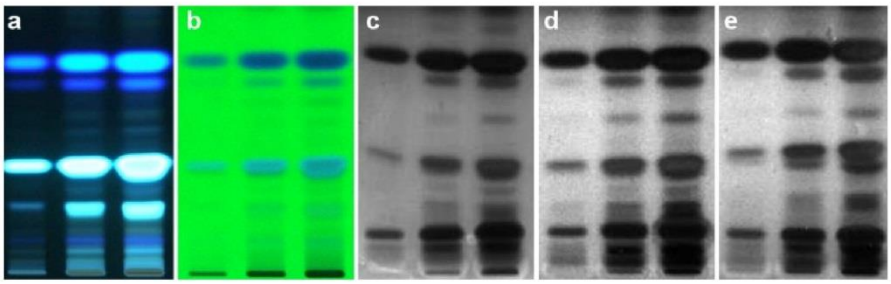

Fig. S-6. Piezoelectric spraying of an *A. fischeri* bacteria suspension: Chromatograms of *P. h.* seed extract after BMP separation (100, 500 and 1000 µg/band) at 366 nm (a), 254 nm (b), *A. fischeri* bioautograms by immersion (c) *versus* piezoelectric spraying with R (d) and B (e) nozzles.

4. PUBLICATION 3

Equivalency calculation of enzyme inhibiting unknowns *in situ* the adsorbent of the effect-directed autogram

Ebrahim Azadniya[a], Gertrud E. Morlock[a,*]

[a]*Chair of Food Science, Institute of Nutritional Science, Interdisciplinary Research Center (IFZ), Justus Liebig University Giessen, Heinrich-Buff-Ring 26-32, 35392, Giessen, Germany*

Published in

Analytical methods, https://doi.org/10.1039/C9AY01465A

Received in revised form 09 July 2019, accepted on 06 September 2019 and first published on 07 September 2019

PAPER

View Article Online
View Journal | View Issue

Equivalency calculation of enzyme inhibiting unknowns *in situ* the adsorbent of the effect-directed autogram

Ebrahim Azadniya[a] and Gertrud E. Morlock[a,*]

Received 00th January 20xx,
Accepted 00th January 20xx

DOI: 10.1039/x0xx00000x

The reliable biochemical quantification of the enzymatically produced signal of enzyme inhibitors has recently been shown within the assay-containing chromatographic bed, meaning *in situ* the adsorbent of the effect-directed autogram. As most enzyme inhibitors discovered in a complex sample are unknown or unidentified, and thus, an external standard calibration cannot be performed, their inhibition potency needs to be estimated by alternative means. Thus, two different modes of equivalency calculation, referring to a potent inhibitor that was either applied or also developed, were investigated, validated and compared, exemplarily on the acetyl- and butyrylcholinesterase (AChE/BChE) inhibition of *Peganum harmala* (*P. h.*) seed extract. Three potent inhibitors, *i. e.* physostigmine (PHY), rivastigmine and piperine, were considered for equivalency calculation. With regard to their hR_F value, band shape and inhibition brightness against the plate background, PHY was most similar in its properties to the unidentified inhibitors in the *P. h.* seed extract, and thus selected as reference. Proven by its low limits of detection, the HPTLC–AChE assay with 1-naphthyl acetate as substrate and Fast Blue B salt as chromogenic reagent was suited to reveal potential differences between the two modes of equivalency calculation. Quantification was studied via PHY zones that were applied *versus* developed on the high-performance thin-layer chromatography (HPTLC) plate. Both intraday precision and reproducibility showed the same trend, *i. e.* the equivalency calculation via developed PHY bands was more repeatable than applied ones. The steeper slope of the calibration curve of developed PHY bands offered a more sensitive quantification. The resulting equivalent inhibition of the ChE inhibitors in 1 µg/band of *P. h.* seed extract showed a bias of ca. 30% when calculated via applied *versus* developed PHY bands, whereby the total AChE-to-BChE inhibition ratio (ca. 2.4) of the ChE inhibitors in 1 µg/band of *P. h.* seed extract remained almost the same. As a result, the enzyme inhibition equivalently calculated via developed reference bands is more reliable and sensitive than via applied ones. When selecting the faster procedure (applied band pattern) for routine equivalency calculation as a compromise, a potential bias has to be taken into account.

1. Introduction

Hyphenation high-performance thin-layer chromatography (HPTLC) with other techniques especially effect-directed analysis (EDA) makes it an unique technique for fast (bio)profiling[1-3], including enzyme inhibition equivalency calculation[4-6] and bioquantification[7] of active compounds *in situ* the planar chromatogram without any previous fractionation steps. The straightforward HPTLC–EDA protocol can be an appropriate alternative for the tedious classical approach of bioassay-guided screening and fractionation of active compounds in complex plant extracts. The direct in flow combination of high-performance liquid chromatography with biochemical assays[8] is still sophisticated, *e. g.*, due to instrumental complexity, intolerance of enzymes to the organic solvents and peak diffusion by longer reaction times[9]. Such limitations of column-derived methods are not existent for planar chromatographic methods providing the solvent-free chromatogram and desirable reaction time owed to its offline and open system.

HPTLC–EDA was implemented, *e. g.*, for *Bacillus subtilis*[3,7,10,11], *Aliivibrio fischeri*[12] and planar yeast estrogen screen (pYES)[13,14] as microbiological, for acetyl-/butyrylcholinesterase (AChE, BChE)[2,15,16], α-/β-glucosidase[17,18] and tyrosinase[5,6,19] as biochemical, and for 2,2-diphenyl-1-picrylhydrazyl ($DPPH^{\bullet}$)[20,21] and 2,2'-azino-bis(3-ethylbenzothiazoline-6-sulphonic acid) ($ABTS^{\bullet+}$)[22] as microchemical assays. Using the straightforward HPTLC–EDA protocol, single active components are figured out among the thousands of compounds present in a complex sample. It is not only suited for screening for active components, but also for their individual quantification based on the signal obtained by the enzyme inhibition or antimicrobial activity (bioquantification). For example, comparison of the negative logarithm of the minimal inhibitory quantity of the least observable band (in mole; pMIQ) on the TLC–AChE autograms and negative logarithm of IC_{50} (in M; pIC_{50}) values measured by microplate spectrophotometric AChE assay showed 83% of 138 AChE inhibitors were potent inhibitors in both methods.[23] Potent AChE inhibitors applied in clinical practice should have pIC_{50} values > 5 which were connected to pMIQ values higher than 10.5.[23,24]

The best *scenario* for quantitative evaluation of the activity *in situ* the HPTLC–EDA autogram is the co-development of the reference compound, if identified and available. If not, an equivalency calculation has recently been reported in reference to a well-known active compound[5] (often used in assays as positive control). Ciprofloxacin or marbofloxacin[7] were used as well-known antibiotics as reference in *B. subtilis* bioassays,

[a] *Chair of Food Science, Institute of Nutritional Science, and Interdisciplinary Research Center, Justus Liebig University Giessen, Heinrich-Buff-Ring 26-32, 35392 Giessen, Germany, Gertrud.Morlock@uni-giessen.de, Tel.: +49-641-99-39141; fax: +49-641-99-39149.*

alkaloids like (±)-huperzine-A[23] and galantamine[25], or carbamates like physostigmine (PHY)[26] in AChE assays, kojic acid[5,6] in tyrosinase assays and ascorbic[20,21] or gallic acid[20] in DPPH$^{\bullet}$ radical scavenging assays.

As an example, the AChE inhibition of alkaloids isolated from *Peganum nigellastrum* Bunge seeds was visually compared to galantamine (0.1-1000 ng/band applied as pattern).[25] In another TLC study, the intensity of AChE inhibitors in different plant extracts was visually compared with the co-developed PHY reference (6–42 ng/band).[26] In a third study that used the Ellman's reagent, the equivalency calculation of the HPTLC–AChE inhibition was performed via a PHY calibration curve on another, separate plate.[27] The latter is not recommended in HPTLC, as absolute signal values vary from plate to plate. For reliable results in HPTLC, it is well-known that external calibrations have to be performed on the same plate as the samples.

For equivalency calculation, the chemical similarity of the discovered, unidentified active compound and the reference compound should be considered. As unidentified, it gets hard to select the reference from a similar structural group; however, the planar chromatogram is helpful to characterize the unidentified active compound in its polarity, spectral and chromatographic properties. Integration of a reference compound challenges the method development for new samples due to their different chromatographic interaction with mobile/stationary phases. Therefore, it was of interest to find more simple alternatives. After separation, the reference compound could be applied as track pattern in different amounts, however, the dimension of the resulting bias of this simplification was unclear. In the current study, two quantitative modes (applied and developed) were compared for equivalency calculation of the AChE/BChE inhibition of a medicinal plant referring to a well-selected known inhibitor. The recently developed, new piezoelectric spraying workflow[4] was applied due to its reported advantages.

2. Experimentals

2.1. Reagents and materials

Lyophilized powder of BChE (equine serum) and AChE (electric eel, *Electrophorus electricus*), Fast Blue B salt, rivastigmine (RIV) tartrate and piperine (PIP) were provided from Sigma Aldrich, Steinheim, Germany. 1-Naphthyl acetate and physostigmine (PHY) were purchased from Panreac, Barcelona, Spain and Santa Cruz Biotechnology, Heidelberg, Germany, respectively. Analytical grade solvents were used. Ethyl acetate and ammonia (25%) were obtained from Th. Geyer, Berlin, Germany. Tris(hydroxymethyl)aminomethane (Tris), hydrogen chloride (HCl) and bovine serum albumin were purchased from Carl Roth, Karlsruhe, Germany. Bi-distilled water was prepared with a Destamat Bi 18 E (Heraeus, Hanau, Germany). Ethanol was provided from Fisher Scientific, Schwerte, Germany. HPTLC plates silica gel 60 F_{254} were purchased from Merck, Darmstadt, Germany. *Peganum harmala* (*P. h.*) seeds were bought from Dehghanzadeh medicinal plant store in Sari, Iran.

2.2. Preparation of solutions

Milled *P. h.* seed (1 g, 0.5 mm sieve) were extracted with 10 mL ethanol and water 3:2, *V/V* (100 mg/mL) on the magnetic stirrer at room temperature for 30 min, followed by 30 min ultrasonication and 15 min centrifugation at 756 × *g*. The supernatant was diluted 1:200 with methanol (0.5 mg/mL). Standards solutions of PHY (0.1 µg/mL), RIV and PIP (each 200 µg/mL) were prepared in methanol. Enzyme solutions (6.6 units/mL AChE or 3.3 units/mL BChE) were prepared by dissolving the lyophilized powder of each enzymes and bovine serum albumin (1 mg/mL) in Tris-HCl buffer (0.05 M, pH 7.8). An ethanolic 1-naphthyl acetate solution and aqueous Fast Blue B salt solution (each 3 mg/mL) were mixed 1:2 as substrate-chromogenic solution.

2.3. HPTLC method

The *P. h.* seed extract solution (2-4 µL/band, 1-2 µg/band) and reference compound solutions (PHY 1-15 µL/band, 0.1-1.5 ng/band; RIV and PIP 10 µL/band, 2000 ng/band) were applied as 8-mm bands on the HPTLC plate using the Automatic TLC Sampler 4 (ATS 4, CAMAG, Muttenz, Switzerland). After 5 min chamber saturation, the plates were developed with a mobile phase consisting of ethyl acetate - methanol - ammonia (25%) 8.5:1.1:0.4, *V/V/V*, up to 85 mm in the Twin Trough Chamber. After 10 min drying in the Automatic Developing Chamber 2 (ADC 2, CAMAG), chromatograms were documented at 254 nm and 366 nm using the TLC Visualizer 2 (CAMAG). All instrumentation was controlled by winCATS software (version 1.47.2018, CAMAG).

2.4. Track pattern application

After the HPTLC development, each reference compound solution (PHY 0.1-1.5 ng/band; RIV and PIP 200-2000 ng/band) was applied as 8-mm band array using the ATS 4 (CAMAG) and the FreeMode option of the winCATS software (CAMAG). It was arranged vertically as a track pattern consisting of 5 or 6 bands with a 15-mm interval in the range of 1-10 or 1-15 µL/band.

2.5. Piezoelectric spraying of the HPTLC–enzyme assays

The ChE assays were carried out according to our latest piezoelectric spaying procedure[4] (Derivatizer, CAMAG, hood and tray for 20 × 10 cm plates, green and red nozzles at speed level 6) using the modified Marston's method[2,15,16]. Briefly, the chromatograms were pre-wetted with 1 mL Tris-HCl buffer. It was necessary to clean the bottom side of nozzles to avoid a dropping on the plate in the next step. Then, 3 mL of the enzyme solution were sprayed. The plate was incubated at 37 °C for 25 min in a humid plastic box covered by wet filter paper, followed by spraying of 0.5 mL substrate-chromogenic solution and drying (5 min at ambient air, then 10 min by the ADC 2 humidity control via molecular sieve). The ChE inhibitors were documented as white or bright bands on a purple plate background at white light illumination (transmission and reflection modes, automatic capture of the image).

2.6. Reference compound selection

The three reference compound solutions (each 10 µL/band) PHY (1 ng/band), RIV and PIP (2000 ng/band) as well as 4 µL of *P. h.* seed extract (2 µg/band) were applied and developed. After plate drying, 1-10 µL of the same reference compounds, PHY (0.1-1 ng/band), RIV and PIP (200-2000 ng/band) were applied as 5-band track pattern, and subjected to the assay as described in 2.5.

2.7. Equivalency calculation

The reference compound PHY was applied four times at 6 calibration levels (1-15 µL/band, 0.1-1.5 ng/band). *P. h.* seed extract was applied three times (2 µL/band, 1 µg/band). After development and plate drying, PHY was applied as a 6-band calibration pattern on three different tracks. The ChE assays were performed. The enzyme inhibition densitograms of both assays were measured by inverse scan at 546 nm using the mercury lamp (absorbance measurement). A software trick (select florescence mode without optical filter) was used to avoid the automatic peak conversion when bright zones are measured on a darker, colored background using the TLC Scanner 4 (CAMAG). The experiments for both assays were performed four times (n = 4).

3. Results and discussion

For the first time, the activities of natural, unidentified AChE and BChE inhibitors recorded by densitometry were quantitatively compared and validated with regard to three different reference compounds. In contrast to literature[25-27] and without the least isolation step[25], quantitative calculations were directly performed *in situ* the autogram. The recently developed ChE piezoelectric spraying workflow was employed, as it provided a good basis (*e.g.*, homogeneous background) for this quantitative study. The results of equivalency calculation via a selected, co-developed reference were compared with a faster protocol, in which it was only applied as calibration pattern on a single track.

3.1. Selection of the reference compound

First, an appropriate reference inhibitor was figured out for the equivalency calculation of natural ChE inhibitors in the *P. h.* seed extract. The activity of unidentified natural inhibitors or identified ones that are not available (or affordable) as standard compound, can at least be compared with a reference compound. Well-known inhibitors used in medicinal treatments can be selected as reference to describe the equivalent inhibition potential of unidentified inhibitors in a plant extract[5]. Positive control substances used as proof of the proper assay performance and for visual comparison[25,26] might be further potential candidates for a reference. Hence, for the AChE assay, three reference compounds were selected and investigated, *i. e.* the alkaloid PIP[5] and the carbamates RIV and PHY[15,26]. For the quantitative comparison by inverse densitometric scanning[5], the reference band should be as similar as possible to the unidentified inhibitor band with regard to inhibition brightness against the purple plate background, hR_F value and band shape. PIP was excluded due to its high hR_F value near the solvent front in the given chromatographic system (Fig. 1). Regarding band brightness, PHY matched best to the natural ChE inhibitors of the *P. h.* seed extract. A 5-band pattern was used to evaluate the quality of the reference compounds over a selected working range. RIV bands were very bright at the given amounts (application of lower amounts recommended), while PHY bands were less bright and more similar in shape to the natural ChE inhibitors (Fig. 1). Additionally, the hR_F value of PHY was in between the two AChE inhibitors of the *P. h.* sample and showed the most similar chromatographic behavior. Thus, PHY was selected as reference compound.

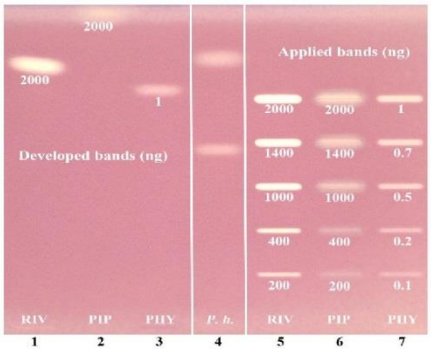

Figure 1 - Selection of the reference compound: HPTLC–AChE autogram of the different reference compounds RIV (tracks 1 and 5), PIP (tracks 2 and 6) and PHY (tracks 3 and 7) applied as usual (tracks 1-3) and as track pattern (tracks 5-7) as well as *P. h.* seed extract (track 4, 2 µg/band); given numbers are standard amounts as ng/band.

3.2. Equivalency calculation via developed *versus* applied mode

Sharply bounded, bright ChE inhibition bands and a homogenously colored plate background were precondition for accurate quantifications *in situ* the enzymatic assay autograms. Thus, the HPTLC–AChE/BChE assays were performed according to the recently developed multi-step piezoelectric spraying workflow.[4] All in all, five active bands (Fig. 2B and E, no. 1-5) were discovered and thus targeted for equivalency calculation by referring to the PHY band. The mere application of the reference compound was faster, but required a proof. Hence, the two different options for equivalency calculation (via applied *versus* developed PHY) were compared to figure out a potential bias. The *P. h.* seed extract (1 µg/band each, n = 3) and the different calibration levels of PHY (0.1 to 1.5 ng/band) were co-developed. Before the assay application, the calibration patterns of PHY were post-chromatographically applied as track (n = 3, Fig. 2B and E). It is worthy to note that in a parallel study[4], the five main inhibition bands detected in the *P. h.* seed extract were identified and assigned to be the AChE-inhibiting harmine (1) and harmaline (2), and the BChE-inhibiting harmol (3), vasicine (4) and deoxyvasicine (5). For statistics, the *P. h.* seed extract sample was applied three times. The PHY calibration pattern was also applied three

times on the same plate, as one calibration afforded only a single track (in contrast, the external standard calibration for the developed PHY zones was applied only once). Three repetitions of this plate were performed on different days (n = 4), each for the BChE and AChE assay. For both ChE assays, the two different modes of equivalency calculations as well as the resulting precisions, limits of detection (LODs), accuracies/bias and IC_{50} values were compared as follows.

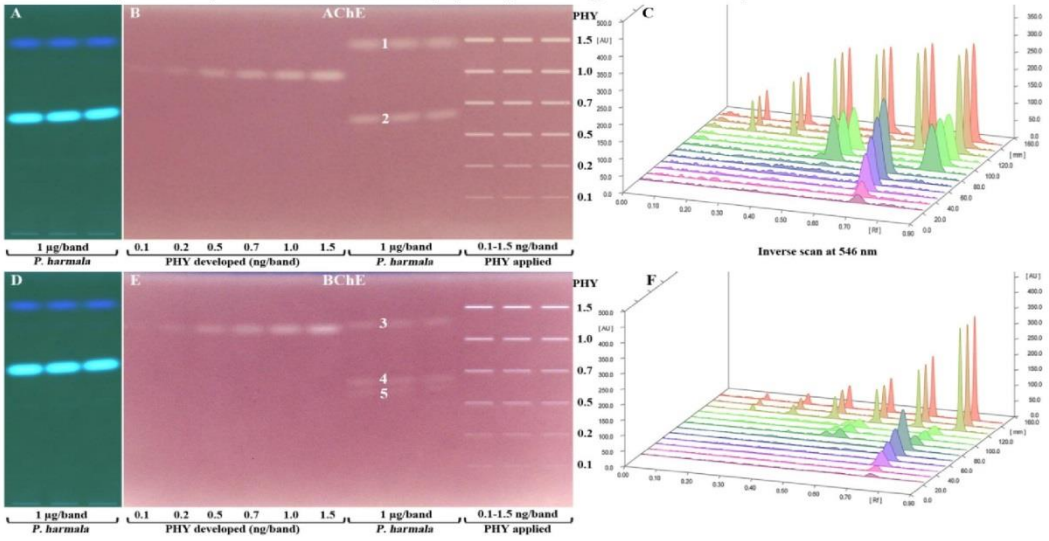

Figure 2 - Equivalency calculation of five ChE inhibition bands in the *P. h.* seed extract by referring to PHY as developed *versus* merely applied bands: HPTLC–FLD chromatograms at UV 366 nm (A and D), HPTLC–ChE autograms at white light illumination (B and E) and densitograms measured *in situ* the enzyme assay autograms by inverse scan at 546 nm (C and F).

3.3.Repeatability, intraday precision and reproducibility

The threefold applications were used for calculating peak area repeatabilities on the same plate, which for example, were between 2 and 6% for *P. h.* bands no. 1-5, and between 1 and 5% for PHY applied as pattern (%*RSD*, n = 3). Consequently, values obtained on the same plate were found to be reliable.

Also, it was investigated whether a one-, two, or three-fold applied calibration pattern of PHY was recommended on each plate. It turned out that the equivalently calculated value did not differ if either one pattern or the mean of two or three patterns were used for equivalency calculation. For example, the equivalently calculated values of PHY equal to 1 µg/band *P. h.* seed extract were 0.98/1.00/1.01 ng/band PHY using one/two/three calibration patterns. Thus, one calibration pattern was found to be sufficient for routine use, as results were comparable.

The whole analysis was repeated at the same day for intraday precision (%*RSD*, n = 2, two plates). For both ChE assays, the intraday precisions obtained for equivalency calculation of the *P. h.* seed extract bands no. 1-5 showed a mean precision of 5% (between 2 and 12%) via the developed mode and a mean precision of 11% (between 6 and 20%) via the applied mode.

The reproducibility on different days and plates (Table 1) revealed that the ChE inhibition band shape of developed PHY (%*RSD* of 5-12%) was more homogenous and repeatable, if compared to merely applied PHY (%*RSD* of 7-18%). The worse precision value for only applied zones, for which no chromatography error is expected, was explained by the lower mean calibration slope for applied (1500 AU) *versus* developed zones (2250 AU), which is more susceptible to variations (small signal changes cause major changes in the result). Combining chromatography with enzymatic reactions is much more challenging for quantifications. The biochemical-analytical HPTLC–EDA protocol includes several steps such as chromatographic separation, plate neutralization (in case of using acidic mobile phase), plate pre-wetting, enzyme solution spraying, incubation, substrate-chromogenic solution spraying, plate drying and densitometric evaluation, and thus, precisions up to 15 % are considered to be acceptable.

3.4.Capability of detection

The respective LOD of the ChE-inhibiting PHY (Table 1) was calculated via the linear calibration range (AChE 0.1-0.7 ng/band and BChE 0.1-1.5 ng/band) based on 3.3 STEYX/slope (MS-Office). The S/N value of 8 (AChE) or 5 (BChE) for the lowest calibration level at 0.1 ng/band confirmed the calculated low LODs of PHY for both ChE assays (Table 1, AChE 0.03 ng/band and BChE 0.05 ng/band). In comparison to literature, our LODs were much lower than those reported by Marston *et al.* (1 ng/band)[15] and very close to that of Yang *et al.* (0.01 ng/band)[28]. With regard to different substrates, the LODs obtained by our method (1-naphthyl acetate as substrate and Fast Blue B salt as chromogenic reagent) showed lower values than the combination of 4-methoxylphenyl acetate as substrate and potassium ferricyanide/iron chloride hexahydrate as

chromogenic reagent (LOD 1 ng/band)[29] or the modified Ellman's method (LODs 10-600 ng/band)[27,30,31].

The comparison of the S/N ratio at 0.1 ng/band PHY showed higher ones for applied (S/N 24 for AChE and S/N 9 for BChE assays, Table 1) than developed PHY (S/N 8 for AChE and S/N 5 for BChE assays, Table 1). Thus, as expected, LODs of applied PHY were lower than that for developed PHY. In a reported normal and reversed phase TLC–AChE procedure with indoxyl acetate as chromogenic substrate(turns to blue fluorescent form), the LOD of a merely applied PHY band was 0.1 ng/band.[32] Therefore in our LOD study being even lower (S/N 24 for AChE and S/N 9 for BChE assays) at 0.1 ng/band, the selected HPTLC–AChE with 1-naphthyl acetate as substrate and Fast Blue B salt as chromogenic reagent was the most sensitive method with regard to LODs of PHY, and thus suited best for this quantitative investigation. In a recent study, the LOD of PHY was determined via a microtiter plate ChE assay (data not shown) which revealed that the HPTLC–AChE needs a lower substance amount to show an equivalent inhibition zone response (0.03 or 0.04 ng/8-mm band) in comparison to a microtiter plate result (ng/well). In order to assess our HPTLC–AChE results, the pIC_{50} was calculated via the pMIQ value for comparison with the microtiter plate results.[23]

3.5.Analytical response and IC_{50} value

If compared to peak height, the calibration range was broader for evaluation via peak area, especially evident by the peak height signal saturation for the AChE assay (Fig. 2C). The slope of the linear calibration (peak area) in the range of 0.1-1.5 ng/band PHY was compared for both calibration modes. For example for the BChE assay, the calibration via developed PHY showed a higher slope (2250), and thus, was more sensitive than the calibration via applied PHY (slope of 1500). The calibration curves of AChE were polynomial in both modes. The linear rang of the developed mode was 0.1-0.7 ng/band. In the same range, its applied mode was hardly linear which challenged the slope comparison. Nevertheless, the same outcome was obtained: in the HPTLC-AChE assay, the slope of developed PHY (mean 4660) was higher than in the applied mode (mean 3290). Thus, it was found that peak area evaluation and the developed mode were slightly superior to peak height evaluation and the applied mode. In the developed mode, the determination coefficient of the polynomial calibration for AChE and linear calibration for BChE (both 0.1-1.5 ng/band) was 0.999 in both cases. In the applied mode, it was 0.990 for AChE (polynomial calibration) and 0.993 for BChE (linear calibration).

The IC_{50} value for PHY was calculated based on the pMIQ value. The lowest, experimentally proven inhibition band for PHY was 0.1 ng/band or 3.6×10^{-13} mol. The corresponding pMIQ would be 12.4 mol for both HPTLC–ChE assays. Our result showed slightly higher pMIQ value in comparison to di Giovanni *et al*. (11.8 mol). The extrapolated IC_{50} of PHY was estimated as 1.25 µM and pIC_{50} of 5.9, which was comparable with pIC_{50} of PHY from Ellman's (pIC_{50} of 5.61) and Marston's (pIC_{50} of 5.86) microtiter plate methods. It was above, but close to the cut-off point (pMIQ 10.5 and pIC_{50} 5.0) that considers a compound as an active one.[23]

Table 1. Equivalency calculation and figures of merit of the ChE inhibition bands in *P. h.* seed extract (recorded by absorption measurement at 546 nm) referring to PHY either as applied or developed band; three repetitions were performed on four plates and on different days (n = 4).

Assays	PHY	**Developed mode** (n = 4)						**Applied mode** (n = 4)		
		Mean amount	Reproducibility		Mean amount	Reproducibility		Mean amount	Reproducibility	
		ng/band, peak height	SD	%*RSD*	ng/band, peak area	SD	%*RSD*	ng/band, peak area	SD	%*RSD*
AChE	Equal to band 1 (harmine)	0.9	0.05	6	0.9	0.07	8	1.2	0.15	12
	Equal to band 2 (harmaline)	0.9	0.05	6	1.0	0.12	12	1.4	0.10	7
	Equal to 1 µg/band *P. h.* seed extract	**1.8**	0.09	5	**1.9**	0.19	10	**2.6**	0.24	9
	LOD (ng/band)	0.03			0.04					
	S/N ratio at 0.1 ng/band[a]	8						24		
	Determination coefficient R^2	0.999			0.999			0.990		
BChE	Equal to band 3 (harmol)	0.3	0.03	9	0.3	0.03	9	0.5	0.09	18
	Equal to band 4 (vasicine)	0.3	0.02	8	0.3	0.01	5	0.4	0.05	14
	Equal to band 5 (deoxyvasicine)	0.2	0.01	7	0.2	0.01	7	0.2	0.02	8
	Equal to 1 µg/band *P. h.* seed extract	**0.8**	0.04	5	**0.8**	0.05	7	**1.1**	0.14	13
	LOD (ng/band)	0.05			0.05					
	S/N ratio at 0.1 ng/band[a]	5						9		
	Determination coefficient R^2	0.999			0.999			0.993		
AChE/BChE inhibition ratio		**2.3**			**2.4**			**2.4**		

[a]via peak height

3.6.Accuracy/bias

The bias between the two different modes of equivalency calculation was investigated (accuracy of sample analysis) and accounted for ca. 30% (Table 1). Referring to calibration via the developed PHY, 0.8 ng was equal to the BChE inhibition of 1 µg *P. h.* seed extract, whereas it was 1.1 ng when referring to the calibration via the applied PHY. In the developed mode, the calibration range covered well all five ChE inhibition bands via both, peak area and peak height. Almost the same PHY amount that was equal to the ChE inhibition of 1 µg/band *P. h.* seed extract was obtained either by peak area or peak height, *i.e.* 0.8/0.8 and 1.8/1.9 ng PHY for BChE and AChE assay, respectively (Table 1). Using the same calibration range in the applied mode, only the calculation via peak area did work, since the merely applied PHY bands were sharper in the peak form and caused higher peak height signals that shifted the BChE-inhibiting bands of the *P. h.* seed extract out of the lower calibration range (Fig. 2C and F). The total AChE inhibition of 1 µg/band of *P. h.* seed extract was ca. 2.4 times stronger than its BChE inhibition (Table 1). This AChE/BChE inhibition ratio remained almost the same, and it made no difference whether either applied or developed PHY was used for equivalency calculation. As expected, relative values are less influenced.

In conclusion, a higher accuracy was obtained via an appropriate co-developed reference inhibitor for the enzyme inhibition equivalency calculation. This was expected due to their similar properties with regard to signal intensity, band/peak shape and more sensitive calibration. Nevertheless, the bias caused by the faster bioanalytical workflow (merely applied track pattern) for equivalency calculation might be acceptable as a compromise.

4. Conclusions

Most enzyme inhibitors discovered in a complex sample are unknown or unidentified, and their inhibition potency needs to be estimated by equivalency calculation. Referring to the known ChE inhibitor PHY, two modes of equivalency calculation were compared, *i. e.* via developed PHY bands, and as a faster and simpler alternative, merely applied PHY bands. This quantification/calculation was performed without the least isolation step and at a much lower working range, if compared to literature. The equivalency calculation of unidentified ChE inhibitors in *P. h.* seed extract was proven to be more reliable and sensitive when using developed PHY bands. However, the effort for the method development is increased. If the faster protocol of an applied track pattern is used for equivalency calculation, an additional bias is expected that was ca. 30% in our study. In contrast to this bias, the AChE/BChE inhibition ratio was the same, as it is a relative value.

Conflicts of interest

There are no conflicts to declare.

Acknowledgments

Thank is owed to Kathrin Billerbeck, Isabelle Thomä and Jonas Baake to work on this project as part of their thesis as well as Merck, Darmstadt, Germany for providing HPTLC plates. Instrumentation was partially funded by the Deutsche Forschungsgemeinschaft (DFG, German Research Foundation) - INST 162/471-1 FUGG; INST 162/536-1 FUGG.

References

1. E. Azadniya and G. E. Morlock, *J. Chromatogr. A*, 2018, **1533**, 180-192.
2. S. Hage and G. E. Morlock, *J. Chromatogr. A*, 2017, **1490**, 201-211.
3. M. Jamshidi-Aidji and G. E. Morlock, *J. Chromatogr. A*, 2015, **1420**, 110-118.
4. E. Azadniya and G. E. Morlock, *J. Chromatogr. A*, 2019, **1602**, 458-466.
5. M. Jamshidi-Aidji and G. E. Morlock, *Anal. Chem.*, 2018, **90**, 14260-14268.
6. J. Zhou, Q. Tang, T. Wu and Z. Cheng, *Phytochem. Anal.*, 2017, **28**, 115-124.
7. M. Jamshidi-Aidji and G. E. Morlock, *Anal. Chem.*, 2016, **88**, 10979-10986.
8. C. F. de Jong, R. J. Derks, B. Bruyneel, W. Niessen and H. Irth, *J. Chromatogr. A*, 2006, **1112**, 303-310.
9. T. A. van Beek, K. K. Tetala, I. I. Koleva, A. Dapkevicius, V. Exarchou, S. M. Jeurissen, F. W. Claassen and E. J. van der Klift, *Phytochem. Rev.*, 2009, **8**, 387-399.
10. A. Ramírez, R. Gutiérrez, G. Díaz, C. González, N. Pérez, S. Vega and M. Noa, *J. Chromatogr. B*, 2003, **784**, 315-322.
11. I. Choma, *J. Liq. Relat. Techn.*, 2006, **29**, 2083-2093.
12. W. Schulz, W. Seitz, S. Weiss, W. Weber, M. Böhm and D. Flottmann, *J. Planar Chromatogr.-Mod. TLC*, 2008, **21**, 427-430.
13. S. Buchinger, D. Spira, K. Bröder, M. Schlüsener, T. Ternes and G. Reifferscheid, *Anal. Chem.*, 2013, **85**, 7248-7256.
14. I. Klingelhöfer and G. E. Morlock, *J. Chromatogr. A*, 2014, **1360**, 288-295.
15. A. Marston, J. Kissling and K. Hostettmann, *Phytochem. Anal.*, 2002, **13**, 51-54.
16. R. Akkad and W. Schwack, *J. Chromatogr. B*, 2010, **878**, 1337-1345.
17. C. A. Simões-Pires, B. Hmicha, A. Marston and K. Hostettmann, *Phytochem. Anal.*, 2009, **20**, 511-515.
18. M. Jamshidi-Aidji, J. Macho, M. B. Mueller and G. E. Morlock, *J. Liq. Relat. Techn.*, 2019, 1-8.
19. J. Taibon, A. Ankli, S. Schwaiger, C. Magnenat, V.-I. Boka, C. Simões-Pires, N. Aligiannis, M. Cuendet, A.-L. Skaltsounis and E. Reich, *Planta Med.*, 2015, **81**, 1198-1204.
20. O. N. Pozharitskaya, S. A. Ivanova, A. N. Shikov and V. G. Makarov, *J. Sep. Sci.*, 2007, **30**, 1250-1254.
21. O. N. Pozharitskaya, S. A. Ivanova, A. N. Shikov and V. G. Makarov, *Phytochem. Anal.*, 2008, **19**, 236-243.
22. V. Danciu, A. Hosu and C. Cimpoiu, *J. Planar Chromatogr.-Mod. TLC*, 2016, **29**, 306-309.
23. S. Di Giovanni, A. Borloz, A. Urbain, A. Marston, K. Hostettmann, P.-A. Carrupt and M. Reist, *Eur. J. Pharm. Sci.*, 2008, **33**, 109-119.
24. T. Mroczek, *J. Chromatogr. A*, 2009, **1216**, 2519-2528.
25. X.-y. Zheng, Z.-j. Zhang, G.-x. Chou, T. Wu, X.-m. Cheng, C.-h. Wang and Z.-t. Wang, *Arch. Pharmacal. Res.*, 2009, **32**, 1245-1251.

26. H. R. Adhami, H. Farsam and L. Krenn, *Phytother. Res.*, 2011, **25**, 1148-1152.
27. A. H. Abou-Donia, F. A. Darwish, S. M. Toaima, E. Shawky and S. S. Takla, *J. Chromatogr. B*, 2014, **955**, 50-57.
28. Z. Yang, X. Zhang, D. Duan, Z. Song, M. Yang and S. Li, *J. Sep. Sci.*, 2009, **32**, 3257-3259.
29. Z. D. Yang, Z. W. Song, J. Ren, M. J. Yang and S. Li, *Phytochem. Anal.*, 2011, **22**, 509-515.
30. I. K. Rhee, M. van de Meent, K. Ingkaninan and R. Verpoorte, *J. Chromatogr. A*, 2001, **915**, 217-223.
31. I. J. Vieira, W. L. Medeiros, C. S. Monnerat, J. J. Souza, L. Mathias, R. Braz-Filho, A. C. Pinto, P. M. Sousa, C. M. Rezende and R. D. A. Epifanio, *An. Acad. Bras. Cienc.*, 2008, **80**, 419-426.
32. I. A. Ramallo, P. García and R. L. Furlan, *J. Sep. Sci.*, 2015, **38**, 3788-3794.

TOC

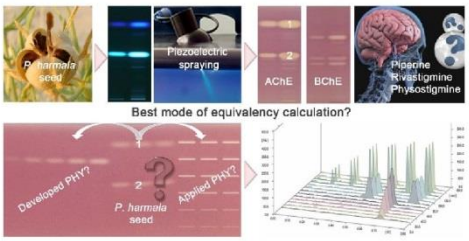

Equivalency calculation of unidentified acetyl- or butyrylcholinesterase inhibiting bands of a medicinal plant (*P. harmala*) referring to a medicinal reference (physostigmine): developed bands led to more reliable and sensitive results, whereas using merely applied bands was faster and simpler.

Please do not adjust margins

5. PUBLICATION 4

Incorporating the S9 system into methods for acetylcholinesterase inhibition and application to food contact materials

Julie Mollergues[a,‡], Ebrahim Azadniya[b,‡], Thomas Stroheker[a], Kathrin Billerbeck[b], Gertrud E. Morlock[b,*]

[a]*Chemical Food Safety group, Nestlé Research Center, Lausanne, Switzerland*

[b]*Chair of Food Science, Institute of Nutritional Science, Interdisciplinary Research Center (IFZ), Justus Liebig University Giessen, Heinrich-Buff-Ring 26-32, 35392, Giessen, Germany*

Ready to submit in

Analytical Chemistry

Incorporating the S9 system into methods for acetylcholinesterase inhibition and application to food contact materials

Julie Mollergues[a,‡], Ebrahim Azadniya[b,‡], Thomas Stroheker[a], Kathrin Billerbeck[b], Gertrud E. Morlock[b,*]

[a]Chemical Food Safety group, Nestlé Research Center, Lausanne, Switzerland

[b]Chair of Food Science, Institute of Nutritional Science, and Interdisciplinary Research Center (IFZ), Justus Liebig University Giessen, Heinrich-Buff-Ring 26-32, 35392 Giessen, Germany

*Corresponding Author: fax +49-641-99-39149; Gertrud.Morlock@uni-giessen.de

ABSTRACT: The metabolizing S9 enzyme mixture, mimicking the biotransformation reactions in the liver, was incorporated into two orthogonal methods for analysis of the acetylcholinesterase (AChE) inhibition. For a fluorometric microtiter plate assay, the incorporated S9 mixture interfered with the final detection product that was further reduced to the non-fluorescent hydroresorufin. In contrast, it was successfully incorporated into a high-performance thin-layer chromatography (HPTLC) method. The separation layer provided an ideal surface for the *in situ* interaction between chemicals and S9 mixture at the start zone. Different application orders/areas and plate wetting modes were investigated for the enzymatic on-surface reaction of the new HPTLC–S9–AChE workflow. After on-plate metabolization and separation, the AChE/substrate/chromogenic reagent solutions were sprayed piezoelectrically, resulting in a homogeneous plate background. The determined limits of detection (LODs) of six AChE inhibiting chemicals, including eserine, the pesticides chlorpyrifos, quinalphos and parathion as well as tris(nonylphenyl) phosphite and nonylphenol released from food contact materials (FCMs), were compared between both methods and with those after metabolic activation. The thresholds of toxicological concern (TTCs) of AChE-inhibiting packaging migrants were compared with the LODs obtained by the HPTLC–S9–AChE method. The direct toxicity assessment of FCMs via their respective TTCs was achieved by a 200-fold enrichment of the two migrates and one extract of a white polyurethane coated can, simply by solvent evaporation during spray-on area application. Hence, two migrates and one extract were directly analyzed without pre-dilution/concentration with this straightforward HPTLC–S9–AChE method, which is standardized, automated in its important steps, and highly efficient (9-10 Euro/plate, 3-4 h analysis time/plate).

Food contact materials (FCMs) are susceptible to release substances migrating into food and categorized as intentionally added substances (IAS) or non-intentionally added substances (NIAS). The latter are, for example, impurities in the starting materials, break-down products of FCMs, unwanted side-products or various contaminants from the recycling process.[1] These substances should not interfere with the organoleptic and sensory aspects of the food, and more important should not impair the safety of the packed food.[2] As a pragmatic and convenient tool, the threshold of toxicological concern (TTC) was developed to assess chemicals with **limited** toxicological data.[3-5] It is recognized and widely used in **risk assessment** of substances, for which toxicological data are **lacking**.[6-7] The assessment follows a decision tree starting with questioning on the presence of alerts for potential genotoxicity. A second level consists in a specific threshold of 0.3 µg/kg body weight/day for chemicals structurally similar to organophosphates (OPs). Such threshold was calculated from the distribution of the acceptable daily intake values of OPs and carbamates (CBs), based on their common acetylcholinesterase (AChE) inhibiting capacity. This enzyme hydrolyses the excitatory neurotransmitter acetylcholine (ACh) and allows cholinergic-sensitive neurons to return to its resting state. The inhibition of AChE triggers neuronal overstimulation resulting in severe neurotoxicity.[8] If chemicals are not similar to OPs, the third level consists in their classification in the three Cramer classes.[9] Some of the packaging chemicals (*e.g.* phosphites used as antioxidants) also inhibit the activity of AChE (unpublished internal results). Therefore, also their identification in packaging migrants is relevant for safety assessment.

In addition, some chemicals require metabolic biotransformation to be active. Biotransformation is generally divided into phase I (hydrolysis, oxidation and reduction) and phase II (conjugation) reactions. Cytochromes P450 play a dominant role in the phase I metabolism and are involved in the bioactivation of a variety of genotoxic chemicals or endocrine active substances.[10] Oxidation of some OPs (*e.g.*, parathion or chlorpyrifos) into their oxon analogs increased significantly the inhibitory potential of the parent substance.[11-13] Hence, the incorporation of a metabolizing system such as the S9 fraction of rat liver, mimicking the phase I reactions,[10,14] is strongly recommended in any assay aimed at measuring the AChE inhibition.

In this context, a rapid separation and sensitive detection of AChE inhibitors would contribute to the assessment of such uncharacterized complex mixtures. It should be sensitive enough to detect traces of AChE inhibitors to be compared with the TTC threshold for OPs, but not oversensitive to stay relevant in a context of safety assessment for decision making. In literature, mainly colorimetric

methods according to Ellman were reported for assessing the activity of AChE,[15-17] though fluorescence detection was more sensitive.[18] In cuvette, microtiter plate or dot-blot assays, either only a sum parameter is achievable for a complex sample, or fractions need to be isolated a priori. In contrast, high-performance thin-layer chromatography (HPTLC) hyphenated with the AChE assay separates complex samples and points to single active zones *in situ* the autogram.[19-22] In detail, organophosphate and carbamate insecticides were investigated.[23-26] Recently, the HPTLC–AChE workflow has been optimized.[27,28] Many advantages were discussed for the straightforward workflow without any previous fractionation.[29,30] The identification of active compounds was demonstrated by coupling HPTLC with techniques for structure elucidation, *e.g.*, nuclear magnetic resonance spectroscopy and high-resolution mass spectrometry (HRMS).[31,32]

According to our preliminary data (not shown), the fluorometric 10-acetyl-3,7-dihydroxyphenoxazine (Amplex® Red) ChE/AChE assay was more sensitive than colorimetric assays. Briefly, AChE converted acetylcholine into choline, which was oxidized by choline oxidase into betaine and H_2O_2 to react in the presence of horseradish peroxidase with Amplex® Red in a 1:1 stoichiometric reaction to generate the highly fluorescent product resorufin. In this study, the limits of detection (LODs) of the sensitive fluorometric assay were compared with the optimized HPTLC–AChE method which AChE hydrolyses the 1-naphthyl (substrate) to 1-naphthol reacting with Fast Blue B salt (chromogenic agent) to produce a purple plate background.[27] The LODs of each method were assessed based on a selection of chemicals consisting of OPs (chlorpyrifos, quinalphos, parathion) and a CB (eserine). These classes of chemicals are well-known to exert AChE inhibition.[8,11] This selection allowed also to assess the feasibility and efficacy of the metabolizing S9 system to be implemented in both methods. In addition, the packaging chemicals tris(nonylphenyl) phosphite and nonylphenol were tested to investigate on a potential activity on the AChE. As proof of principle, two migrates and one extract of a white polyurethane coated can were investigated as typical samples in the food-packaging field.

EXPERIMENTAL SECTION

Chemicals and Materials. Lyophilized powder of AChE (*Electrophorus electricus*, electric eel), ACh, Fast Blue B salt, chlorpyrifos (CP), quinalphos (QP), parathion (PT), nonylphenol (NP), tris(nonylphenyl) phosphite (TNPP), dimethyl sulfoxide (DMSO), β-nicotinamide adenine dinucleotide phosphate (β-NADPH), reduced tetra(cyclohexylammonium) salt, glucose-6-phosphate, glucose-6-phosphate dehydrogenase, magnesium chloride hexahydrate, horseradish peroxidase, and choline oxidase were provided from Sigma Aldrich (Steinheim, Germany). Eserine (ER) was purchased from LabForce (Muttenz, Switzerland). The Amplex® Red ACh/AChE assay, ethanol and methanol were obtained from Thermo Fisher Scientific (Loughborough, UK, or Schwerte, Germany; kit A-12217). Rat fraction S9 induced with a mixture of β-naphtoflavone/phenobarbital was purchased from Xenometrix (Allschwil, Switzerland). 1-Naphthyl acetate was purchased from Panreac (Barcelona, Spain). *n*-Hexane and ethyl acetate (both analytical grade for mobile phase) were obtained from Th. Geyer (Berlin, Germany). Hydrogen chloride (HCl), tris(hydroxymethyl)aminomethane (Tris), sodium monohydrogen phosphate, formic acid (96 %) and bovine serum albumin were purchased from Carl Roth (Karlsruhe, Germany). Bidistilled water was prepared with a Destamat Bi 18 E (Heraeus, Hanau, Germany). For migration simulation, *n*-hexane (for residue analysis), ethanol and acetone (both SupraSolv®) as well as HPTLC plates silica gel 60 F_{254} were purchased from Merck (Darmstadt, Germany). The FCM sample was a white polyurethane coated can manufactured for R&D purposes.

Fluorometric Assay. Stock concentration of the six chemicals were prepared in DMSO to a final concentration of 250 mM. An aliquot (4.8 µL) was diluted into 295.2 µL Tris-HCl buffer (0.03 M, pH 8). A dose-range was prepared with serial dilutions of this starting solution in the same buffer containing 1.6 % DMSO to have a final DMSO concentration in wells at 0.4 % (fluorescence signal decreased at 0.8 %; data not shown). Fifty microliters of each dose (in triplicates) was transferred into a black 96 well-plate. The plate was incubated at room temperature on a plate shaker for 30 min. Lyophilized AChE was dissolved in the Tris-HCl buffer. This AChE solution (50 µL, 0.2 U/mL) was added on top of each well. Positive and negative control (100 µL each) consisting of 10 µM hydrogen peroxide (H_2O_2) and Tris-HCl buffer, respectively, was also transferred into the plate (triplicate). After 15 min, 100 µL of working solution (0.14 mM Amplex® Red, 8 units/mL horseradish peroxidase, 0.4 U/mL choline oxidase and 0.18 mM ACh chloride) was added in each well (including positive and negative controls) and the kinetic fluorescence measurement was launched. The final concentration of AChE was 0.05 U/mL. Every chemical was tested from the nanomolar to the millimolar range. Fluorescence of resorufin was measured at 37 °C, every 120 s for 1 h at excitation and emission wavelengths of 560 and 620 nm, respectively. The procedure with the incorporated S9 system was nearly the same as described above, except that serial dilutions of the chemicals were prepared in buffer containing 0.1 mg/mL S9, 0.17 mM β-NADPH, 3 mM glucose-6-phosphate, 5 mM magnesium chloride hexahydrate and 0.3 U/mL glucose-6-phosphate dehydrogenase (S9 mixture).

Solutions and Samples for HPTLC. Ethanolic solutions of CP, QP, ER, PT, NP and TNPP (1 mg/mL) were diluted 1:10 and 1:100 (0.1 and 0.01 mg/mL). White polyurethane coated cans were filled with 300 mL of food simulant (ethanol 95 % or ethanol 50 %) and incubated at 60 °C for 10 days for migration or extracted at room temperature with *n*-hexane–acetone, 1:1, for 16 ±1 h. AChE solution (6.6 units/mL) was prepared by dissolving the lyophilized enzyme powder and bovine serum albumin (1 mg/mL) in Tris-HCl buffer (0.05 M, pH 7.8). The substrate-chromogenic solution was prepared by mixing 1:2 an ethanolic solution of 1-naphthyl acetate and an aqueous solution of Fast Blue B salt (3 mg/mL each).

LOD Study by HPTLC–S9–AChE via bandwise application and immersion of solutions. A set of plates was prewashed twice by chromatography with methanol and water 3:1 (*V*/*V*), dried at 120 °C in a clean oven for 1 h, covered with a clean counter glass plate and stored wrapped in aluminum foil until use. Ethanolic standard solutions were applied on HPTLC plates silica gel 60 F_{254} as 8-mm bands, each at five different levels in the range of 0.5-10 µL/band (overall range for all six chemicals 0.1-1000 ng/band) using the Automated TLC Sampler (ATS4, CAMAG, Muttenz

Switzerland). After drying for 2 min, the application bands were pre-wetted by immersing (3-s immersion time, 3.5-cm/s immersion speed) the plate up 10 mm in water (6 mL in the 20 × 10 cm Biostep dipping chamber). Then, immediately S9 mixture (7 µL each, 0.1 mg/mL) was sprayed on top, then plates were incubated at room temperature (RT) for 30 min in the humid box. Plates were dried for 20 min in humidity control mode of Automatic Developing Chamber 2 (ADC 2, CAMAG). After 5 min chamber saturation, the dried plates were developed up to 70 mm in the Twin Trough Chamber (CAMAG, 20 × 10 cm), each with an optimized mobile phase (MP): Ethyl acetate–methanol–water, 5:5:2 (MP1 for ER), *n*-hexane–ethyl acetate–ethanol, 16:3:1 (MP2 for QP and PT) and *n*-hexane–toluene–ethyl acetate, 5:4:1 (MP3 for CP, NP and TNPP). Dried chromatograms were documented at 254 and 366 nm as well as white light illumination using the TLC Visualizer (CAMAG). Chromatograms were immersed in the AChE solution at an immersion speed of 3.5 cm/s for 2 s using the Immersion Device III (CAMAG). After evaporation of the liquid film on the surface, the plate was incubated at 37 °C in a humid box for 25 min. The plate was immersed into the substrate-chromogenic solution for 1 s at an 3.5-cm/s immersion speed, after evaporating the solvents and drying at RT for 4 min, dried for 10 min in ADC 2 and documented under white light illumination.

Matrix Effect and Recovery Study by HPTLC–S9–AChE. Two migrates and one extract were spiked by 6 chemicals at a concentration level of the calibration curve (Table S-1) and applied in duplicate to be studied with and without S9 and repeated (n = 3). The main inhibition band of each chemical in the spiked samples was compared to the corresponding inhibition band of pure chemical in the same autogram. The peak area ratios were reported as recovery (%; peak area of chemical in spiked sample/peak area of chemical × 100).

Sample Analysis by HPTLC–S9–AChE via area application and piezoelectric spraying. Can migrates, extract and corresponding blanks were applied on prewashed HPTLC plates silica gel 60 F_{254} as area (8 × 10 mm, 200 µL each) at a dosage speed of 1000 nL/s and needle temperature of 50 °C. The applied areas were focused two times with 2 mL methanol up to 20 mm. On top of the focused application areas, the S9 mixture solution (0.1 mg/mL) was applied as an area (84 × 3 mm, 110 µL, 200 nL/s, no nozzle heat). After aqueous plate wetting *via* piezoelectric spraying (2 mL water, green nozzle, spraying level 6, Derivatizer, CAMAG) and incubation at RT in a humid box for 30 min, the dried plate (20 min, ADC 2) was developed first with a polar mixture consisting of ethyl acetate–methanol–water, 17:2:1 (MP4) up to 50 mm. After drying for 2 min, a second development was performed using a less polar mixture of toluene–*n*-hexane–ethyl acetate–ethanol, 9:8:3:1 (MP5) up to 85 mm. All AChE assay solutions were piezoelectrically sprayed (spraying level 6) as follows[27]: The plate was wetted first with 1 mL Tris-HCl buffer and then with the enzyme solution (green nozzle, 3 mL), followed by incubation in a humid box at 37 °C for 25 min. The substrate-chromogenic solution (red nozzle, 0.5 mL) was sprayed, followed by drying (4 min at RT and 10 min in ADC 2) and documentation as white zones on a purple background under white light illumination (automatic capture of the image).

Data Analysis. In the fluorometric assay, the AChE activity was expressed as the production of hydrogen peroxide (pmol) per minute. The measured fluorescence (F) is proportional to the concentration of the fluorescent molecule resorufin (C) in the sample: $F = K^*C$. The positive control H_2O_2 was used to determine the constant K, using the command "Column statistics" in GraphPad Prism software version 7.03 (GraphPad, La Jolla, CA): $K = F(H_2O_2)/C(H_2O_2)$. In order to calculate the resorufin concentration in each sample, the measured F value is divided by the calculated constant K: $C = F\ (measured)\ /\ K$. The Amplex® Red reaction is stoichiometric. Hence, the amount of resorufin is equal to the amount of H_2O_2 produced. Each chemical was tested in three independent experiments (n = 3). Each concentration was tested in technical triplicate. AChE activity has been calculated by the software as described above taking into account the triplicate values and standard deviations (SD). LOD and limits of quantitation (LOQ) were calculated for each standards assay as follow: LOD = mean (vehicle control) – 3 SD and LOQ = mean (vehicle control) – 10 SD.

The enzyme inhibition densitograms of the HPTLC–S9–AChE analysis were obtained by absorbance measurement at 546 nm (mercury lamp) using an inverse scan (trick to avoid peak conversion to negative peaks by selection of fluorescence mode without optical filter as software parameter; TLC Scanner 4, CAMAG). The peak area of the inhibition zones of the six chemicals were plotted *versus* their five concentration levels. LODs were determined according to the standard deviation of response (Sy) and slope (m) of the calibration curve method as LOD = 3.3 (Sy/m) (MS Excel: "SLOPE" function was used for "m" and "STEYX" for Sy). Secondly, the S/N ratio was checked to be 3 in the lower concentration level of the calibration curve as the closet point to the LODs. For precision study (± SD), three experiments were performed per chemical (n = 3).

RESULTS AND DISCUSSION

The sensitive fluorometric assay was compared with the recently developed HPTLC–AChE method for piezoelectric spraying[27] based on the Marston's method.[19] The incorporation of the S9 system was investigated, validated (LOD, recovery, calibration curve, working range, precision) and finally applied to the analysis of can migrates and extracts as proof of concept.

Feasibility of incorporating the S9 system in the fluorometric assay. The incorporation of an exogenous metabolizing system in the fluorometric method (Figure 1) encounters some issues. CP induced the inhibition of the enzyme (red dose response) with an IC_{50} of 7.82×10^{-4} M (Figure 2). The oxon form of CP was also tested (purple dose response curve) and its inhibition activity was much more potent as compared to the parental compound with an IC_{50} of 2.01×10^{-6} M (2 log lower). The AChE inhibition of CP after S9 treatment (dashed blue curve) did not appear to differ greatly from that of its pure metabolite CP oxon, with an IC_{50} similar to the CP-oxon (2.67×10^{-6} M) suggesting that either the oxon form was the main component of the metabolite mixture, or the other metabolites present similar inhibition activity, or both. This method did not allow identifying and discriminating the different metabolites. However, a drop in the maximum activity (efficacy of the response) was observed with an AChE activity 3 times lower when CP was co-incubated with S9 and cofactors (dashed blue

curve), as compared to the parental compound (dotted red curve). A similar decrease in AChE activity was also detected when CP was incubated solely with cofactors (dash-dotted green curve). The same shift in the fluorescence signal was observed with the five other chemicals, in the presence of the S9 mixture or cofactors (Figure S-1). Nonetheless, the co-incubation of the parental compound with the S9 mixture allowed the biotransformation into potent metabolites, as demonstrated with PT, QP and CP. The S9 mixture did not influence the response of ER, NP and TNPP. The investigation revealed that the S9 mixture interfered with the final detection system, *i.e.* production of the redox resorufin. This fluorescent chemical was reported in the literature to be reduced into colorless, non-fluorescent compounds by the NADPH-cytochrome P450 reductase.[10, 41-42] Considering the presence of this enzyme in the rat liver S9 and the use of β-NADPH as a cofactor, the decrease in fluorescence would be explained by the conversion of resorufin in its non-fluorescent metabolites. Hence, the addition of S9 mixture was not suitable in the fluorometric assay.

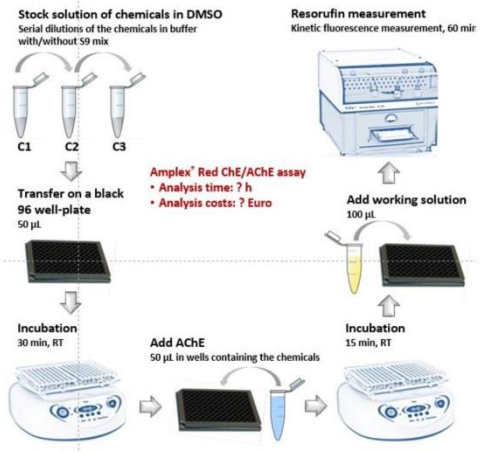

Figure 1. Workflow of the fluorometric Amplex® Red ChE/AChE assay.

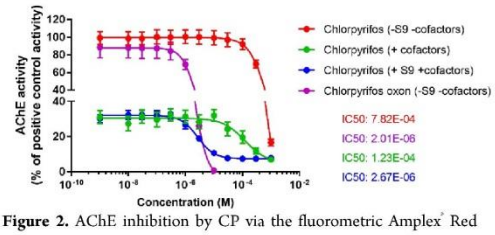

Figure 2. AChE inhibition by CP via the fluorometric Amplex® Red ChE/AChE assay.

Incorporation of the S9 System into the HPTLC–AChE Method. Three different modes of plate wetting (without, before or after S9 application) were investigated as well as various amounts of S9 (0-8 µg/band, 0-20 µL/band, 0.4 mg/mL). The HPTLC–S9–AChE method was performed with wetting the applied chemicals by immersion in 6 mL water, followed by S9 application (2.0 µg/band, 5 µL/band, 0.4 mg/mL). The wetting was necessary for successful on surface reactions of the metabolic phase I, as evident for CP, QP and PT (Figure S-2). In order to find the optimum dose, an S9 mixture range of 0-1 µg/band (0-10 µL, 0.1 mg/mL) was applied on a fix amount of each chemical, *i.e.* CP (400 ng/band), QP (10 ng/band), ER (0.7 ng/band), PT (50 ng/band), NP (500 ng/band) and TNPP (1000 ng/band). In addition, the S9 mixture (0.5 µg/band) was applied as a control. After development and absorbance measurement, the peak area of the inhibition bands were plotted *versus* the amount of added S9 mixture (Figure 3, Table S-2). All curves showed the same trend, *i.e.* a maximum around 0.7 µg/band. This optimal amount was selected for the following experiments. The plate wetting via immersion was compared before and after the S9 mixture application. The prior wetting was preferred to avoid any zone shifts and a resulting uneven plate background.

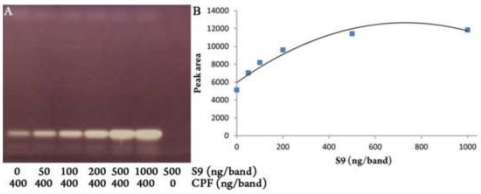

Figure 3. Optimization of the S9 mixture addition, shown for metabolization of CP: HPTLC–S9–AChE autogram under white light illumination (A), and after absorbance measurement, respective dose response curve (B).

Table 1. LODs of the six chemicals measured with/without S9 mixture via HPTLC–AChE *versus* fluorometric Amplex® Red ChE/AChE assay.

Chemicals	S9 mixture	HPTLC–AChE	Amplex® Red ChE/AChE assay	
		Mean LOD ± SD (n = 3)	Mean LOD ± SD (n = 3)	
		[ng/band, µg/mL]	[ng/well]	[µg/mL]
CP	-	17.2 ± 5.0	3797 ± 2975	19.0 ± 14.8
	+	0.28 ± 0.08	19.6 ± 11.7	0.10 ± 0.06
QP	-	0.3 ± 0.1	616 ± 1565	3.08 ± 1.56
	+	0.08 ± 0.02	13.8 ± 2.94	0.07 ± 0.01
ER	-	0.07 ± 0.03	0.63 ± 0.47	0.0032 ± 0.002
	+	0.05 ± 0.02	2.97 ± 2.27	0.01 ± 0.01
PT	-	16.9 ± 5.0	ND	ND
	+	0.20 ± 0.05	123.6 ± 109.4	0.62 ± 8.70
NP	-	64.0 ± 10.0	6345 ± 2189	31.7 ± 10.9
	+	34.0 ± 5.0	ND	ND
TNPP	-	500 (S/N 3.5)	10764 ± 4014	53.8 ± 20.1
	+	500 (S/N 3.5)	ND	ND

ND: not detectable

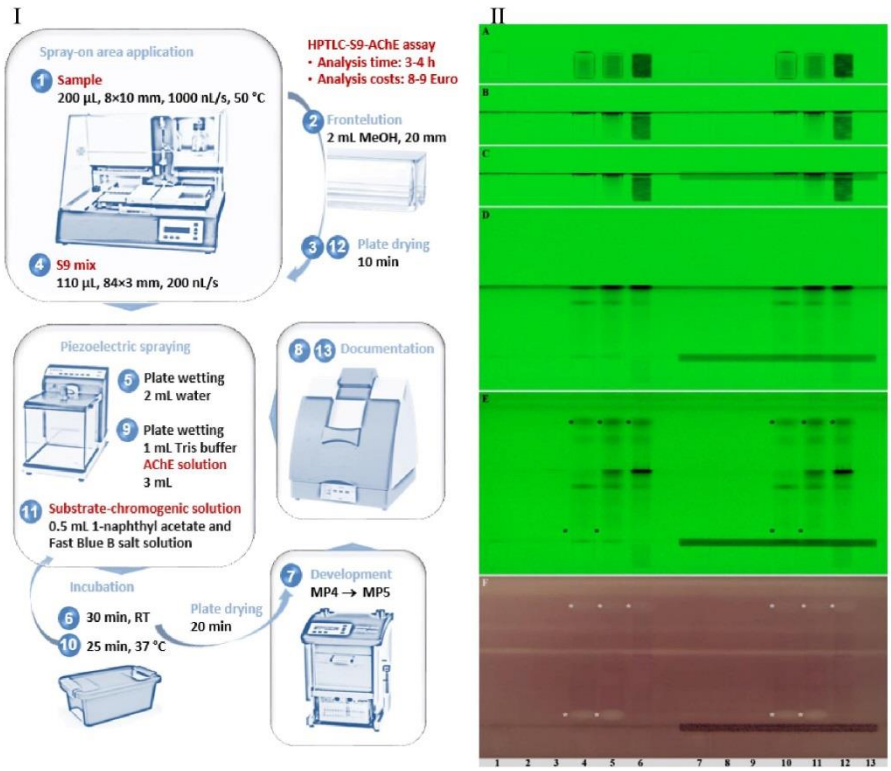

Figure 4-I. Workflow of the HPTLC–S9–AChE assay with piezoelectric spraying of all assay solution; framed steps are automated; steps 1, 2, 4, 7 and 13 are illustrated in **II** as HPTLC–UV chromatograms at 254 nm after area application (A), focusing of the start area by frontelution (B), S9 mixture application (C, only region of interest depicted in A-C), first development up to 50 mm with MP4 (D) and second development up to 85 mm with MP5 (E) as well as HPTLC–AChE autogram (F, tracks 1-6) *versus* HPTLC–S9–AChE autogram (F, tracks 7-13) under white light illumination: blanks of can migrates (tracks 1 and 7: ethanol 50%; tracks 2 and 8: ethanol 95%), *n*-hexane–acetone extract (tracks 3 and 9) and S9 mixture (track 13) *versus* can migrates (tracks 4 and 10: ethanol 50%; tracks 5 and 11: ethanol 95%) as well as *n*-hexane–acetone extract (tracks 6 and 12)

Determination of the LODs of the six chemicals. For each chemical, the LODs for both methods in the absence or presence of the S9 mixture were determined (Table 1). In general, the same workflow was used for both methods. For HPTLC, the S9 mixture including prior plate wetting was either applied or not. However, the generally used MP3 (except MP1 for ER) needed to be adjusted after the on surface metabolization of QP and PT, resulting in MP2. The HPTLC–AChE results revealed that PT showed almost a similar inhibiting activity as CP even without metabolic activation via the S9 mixture. Apart from very close results of both methods for CP, other compounds showed mostly similar LODs with some exceptions like QP and PT in HPTLC-AChE and, NP and TNPP in HPTLC-S9-AChE showed lower LODs, while, ER and TNPP showed lower LODs in the fluorometric AChE assay (Table 1, Figures S-3 to S-8). The HPTLC–S9–AChE and fluorometric AChE assay results showed that the LODs improved for CP, QP and PT after their metabolic activation. These findings were in accordance to literature, in which QP, CP and PT were reported to be activated into their oxon forms by CYP1A2 and 2B6[33-36]. These two CYP families induced by β-naphtoflavone and phenobarbital, respectively, are mainly present in our S9 mixture used.

Matrix Effect on the AChE Inhibition. The recovery values of chemicals spiked food simulants and extract showed different trends for six chemicals with and without S9 mixture treatment (Table S-1). For example, matrix effect increased the inhibition of CP (except ethanol 50 %, no change), ER and PT, and decreased that in NP and especially for TNPP but showed no change in QP. The S9 mixture treatment on chemical spiked food simulants and extract showed no impact on matrix influence on CP, QP and ER inhibition (the same trend as no S9 mixture treatment) but this treatment could counteract the matrix effect on PT by decreasing the inhibition. However, this S9 mixture treatment showed almost no change for inhibition of NP and decreased the inhibition of TNPP (except ethanol 50 %, no change), even matrix effect (without S9 mix) showed more decrease in inhibition of NP and TNPP.

Method Comparison and Benchmarking. Based on the LOD of each chemical expressed in µg/mL (Table 1), both methods were similarly sensitive. However, when expressed in absolute quantity (ng/band or ng/well), the HPTLC–AChE method appeared to be more sensitive. This is due to the principle of the test, requiring less material to be applied on the plates than to be put in the wells. Indeed, in the fluorometric method, the tested substances were dissolved in DMSO, as it is a known carrier of water-insoluble substances and miscible in a wide range of organic solvents. However, our internal data (not shown) demonstrated that DMSO affects the activity of the AChE enzyme at a concentration ≥ 0.8% and the same for standard solutions contains DMSO in HPTLC–AChE (not shown). In the Amplex® Red ChE/AChE assay, the chemicals were tested in a wide range of concentration at a fix volume (200 µL per well). On the contrary, in the HPTLC–AChE, the initial concentration was fixed, and only the volume of application on the HPTLC plate changed, and consequently the quantity of chemicals varied per band. This is especially useful in cases where only a small amount of sample is available. Another advantage of this method is the direct application of a sample without a pre-dilution, which is the case in most bioassays (cell or enzyme-based systems). Above all, the powerful key aspect was the separation of samples. By this, treasured information on single compounds in complex samples was obtained, and matrix interference was avoided.

Using the HPTLC–S9–AChE assay, one HPTLC plate was used for one chemical, which was applied 2-fold at 4 different concentrations with and without S9 mixture 16 tracks. Along with the blanks, it summed up to be 18 tracks. Positive/negative controls were applied as track pattern in the upper plate region. Also in the Amplex® Red ChE/AChE assay, one 96-well microtiter plate was used for the analysis of one chemical. The threefold application of 12 concentrations with and without S9 mixture (72 wells), in addition some blanks and positive/negative controls summed up to be 96 wells. The total incubation time was 45 min for the Amplex® Red ChE/AChE assay, whereby it was 55 min for the HPTLC–S9–AChE assay.

Calculating the analysis time for the HPTLC–S9–AChE assay, it took 3 or 4 h, depending on the protocol (immersion and bandwise application versus piezoelectric spraying and area application). The running costs were 8-9 Euro per plate (Table S-3). Calculating the analysis time for the Amplex® Red ChE/AChE assay, it took … h. The running costs were … Euro (Table S-3).

Selection of the Preferred Method. Regardless of the sensitivity of both methods, the ranking of the inhibition potency of the six chemicals was conserved as follows: ER > QP > CP ≈ PT > NP > TNPP for the fluorometric assay. The same order applied for the HPTLC–AChE method, except for PT > CP. The most potent AChE inhibitor of both systems, *i.e.* ER, was not affected by the S9 mixture. The two packaging substances NP and TNPP showed the weakest AChE inhibition, observed only at the highest dose in the fluorometric method (66 and 20.7 µg/mL, respectively). This inhibition disappeared with the S9 mixture pre-incubation, suggesting a biotransformation into non-inhibiting metabolites. In the manufacturing process, the antioxidant TNPP is known to be subjected to hydrolysis, leading to the production of NP,[37] which exerts estrogenic activity both *in vitro* and *in vivo*.[38-41] These two chemicals were not expected to exert AChE inhibition, and no dose-response relationship was observed. This suggests that such results should be interpreted with caution: the test system measured an enzymatic inhibition, which may be unspecific in presence of a large amount of the chemical.

Based on the successful integration of the S9 system for metabolization, the much lower matrix effect, the separation/assignment of single inhibitors and the possibility of applying small sample volumes, the HPTLC method was preferred for testing of FCMs, as shown for can migrates and extracts in the following.

Determination of a Threshold for the HPTLC–S9–AChE Assay. The TTC of 0.3 µg/kg bw/day for OPs and CBs was used as a starting point to define a threshold for the screening of uncharacterized packaging mixtures, *e.g.*, FCM migrates or extracts. Therefore, this oral exposure has to be converted into a testing dose in the HPTLC–AChE assay. In 2016, the EFSA panel on Food Contact Materials, Enzymes, Flavourings and Processing Aids defined four food intake *scenarios* based on the type of packed products.[42] In a conservative approach, it was considered that the packaging substances might leach from FCMs belonging to the first category, for which the food consumption to be applied for the estimation of the exposure is 0.15 kg/kg bw/day. This food intake *scenario* served as the basis to determine the equivalent in TTC per kg of food: 0.3 µg in 0.15 kg of food equals 2 µg "TTC equivalent"/kg of food. In this study, migration and extraction were performed by filling the can with 300 mL of food simulant. Considering that 1 liter of food simulant mimicks 1 kg of packed food, a level of 2 µg "TTC eq."/kg of food corresponds then to a quantity of 0.6 µg "TTC eq." in the can, *i.e.* 2 ng/mL.

CP, QP and PT were part of the database used to define the TTC for OPs[43]. Their respective acceptable daily intake values (1, 0.5 and 0.6 µg/kg bw/day, respectively) are close to the TTC. Based on their LODs (0.28, 0.08 and 0.20 ng/band, respectively) reported in HPTLC in the presence of the S9 mixture, a FCM migrate or extract containing 2 ng "TTC eq."/mL would be detected with tested volumes as low as 140 µL, 40 µL and 100 µL, respectively. Again, for a conservative approach, the highest volume was selected. In addition, an uncertainty factor of 1.4 was applied to reflect the loss of AChE inhibition activity observed with TNPP due to the migrant matrix (ethanol 95 %) in presence of the S9 mixture (Table S-1). By applying this uncertainty factor, it is recommended to start testing a packaging migrate or extract with a sample volume of 200 µL. The spray-on application parameters (dosage speed and needle temperature) were also optimized for 400 µL demonstrating the potential for higher application volumes.

Analysis of White Polyurethane Coated Can. Along with blanks, the can migrates and extract (200 µL each) were applied as area. The initial HPTLC–S9–AChE results of can migrates and extract revealed that these samples contained inhibitors with quite different polarity. For their separation, a two-step HPTLC development (first polar, then less polar mobile phase) was set up (Figures 4 and 5). An inhibition band at the lower hR_F (Figure 4-IIF, tracks 4, 5, 10 and 11), present in both migrates, but absent in the extract, was observed as well as further inhibition zones at a higher hR_F (Figure 4-IIF, tracks 4-6 and 10-12). The same profile of inhibition bands was observed in the absence and presence of S9 mix, suggesting that the AChE inhibitor(s) present in the bands were not impacted

by the CYP450 in the S9 mix. This could additionally be proven using a different system selectivity or HRMS. A follow-up of these results can consist in the identification of the molecules present in the inhibition band and therefore their quantification or equivalency calculation[28] to run out a toxicological risk assessment.

CONCLUSIONS

In this study, we demonstrated that the HPTLC hyphenated with the AChE inhibition assay is a very sensitive tool allowing the detection of chemicals at levels consistent with the TTC for OPs and CBs. In addition, it was suitable for the successful implementation of the S9 mixture metabolism system. Assessing the *in vitro* biological activity of the packaging migrants often required an additional step of concentration into a solvent suitable for cell or enzyme-based assays, with the subsequent risk of contamination of the sample preparation. Here, the high sensitivity of the method allowed the direct application of the can migrate or extract on the HPTLC plate, followed by separation and AChE assay. Single AChE inhibitors were found via this helpful biochemical-analytical tool. The same approach can be investigated for other toxicities of interest (*e.g.*, genotoxicity or endocrine activity) and for other families of complex mixtures (plant extracts).

ASSOCIATED CONTENT

Supporting Information

The Supporting Information is available free of charge on the ACS Publications website.

AUTHOR INFORMATION

Corresponding Author

*Phone: +49-641-99-39141. Fax: +49-641-99-39149. E-mail: Gertrud.Morlock@uni-giessen.de.

Author Contributions

The manuscript was written by all authors, with the exception of KB. JM… TS… EA…. GM….

‡These authors contributed equally.

ACKNOWLEDGMENT

Thank is owed to Benoit Schilter and Maricel Marin-Kuan for fruitful discussions.

REFERENCES

1. Koster, S.; Leeman, W.; Verheij, E.; Dutman, E.; van Stee, L.; Nielsen, L. M.; Ronsmans, S.; Noteborn, H.; Krul, L., A novel safety assessment strategy applied to non-selective extracts. *Food and Chemical Toxicology* **2015,** *80*, 163-181.
2. EU, European Regulation, no. 1935/2004 of the European Parliament and of the Council of 27 October 2004 on materials and articles intended to come into contact with food and repealing Directives 80/590/EEC and 89/109/EEC. Official Journal of the European Union: 2004; Vol. L 338/4.
3. Munro, I.; Kennepohl, E.; Kroes, R., A procedure for the safety evaluation of flavouring substances. *Food Chem. Toxicol.* **1999,** *37* (2-3), 207-232.
4. Kroes, R.; Galli, C.; Munro, I.; Schilter, B.; Tran, L.-A.; Walker, R.; Würtzen, G., Threshold of toxicological concern for chemical substances present in the diet: a practical tool for assessing the need for toxicity testing. *Food Chem. Toxicol.* **2000,** *38* (2-3), 255-312.
5. Kroes, R.; Renwick, A.; Cheeseman, M.; Kleiner, J.; Mangelsdorf, I.; Piersma, A.; Schilter, B.; Schlatter, J.; Van Schothorst, F.; Vos, J., Structure-based thresholds of toxicological concern (TTC): guidance for application to substances present at low levels in the diet. *Food Chem. Toxicol.* **2004,** *42* (1), 65-83.
6. EFSA; WHO, Review of the Threshold of Toxicological Concern (TTC) approach and development of new TTC decision tree. *EFSA Supporting Publications* **2016,** *13* (3), 1006E.
7. FDA, U. S., Threshold of regulation for substances used in food-contact articles. 21 CFR 170.39. https://www.ecfr.gov/cgi-bin/text-idx?SID=fff8b1d85cc676bb4a448a1f84d7b443&mc=true&node=se21.3.170_139&rgn=div8, 1995.
8. Moser, V. C.; Ashmer, M.; Richardson, R. J.; Philbert, M. A. In Casarett and Doull's toxicology: the basic science of poisons, 8th ed.; Klaassen, C. D, Ed.; McGraw-Hill Education: New York, 2013; pp 733-930.
9. Cramer, G. M.; Ford, R. A.; Hall, R. L., Estimation of toxic hazard--a decision tree approach. *Food and cosmetics toxicology* **1978,** *16* (3), 255-76.
10. Parkinson, A.; Ogilvie, B. W.; Buckley, D. B.; Kazmi, F.; Czerwinski, M.; Parkinson, O. In Casarett and Doull's toxicology : the basic science of poisons, 8th ed.; Klaassen, C. D, Ed.; McGraw-Hill Education: New York, 2013; pp 185-366.
11. Colovic, M. B.; Krstic, D. Z.; Lazarevic-Pasti, T. D.; Bondzic, A. M.; Vasic, V. M., Acetylcholinesterase inhibitors: pharmacology and toxicology. *Curr. Neuropharmacol.* **2013,** *11* (3), 315-335.
12. Amitai, G.; Moorad, D.; Adani, R.; Doctor, B. P., Inhibition of acetylcholinesterase and butyrylcholinesterase by chlorpyrifos-oxon. *Biochem Pharmacol* **1998,** *56* (3), 293-9.
13. Jan, Y. H.; Richardson, J. R.; Baker, A. A.; Mishin, V.; Heck, D. E.; Laskin, D. L.; Laskin, J. D., Novel approaches to mitigating parathion toxicity: targeting cytochrome P450-mediated metabolism with menadione. *Ann N Y Acad Sci* **2016,** *1378* (1), 80-86.
14. Brandon, E. F.; Raap, C. D.; Meijerman, I.; Beijnen, J. H.; Schellens, J. H., An update on in vitro test methods in human hepatic drug biotransformation research: pros and cons. *Toxicol Appl Pharmacol* **2003,** *189* (3), 233-46.
15. Ellman, G. L.; Courtney, K. D.; Andres, V., Jr.; Feather-Stone, R. M., A new and rapid colorimetric determination of acetylcholinesterase activity. *Biochem Pharmacol* **1961,** *7*, 88-95.
16. Worek, F.; Eyer, P.; Thiermann, H., Determination of acetylcholinesterase activity by the Ellman assay: a versatile tool for in vitro research on medical countermeasures against organophosphate poisoning. *Drug Test Anal* **2012,** *4* (3-4), 282-91.
17. Benabent, M.; Vilanova, E.; Sogorb, M. A.; Estevez, J., Cholinesterase assay by an efficient fixed time endpoint method. *MethodsX* **2014,** *1*, 258-63.
18. Li, S.; Zhao, J.; Huang, R.; Santillo, M. F.; Houck, K. A.; Xia, M., Use of high-throughput enzyme-based assay with xenobiotic metabolic capability to evaluate the inhibition of acetylcholinesterase activity by organophosphorous pesticides. *Toxicology in Vitro* **2019,** *56*, 93-100.
19. Marston, A.; Kissling, J.; Hostettmann, K., A rapid TLC bioautographic method for the detection of acetylcholinesterase and butyrylcholinesterase inhibitors in plants. *Phytochem. Anal.* **2002,** *13* (1), 51-54.
20. Zheng, X.-Y.; Zhang, Z.-J.; Chou, G.-X.; Wu, T.; Cheng, X.-M.; Wang, C.-H.; Wang, Z.-T., Acetylcholinesterase inhibitive activity-guided isolation of two new alkaloids from seeds of *Peganum nigellastrum* Bunge by an *in vitro* TLC-bioautographic assay. *Arch. Pharmacal. Res.* **2009,** *32* (9), 1245-1251.

21. Adhami, H. R.; Farsam, H.; Krenn, L., Screening of medicinal plants from Iranian traditional medicine for acetylcholinesterase inhibition. *Phytother. Res.* **2011,** *25* (8), 1148-1152.
22. Hage, S.; Morlock, G. E., Bioprofiling of *Salicaceae* bud extracts through high-performance thin-layer chromatography hyphenated to biochemical, microbiological and chemical detections. *J. Chromatogr. A* **2017,** *1490*, 201-211.
23. Mendoza, C.; Wales, P.; McLeod, H.; McKinley, W., Enzymatic detection of ten organophosphorus pesticides and carbaryl on thin-layer chromatograms: an evaluation of indoxyl, substituted indoxyl and 1-naphthyl acetates as substrates of esterases. *Analyst* **1968,** *93* (1102), 34-38.
24. Akkad, R.; Schwack, W., Multi-enzyme inhibition assay for the detection of insecticidal organophosphates and carbamates by high-performance thin-layer chromatography applied to determine enzyme inhibition factors and residues in juice and water samples. *J. Chromatogr. B* **2010,** *878* (17-18), 1337-1345.
25. Akkad, R.; Schwack, W., Effect of bromine oxidation on high-performance thin-layer chromatography multi-enzyme inhibition assay detection of organophosphates and carbamate insecticides. *J. Chromatogr. A* **2011,** *1218* (19), 2775-2784.
26. Akkad, R.; Schwack, W., Determination of organophosphorus and carbamate insecticides in fresh fruits and vegetables by high-performance thin-layer chromatography-multi enzyme inhibition assay. *J. AOAC Int.* **2012,** *95* (5), 1371-1377.
27. Azadniya, E.; Morlock, G. E., Automated piezoelectric spraying of biological and enzymatic assays for effect-directed analysis of planar chromatograms. *J. Chromatogr. A*, in print **2019**.
28. Azadniya, E.; Morlock, G. E., Equivalency calculation of enzyme inhibiting unknowns *in situ* the adsorbent of the effect-directed autogram, in submission, **2019**.
29. Morlock, G. E. In Instrumental Methods for the Analysis and Identification of Bioactive Molecules, American Chemical Society: 2014; Vol. 1185, pp 101-121.
30. Morlock, G. E. In Reference Module in Chemistry, Molecular Sciences and Chemical Engineering, Elsevier: 2018. (place ? pp ?)
31. Azadniya, E.; Morlock, G. E., Bioprofiling of *Salvia miltiorrhiza* via planar chromatography linked to (bio)assays, high resolution mass spectrometry and nuclear magnetic resonance spectroscopy. *J. Chromatogr. A* **2018,** *1533*, 180-192.
32. Morlock, G. E. In Mass Spectrometry Handbook, 1st ed.; Lee, M. Ed.; Wiley: Hoboken, NJ, 2012; pp1181-1206.
33. Dwivedi, P. D.; Das, M.; Khanna, S. K., Role of cytochrome P-450 in quinalphos toxicity: effect on hepatic and brain antioxidant enzymes in rats. *Food Chem Toxicol* **1998,** *36* (5), 437-44.
34. Buratti, F. M.; Volpe, M. T.; Meneguz, A.; Vittozzi, L.; Testai, E., CYP-specific bioactivation of four organophosphorothioate pesticides by human liver microsomes. *Toxicol Appl Pharmacol* **2003,** *186* (3), 143-54.
35. Bicker, W.; Lammerhofer, M.; Genser, D.; Kiss, H.; Lindner, W., A case study of acute human chlorpyrifos poisoning: novel aspects on metabolism and toxicokinetics derived from liquid chromatography-tandem mass spectrometry analysis of urine samples. *Toxicol Lett* **2005,** *159* (3), 235-51.
36. Gupta, B.; Rani, M.; Salunke, R.; Kumar, R., In vitro and in vivo studies on degradation of quinalphos in rats. *Journal of Hazardous Materials* **2012,** *213-214*, 285-291.
37. Fernandes, A. R.; Rose, M.; Charlton, C., 4-Nonylphenol (NP) in food-contact materials: analytical methodology and occurrence. *Food Addit Contam Part A Chem Anal Control Expo Risk Assess* **2008,** *25* (3), 364-72.
38. Preuss, T. G.; Gehrhardt, J.; Schirmer, K.; Coors, A.; Rubach, M.; Russ, A.; Jones, P. D.; Giesy, J. P.; Ratte, H. T., Nonylphenol isomers differ in estrogenic activity. *Environ Sci Technol* **2006,** *40* (16), 5147-53.
39. Uchiyama, T.; Makino, M.; Saito, H.; Katase, T.; Fujimoto, Y., Syntheses and estrogenic activity of 4-nonylphenol isomers. *Chemosphere* **2008,** *73* (1 Suppl), S60-5.
40. Veyrand, J.; Marin-Kuan, M.; Bezencon, C.; Frank, N.; Guerin, V.; Koster, S.; Latado, H.; Mollergues, J.; Patin, A.; Piguet, D.; Serrant, P.; Varela, J.; Schilter, B., Integrating bioassays and analytical chemistry as an improved approach to support safety assessment of food contact materials. *Food Addit Contam Part A Chem Anal Control Expo Risk Assess* **2017,** *34* (10), 1807-1816.
41. ECHA *Support document for identification of 4-nonylphenol, branched and linear as substances of very high concern because due to their endocrine disrupting properties they cause probable serious effects to the environment which give rise to an equivalent level of concern to those of CMRs and PBTs/vPvBs*; European Chemical Agency: 2012.
42. EFSA Panel on Food Contact Materials, E., Flavourings and Processing Aids (CEF), Scientific opinion: Recent developments in the risk assessment of chemicals in food and their potential impact on the safety assessment of substances used in food contact materials. *EFSA Journal* **2016,** *14* (1), 28.
43. Kroes, R.; Galli, C.; Munro, I.; Schilter, B.; Tran, L.; Walker, R.; Wurtzen, G., Threshold of toxicological concern for chemical substances present in the diet: a practical tool for assessing the need for toxicity testing. *Food Chem Toxicol* **2000,** *38* (2-3), 255-312.

Supplementary data

Incorporating the S9 system into methods for acetylcholinesterase inhibition and application to food contact material

Julie Mollergues[a,‡], Ebrahim Azadniya[b,‡], Thomas Stroheker[a], Kathrin Billerbeck[b], Gertrud E. Morlock[b,*]

[a]Chemical Food Safety group, Nestlé Research Center, Lausanne, Switzerland

[b]Chair of Food Science, Institute of Nutritional Science, and Interdisciplinary Research Center (IFZ), Justus Liebig University Giessen, Heinrich-Buff-Ring 26-32, 35392 Giessen, Germany

[‡]Both authors contributed equally.

*Corresponding Author: fax +49-641-99-39149; Gertrud.Morlock@uni-giessen.de

Table of Contents

Table S-1. Recovery (%) and detectability (S/N ratio) for the original and spiked two migrates and one extract with and without S9 metabolization.

After metabolization with S9 mixture	**AChE inhibitor**								
Intense change	**CP**			**QP**			**PT**		
	Amount [ng/band]	Mean recovery [%], *n* = 3	S/N ratio	Amount [ng/band]	Mean recovery [%], *n* = 3	S/N ratio	Amount [ng/band]	Mean recovery [%], *n* = 3	S/N ratio
Pure standards	100		6	1		8	100		4
Pure standards+S9	2.5		4	1		9	2.5		3
spiked EtOH 50%	100	**106**	6	1	**101**	9	100	**115**	4
spiked EtOH 50%+S9	2.5	**77**	3	1	**103**	9	2.5	**84**	3
spiked EtOH 95%	100	**131**	8	1	**109**	9	100	**177**	6
spiked EtOH 95%+S9	2.5	**110**	3	1	**107**	9	2.5	**87**	3
spiked Hex-Act	100	**105**	5	1	**104**	8	100	**107**	4
spiked Hex-Act+S9	2.5	**106**	3	1	**94**	7	2.5	**117**	2
Less change	**ER**			**NP**			**TNPP**		
	Amount [ng/band]	Mean recovery [%], *n* = 2	S/N ratio	Amount [ng/band]	Recovery [%]	S/N ratio	Amount [ng/band]	Recovery [%]	S/N ratio
Pure standards	0.5		3	250		9	1000		12
Pure standards+S9	0.5		3	250		6	1000		11
spiked EtOH 50%	0.5	**108**	3	250	**85**	8	1000	**60**	9
spiked EtOH 50%+S9	0.5	**112**	3	250	**105**	7	1000	**115**	11
spiked EtOH 95%	0.5	**134**	3	250	**69**	6	1000	**38**	6
spiked EtOH 95%+S9	0.5	**119**	3	250	**99**	7	1000	**66***	8
spiked Hex-Act	0.5	**134**	4	250	**81**	8	1000	**82**	11
spiked Hex-Act+S9	0.5	**123**	4	250	**136**	9	1000	**95**	10

n-Hexane (Hex), ethanol (EtOH), acetone (Act)
*value used for TTC

Table S-2. Optimum amount of S9 (100 mg/L, 0-10 µL applied, 0-1000 ng/band) for six selected chemicals via HPTLC–S9–AChE.

Chemical	Concentration [mg/L]	Volume applied [µL]	Amount [ng/band]	Max point of S9 in curve (ng/band)
CP	100	4	400	733
QP	10	1	10	777
ER	0.1	7	0.7	577
PT	10	5	50	756
NP	100	5	500	-
TNPP	100	10	1000	-
			Mean	**710**

Table S-3. Calculation of analysis time and running costs per plate for the HPTLC–S9–AChE method.

HPTLC–S9–AChE workflow	**Analysis time (min)**	
for one plate	**Immersion Band**	**Piezoelectric spraying Area**
Sample application	20	60
Focusing	-	10
Drying	1	2
Wetting	5	-
S9 application	20	20
Wetting	-	5
Incubation	30	30
Drying	20	20
Development	25	60
Documentation	2	2
Enzyme application	5	5
Incubation	25	25
Substrate application	5	3
Drying	10	10
Documentation	2	2
Scanning	3	3
Total time (min)	**173**	**257**
Total time (h)	**2.9**	**4.3**

	Running costs (Euro)	
HPTLC plate (20 x 10 cm)	7.0	7.0
Solvent (8 mL)	0.5	0.5
Enzyme (6.6 U/mL)/plate	1.3 (2 mL,13.3 U)	2.0 (3 mL, 20 U)
S9 mixture (0.1 mg/mL S9 + cofactors), 7 µL/band or 11 µg/area	0.1	0.1
	8.9	**9.6**

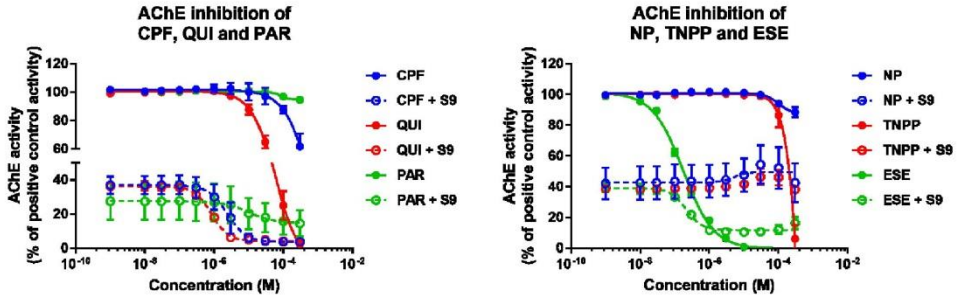

Figure S-1. AChE inhibition by six chemicals via the fluorometric Amplex® Red ChE/AChE assay.

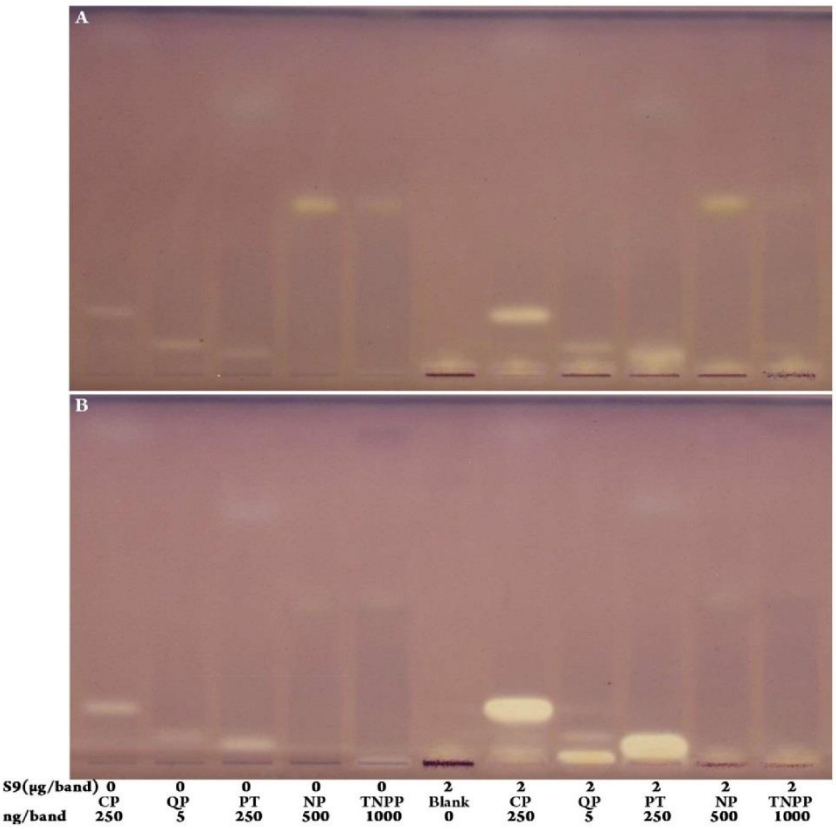

Figure S-2. HPTLC-AChE autograms of the five chemicals without and with metabolization by the S9 mixture (2 µg/band) documented under white light illumination (A) and after additional plate wetting (B).

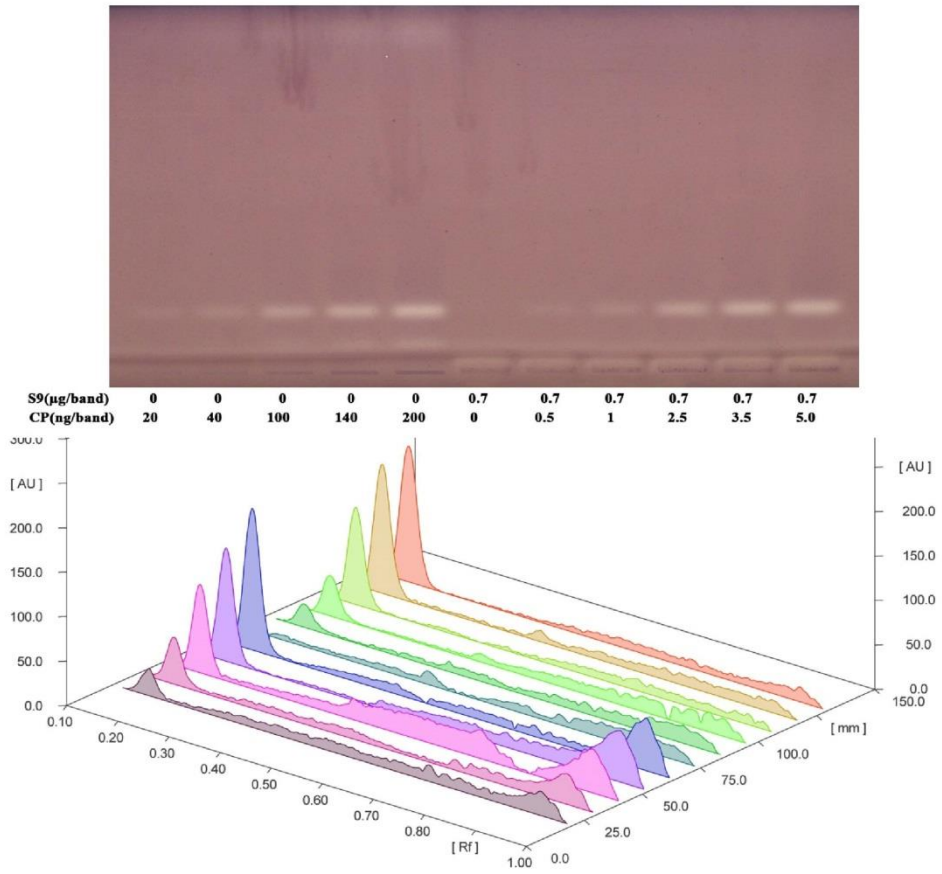

Figure S-3. HPTLC–S9–AChE autogram of CP developed with MP3 and its corresponding densitogram.

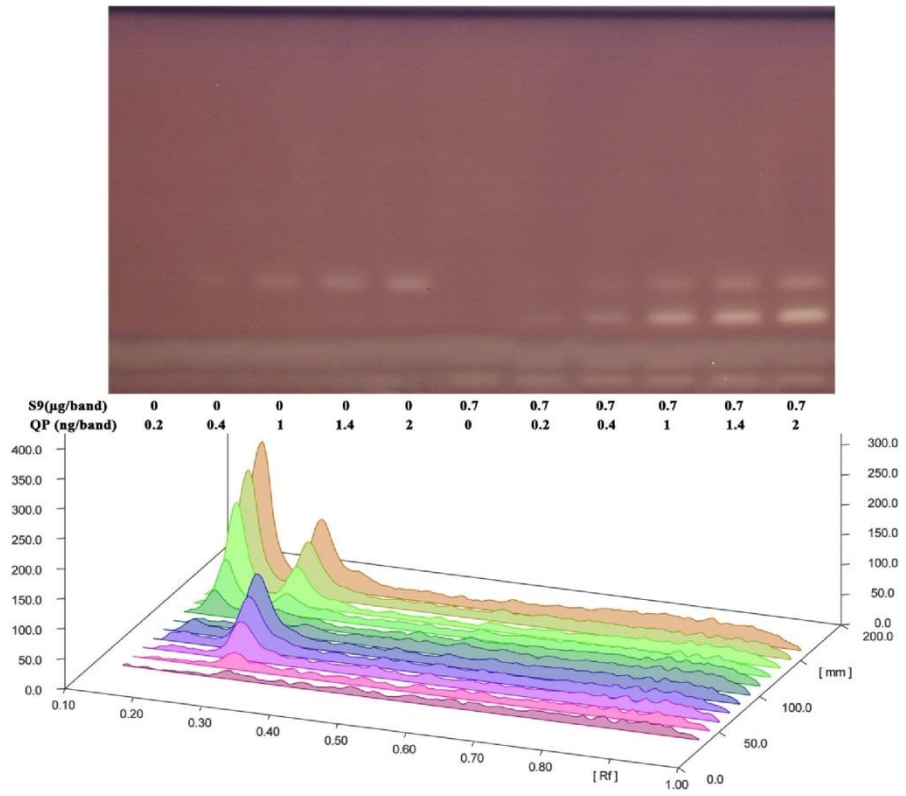

Figure S-4. HPTLC–S9–AChE autogram of QP developed with MP2 and its corresponding densitogram**.**

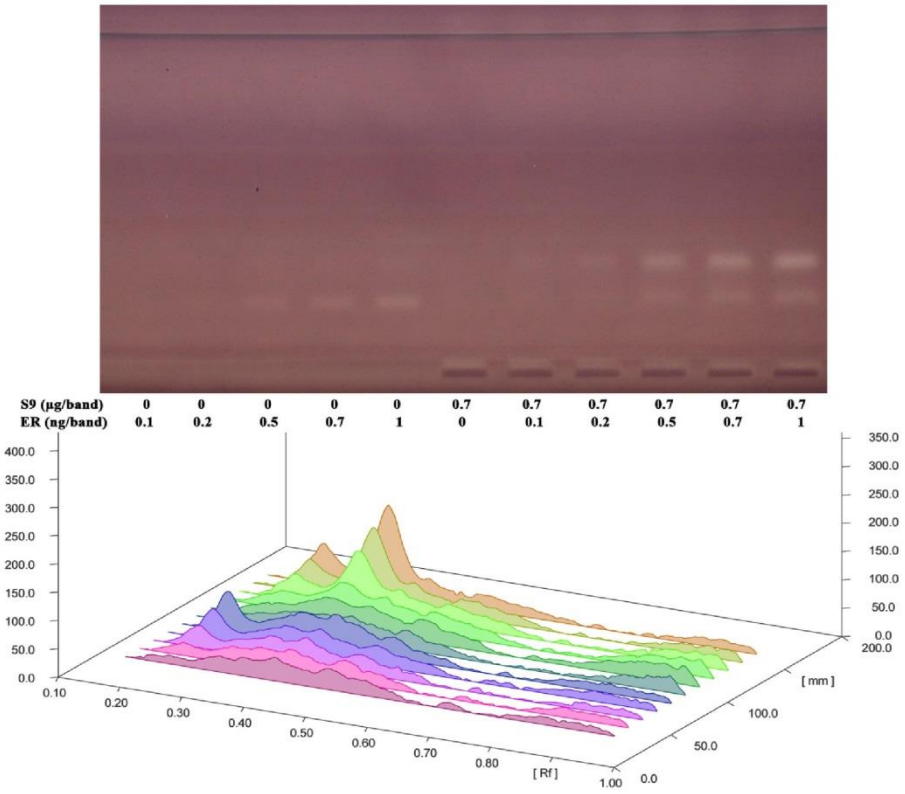

Figure S-5. HPTLC–S9–AChE autogram of ER developed with MP1 and its corresponding densitogram.

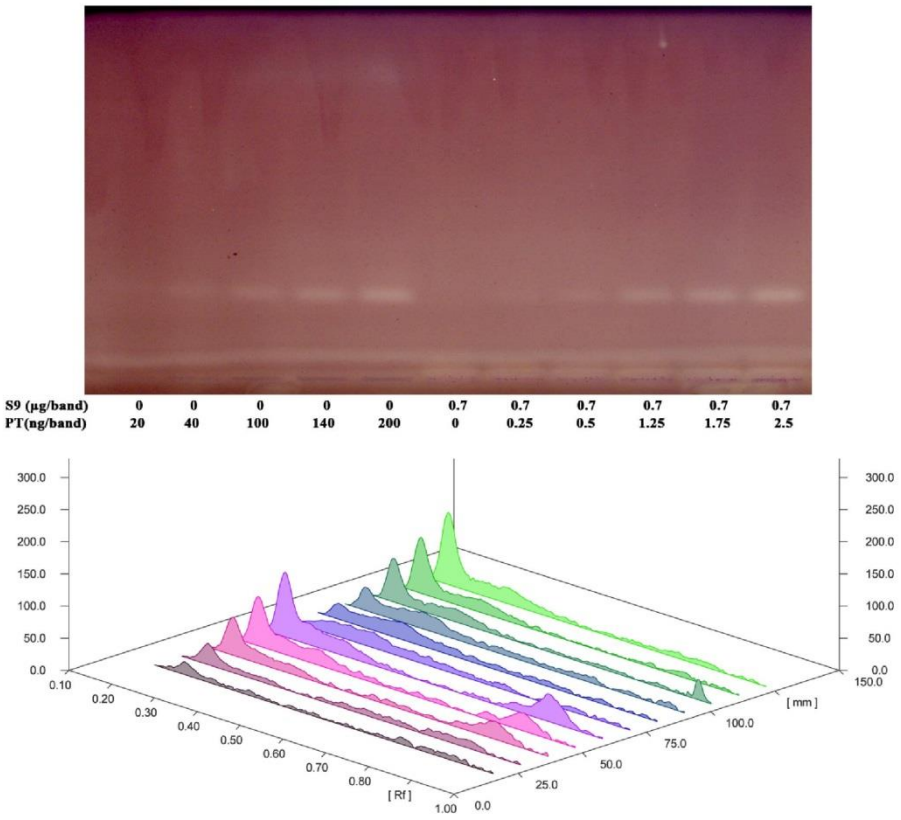

Figure S-6. HPTLC–S9–AChE autogram of PT developed with MP2 and its corresponding densitogram.

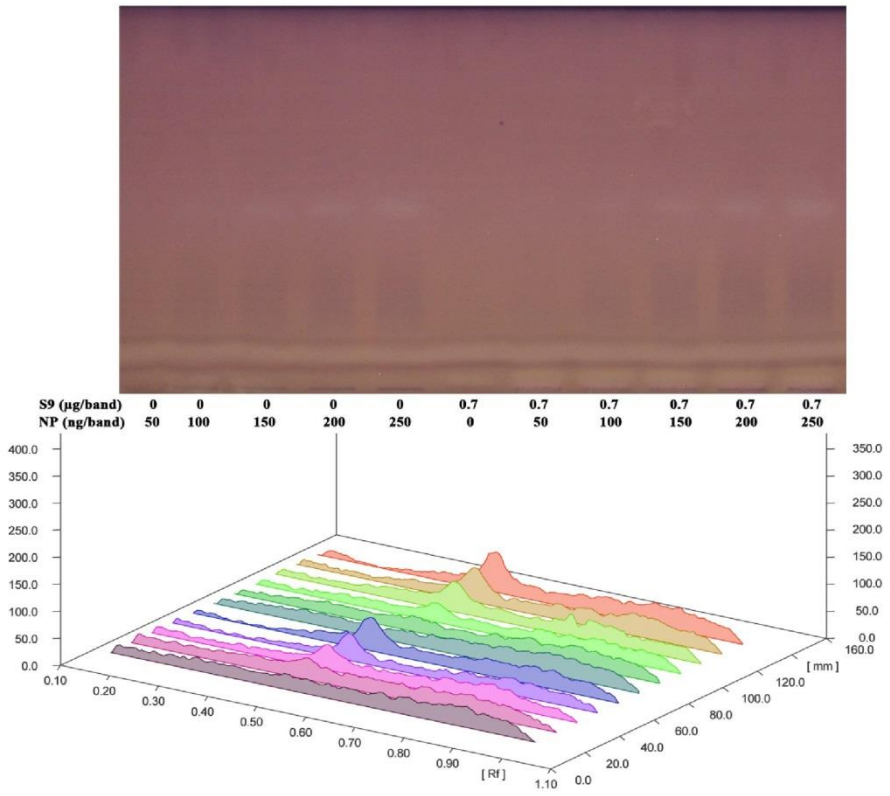

Figure S-7. HPTLC–S9–AChE autogram of NP developed with MP3 and its corresponding densitogram**.**

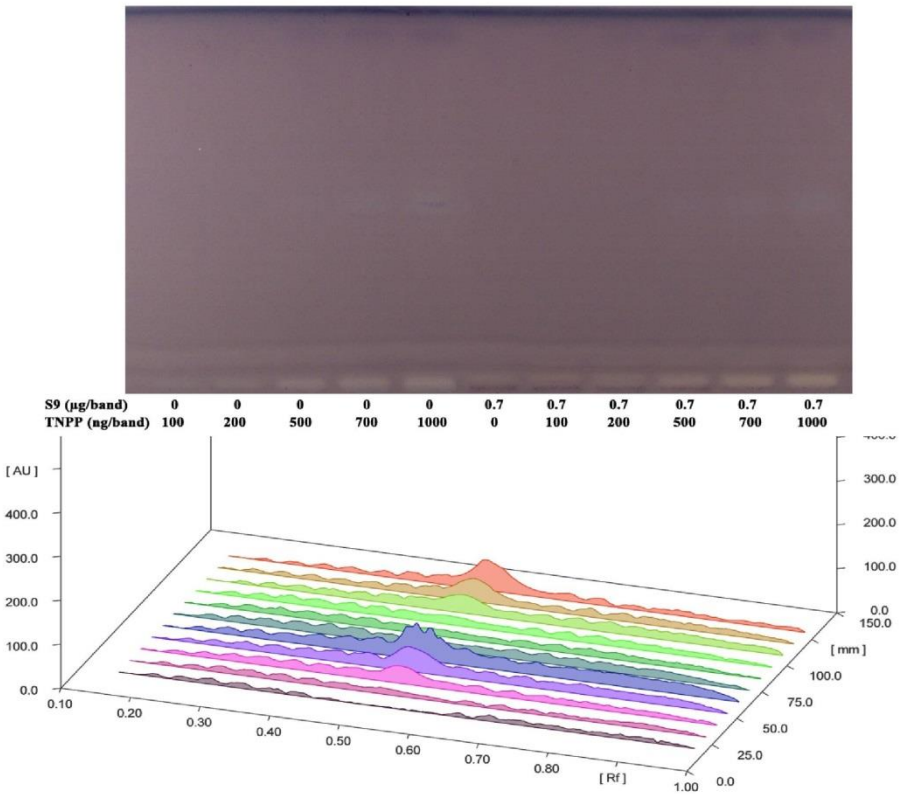

Figure S-8. HPTLC–S9–AChE autogram of TNPP developed with MP3 and its corresponding densitogram.

6. PUBLICATION 5

From bioprofiling to quantification of bioactive compounds via a direct workflow of planar chromatography–effect-directed analysis-nuclear magnetic resonance spectroscopy

Ebrahim Azadniya[a,b,c], Luca Goldoni[c], Tiziano Bandiera[d], Gertrud E. Morlock[a,b,*]

[a]*Chair of Food Science, Institute of Nutritional Science, Interdisciplinary Research Center, Justus Liebig University Giessen, Heinrich-Buff-Ring 26-32, 35392 Giessen, Germany*

[b]*TransMIT Center of Effect-Directed Analysis, Kerkrader Straße 3, 35394 Giessen, Germany*

[c]*Analytical Chemistry Lab,[d] D3 PharmaChemistry, Istituto Italiano di Tecnologia, Via Morego, 30, 16163, Genoa, Italy*

Ready to submit in

Journal of Chromatography A

From bioprofiling to quantification of bioactive compounds via a direct workflow of planar chromatography–effect-directed analysis-nuclear magnetic resonance spectroscopy

Ebrahim Azadniya[a,b,c], Luca Goldoni[c], Tiziano Bandiera[d], Gertrud E. Morlock[a,b,*]

[a]Chair of Food Science, Institute of Nutritional Science, Interdisciplinary Research Center, Justus Liebig University Giessen, Heinrich-Buff-Ring 26-32, 35392 Giessen, Germany

[b]TransMIT Center of Effect-Directed Analysis, Kerkrader Straße 3, 35394 Giessen, Germany

[c]Analytical Chemistry Lab,[d] D3 PharmaChemistry, Istituto Italiano di Tecnologia, Via Morego, 30, 16163, Genoa, Italy

*Corresponding author. Tel.: +49-641-99-39141; fax: +49-641-99-39149.

E-mail addresses:

Gertrud.Morlock@uni-giessen.de (G. E. Morlock),

Ebrahim.Azadniya@chemie.uni-giessen.de (E. Azadniya),

Luca.Goldoni@iit.it (L. Goldoni),

Tiziano.Bandiera@iit.it (T. Bandiera).

Abstract

The sensitivity gap was the main obstacle to achieve a direct workflow from planar chromatogram to NMR spectroscopy. The workflow needs to provide the enough amounts of the active compounds, from a planar chromatogram, in detectable rang of NMR spectroscopy. Here, a straight-forward HPTLC-NMR spectroscopy workflow using a fix chromatographic condition from bioprofiling to isolation of the active zones was established. The dried extracts of *Salvia officinalis*, *Thymus vulgaris*, *Origanum vulgare*, red and green apple peel containing different structural isomers e.g. ursolic (UA), oleanolic (OA), betulinic acids (all $C_{30}H_{48}O_3$) with potential of coelution, were selected as the extreme case studies. The bioprofiling via HPTLC–acetylcholinesterase, –tyrosinase and –*Bacillus subtilis* (bio)assays revealed the UA-OA as a coeluted (bio)active zone collected then via the HPTLC isolation (using one plate) for quantitative NMR (qNMR) spectroscopy. However both NP-HPTLC and HRMS showed the same hR_F values and molecular ions respectively for UA and OA, the ^{1}H NMR spectra indicated a distinct allylic 1H-18 signals (UA 2.20 ppm and OA 2.85 ppm) in UA:OA (40:60) and isolated UA-OA zones solutions. The PUlse Length-based CONcentration determination (PULCON) procedure calibrated by maleic acid standard solution was used for UA and OA quantification. In case of partially signal overlap with those of the matrix, results were compared with those obtained by ^{1}H deconvoluted spectrum (MestReNova) and the ones obtained from ^{1}H-^{13}C Heteronuclear Single Quantum Coherence cross peaks. The results of PULCON (n=2) was compared with those of pre- and post-chromatographic derivatization HPTLC (n=3), which revealed a high correlation (R^2 = 0.972) between two orthogonal methods. The efficiency of HPTLC isolation procedure was assessed by comparing the amount of UA and OA in the isolated samples and the crude extracts solutions via derivatization HPTLC. The HPTLC isolation procedure using the same chromatographic condition as derivatization HPTLC and HPTLC–bioprofiling showed 82 % (mean) efficiency and provided detectable amount of UA and OA (0.27-4.67 mM) in qNMR spectroscopy. The direct HPTLC-NMR workflow with low solvent consumption (16 mL) can be a proper alternative for bioactivity-guided fractionation strategy to reach NMR spectra of active compounds.

Keywords

Quantitative NMR (qNMR), PULCON, HPTLC isolation, Biochemical/biological profiling; *Lamiaceae*, apple peel.

1. Introduction

Structural confirmation and quantification of the compounds related to the active zones are the ultimate targets after a biological/biochemical profiling of samples by (HP)TLC–effect-directed analysis (EDA). The employment of spectrometric techniques especially MS [1] and NMR spectroscopy [2-5], after bioprofiling, provides the structural information on active compounds. However, the combination of (HP)TLC and NMR spectroscopy was not considered deservedly, due to the significant difference in sensitivity between NMR spectroscopy (mM or hundreds μg/tube) and mainly ng/band for HPTLC [4, 5]. Then, supplying a sufficient amount of the (bio)active zones isolated from the HPTLC/preparative layer chromatography (PLC) is the main requirement for the NMR spectra appropriate to confirm both the chemical structure and the analyte quantification by quantitative NMR (qNMR) spectroscopy. Otherwise, other techniques i.e. column based separation [6-8] or elution compounds from the HPTLC plate using an elution head-based interface [2, 3, 9] were used for NMR spectroscopy sample preparation. The latter two methods were inefficient procedures because of time-consuming steps including fractionation/stamping, evaporation and high consumption of solvent and HPTLC plates [2, 3, 6-9].

The low chromatographic resolution of (HP)TLC sometimes causes the coelution of sample components. The worst case *scenario* is the coelution of two structural isomers hardly recognized in high-resolution (HR)MS, and sometimes by MS^n technique, due to their similar base peak. Despite their structural similarity, structural isomers have some protons in chemically diverse environments leading to signals at different chemical shifts of ^1H NMR spectrum, allowing determining them especially in a coeluted active zone found by HPTLC–EDA, here as the case study.

NMR spectroscopy is an orthogonal technique for simultaneous identification and quantification of several compounds. In compare to HPLC and GC which need reference standards of analytes, qNMR spectroscopy quantifies all the analytes of several spectra, just with a single reference compound [10]. In NMR spectroscopy the peak intensity is directly proportional to the number of nuclei generating such a signal that, in turn, is linearly related to the analyte amount in solution (absolute concentration) [10-13]. Additionally, HPLC [14] and GC [15] can perform the multi-analytes quantification via internal standard addition but the response factor of each analyte needs to be calculated, whereas the NMR spectroscopy returns homogenous response factor for all the analytes and all the signals.

The qNMR spectroscopy can be fulfilled in two ways, by relative and absolute quantitation methods. Relative mode provides molar ratio between two compounds [4] while the absolute compound quantitation measures the actual amount of an analyte [10, 12]. Absolute mode requires an internal or external reference compound to calibrate the NMR signal. In the internal standard method, a weighed amount of a reference standard (or a measured volume of a known concentration solution) is added into a fix volume of sample and the intensity of its signal is used for quantification of all the other species in the same spectrum. The proper standard as internal should have at least one signal separated from those of the sample, a similar solubility in the same solvent and no chemical interaction with analytes and matrix [11, 12]. Those requirements are not trivial at all, when dealing with natural extracts in polar protic solvents. However, the main drawback is the sample contamination with the internal standard added, on the contrary, the external reference methods utilize a reference compound in a separate solution and its NMR signal intensity is used to quantify several compounds in different spectra [12]. Among them one of the most innovative is the PUlse Length-based CONcentration determination (PULCON) method, that correlates the NMR signal intensity of a reference standard to those ones of analytes in different spectra, after the 90° pulse correction on each sample tube, according to the principle of reciprocity [16, 17]. The procedure is implementable on all type of NMR spectrometers without specific hardware configuration and, once calibrated, can measure concentrations of samples for months [13, 16, 17]. The use of high field magnets and cryoprobes, used here, improved the sensitivity of spectrometers, lowering down the limit of detection (LOD) to the micro-molar (μM) range to measure low amount analytes even in complex biological matrices by PULCON [18], with acceptable experiment times (~18 min).

The current study investigates the efficiency of HPTLC-NMR workflow for isolation, structural confirmation and quantification of structural isomers in a coeluted (bio)active zone found after an HPTLC–EDA as a tough *scenario*. Different natural extracts containing several structural isomers were selected and after bioprofiling, the ursolic and oleanolic acids, as a coeluted (bio)active zone, was isolated via HPTLC and measured by a set up qNMR spectroscopy. As an alternative, two dimensions (2D) spectra, e.g. Heteronuclear Single Quantum Coherence (HSQC) and Heteronuclear Multiple Bond Correlation (HMBC), were used too, to spread out the signals into 2D [19].

Finally, the results of qNMR spectroscopy were compared with those obtained from pre- and post-chromatographic derivatization HPTLC. The latter method was used for evaluation of the HPTLC isolation efficiency by comparison of UA and OA amount in between the isolated samples and the crude extracts.

2. Materials and methods

2.1. Chemicals and materials

Analytical grade solvents were used for chromatography and sample preparation. Acetone, toluene, ethyl acetate, methanol, chloroform, sulfuric acid (98%), anisaldehyde, Müller–Hinton broth, polyethylene glycol (PEG) 8000 and 3-(4,5-dimethylthiazol-2-yl)-2,5-diphenyl-tetrazolium bromide (MTT, ≥98%) were purchased from Carl Roth, Karlsruhe, Germany. Carvacrol (Car), thymol (Thy), betulinic acid (BA), maslinic acid (MA), Fast Blue B Salt (FBS), tyrosinase from mushroom, acetylcholinesterase (AChE) from *Electrophorus electricus*, sodium and potassium chloride, sodium monohydrogen phosphate, bovine serum albumin (BSA), 3-(cyclohexylamino)-1-propanesulfonic acid (CAPS) and Tris were provided from Sigma-Aldrich, Steinheim, Germany. Maleic acid standard (99.99% with 0.09% uncertainty) for qNMR was provided as reference materials from Fluka Analytics (ISO guide 35). Hydrogen chloride (HCl, 37%), iodine, *Bacillus subtilis* (BGA, ATCC 6633) spores and HPTLC plate silica gel 60 F_{254} were purchased from Merck, Darmstadt, Germany. MS-grade methanol was provided from Fisher Scientific, Schwerte, Germany. Corosolic acid (CA), rosmanol (Ros) were purchased from Phytolab, Vestenbergsgreuth, Germany. Ursolic acid (UA, 95%) and oleanolic acid (OA, 90%) were provided from Cayman Chemical, Hamburg, Germany. L-DOPA and 1-naphthyl acetate (97%) were obtained from Santa Cruz Biotechnology, Dallas, U.S.A., and Panreac, Barcelona, Spain respectively. The HPTLC plates were prewashed twice by chromatography with methanol and water (3:1), after second time, dried at 120 °C in a clean oven for 30 min, then covered with a clean counter glass plate and wrapped in aluminum foil for NMR spectroscopy and HRMS experiments. NMR tubes (3 mm SVPC-3-103.5-96PK) were purchased from Norrell and CD_3OD (D4, D 99,96%, water < 0.02%) from Eurisotop. The Mettler® Toledo XP205 analytical balance (certified uncertainty 0.013 mg) and Rainin pipettes P1000 (volume uncertainty for 100 µL, 500 µL and 1000 µL were 2.53 µL, 4.27 µL and 2.44 µL respectively) and P10 (volume uncertainty for 10 µL was 0.18 µL) were used for qNMR spectroscopy standard and sample solutions preparation.

2.2. Sample, standard and reagent solutions preparation

For HPTLC–EDA experiments, the methanolic solutions of all standards (UA, OA, BA, CA, MA, Thy, Car and Ros) in concentration of 1 mg/mL as stock solution were prepared and then diluted to 0.1 mg/mL. For pre- and post-chromatographic derivatization HPTLC, the 0.1 mg/mL solutions of OA, MA and CA were diluted again to 0.05 mg/mL, 0.025 mg/mL and 0.01 mg/mL respectively. For NMR experiments, the UA (2.52 mg) and OA (2.61 mg) were weighted, and dissolved in 1 mL CD_3OD (UA 5.52 mM and OA 5.71 mM). Standard solutions of maleic acid for PULCON calibration as well as accuracy and precision measurements were freshly prepared by independent weights (1.15-1.27 mg) and dissolving in CD_3OD (3622-4000 µL) to reach exactly 2.74 mM. Maleic acid solution as internal reference was prepared by dissolution of 2.56 mg of maleic acid in 400 µL CD_3OD (55.14 mM) then 10 µL of that was added into 250 µL of sample solutions to reach 2.12 mM.

The dried powder of *Salvia officinalis* (Sage), *Thymus vulgaris* (Thm), *Origanum vulgare* (Org) from Ostmann (Ostmann Gewürze GmbH, Bielefeld, Germany), and red apple (Jonagored) and green apple (Granny Smith) from Lidl shop in Giessen, Germany were purchased. After peeling the apples (1 kg), the green apple peel (GAP) 86.6 g and the red apple peel (RAP) 88.2 g, were dried in 80 °C ± 5 for 4 h (each 30 min removing the vapor by opening the oven) to get dried GAP (17 g) and RAP (20 g). Ten grams dried milled powder of each sample was extracted two times with 100 mL acetone at room temperature for 15 min on the stirrer, followed by 15 min ultrasonication and centrifugation at 756 × *g* for 10 min. The upper phases (50 mg/mL) were collected and dried to get Sage (950 mg), Org (680 mg), Thm (550 mg), GAP (630 mg) and RAP (790 mg) dried extracts. Methanolic extract solutions were prepared by dissolution of 100 mg of each dried extract in 10 mL methanol (10 mg/mL) used for HPTLC isolation and MS, and diluted to 1 mg/mL for HPTLC–EDA and pre- and post-chromatographic derivatization HPTLC. The isolated sample solutions (10 mg/mL) were prepared by dissolving of the residual of HPTLC-isolated zone in CD_3OD (see 2.3). The crude sample solutions for qNMR were prepared as 10 mg/mL by dissolving 10 mg of each dried extract in 1 mL CD_3OD, then after centrifugation at 756 × g for 10 min, 250 µL of supernatant was transferred into 3-mm NMR tube.

AChE enzyme solution (6.6 units/mL) was prepared in Tris-HCl buffer (0.05 M, pH 7.8) plus adding BSA (1 mg/mL). The mixture of ethanolic solution of 1-naphthyl acetate and aqueous solution of FBS (both 3 mg/mL, 1:2 v/v) was used as the substrate-chromogenic solution for AChE assay. After mixing, the solution was ultrasonicated for 30 min with 10 min vortex interval.

Tyrosinase enzyme solution (400 units/mL) was prepared in phosphate buffer (0.02 M, pH 6.8). Substrate of tyrosinase assay was prepared by dissolving 4.5 mg/mL L-DOPA, 2.5 mg/mL CAPS and 75 mg/mL PEG 8000 in phosphate buffer followed by 30 min ultasonication with 10 min vortex interval.

2.3. Application and separation on HPTLC

Five different extracts and standard solutions were applied as 8-mm bands (except for HPTLC isolation) on a HPTLC plate silica gel 60 F_{254} using the Automatic TLC Sampler 4 (ATS 4, CAMAG, Muttenz, Switzerland). For (bio)profiling via *B. subtilis*, AChE and tyrosinase (bio)assays, 10 µL of 1 mg/mL extracts solutions (10 µg/band) and 1 µL of 1 mg/mL (1 µg/band) each standard solutions were applied. For MS experiments, 2 µL of 10 mg/mL extracts solutions (20 µg/band) as well as 1 mg/mL UA, OA and BA (2 µg/band) were applied on a prewashed HPTLC. For pre- and post-chromatographic derivatization HPTLC, 1-4 µL/band of UA 0.1 mg/mL (100-400 ng/band), MA 0.025 mg/mL (25-100 ng/band) and CA 0.01 mg/mL (10-40 ng/band), and 0.5-4 µL/band of OA 0.05 mg/mL (25-200 ng/band) as well as 1 µL of 1 mg/mL of each extract solution (except for Org 4 µL of 1 mg/mL) and isolated sample solutions (1 mg/mL) were applied. The isolated sample solutions (10 mg/mL) in CD_3OD (already used for qNMR) were diluted with methanol to 1 mg/mL. Plates were developed with 10 mL of the optimized mobile phase containing toluene–methanol–ethyl acetate 17:2:1 v/v up to 70 mm in the Automatic Developing Chamber 2 (ADC 2, CAMAG) after 5 min chamber saturation at around 50 % relative humidity of the air at 25 °C, then, automatically dried for 3 min under a cold stream of air in the ADC 2.

The HPTLC isolation for NMR spectroscopy experiments was performed by area application of 1 mL (150 mm × 3 mm) and 150 µL (25 mm × 3 mm) of each extract solution (10 mg/mL) on a prewashed HPTLC plate and then development with mentioned mobile phase up to 70 mm. After development, the smaller part was cut by smartCut Plate Cutter (CAMAG) and derivatized to find the position of favorite band on the bigger piece. The zone of interest was scraped off and extracted three times with 2 mL methanol. After centrifugation, the supernatant was collected and then evaporated to dryness under nitrogen stream. The residue was dissolved in 1 mL CD_3OD (10 mg/mL).

2.4. Pre- and post-chromatographic derivatization HPTLC

After application, the plate was developed up to 12 mm in iodine solution (1 % w/v, 1 g iodine in 100 mL chloroform) [20]. After removing iodine liquid by contacting bottom of the plate to a paper tissue, plate was covered by a counter glass, wrapped in aluminum foil and incubated for 10 min in incubator at 27 °C. Then the extra iodine was removed by a cold stream of air from a hair dryer. After development, the plate was derivatized by immersion (time 2 s, speed 3.5 s/cm) in anisaldehyde-sulfuric acid reagent with TLC Immersion Device III (CAMAG) and heated up on the TLC Plate Heater (CAMAG) at 110 °C for 5 min. Chromatograms were documented at 366 nm and white light illumination. In order to perform quantification, plates were scanned in absorption mode at 665 nm with tungsten lamp (slit dimension 5.00 × 0.2 mm and scanning speed 20 mm/s).

2.5. HPTLC–EDA

The developed HPTLC plates (chromatograms) were subjected to *B. subtilis,* AChE and tyrosinase (bio)assays. Immersion was performed by the TLC Immersion Device III (CAMAG) and incubated in a humid box covered with wet filter papers. Documentation of the (bio)autograms were performed under white light illumination (reflectance mode) using the TLC Visualizer (CAMAG).

2.5.1. HPTLC–*B. subtilis* bioassay

Antibacterial screening was performed according to our former method [21]. Briefly, the chromatogram was dipped (time 6 s, speed 3.5 cm/s) into the *B. subtilis* suspension (OD_{600nm}= 0.8), incubated at 37 °C for 2 h and then visualized by dipping (time 1 s, speed 3.5 cm/s) into a 0.2 % PBS-buffered MTT solution and incubation at 37 °C for 30 min followed by heating at 50 °C for 5 min on the TLC Plate heater (CAMAG). The documented bioautogram revealed that the active microorganism reduced MTT into a purple formazan as plate background, whereas, the antimicrobial substances showed white zones which prove no activity of microorganism [21, 22].

2.5.2. HPTLC–AChE assay

The AChE assay was implemented according to the latest modified procedures [23-25] of the Marston's method [26]. Concisely, the chromatogram was immersed (time 2 s, speed 3.5 cm/s) into the enzyme solution. The plate was incubated at

37 °C for 25 min and then, immersed (time 1 s, speed 3.5 cm/s) into the substrate-chromogenic reagent solution, followed by drying in ambient temperature for 5 min and then ADC 2 (CAMAG) for 10 min in humidity control mode. The AChE inhibitors were documented as white active zones in a purple background.

2.5.3. HPTLC–tyrosinase assay

Tyrosinase inhibitors were detected using the Derivatizer (CAMAG, hood and tray for 20 × 10 cm plates) based on CAMAG suggested procedure which were recently improved in our laboratory [5, 27, 28]. The chromatogram was placed in the Derivatizer, sprayed with 2 mL of substrate solution, and subsequently dried for 2 min using a cold stream of air from a hair dryer. Then, it was sprayed with 2 mL enzyme solution and incubated at room temperature for 15 min. The drying and documentation steps were performed as reported for the AChE assay. The tyrosinase inhibitors appeared as white/light yellow zones in gray background.

2.6. Characterization of active zones via HPTLC–HRMS

The samples and standards were applied twice and after development the chromatogram was cut by smartCut Plate Cutter (CAMAG) in two pieces, one for derivatization with anisaldehyde-sulfuric acid reagent and another for HRMS. On the latter, the positions of favorite zones were marked using a soft pencil. An elution head-based interface (Plate Express, Advion, Ithaca, NY, USA) transferred the favorite substances to the heated electrospray ionization (HESI) source connected to a Q Exactive Plus Hybrid Quadrupole-Orbitrap Mass Spectrometer (Thermo Fisher Scientific, Dreieich, Germany). The zones of interest were tightly fixed by the oval elution head (4 mm × 2 mm, 320 N) and eluted for 60 s at F=0.1 mL/min using methanol for the positive/negative ionization mode. All mass spectra were recorded in the full scan mode between *m/z* 100 and *m/z* 1000. Sodium diisooctyl phthalate (*m/z* 413.26623) and monosodium diformate (*m/z* 112.98563) were used as lock mass for positive and negative modes respectively. The settings for both modes included spray voltage +/- 3.5 kV and capillary temperature 270 °C. The MS data processing was performed with Xcalibur 3.0.63 software (Thermo Fisher Scientific). A representative plate background (similar hR_F position as the zone of interest) as well as a piece of clean aluminum plate as system background were subtracted from the analyte mass spectrum.

2.7. NMR spectroscopy

2.7.1. 1D and 2D NMR spectroscopy experiment

All NMR experiments were acquired on a 600 MHz NMR spectrometer (Avance III, Bruker, Rheinstetten, Germany) equipped with a 5 mm QCI cryoprobe with z shielded pulsed-field gradient coil. 250 µL of each isolated sample or standard solutions were transferred into a 3-mm NMR tubes which were stored in cooled rack (at 6°C) in a sample case before being handled by the SampleJet (Bruker) automation system. The temperature inside the probe was actively monitored at 298K and each sample was let to equilibrate for 3 min before pre-acquisition routines. The matching and the shimming map were manually optimized on the first NMR tube and, then, automatic matching and tuning, and spectra resolution were finely adjusted on each sample-tube. Typically, 128 transients were accumulated, after a 90° pulse being applied (optimized by an automatic pulse calculation routine [29]), with 64K of digitalization points, a relaxation delay of 30 s, over a spectral width of 20.55 ppm (offset at 4.7 ppm), by using a fixed receiver gain (11.3). For Org samples (isolated and crude) the number of transients was increased to 256 to achieve the S/N ratio of 13 for OA signal at 2.85 ppm. Spectra were manually phased and the baseline automatically corrected. An exponential apodization function equivalent to 0.1 Hz was applied to FIDs before the Forier transform. The bias and slope correction of integral were applied only if signals were overlapped at their peak base. The parameters for ^{1}H-^{13}C HSQC experiment (multiplicity edited HSQC, "*hsqcedetgpsp.3*" pulse sequence of Bruker library) were: 16 FIDs (except for Org, with 64 scans), 2048 digit points, 400 increments and $^{1}J_{CH}$ = 145 Hz, a spectral width of 10.01 ppm for ^{1}H and 180.0 ppm for ^{13}C, with a transmitter frequency offset at 4.0 and 90.0 ppm respectively. The ^{1}H-^{13}C HMBC experiment ("*hmbcgpndqf*" pulse sequence of Bruker library) were recorded for UA, OA, model solutions (mix UA:OA 40:60 w/w) and samples by using 64-256 FIDs (depending on sample concentration), 2048 digit points, 128 increments and $^{1}J_{CH}$ long range = 10 Hz, a spectral width of 10.01 ppm for ^{1}H and 222.1 ppm for ^{13}C, with a transmitter frequency offset at 4.67 and 99.8 ppm respectively. All spectra were collected by means of TopSpin 3.5 PL7 software and processed with TopSpin 3.2 (Bruker). All the chemical shifts were referred to the not deuterated methanol residual solvent peak at 3.31 ppm for ^{1}H and 49.00 ppm for ^{13}C respectively.

2.8. qNMR with internal reference standard and PULCON

The ^{1}H NMR spectra of isolated sample solutions were recorded after adding 10 µL (55.14 mM) of maleic acid solution into 250 µL sample solution. The concentration of UA and OA was calculated by means of the ratio between an integrated peak

intensity of analytes and that of reference, each normalized to the number of resonances (^{1}H) which generate the signals, according to the equation 1 [11].

$$Cx = \frac{Ix\ Nstd}{Istd\ Nx}\ Cstd \quad \textbf{equation 1}$$

Where I, N, and C, are respectively the integrated peak intensity, number of nuclei and concentration of analyte (x) and standard (std).

For PULCON method, the ^{1}H NMR spectra of each isolated sample, crude extract as well as a known concentration of maleic acid solutions were recorded. The concentrations of analytes were calculated from the ratio between the integrated intensity of analyte peak (UA 2.20 ppm and OA 2.85 ppm) and that of reference, acquired in an independent spectrum, after the normalization by the number protons generating such signals and by correcting for the 90° pulse measured on each sample-tube, according to equation 2 [30].

$$C_x = \frac{I_x\ T_x\ P90_x\ NS_{std}}{I_{std}\ T_{std}\ P90_{std}\ NS_x}\ F\ C_{std} \quad \textbf{equation 2}$$

Where C, I, T, P90, NS, F are respectively the concentration of analyte (x) and standard (std), the integrated peak intensity, the temperature (K), the 90° pulse length, the number of transients, and F is the factor to take different experimental scheme into account.

3. Results and discussion

3.1. Bioprofiling of natural extracts

In all samples and among the eight standards which were selected as structural isomers, UA and OA showed the most active bands in AChE, tyrosinase, and *B. subtilis* (bio)assays (Fig. 1). These results were in accordance with other research about cholinesterase [31] and tyrosinase [32] inhibitions as well as the antibacterial properties against *B. subtilis* [33] of UA and OA. Although CA and MA showed (bio)activity and coelution, their inhibition of tyrosinase and AChE revealed less intensity compared to UA and OA due to their less amount. Moreover, Ros and BA as well as Thy and Car showed (bio)activity but they were well separated from other structural isomers; therefore we left them out and focused on UA-OA coeluted (bio)active zones of these natural extracts (Fig. 1). UA-OA zones were isolated by HPTLC and then quantified as a coeluted (bio)active zone via qNMR. Although UA and OA can be separated by GC [34] and RP-HPTLC [35]/-HPLC [35, 36], we continued with normal phase chromatography workflow due to its higher compatibility to most bioassays and enzymatic inhibition assays. In addition, using the same chromatographic system as bioprofiling for isolation was useful to collect right active zone in a similar hR_F for NMR spectroscopy (Fig. 2).

3.2. Signal assignment of UA and OA as two structural isomers via 1D and 2D NMR

Even though UA and OA, as two different hydroxy pentacyclic triterpen acids, showed similar hR_F values on NP-HPTLC (Fig. 1) as well as similar molecular ions in HRMS spectra (Table 1), the ^{1}H NMR spectrum returned distinct allylic 1H-18 signals i.e. 2.20 ppm for UA and 2.85 ppm for OA in CD_3OD. Such signals were typically in regions of the ^{1}H NMR spectrum not overcrowded in solutions of UA and OA individual standard, their model mixtures (UA:OA 70:30 and 40:60, Fig. 3) and isolated band from our natural extracts (Fig. 4B and D) to ensure good selectivity. The chemical shift of the allylic 1H-18 in structural isomers (UA and OA) is determined by methyl substitution in ring E (Fig. 5, C-29 and C-30) in vicinal or geminal configuration in UA and OA respectively. The fine structure of 1H-18 signals ((UA, 2.20 ppm, 1H, *d*, *J* (Hz) = 11.26 and OA, 2.85 ppm, 1H, *dd*, *J* (Hz) = 13.97, 4.60 Hz, 1H)) is determined by the number of protons in chemical environment and by the value of constant couplings. Both chemical shift and signal multiplicity (the *dd* splitting in 1H-18 OA is a result of correlation of 1H-18 with two chemically unequivalent protons on 2H-19) were essential for the isomer identification. However, it can get problematic if diagnostic signals (at 2.20 and 2.85 ppm) even only partially overlap with other signals of the matrix [36] and particularly is evident in crude NMR spectra (Fig. 6A). In case of partially overlap, the identification of UA and OA can be provided by 2D NMR spectroscopy, i.e. ^{1}H-^{13}C HSQC and ^{1}H-^{13}C HMBC techniques which allow to spread out signals into two dimensions (with a huge spectral width at the carbon compared to that of proton), decreasing therefore the peak overcrowding. The ^{1}H-^{13}C cross correlation in HSQC spectrum, ensures also that the observed peak belongs to the analyte of interest, whereas analyte structure identity is determined by the ^{1}H-^{13}C HMBC experiment by long distance ^{1}H-^{13}C interactions. Indeed, the ^{1}H-^{13}C HMBC cross correlation peaks of signals at 2.20 ppm and 2.85 ppm return characteristic fingerprints along the dimension of the carbon, particular for UA and OA respectively [36]. The 2D NMR techniques were therefore implemented in our protocol of analyses to ensure the specificity of method for UA and OA in all the samples.

^{1}H-^{13}C HSQC spectra of a model mixture of UA:OA mixture (40:60) and isolated samples solutions were acquired, then, in which the ^{1}H and ^{13}C in position 18 return two different cross correlation peaks respectively at 2.20 ppm and 54.9 ppm for UA and 2.85 ppm and 43.4 ppm for OA (Fig. 7) used for volume peak integration.

The ^{1}H-^{13}C HMBC spectrum of UA:OA mixture (40:60, Fig. 8, Table 2) as well as isolated samples solution showed two series of cross-peaks for the two isomers resulting via correlation of the 1H-18 with neighboring carbons in the rings C, D and E such C-13, C-17 and C-19 (two-bonds correlation) and C-12, C-14, C-16, and C-28 (three-bonds correlation) respectively for UA and OA. A clear distinctive 1,3 HMBC cross correlation was that of the H-18 with C-29 since is typical of ursolic acid only.

3.3. Quantitative measurement method: internal reference method *versus* PULCON

Both internal standard and PULCON procedures for analyte quantification by NMR were explored by using a maleic acid reference solution as internal standard, directly added to the sample tube or used in a separate tube, as external reference. The integration of district signals related to 1H-18 signals (Fig. 4A, UA, 2.20 ppm and OA, 2.85 ppm) in ^{1}H NMR spectra were used for analyte quantification. However, after the internal standard addition, a signal drift was observed (Fig. 4C and E) that was ascribed to the effect of maleic acid. Maleic acid, indeed, has two acidic functions that change the pH in polar solvents such as the methanol. A signal drift can have a detrimental effect, due to the selectivity loss caused by the overlap of diagnostic signal with those of the matrix. Internal standard method was, therefore, rejected. External standard based NMR methods do not have such drawbacks, being the reference standard in a separate tube [10]. The PULCON method, proved to be more suitable than internal standard for the quantitative study of natural extracts. On other hand, the isolated zone contained ions due to using silica gel HPTLC plate for isolation (Fig. 2) showed a drift (around 0.05 ppm) compared to model solution spectrum (Fig. 4B and D, UA, 2.25 ppm and OA, 2.90 ppm) but it did not cause signal overlap as much as internal standard especially for Org (Fig. 4D *vs.* E).

3.4. Comparison of the PULCON results with HPTLC

Quantitative ^{1}H NMR of UA and OA in five isolated (bio)active zones from Sage, Org, Thm, GAP and RAP extract solutions were performed by PULCON procedure. NMR spectrum of each sample was recorded twice (n=2) and the concentration of UA (0.72-4.67 mM) and OA (0.27-1.83 mM) in all samples was referred to maleic acid external standard 2.74 mM solution. For those signals overlap to those of matrix, deconvolution in MestreNova and volume peak integration via HSQC were performed (Table 3) as comparison (see 3.5).

The same isolated sample solutions (in CD_3OD) used for NMR experiments, after 10 times dilution, were analyzed thrice (n=3) by HPTLC. The quantification of UA and OA was performed after a pre- and post-chromatographic derivatization HPTLC (Fig. 9), the efficiency of HPTLC isolation was assessed by comparison between the amount of UA and OA in isolated samples and extract solutions (Table 3). Then the qNMR results were compared to those obtained by HPTLC. This derivatization HPTLC method separated and detected MA and CA, as well (Fig. 9) and can be used for quantification these compounds. According to extract solutions results in Table 3, amount of UA and OA in dried extracts was 38-241 mg/g and 11-96 mg/g while amount of UA and OA in dried milled powder was 3-18 mg/g and 1-9 mg/g. However, quantification of UA and OA due to peak overlapping was not possible in crude extracts via qNMR (Fig. 6A).

The comparison of two methods based on orthogonal techniques (NMR spectroscopy and planar chromatography) showed a high correlation between the quantitative results (Fig. 10). The HPTLC isolation (Fig. 2) efficiency (mean 82 %) revealed that after finding an (bio)active zone, the structural confirmation of the expected compound(s) and their quantification can be more precisely done via an efficient isolation step with around 18 % loss of favorite compounds, but the ratio between the interested compounds were close to those of extract solutions (Table 3). The HPTLC-NMR workflow with a fast and cost-effective procedure with 16 mL solvent consumption (10 mL mobile phase and 3 × 2 mL methanol for extraction) can be a proper alternative for bioactivity-guided fractionation strategy using column chromatography long procedure with high consumption of solvents and long evaporation time. The one-step HPTLC isolation with 10000 times more sample application in comparison with common HPTLC workflow (1 µg/band for pre- and post-chromatographic derivatization HPTLC *versus* 10000 µg/area for HPTLC isolation) using the same chromatographic condition as HPTLC–EDA (10 µg/band), provided enough active compound for NMR spectroscopy (0.27-4.67 mM or 123-2133 µg of UA/OA). In addition, HPTLC isolation (Fig. 2) removed the matrix and made the NMR spectra less crowded compare to crude sample spectra (Fig. 6A *vs.* 6B). In another study, ^{1}H qNMR and quantitative ^{1}H-^{13}C HSQC (in case of complex samples matrix) were performed using classical internal and external standard

calibration curve [36]. This procedure needed several serial dilutions of UA and OA standard solutions in expensive deuterated solvents and many NMR spectra just for drawing a calibration curve, while in PULCON method, one external standard is enough for quantification of several analytes in different samples.

3.5. Deconvolution and HSQC volume peak integration

When the peak of interest is partially overlaps to those of the matrix, a deconvolution algorithm can be applied to separate the contributions to the signal, performing by MestreNova line fitting algorithm (MestReNova 11.0). The NMR peak is deconvoluted into component peaks by using suitable percentage of Lorentzian and Gaussian character to properly fit the peak shape. Then an artificial spectrum is generated as sum of each component, where the signals of the matrix are not added. The same deconvolution procedure was applied to peak not disturbed by matrix signal and the resulting artificial integrated peak intensity was calibrated to the value of concentration, measured by PULCON in the ^{1}H NMR original spectrum (before the deconvolution). The concentration of another structural isomer (UA or OA) was, then, inferred from the integral ratio performed on the artificial spectrum, thus eliminating the matrix contribution.

The ^{1}H-^{13}C HSQC experiment, instead, is suitable to verify the analyte concentration when the peak overlap is more pronounced. The main limit in using 2D technique for quantitative purposes is that the signal is proportional not only to the analyte concentration in the active volume of NMR tube in the coil, as it is for ^{1}H NMR spectrum but it depends on 2D NMR experimental acquisition parameter (e.g. delays), the constant couplings (J_{HH} and J_{CH}) and the intrinsic relaxation times of the resonances (T1 and T2) [31]. In our case, the signal of interest is the same (C18-H18) for both isomers as well the acquisition parameters thus the site specificity in peak intensity measuring derives only from difference in one J_{HH}, rather than from all the factors previously mentioned. However, the quantification by deconvolution and by ^{1}H-^{13}C HSQC experiments was used only as a comparison (Table 3). The concentration of isolated isomer signals measured by PULCON ^{1}H qNMR was used to calibrate the same signal (integrated volume peak intensity) in the ^{1}H-^{13}C HSQC experiment. Then, the concentration of the other isomer was inferred from the ratio between the integrated volume peak intensity of the two isomer signals detected in the ^{1}H-^{13}C HSQC experiment, after verifying that the matrix signals were spread out, far from those of interests.

3.6. Figure of merit of qNMR spectroscopy and pre- and post-chromatographic derivatization HPTLC

The intra-day and intermediate precision (repeatability) of PULCON method was estimated by calculating the relative standard deviation (*RSD*% < 3) of ^{1}H qNMR spectroscopy measurements of three individual maleic acid solution (2.74 mM) each run in three replicates in three different days (Table 4). Detectability of qNMR was defined as S/N ratio of UA (43-104) and OA (13-43) in ^{1}H NMR spectra of all isolated sample solutions using TopSpin 3.2 (Table 3). While the LODs of HPTLC method were calculated as 16 ng/band and 7 ng/band for UA and OA respectively, based on 3.3 STEYX/Slope (MS-Office) in the linear rang of calibration curves (linearity 100-400 ng/band for UA and 25-200 ng/band for OA). The S/N ratios of UA and OA in HPTLC were defined in the lowest level of calibration curve as S/N = 24 for UA at 100 ng/band and S/N = 4 for OA at 25 ng/band. The *RSD*% values (1-10 %) for HPTLC was reported in Table 3.

4. Conclusions

The HPTLC-NMR spectroscopy workflow is a straightforward and efficient procedure (mean 82 %) for determination, structural confirmation and quantification of bioactive compounds even in case of coelution of structural isomers. The one-step HPTLC isolation with a high sample application in the same chromatographic condition as HPTLC–EDA provides enough active compound for qNMR spectroscopy. A fast and cost-effective HPTLC isolation of (bio)active compounds is an appropriate alternative instead of costly and long bioactivity-guided fractionation strategy. PULCON procedure as an orthogonal technique is able to quantify structural isomers of (bio)active compounds in natural products and medicinal plant extracts without making any contamination in sample solutions. The quantification results presented a high correlation between those obtained by PULCON and the ones from HPTLC technique, demonstrating as the combination of the two, to be a cheap and reliable method. In case of peak overlapping with matrix signals the deconvolution and HSQC volume peak integration are the other alternatives to reach to pure signal without matrix interference.

Acknowledgment

Thank is owed to DAAD lab rotation fund given via International Giessen Graduate Centre for the Life Sciences (GGL),

Merck, Darmstadt, Germany for providing HPTLC plates, and Silvia Venzano for precious suggestions for accurate weighing.

Appendix A. Supplementary data

Supplementary data of with this article is available, in the online version, at

References

[1] G.E. Morlock, Chromatography combined with bioassays and other hyphenations – the direct link to the compound indicating the effect, in: Instrumental Methods for the Analysis and Identification of Bioactive Molecules, American Chemical Society, 2014, pp. 101-121.

[2] H.R. Adhami, U. Scherer, H. Kaehlig, T. Hettich, G. Schlotterbeck, E. Reich, L. Krenn, Combination of bioautography with HPTLC–MS/NMR: a fast identification of acetylcholinesterase inhibitors from Galbanum, Phytochem. Anal. 24 (2013) 395-400.

[3] E.M. Grzelak, C. Hwang, G. Cai, J.-W. Nam, M.P. Choules, W. Gao, D.C. Lankin, J.B. McAlpine, S.G. Mulugeta, J.G. Napolitano, Bioautography with TLC-MS/NMR for rapid discovery of anti-tuberculosis lead compounds from natural sources, ACS Infect. Dis. 2 (2016) 294-301.

[4] E. Azadniya, G.E. Morlock, Bioprofiling of *Salvia miltiorrhiza* via planar chromatography linked to (bio)assays, high resolution mass spectrometry and nuclear magnetic resonance spectroscopy, J. Chromatogr. A 1533 (2018) 180-192.

[5] E. Azadniya, L. Goldoni, T. Bandiera, G.E. Morlock, HPTLC-qNMR to quantify co-eluted isomers in (bio)active zones, in: 11th annual GGL conference on life sciences, Giessen, Germany, 2018.

[6] X.-y. Zheng, Z.-j. Zhang, G.-x. Chou, T. Wu, X.-m. Cheng, C.-h. Wang, Z.-t. Wang, Acetylcholinesterase inhibitive activity-guided isolation of two new alkaloids from seeds of *Peganum nigellastrum* Bunge by an *in vitro* TLC-bioautographic assay, Arch. Pharmacal Res. 32 (2009) 1245-1251.

[7] L. Gu, T. Wu, Z. Wang, TLC bioautography-guided isolation of antioxidants from fruit of *Perilla frutescens* var. *acuta*, LWT-Food Sci. Technol. 42 (2009) 131-136.

[8] E.F. Queiroz, J.-L. Wolfender, K. Atindehou, D. Traore, K. Hostettmann, On-line identification of the antifungal constituents of *Erythrina vogelii* by liquid chromatography with tandem mass spectrometry, ultraviolet absorbance detection and nuclear magnetic resonance spectrometry combined with liquid chromatographic micro-fractionation, J. Chromatogr. A 974 (2002) 123-134.

[9] A. Gössi, U. Scherer, G. Schlotterbeck, Thin-layer chromatography–nuclear magnetic resonance spectroscopy – a versatile tool for pharmaceutical and natural products analysis, CHIMIA Int. J. Chem. 66 (2012) 347-349.

[10] S.K. Bharti, R. Roy, Quantitative ^{1}H NMR spectroscopy, Trends Anal. Chem. 35 (2012) 5-26.

[11] Y.B. Monakhova, M. Kohl-Himmelseher, T. Kuballa, D.W. Lachenmeier, Determination of the purity of pharmaceutical reference materials by ^{1}H NMR using the standardless PULCON methodology, J. Pharm. Biomed. Anal. 100 (2014) 381-386.

[12] C.H. Cullen, G.J. Ray, C.M. Szabo, A comparison of quantitative nuclear magnetic resonance methods: internal, external, and electronic referencing, Magn. Reson. Chem. 51 (2013) 705-713.

[13] R. Watanabe, C. Sugai, T. Yamazaki, R. Matsushima, H. Uchida, M. Matsumiya, A. Takatsu, T. Suzuki, Quantitative nuclear magnetic resonance spectroscopy based on PULCON methodology: application to quantification of invaluable marine toxin, okadaic acid, Toxins 8 (2016) 294.

[14] E. Cífková, M. Holčapek, M. Lísa, M.n. Ovčačíková, A.n. Lyčka, F.d.r. Lynen, P. Sandra, Nontargeted quantitation of lipid classes using hydrophilic interaction liquid chromatography–electrospray ionization mass spectrometry with single internal standard and response factor approach, Anal. Chem. 84 (2012) 10064-10070.

[15] L. Bai, D.D. Carlton Jr, K.A. Schug, Complex mixture quantification without calibration using gas chromatography and a comprehensive carbon reactor in conjunction with flame ionization detection, J. Sep. Sci. 41 (2018) 4031-4037.

[16] L. Dreier, G. Wider, Concentration measurements by PULCON using X-filtered or 2D NMR spectra, Magn. Reson. Chem. 44 (2006) S206-S212.

[17] G. Wider, L. Dreier, Measuring protein concentrations by NMR spectroscopy, JACS 128 (2006) 2571-2576.

[18] L. Goldoni, T. Beringhelli, W. Rocchia, N. Realini, D. Piomelli, A simple and accurate protocol for absolute polar metabolite quantification in cell cultures using quantitative nuclear magnetic resonance, Anal. biochem. 501 (2016) 26-34.

[19] P. Giraudeau, Quantitative 2D liquid-state NMR, Magn. Reson. Chem. 52 (2014) 259-272.

[20] M. Wójciak-Kosior, Separation and determination of closely related triterpenic acids by high performance thin-layer chromatography after iodine derivatization, J. Pharm. Biomed. Anal. 45 (2007) 337-340.

[21] M. Jamshidi-Aidji, G.E. Morlock, Bioprofiling of unknown antibiotics in herbal extracts: Development of a streamlined direct bioautography using *Bacillus subtilis* linked to mass spectrometry, J. Chromatogr. A 1420 (2015) 110-118.

[22] A. Marston, Thin-layer chromatography with biological detection in phytochemistry, J. Chromatogr. A 1218 (2011) 2676-2683.

[23] R. Akkad, W. Schwack, Determination of organophosphorus and carbamate insecticides in fresh fruits and vegetables by high-performance thin-layer chromatography-multienzyme inhibition assay, J. AOAC Int. 95 (2012) 1371-1377.

[24] Z. Yang, X. Zhang, D. Duan, Z. Song, M. Yang, S. Li, Modified TLC bioautographic method for screening acetylcholinesterase inhibitors from plant extracts, J. Sep. Sci. 32 (2009) 3257-3259.

[25] S. Hage, G.E. Morlock, Bioprofiling of *Salicaceae* bud extracts through high-performance thin-layer chromatography hyphenated to biochemical, microbiological and chemical detections, J. Chromatogr. A 1490 (2017) 201-211.

[26] A. Marston, J. Kissling, K. Hostettmann, A rapid TLC bioautographic method for the detection of acetylcholinesterase and butyrylcholinesterase inhibitors in plants, Phytochem. Anal. 13 (2002) 51-54.

[27] D. Krickeberg, S. Hage, G.E. Morlock, Discovery and characterization of tyrosinase inhibitors in plants, creams and propolis by optimized HPTLC-EI-MS, in, Justus Liebig University of Giessen, Giessen, Germany, September 2017.

[28] M. Jamshidi-Aidji, G.E. Morlock, Fast equivalency estimation of unknown enzyme inhibitors in situ the effect-directed fingerprint, shown for *Bacillus* lipopeptide extracts, Anal. Chem. 90 (2018) 14260-14268.

[29] P.S. Wu, G. Otting, Rapid pulse length determination in high-resolution NMR, J. Magn. Reson. 176 (2005) 115-119.

[30] L. Benedito, A. Maldaner, A. Oliveira, An external reference 1 H qNMR method (PULCON) for characterization of high purity cocaine seizures, Anal. Methods 10 (2018) 489-495.

[31] A. Loesche, A. Köwitsch, S.D. Lucas, Z. Al-Halabi, W. Sippl, A. Al-Harrasi, R. Csuk, Ursolic and oleanolic acid derivatives with cholinesterase inhibiting potential, Bioorg. Chem. 85 (2019) 23-32.

[32] S. Khan, M. Tareq Hassan Khan, M. Nadeem Kardar, Tyrosinase Inhibitors from the Fruits of *Madhuca latifolia*, Curr. Bioact. Compd. 10 (2014) 31-36.

[33] K.I. Wolska, A.M. Grudniak, B. Fiecek, A. Kraczkiewicz-Dowjat, A. Kurek, Antibacterial activity of oleanolic and ursolic acids and their derivatives, Cent. Eur. J. Biol. 5 (2010) 543-553.

[34] A. Caligiani, G. Malavasi, G. Palla, A. Marseglia, M. Tognolini, R. Bruni, A simple GC–MS method for the screening of betulinic, corosolic, maslinic, oleanolic and ursolic acid contents in commercial botanicals used as food supplement ingredients, Food Chem. 136 (2013) 735-741.

[35] M. Martelanc, I. Vovk, B. Simonovska, Separation and identification of some common isomeric plant triterpenoids by thin-layer chromatography and high-performance liquid chromatography, J. Chromatogr. A 1216 (2009) 6662-6670.

[36] V.G. Kontogianni, V. Exarchou, A. Troganis, I.P. Gerothanassis, Rapid and novel discrimination and quantification of oleanolic and ursolic acids in complex plant extracts using two-dimensional nuclear magnetic resonance spectroscopy—Comparison with HPLC methods, Anal. Chim. Acta 635 (2009) 188-195.

Table 1. HPTLC–HRMS data of UA and OA standards and active zones at the same hR_F in *Lamiaceae* and apple peel dried extracts

No.	ID	Modes	Observed *m/z*	Theoretical *m/z*	Molecular ion	Mass error (ppm)	Assignment	Confirmed substance
1	UA standard	Neg (-)	455.35360	455.35307	$C_{30}H_{47}O_3^-$	1.17	$[M-H]^-$	UA
		Pos (+)	479.34977	479.34957	$C_{30}H_{48}O_3Na^+$	0.43	$[M+NA]^+$	Sodium adduct UA
			501.33157	501.33151	$C_{30}H_{47}O_3Na_2^+$	0.12	$[M-H+2Na]^+$	Sodium adduct UA
2	OA standard	Neg (-)	455.35367	455.35307	$C_{30}H_{47}O_3^-$	1.32	$[M-H]^-$	OA
		Pos (+)	479.34974	479.34957	$C_{30}H_{48}O_3Na^+$	0.36	$[M+H]^+$	Sodium adduct OA
			501.33145	501.33151	$C_{30}H_{47}O_3Na_2^+$	-0.12	$[M-H+2Na]^+$	Sodium adduct OA
3	All samples	Neg (-)	455.35348-69	455.35307	$C_{30}H_{47}O_3^-$	0.90-1.36	$[M-H]^-$	Both UA and OA
		Pos (+)	479.34965-98	479.34957	$C_{30}H_{48}O_3Na^+$	0.17-0.86	$[M+NA]^+$	Both UA and OA
			501.33154-68	501.33151	$C_{30}H_{47}O_3Na_2^+$	0.06-0.34	$[M-H+2Na]^+$	Both UA and OA

Table 2. HMBC signal assignment for 1H-18 correlated with neighbouring carbons in UA and OA.

C	OA 18-H 18-C (2.85 and 43.4 ppm)	C	UA 18-H 18-C (2.20 ppm and 54.9 ppm)
		29	16.1
16	22.6	16	23.9
		19, 20	38.7
14	41.6	14	41.6
17, 19	45.9	17	47.9
12	122.3	12	125.2
13	143.9	13	138.0
28	180.4	28	180.3

Table 3. Quantification of ursolic (UA) and oleanolic (OA) acids in *Salvia officinalis* (Sage), *Thymus vulgaris* (Thm), *Origanum vulgare* (Org) red apple peel (RAP) and green apple peel (GAP) via PULCON (^{1}H qNMR) and pre- and post-chromatographic derivatization HPTLC

	qNMR (PULCON)							Pre- and post-chromatographic derivatization HPTLC									
	^{1}H NMR			Deconvolution MestreNova		HSQC volume peak integration		Isolated zone			extract solutions			mg/g dried extract	mg/g dried milled powder	Isolation efficiency (%)	Loss %
Sample name	UA (ng/µL)*	UA/OA ratio	S/N ratio	UA (ng/µL)	UA/OA ratio	UA (ng/µL)	UA/OA ratio	UA (ng/µL)	UA/OA ratio	*RSD* %	UA (ng/µL)	UA/OA ratio	*RSD* %	UA	UA	UA	UA
Sage	167	2	62	135	2	141	2	158	2	1	185	2	2	185	18	86	14
Org	32	3	43	32	2	32	2	30	3	2	38	3	8	38	3	80	20
Thm	134	2	54	125	2	161	2	134	2	2	178	2	6	178	10	75	25
GAP	209	4	104	209	4	209	4	206	4	3	241	4	10	241	15	85	15
RAP	132	3	69	114	3	122	3	142	3	3	222	4	7	222	18	64	36
	OA (ng/µL)			OA (ng/µL)		OA (ng/µL)		OA (ng/µL)		RSD %	OA (ng/µL)		RSD %	OA	OA	OA	OA
Sage	80		39	80		80		93		6	96		3	96	9	97	3
Org	13		13	13		13		10		1	11		1	11	1	93	7
Thm	83		41	83		83		56		5	71		7	71	4	78	22
GAP	53		43	59		49		48		1	55		10	55	3	88	12
RAP	45		27	45		45		44		1	57		7	57	4	78	22
															Average	82	18

as well as efficiency of HPTLC isolation of a (bio)active coeluted zone.

*All qNMR results converted to ng/µL of 0.1 mg/mL extracts or ng/0.1 µg of dried extract to be comparable with those of derivatization HPTLC.

Table 4. Intraday and intermediate precision of the PULCON methods for maleic acid measurement.

Sample no.	Maleic acid (mM) Day 1	Day 2	Day 3	Mean	SD	*RSD* %
1	2.76	2.76	2.78	2.77	0.01	0.42
2	2.74	2.74	2.82	2.77	0.05	1.67
3	2.65	2.65	2.74	2.68	0.05	1.94
Mean	2.72	2.72	2.78	-	-	-
SD	0.06	0.06	0.04	-	-	-
RSD %	2.16	2.16	1.44	-	-	-

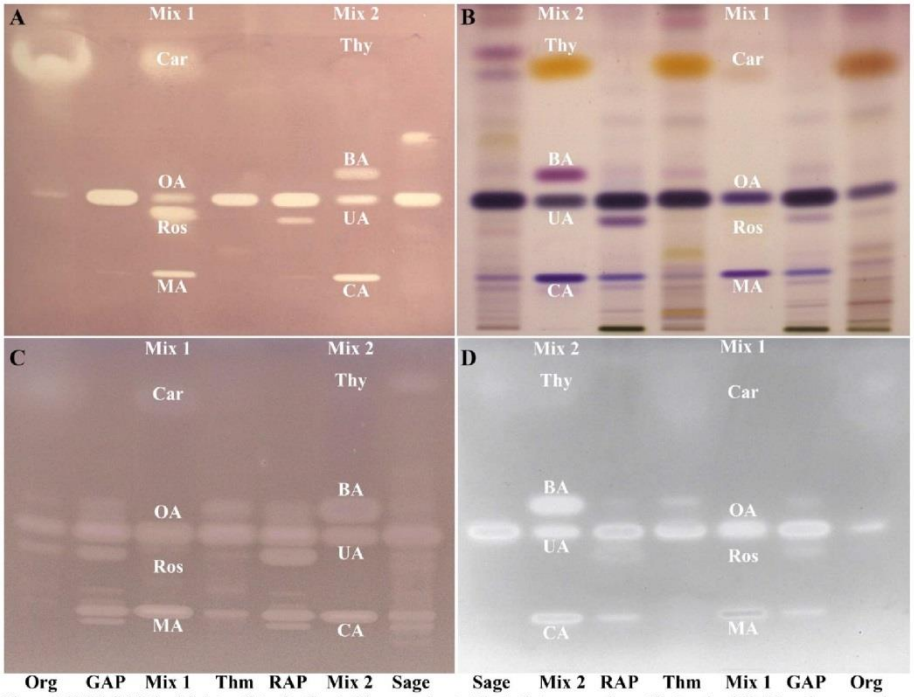

Figure 1. HPTLC–EDA of *Salvia officinalis* (Sage), *Thymus vulgaris* (Thm), *Origanum vulgare* (Org) and red (RAP) and green apple peel (GAP) extract solutions (10 µg/band) along with eight standards (1 µg/band), i.e., maslinic acid (MA), rosmanol (Ros), oleanolic acid (OA), thymol (Thy) as Mix 1 and corosolic acid (CA), ursolic acid (UA), betulinic acid (BA), and carvacrol (Car) as Mix 2, were developed by toluene–methanol–ethyl acetate 17:2:1 up to 70 mm after *B. subtilis* bioassay (A), derivatized with anisaldehyde-sulfuric acid reagent (B) AChE (C) and tyrosinase (D) assays under white light illumination.

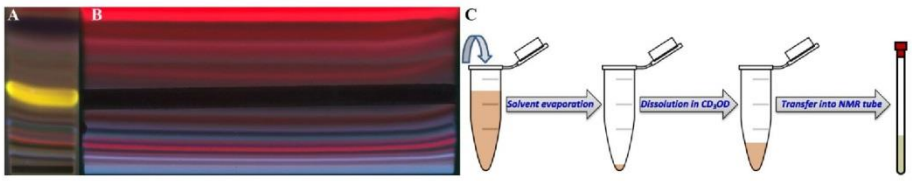

Figure 2. 150 µL (A) and 1 mL (B) of *Origanum vulgare* (Org) extract solution (10 mg/mL) were applied as two areas of 25×3 mm and 150×3 mm (10 mg/area) respectively, on the HPTLC plate (20×10 cm) and developed up to 70 mm; the left part was cut and derivatized with anisaldehyde-sulfuric acid reagent as a pattern for scraping off the active band (B). Scrapped part was extracted 3 times with 2 mL methanol, after evaporation, the residue was dissolved in 1 mL CD_3OD (10 mg/mL), then transferred (250 µL) into a 3-mm NMR tube (C) and afterwards diluted 1:10 for pre- and post-chromatographic derivatization HPTLC.

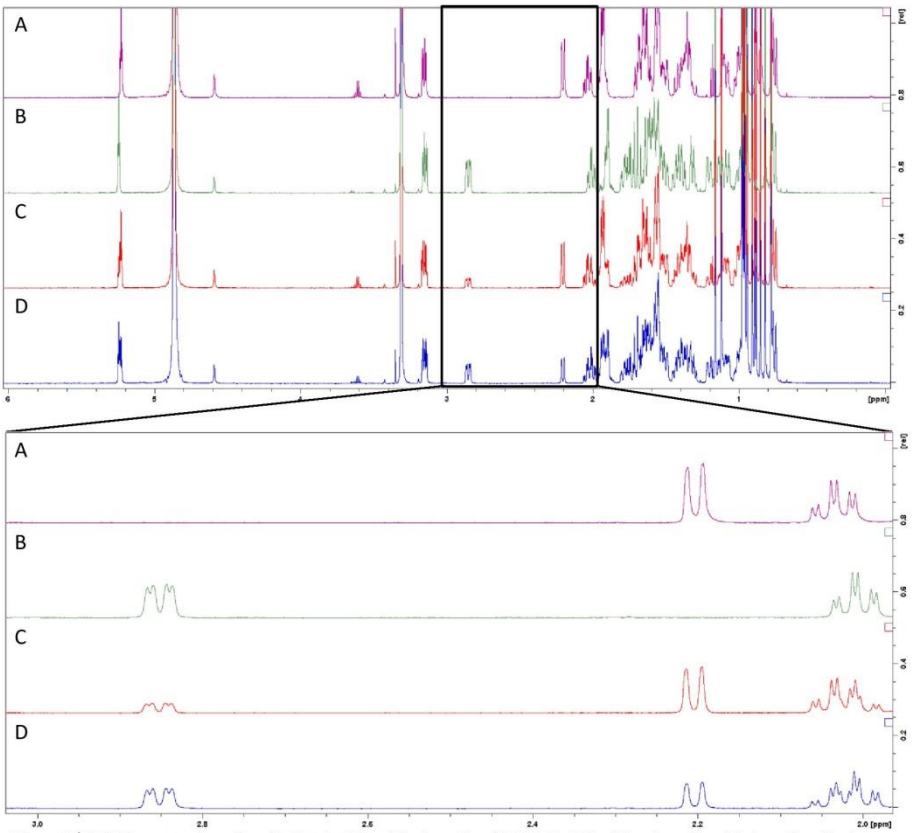

Figure 3. ^{1}H NMR spectra of ursolic acid (UA, A, 5.52 mM), oleanolic acid (OA, B, 5.71 mM) and ursolic acid:oleanolic acid mixture (UA:OA, C, 70:30 and D, 40:60) in CD_3OD.

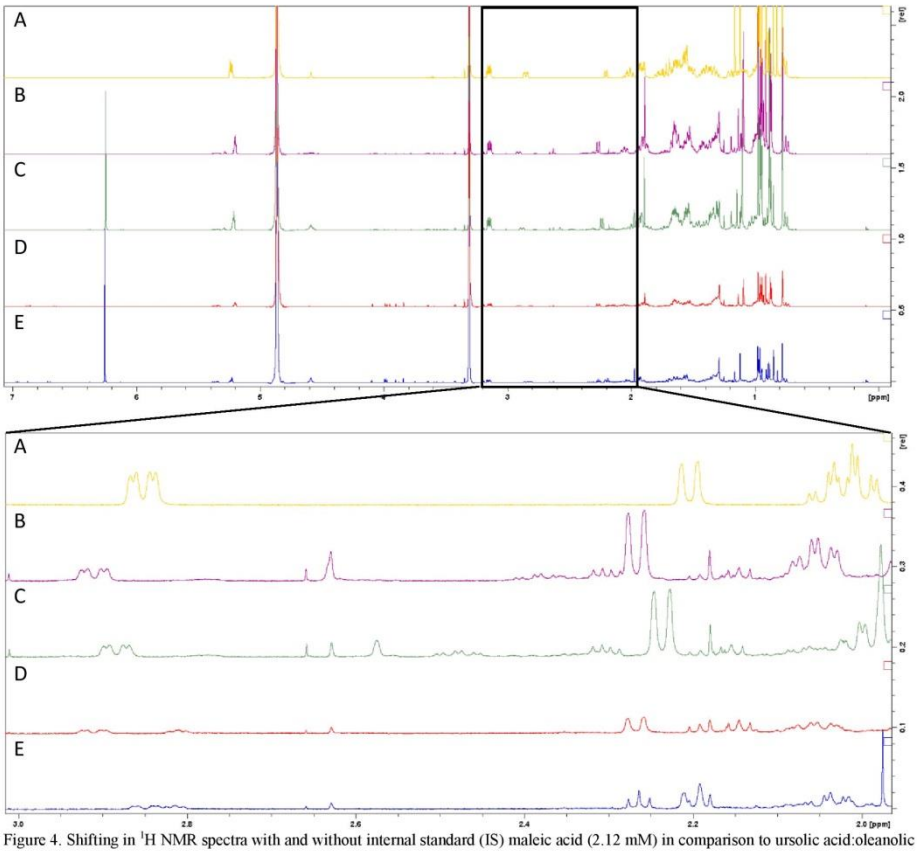

Figure 4. Shifting in ^{1}H NMR spectra with and without internal standard (IS) maleic acid (2.12 mM) in comparison to ursolic acid:oleanolic acid mixture (A, UA:OA 40:60) spectrum. Red apple peel (RAP) isolated sample solution without IS (B) and with IS (C), as well as *Origanum vulgare* (Org) isolated sample solution without IS (D) and with IS (E).

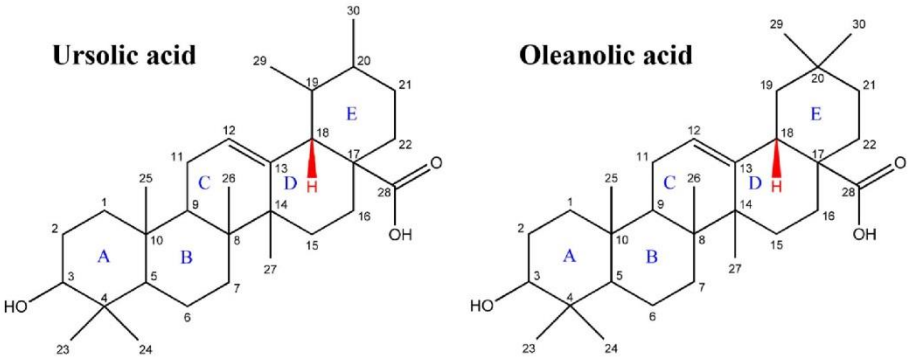

Figure 5. Structures of ursolic and oleanolic acids.

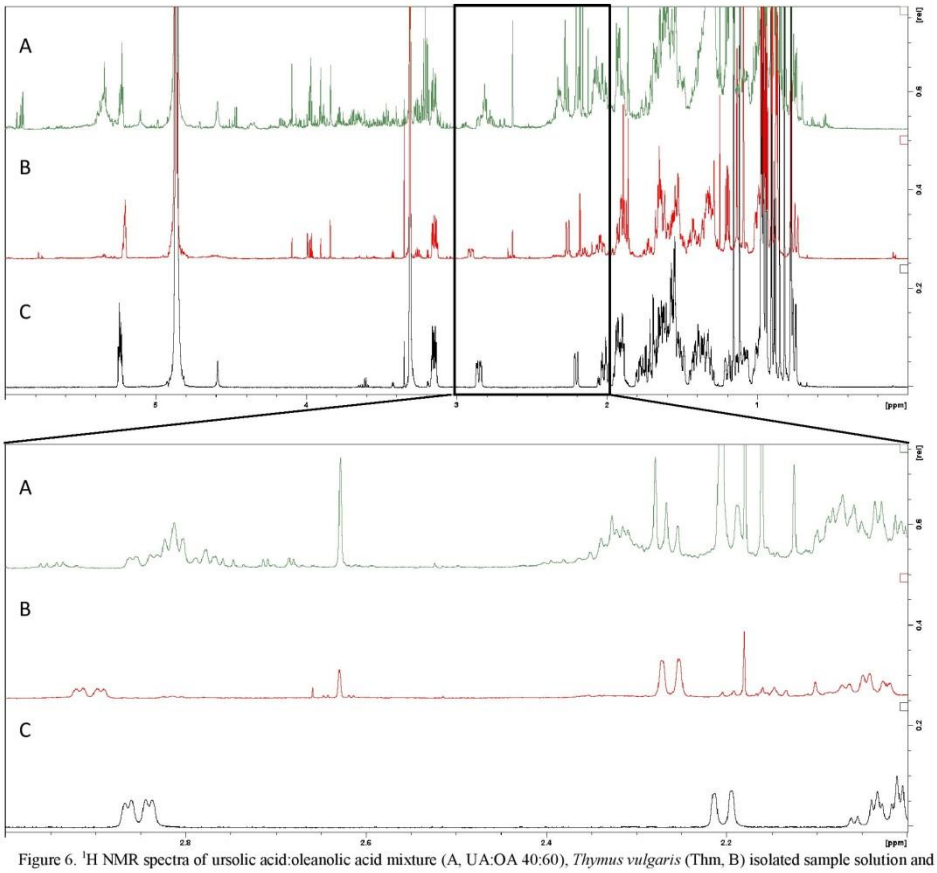

Figure 6. ^{1}H NMR spectra of ursolic acid:oleanolic acid mixture (A, UA:OA 40:60), *Thymus vulgaris* (Thm, B) isolated sample solution and its crude extract solution (C) in CD_3OD.

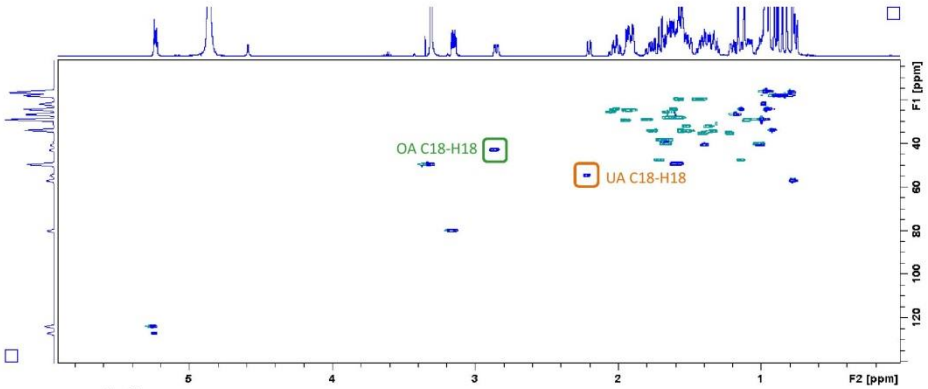

Figure 7. ^{1}H-^{13}C HSQC edited spectrum of ursolic acid:oleanolic acid mixture (UA:OA, 40:60) in CD_3OD.

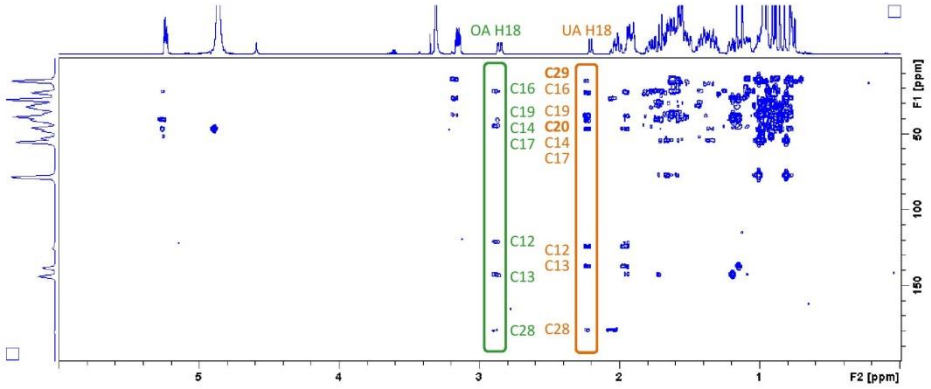

Figure 8. ^{1}H-^{13}C HMBC spectrum of ursolic acid:oleanolic acid mixture (UA:OA, 40:60) in CD_3OD.

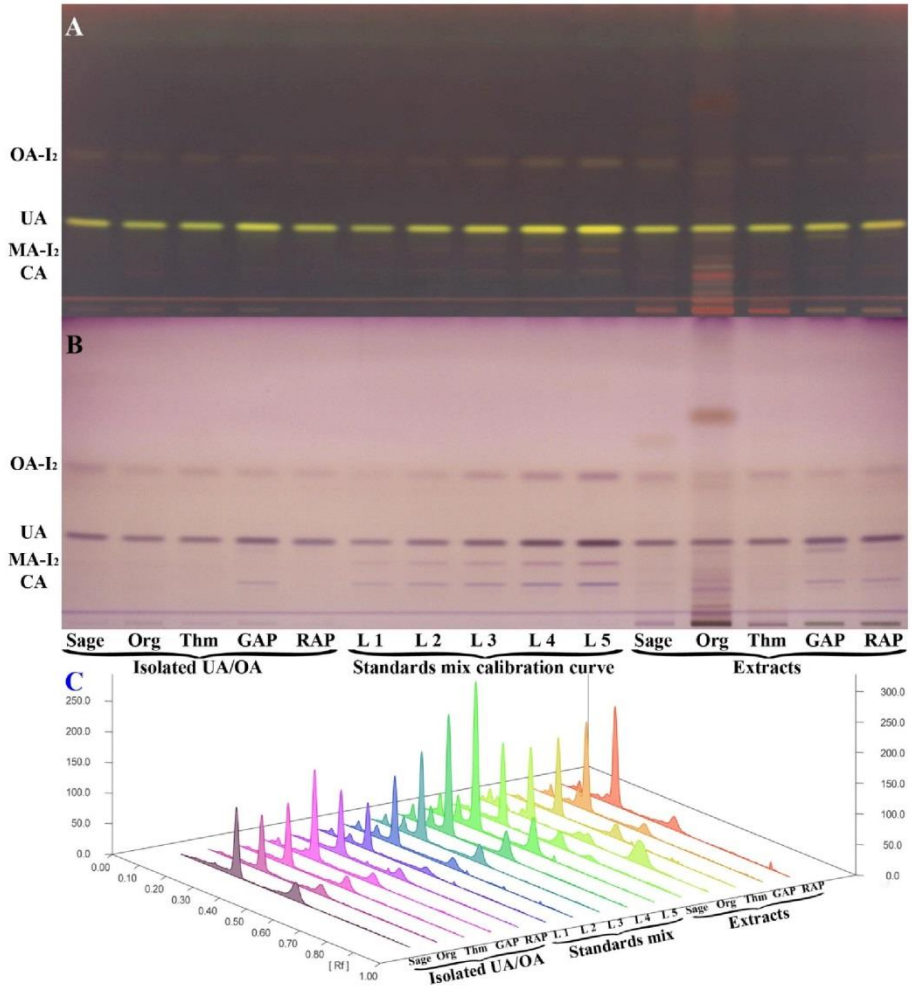

Figure 9. Chromatogram of isolated sample solutions (isolated ursolic/oleanolic acid, UA/OA), standard mixture, UA (100-400 ng/band), OA (25-200 ng/band), corosolic (CA, 10-40 ng/band), maslinic (MA, 25-100 ng/band) acids for calibration as well as *Salvia officinalis* (Sage), *Thymus vulgaris* (Thm), *Origanum vulgare* (Org) and red (RAP) and green apple peel (GAP) extracts solutions (1 µg/band) after iodine pre-chromatographic derivatization and anisaldehyde-sulfuric acid post-chromatographic derivatization reagents, developed by toluene-methanol-ethyl acetate 17:2:1, detected at 366 nm (A) and under white light illumination (B). Densitogram (C) was recorded in absorption mode at 665 nm of tungsten lamp.

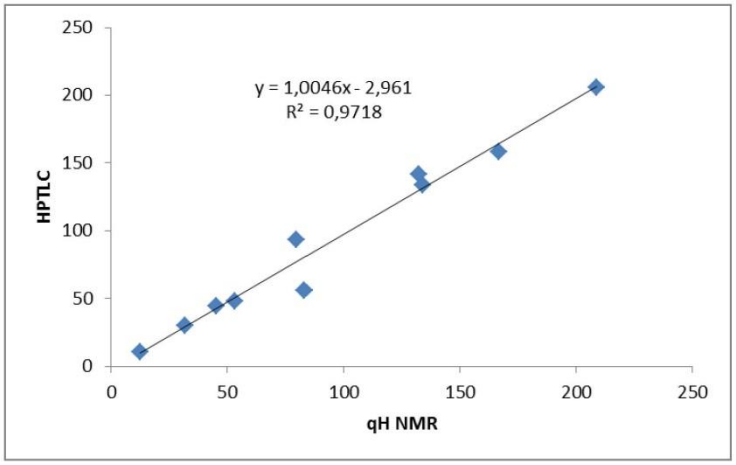

Figure 10. Comparison of two orthogonal methods HPTLC and ^{1}H qNMR (PULCON).